RMIT UNIVERSITY

Sensitive Ambient RF Energy Harvesting

A thesis submitted in fulfilment of the requirements for the degree of Doctor of Philosophy

Negin Shariati

Bachelor of Engineering – Electrical and Electronics

School of Electrical and Computer Engineering

College of Science, Engineering and Health

RMIT University

August 2015

Declaration

I certify that except where due acknowledgement has been made, the work is that of the author alone; the work has not been submitted previously, in whole or in part, to qualify for any other academic award; the content of the thesis is the result of work which has been carried out since the official commencement date of the approved research program; any editorial work, paid or unpaid, carried out by a third party is acknowledged; and, ethics procedures and guidelines have been followed.

Negin Shariati

22 August 2015

To the World

Acknowledgements

The outcomes presented in this thesis could not have been completed without the support of my supervisors. I would like to express my sincere gratitude to Prof. Kamran Ghorbani, A. Prof. Wayne Rowe and A. Prof. James Scott for their expert supervision, for the opportunity to work alongside them and for their valuable input on this research and academic writing. Greatest appreciation for my senior supervisor Prof. Kamran Ghorbani for promoting forward thinking and for his invaluable guidance and support during this PhD program.

A great acknowledgement for Mr. David Welch as the most creative and skilled technical staff member for assistance in fabrication of the rectifier circuits. I would like to acknowledge Dr. Thomas Baum for his input and proof reading of this thesis. Thanks to my colleagues Kashka Sarosh Irani and Grace Sharma for proof reading of this thesis. I would also like to acknowledge Dr. Khashayar Khoshmanesh for his valuable advice.

I would like to express my deepest gratitude to my mother Ms. Masoumeh Gheispour. Thank you for continuously building my confident, inspiring and comforting me to pursue this degree. Big thanks to my little sister Nooshin Shariati for lifting my spirit with her positive energy. I wish to thank my aunt Ms. Mozhgan Shariati for her compassion and for initiating and facilitating my transition in to Australia and my cousin Sanaz Zahedi for her unconditional support and optimism.

Special thanks to my best friend Amir Reza Vahid, for being a tremendous source of encouragement throughout my research. I am deeply grateful for your endless moral support during challenging time.

Abstract

Rectification of microwave signals to generate DC (Direct Current) power has become the subject of research since the 1950's. Radio Frequency (RF) energy harvesting has experienced a rapid development in recent years due to the increasing number of RF transmitter sources producing an abundant ambient microwave energy waste.

Furthermore, the development of wireless power transmission (WPT) technologies has triggered impetus for RF energy harvesting. Hence, RF energy scavenging is a promising solution as it has the potential to provide a sustainable energy source to meet upcoming demands.

Efficient ambient RF energy scavenging is a very challenging issue, as it deals with the low RF power levels available in the environment. The scavengeable power levels are generally unknown and can vary unpredictably; therefore sparking research interest to develop highly sensitive RF energy scavengers to capture ambient RF signals over a range of low input power levels.

This research focuses on a real life RF energy scavenging approach to generate electrical power in urban environments. It aims to develop highly sensitive and efficient ambient RF energy scavenging system and method to harvest a broad range of very low level ambient RF power.

The feasibility of RF energy harvesting through field measurements and maximum available power analysis in metropolitan areas of Melbourne, Australia is investigated. Scavengeable ambient frequency sources with their associated available RF power levels were identified. RF field investigations and analysis identified the scavengeable levels of ambient RF power are lower than previous published works. Available bands vary considerably from location to location which are highly incoherent and are effected by environmental/free-space

conditions. Furthermore, it is demonstrated that commercial frequency bands such as FM (88-108 MHz) and TV (470-890 MHz) provide optimal sources for power scavenging due to their suitable level of the ambient power at a variety of locations. Furthermore, cellular and wireless communication systems (800-1000 MHz) are recommended as alternative power scavenging sources.

In order to investigate the feasibility of harvesting ambient EM (electromagnetic) energy from multiple sources (broadcasting and cellular systems) simultaneously, a new highly sensitive multi-resonant rectifier is proposed operating over a broad input power range (−40 to −10 dBm). The measurement results demonstrate that a two tone input to the proposed dual-band RF energy harvesting system can generate 3.14 and 7.24 times more DC power than a single tone at 490 and 860 MHz respectively, resulting in a measured effective efficiency of 54.3% for a dual-tone input power of −10 dBm. Real environmental measurements indicate the rectifier generates 39.38 μW by harvesting RF energy from two bands simultaneously.

In order to increase the sensitivity and hence the output DC power, harvesting energy over a wider frequency band is investigated. Therefore, the feasibility of harvesting ambient EM energy from FM broadcasting band is examined. A highly sensitive rectenna is proposed which exhibits favourable impedance matching at 89-11 MHz over a broad range of low input power −50 to −10 dBm (0.01 to 100 μW). The proposed FM rectenna with 22% fractional bandwidth delivers a measured power conversion efficiency of 41% with single tone of −10 dBm. An innovative idea that arose from these investigations was an evaluation of the performance of a rectenna system which was embedded into low profile building materials. This enables to harvest ambient RF energy in urban environments, providing a unique way of delivering power to many low energy home or office devices. Based on the

real environmental measurements, the embedded rectenna in plaster generates 175 μW of DC power by harvesting EM energy over the FM frequency band.

Finally, the effect of multi-tone excitation (with constant total input power) on output DC power of the rectifier is analysed to facilitate the comparison between single tone and multiple tones. Various factors such as; different frequency spacing, low input power levels and random phase (incoherency) arrangements were considered in frequency and time domain analysis and also in measurements.

It is demonstrated that the application of multiple tones simultaneously within the matched frequency band and with constant total input power results in a lower total average output power when compared with single-tone case with the same input power.

Contents

List of Figures

List of Tables

Glossary

AC	Alternating Current
ADS	Advanced Design System
BPF	Band Pass Filter
c	Speed of Light (~3×10^8 m/s)
C	Capacitance, unit is Farad
CMOS	Complementary Metal-Oxide-Semiconductor
dB	Decibels
DC	Direct Current
EM	Electromagnetic
f	Frequency
GPS	Global Positioning System
GSM	Global System for Mobile communications
L	Inductance, unit is Henry
LPF	low Pass Filter
HB	Harmonic Balance
HF	High Frequency
Hz	Hertz (cycles per second)
I	Electric current, unit is Ampere
IC	Integrated Circuits
LSSP	Large Signal S-parameter
MHz	Mega-Hertz ($1*10^6$Hz)
PAPR	Peak-to-Average Power Ratio
PCE	Power Conversion Efficiency
R	Resistance, unit is ohm (Ω)
RF	Radio Frequency
RFID	Radio Frequency Identification
SBD	Schottky Barrier Detector
SMT	Surface Mount Technology
SPS	Solar power Satellites
SSP	Space Solar Power

UHF	Ultra High Frequency
V	Electric Potential Difference or Voltage, unit is Volt (V)
VNA	Vector Network Analyser
VSWR	Voltage Standing Wave Ratio
Wi-Fi	Wireless Fidelity
WLAN	Wireless LAN
WPT	Wireless Power Transmission
ε	Permittivity
λ	Wavelength

Chapter 1 – Introduction

1.1 Introduction

With an ever increasing world population and the implications this has on the carbon footprint and energy cost, there is a need to adopt inexpensive and green energy harvesting strategies. This is of paramount importance for the conservation of the environment and the global economy.

Hence, implementing green policies by replacing finite sources of energy with renewable ones (e.g. solar, wind, vibration and ambient radiation) is a long term solution [1, 2].

In recent years, Radio Frequency (RF) energy harvesting has attracted widespread interest due to the increasing number of RF transmitting sources, which have created an abundance of ambient microwave energy sources. These abundant signals are radiated by local electromagnetic (EM) sources such as FM radio stations, TV transmitters, cellular systems, wireless communication systems, to name a few. Hence, RF energy harvesting can provide power continuously.

Furthermore, the development of wireless power transmission (WPT) technologies has triggered impetus for RF energy harvesting. RF energy harvesting has the potential to charge batteries or power electronic devices wirelessly; this is especially useful in remote areas, where accessibility is a problem, or where it is hard to replace batteries (e.g. bridges,

chemical implants, aircraft, etc.). Hence, instead of using batteries which have a limited lifespan and result in environmental pollution, RF energy harvesters can provide electrical power cleanly, safely, and cheaply. This concept has been around for decades, and since the 1950's, devices for powering mobile electronics and wireless sensor networks have evolved.

A prominent advantage of RF energy scavenging is the ability to convert ambient energy into electrical power throughout day and night, both outdoor and indoor. Moreover, RF scavenging has the advantage of diffracting from and penetrating inside building materials. Although ambient microwave signals have very low energy (compared to wind or solar), they radiate energy at all times. RF scavenging can allow for size reduction in the harvesting system (compared to photovoltaic cells or wind turbines) in applications where miniaturisation is essential. Hence, RF energy harvesting is a promising solution to provide a sustainable energy source to meet future demands.

1.2 Motivation

This research aims to generate useful electrical power by harvesting very low density RF signals which are freely available in the atmosphere. Although considerable advances in rectenna (rectifying antenna) designs have been achieved, the vast majority of the published work are dedicated to maximising the system efficiency at often high input power levels (e.g. WPT scenarios). Only a few attempts at using realistic ambient RF energy levels have been reported, however, the achieved efficiencies at ambient power levels were quite low and hence not applicable in real environmental cases.

Moreover, the problems related to input power variation have not been taken into consideration which can lead to unexpected behaviour in the matching network due to diode

non-linearity. Therefore, the great potential of vast ambient RF energy scavenging capabilities has not yet been fully discovered.

The motivation of this thesis is to develop a highly sensitive and efficient ambient RF energy scavenging technique and system to harvest very low ambient RF energies and overcome some of the limitations reported in the prior state-of-the-art solutions. It is believed that using sensitive rectification devices and harvesting multiple RF signals simultaneously can play a vital role in fulfilling this aim. Ultimately, this research hopes to generate a viable energy source in urban environments, predominately for low powered applications (e.g. home and office devices).

1.3 Objectives and Research Questions

This thesis focuses on realistic RF energy scavenging methods to provide electrical energy in urban environments. The aim is to develop highly sensitive and efficient RF energy scavengers. Hence, this research embarks on several objectives which include the followings:

- Identify scavengeable ambient frequency sources.
- Design highly sensitive rectifier/rectenna to harvest a broad range of very low ambient RF energy.
- Harvest ambient RF energy from multiple sources simultaneously.
- Embed an RF energy harvesting system in an appropriate structure (e.g. roof or wall).
- Analyse the effects of multi-tone excitation on the DC output and sensitivity of the rectifier.

In order to achieve these objectives, several research questions were raised as follows:

1. What are the suitable ambient frequency bands for energy scavenging and their available RF power levels?
2. What kind of rectifier topology could enhance the sensitivity and the output DC power when input RF power is low?
3. Should the energy harvesting system be a broad bandwidth, multi bandwidth or a narrow bandwidth?
4. What is the effect of increasing the bandwidth on the output DC power and sensitivity of the rectenna?
5. How does applying multi-tones simultaneously affect the output DC power of the rectenna?
6. How does applying multiple tones with constant total input power and with different phases and spacing affect the output DC power of the rectifier?
7. What is the practicality of using RF energy harvesting systems in urban environments (e.g. home and office devices)?

1.4 Thesis Overview

This thesis aims to investigate the feasibility of RF energy scavenging in Melbourne, Australia. Based on real environmental cases, different RF energy scavengers have been developed and the practicalities of using them in urban environments have been examined. This research presents a sensitive and efficient RF energy harvesting technique and system that can scavenge a wide range of very low ambient power levels. (Throughout this work, the sensitivity is defined as the minimum power necessary to turn on a rectification circuit.)

Chapter 2 presents a comprehensive review of state-of-the-art solutions proposed by researchers in the scientific literature. This chapter compares various sustainable energy harvesting sources and methods and focuses on their associated advantages and disadvantages. The review looks explicitly at the EM energy harvesting approaches; ambient RF energy scavenging and WPT. The basics of a rectenna system are discussed and various rectifier circuit technologies and topologies are reviewed. This chapter also provides a comprehensive review of several recent designs for both ambient and WPT techniques.

Chapter 3 investigates the feasibility of harvesting ambient EM energy in metropolitan areas of Melbourne, Australia. Several RF field measurement results are collected and averaged to establish a comprehensive database. This chapter determines usable frequency ranges with their associated scavengeable power levels. Furthermore, maximum available power analysis for different frequency bands based on antenna aperture and the number of antennas in a given area is provided to estimate the potential of RF energy harvesting. Finally, this chapter compares different rectenna configurations and recommends an alternative solution for ambient RF energy scavenging based on the RF field measurement and analysis outcomes. Chapter 3 answers research question 1 and investigates research question 2.

Chapter 4 discloses a highly sensitive and efficient multi-resonant rectifier. This chapter is dedicated to harvesting RF energy from two frequency bands simultaneously: 478–496 and 852–869 MHz, which are used for broadcasting and cellular systems. These frequency bands are selected based on the results and conclusions from Chapter 3. In this chapter RF energy scavenging from two bands is proposed to enhance the output DC power and sensitivity by scavenging more signals. To clarify the findings, both laboratory and real environmental measurements are carried out. Chapter 4 addresses research questions 2 and 3.

Chapter 5 presents RF energy scavenging from the FM frequency band (based on the outcomes from Chapter 3). In this chapter the effect of widening the bandwidth on the DC output of the rectifier is examined to harvest more RF signals and deliver more power to the rectification device (based on the outcomes from Chapter 4), hence, enhancing the output DC power and sensitivity. Furthermore, the FM rectenna is embedded into building materials (plaster) to provide a sustainable energy source in urban environments for low powered applications (e.g. home and office devices). In order to verify the findings, laboratory experiments along with real environmental measurements are conducted. A realistic case is also presented to estimate the total amount of DC power that could be harvested from outdoor and indoor RF signals for a typical building. Chapter 5 answers research questions 4, 5 and 7.

Chapter 6 investigates the effect of multi-tone excitation (with constant total input power) on the DC response of the rectifier. The effect of applying multi tones with various factors such as: different frequency spacing, low input power levels and random phase arrangement is investigated. This chapter presents frequency domain and time domain analysis of the FM rectifier (designed in Chapter 5). Measurements are also performed to clarify the findings. Chapter 6 addresses research question 6.

Chapter 7 Concludes this thesis and suggests avenues for future research.

1.5 Original Contributions

A summary of the novel and scientific contributions to the existing body of research in the field of RF energy harvesting is provided as follows.

- **Chapter 3 – The feasibility of harvesting ambient EM energy in metropolitan areas of Melbourne, Australia is investigated [P5].**

  RF field measurements and analysis of maximum available power in different suburbs of Melbourne are conducted, which has not been reported previously. Hence the great potential of vast power scavenging capabilities has not yet been fully discovered in order to generate a viable energy source in urban environment.

  It is demonstrated that broadcasting frequency ranges (FM and TV) and cellular systems are preferred power scavenge sources. These field investigations and analysis enable us to design appropriate ambient RF scavengers based on the real environmental cases.

- **Chapter 4 – A new highly sensitive multi-resonant rectifier is proposed to investigate the feasibility of harvesting ambient EM energy from multiple sources simultaneously [P1].**

  A highly sensitive and efficient multi-resonant rectifier which operates at two frequency bands (490 and 860 MHz) and exhibits favourable impedance matching over a broad input power range (−40 to −10 dBm) is proposed.

  Measurement results indicate an effective efficiency of 54.3%, and an output DC voltage of 772.8 mV is achieved for a multi-tone input power of −10 dBm.

Furthermore, the measured output DC power of harvesting RF energy from multiple services (broadcasting and cellular systems) concurrently exhibits a 3.14 and 7.24 fold increase over single frequency rectification at 490 and 860 MHz respectively. The achieved sensitivity and dynamic range demonstrate the usefulness of this innovative low input power rectification technique. The proposed dual resonant rectifier takes the advantage of harvesting RF energy from multiple sources concurrently to enhance the sensitivity, enabling the harvesting of RF energy in urban environments.

- **Chapter 5 – The feasibility of harvesting ambient EM energy from the FM broadcasting band is examined with a highly sensitive rectenna. An innovative idea is also proposed to embed a rectenna system in to the building materials to harvest ambient RF energy in urban environments [P2], [P4], [P6], [P7].**

  The proposed FM band rectenna achieves a sensitivity of −50 dBm (0.01 μW), which to the best of knowledge is the highest sensitivity reported for an ambient energy harvester.

  Measurement results of the RF scavenger indicate an output DC power of 0.14 nW for a single-tone input power of −50 dBm (0.01 μW). An output DC power of 13.3 nW is also achieved from concurrently rectifying seven tones of −50 dBm. The proposed broadband rectenna (with 22% fractional bandwidth) takes the advantage of delivering multiple signals to the diode, hence harvesting very low density ambient signals.

  Furthermore, the practicality of embedding the RF energy harvesting system in building materials is investigated, creating a new structurally integrated energy scavenging scheme. This enables to provide a sustainable, green, and inexpensive

energy source in urban environments predominately for low power applications (e.g. home and office devices).

- **Chapter 6 – The effect of multi-tone excitation (with constant input power) on DC response of the rectifier is investigated [P3].**

  The output power of the FM rectifier in presence of multi concurrent tones (with constant total input power), is compared to a single-tone case with the same input power. Hence, the effect of applying multiple tones with various factors (e.g. frequency spacing, input power and etc.) is analysed and measured to prove the concept.

  It is demonstrated that, applying multiple tones simultaneously (with constant total input power) results in a lower total average output voltage and power, when compared to a single-tone case with the same input power. It was found that this was mainly due to the change in the signal waveform.

1.6 List of Publications

1.6.1 Peer-Reviewed Journal Articles

[P1] **N. Shariati**, W. S. T. Rowe, J. R. Scott, and K. Ghorbani, "Multi-Service Highly Sensitive Rectifier for Enhanced RF Energy Scavenging," *Nature Scientific Reports,* vol. 5, 05/07/online 2015.

[P2] **N. Shariati**, W. S. T. Rowe, and K. Ghorbani, "Sustainable Energy Solution for Urban Environments: Sensitive Rectenna Embedded in Building Materials for Enhanced RF Energy Scavenging" *IEEE Transactions on Circuits and Systems I*, (under review), 2015.

[P3] **N. Shariati**, W. S. T. Rowe, J. R. Scott, and K. Ghorbani, "Multi-tone Excitation Analysis in RF Energy Harvesting Systems" *IEEE Transactions on Microwave Theory and Technique (drafted)*, 2016.

1.6.2 Australia Provisional Patent

[P4] **N. Shariati**, and K. Ghorbani "Sustainable Energy Solution for Urban Environments: Sensitive and Low Cost Rectenna Embedded in Building Materials for Enhanced Ambient RF Energy Scavenging" *Australia provisional patent, Australian Government, IP Right Number: 2015902180*, filed 10th June 2015.

1.6.3 Peer-Reviewed Conference Proceedings

[P5] **N. Shariati,** W. S. T. Rowe, and K. Ghorbani, "RF Field Investigation and Maximum Available Power Analysis for Enhanced RF Energy Scavenging," *42nd European Microwave Conference (EuMC)*, pp. 329-332, 2012.

[P6] **N. Shariati,** W. S. T. Rowe, and K. Ghorbani, "Highly sensitive rectifier for efficient RF energy harvesting," in *44th European Microwave Conference (EuMC)*, pp. 1190-1193, 2014.

[P7] **N. Shariati,** W. S. T. Rowe, and K. Ghorbani, "Highly Sensitive FM Frequency Scavenger Integrated in Building Materials," *45th European Microwave Conference (EuMC)*, pp. 68-71, 2015.

Chapter 2 – Literature Review

1.7 Introduction

This chapter presents a comprehensive review of the state-of-the-art solutions proposed by researchers in scientific literature. It compares various sustainable energy sources and focuses on an approach to EM (electromagnetic) energy harvesting. The basics of a rectenna (rectifying antenna) system is discussed and will be referred later in this thesis. It reviews several rectifier circuit technologies and topologies which have been widely utilised in EM energy harvesting systems. Finally, this chapter thoroughly reviews two methods of EM energy harvesting: WPT (wireless power transmission) and ambient RF energy scavenging.

1.8 Sustainable Energy Sources

The increasing energy demands of the world's population and the quickly diminishing fossil fuel reserves suggest the urgent need to secure alternative green energy resources.

There are two types of energy harvesting: the first one is called ambient energy harvesting which enables systems to harvest green energy from available sources in the environment. In the second approach, a dedicated/fixed source is employed to provide the required energy for portable devices wirelessly and without any air pollution.

Considering the first approach several methods exist for energy harvesting from inexhaustible sources such as: solar, mechanical (e.g. wind, kinetic, vibration), thermal, biomass, undersea and electromagnetic (EM) waves [1-23]. These sustainable sources of energy are in abundance and can be harvested from the environment. A thorough set of reviews for each source is given in the literature [1, 2, 4-23]. Table 2.1 compares the output power that can be obtained from the environmental sources [1]. As will be discussed, the amount of harvested power depends on the environmental conditions.

Table 2.1 Comparison of Ambient Energy Sources and Harvested Power [1,5]

Energy Source	Available Input Power Density	Output Power	Availability
Ambient Light **Indoor** **Outdoor**	 0.1 mW/cm^2 100 mW/cm^2	 10 $\mu W/cm^2$ 10 mW/cm^2	During day
Thermal Energy **Human** **Industrial**	 20 mW/cm^2 100 mW/cm^2	 30 $\mu W/cm^2$ 1-10 mW/cm^2	Continuous
Vibration/Motion **Human** **Industrial**	 0.5 m/s^2@ 1Hz, 1 m/s^2@ 50Hz 1 m/s^2 @ 1Hz, 10 m/s^2@ 1KHz	 4 $\mu W/cm^2$ 100 $\mu W/cm^2$	Depends on the movement
Ambient RF Energy	0.3 $\mu W/cm^2$	0.1 $\mu W/cm^2$ (Cell phone)	Continuous

Solar energy is considered as the leading alternative energy source with the pertinent challenges of uneven worldwide distribution of usable sunlight as well as periods of no sunshine. Solar energy has a high power density during daytime and is hence a good scavenging source in areas where there is sufficient sunlight [1, 4, 6-8]. However, the lack of strong and consistent sunlight constrains the applications in this method of energy harvesting. Furthermore, in order to capture sufficient amounts of ambient solar energy a large area is needed for solar panels. This is due to the low conversion efficiency of this type of energy harvesting system (10% to 40 %) [5].

Similar to solar, wind power generation has a large number of variables and unpredictability. The quantity of energy generated is subject to change according to environmental circumstances [1, 4, 10, 11].

In piezoelectric converters, vibrations cause the deformation of a piezoelectric capacitor and hence voltage or current can be produced. In comparison to other energy harvesting devices, piezoelectric power generators are quite small and lightweight [5]. However, the output power of piezoelectric generators are highly variable when unstable motions (e.g. human motions) are utilised as a driving force and they can produce power as long as there is a movement. Furthermore, low conversion efficiency of piezoelectric power generators limits the applications of this alternative source [1, 4, 13].

Thermal energy is also predominately employed. Based on the thermoelectric effects (e.g. Seebeck or Thomson effect) [1, 4, 5, 16-20], electrical power can be produced by extracting temperature difference in thermoelectric devices. Thermoelectric generators can produce power as long as there is a temperature difference, however they are large and heavy

compared to other energy scavenging devices. Moreover, in order to produce sufficient output power, a large area is required for thermoelectric devices.

Among these green energy sources, there has been a growing interest for radio frequency (RF) energy harvesting due to the advancements in broadcasting and wireless communication systems [1, 4, 5, 23-26], creating an abundance of ambient microwave energy. Although, ambient RF signals have a relatively low energy density compared to other energy sources and are more suited to low power applications, RF signals can be found everywhere and they radiate energy continuously.

Nowadays, there is a great range of ambient RF sources available to us whether in public, office or at home. Television, radio, mobile phones, cordless phones, Wi-Fi, GPS, Bluetooth, and WiMax are some of the most dominant sources. These ambient microwave energy sources are vastly available and radiate freely propagating RF energy and hence have a great potential as a scavenge source to complement other green energy sources such as solar energy.

Hence, RF energy harvesting has experienced a rapid development in recent years mainly due to the increasing number of RF transmitter sources, creating an abundance of ambient microwave energy. Furthermore, the development of WPT technologies [26-28] that allow micro sensors [29-31], mobile electronic devices [32], wireless implantable neural interfaces[33-35] and far-field passive RFID (Radio-frequency identification) [36-40] systems to operate without batteries has triggered impetus for RF energy harvesting which can provide power continuously.

Figure 2.1 illustrates RF energy harvesting process. Ambient RF signals are collected from various EM sources and then are converted into electrical energy using rectenna. Hence, the

output DC energy can be delivered to various applications such as RFID systems and implantable devices.

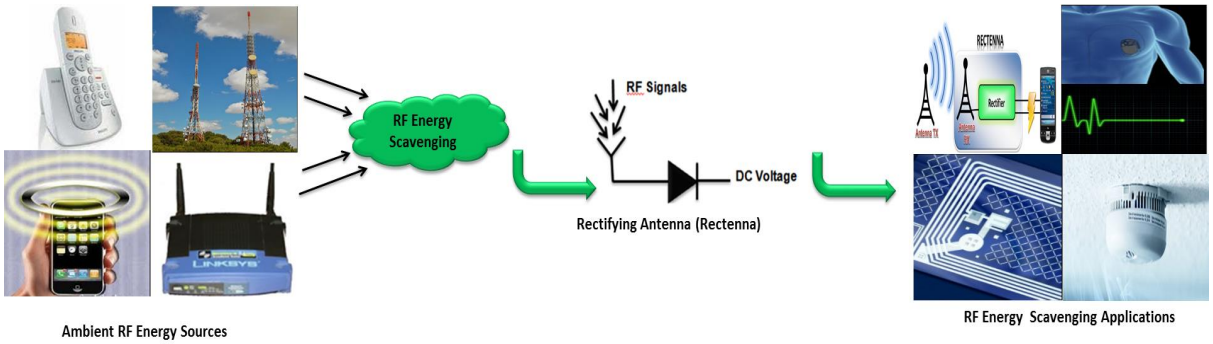

Figure 2.1 RF energy harvesting process.

A prominent advantage of RF scavenging is the ability to convert ambient RF energy into electrical power throughout day and night, both outdoor and indoor. RF propagating wave has the advantage of diffracting from and penetrating inside building materials and hence can be harvested inside the buildings as well.

Furthermore, integrating RF energy harvesting systems with other harvesting technologies (e.g. solar cells, piezoelectric) in a hybrid mode can provide an efficient energy regenerating solution [41-43]. Moreover, RF scavenging systems have a small form factor and can allow for size reduction in the harvesting system, in comparison with other energy sources (e.g. photovoltaic cell, wind turbine), in applications where miniaturisation is essential [34].

Therefore, ambient RF energy scavenging can overcome some of the identified disadvantages in the prior state-of-the-art solutions. A thorough set of reviews is given in in Section 2.4, providing more detail for this energy harvesting technique.

1.9 Electromagnetic Energy Harvesting Systems

Rectification of microwave signals to provide DC power has been the subject of research for almost half a century [26, 44-47]. The word rectenna is a compound of "rectifier" and "antenna". An antenna receives RF signals from the air and the rectifier converts the RF signals into direct current to obtain electrical power. The concept of wireless energy harvesting had been raised by Nikola Tesla and Heinrich Hertz [24, 26, 48-51] and the rectenna concept, to produce DC power was initially patented by W.C. Brown in the 19th century, which demonstrated a novel RF to DC converter [44].

The general block diagram of the energy harvesting system is depicted in Figure 2.2 [31]. As shown, an EM source is responsible for generating and radiating RF/microwave energy into free-space (i.e. atmosphere). A receiving antenna captures the propagated RF energy from the atmosphere and transfers it to the rectifier circuit via an input filter and a matching network. The input filter is responsible for rejecting harmonics generated by the non-linear rectification device, avoiding re-radiation of these harmonics back into free-space. The matching stage ensures the maximum power is transferred from the source to the rectifier. In absence of an impedance matching network, the RF energy captured by the receiving antenna will be reflected back to the source, thus little energy is seen at the rectifier. The rectifying circuit is the core of an energy harvesting circuit which converts the received RF signals to the useful DC power. This circuit includes rectification device (diode/transistor) and capacitor. In a typical rectifier design, various topologies and technologies can be employed to rectify RF power (this will be discussed later). An output DC pass filter (low pass filter (LPF)) is included to provide a clean and levelled DC power by removing AC content and

associated ripple that may form at the output of the rectification stage. The output capacitor of the LPF can also be used as a storage component.

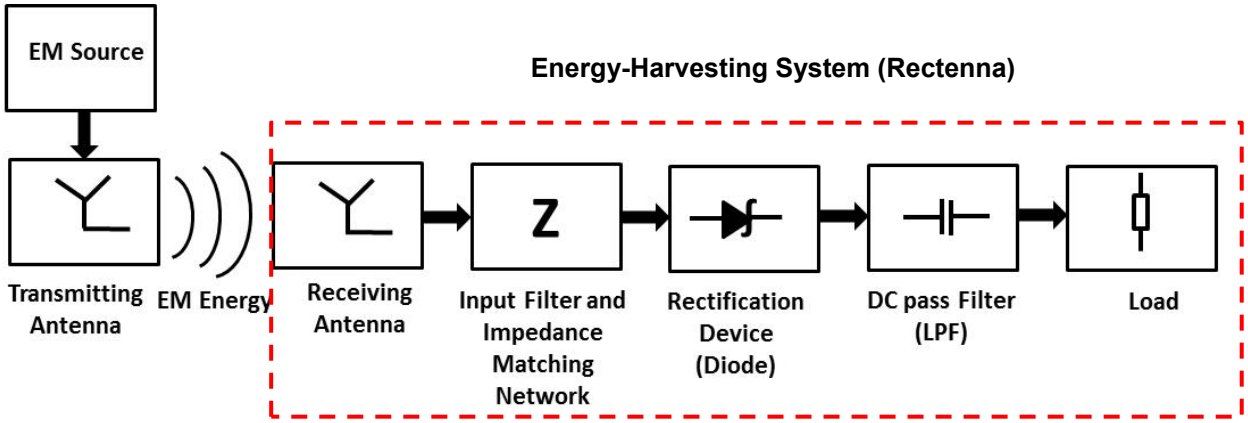

Figure 2.2 General block diagram of the RF energy harvesting system (Rectenna).

1.9.1 Rectifier Circuit Technologies and Topologies

Rectifier plays a vital role in energy-harvesting systems and its related discoveries has been granted around 18 Nobel Prizes, demonstrating its importance in our modern society [3]. Rectifier technologies fall in to two main categories: diode-based and transistor-based. However, transistors are developed based on diode effects. Hence, a diode is the key component of any energy converter and can be found in various harvesting system such as solar, wind, thermal, kinetic, RF and so on [3].

Focusing on RF energy harvesting, Schottky Barrier Detector (SBD) are widely utilised in microwave rectifiers due to several advantages such as: low threshold voltage (high

efficiency), high saturation current (high output), fast rectifying feature ref (short transit time) and low series resistance and junction capacitance [3, 52-54].

While SBD-rectifiers present numerous advantages, there exist some limitations which should be considered in rectifier design [52-54], such as large variation of input impedance with input power and frequency, high reverse leakage current, limited junction temperature (the maximum junction temperature of a Schottky diode rectifier is normally limited to the range of 125°C to 175°C), limited reverse voltage (Schottky diodes have a limited reverse voltage capability with a maximum of around 100 V).

Transistor-based rectifiers also have some advantages and disadvantages. These rectifiers are typically very compact and small, as a result of advances in complementary metal-oxide-semiconductor (CMOS) technology [5]. CMOS technology is widely utilised to design integrated circuits (IC) as well as to reduce the leakage current, providing high conversion efficiency RF harvesting systems. The small form factor and integrated design, low cost and short rise time of the transistor-based rectifiers could make them an optimum solution in application where miniaturisation is essential and cost is important; such as in RFID systems. However, complicated design procedure and large voltage drops across the transistors (especially at low available input powers) need be considered.

As discussed earlier, the rectifier circuit is the core of any energy harvesting system and its sensitivity and efficiency determine the whole system performance. Hence, from a design perspective, various topologies such as voltage doublers or multipliers have been employed in order to increase the RF to DC conversion efficiency and the output DC voltage for specific applications [28, 47, 55-63]. These topologies are transistor-based or diode-based; however, diode-based rectifiers are most frequently used and will be focused on in this thesis [62].

When the amount of output DC voltage of a rectenna is under the required level to turn on an electronic device (e.g. RFID), charge pumps (which are amplitude amplifying circuits) can perform RF-DC rectification and boost the output voltage simultaneously [28, 47, 55-63] . Therefore, cascaded diode-capacitor stages are used to set up the output voltage to the required levels (See Figure 2.3). The idea is to use each stage as a biasing point for the next stage, hence increasing the output voltage.

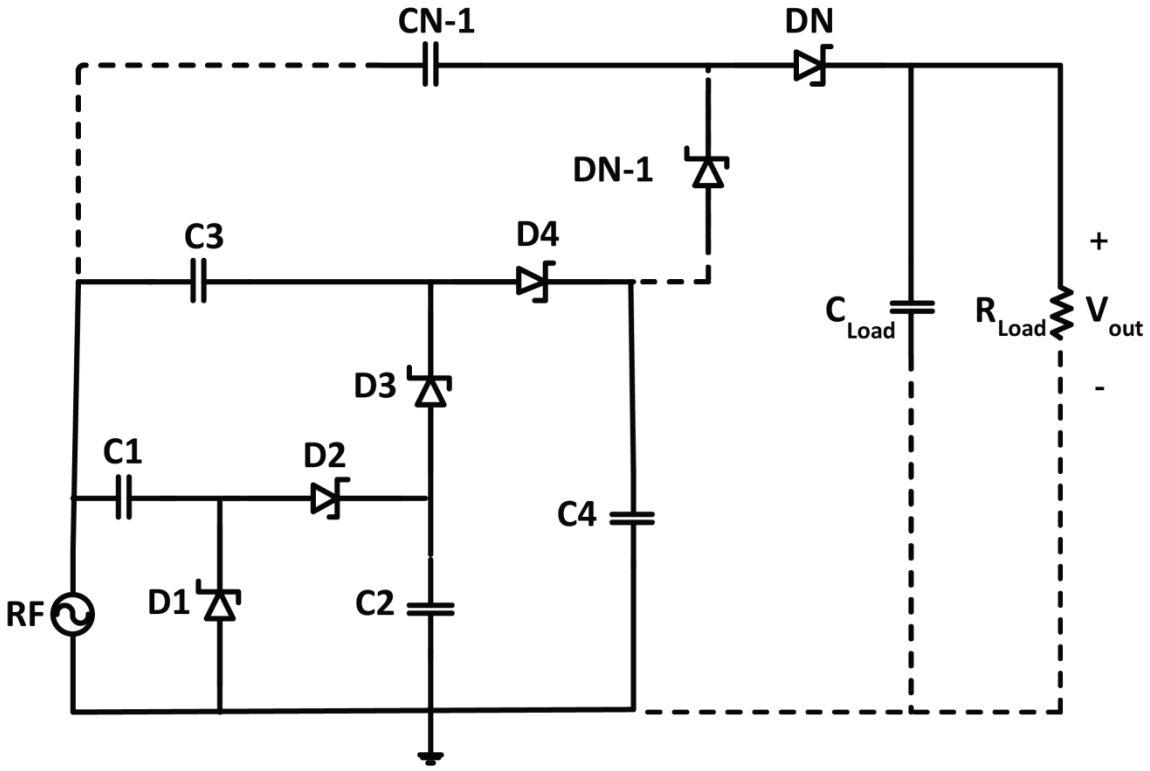

Figure 2.3 Charge pump (amplitude amplifying) structure with cascaded diode-capacitor stages [62].

Although, the higher number of multiplier stages typically results in higher output voltage levels, these numbers should be determined precisely based on the available input power level and to fulfill the design goals for different applications [47]. Due to the power consumption and dissipations of diodes and other components, increasing the number of rectifying devices may result in a lower output DC power and hence degrading the RF-DC

conversion efficiency, specially, at very low input power levels. Therefore, there is a tradeoff between the number of multiplier stages, the amount of achievable output DC voltage and efficiency.

Some of the widely utilised topologies are explained in [62] and it should be noted that traditional structures can be modified to fulfill the design requirements.

1.10 Electromagnetic Energy Harvesting Approaches

There are two methods for EM energy harvesting; ambient energy scavenging from environmental scattered RF signals and WPT using a dedicated RF source [23]. The general block diagram of the RF energy harvesting system was shown in Figure 2.2. The only difference between WPT and ambient energy scavenging is the electromagnetic (EM) source. Electromagnetic (EM) energy source is known in WPT scenario (e.g. a dedicated/fixed transmitter) whilst it is unknown in ambient RF scavenging (e.g. broadcasting and wireless communication systems).

1.10.1 Wireless Power Transmission (WPT)

A process of transmitting energy from an electromagnetic source to a load via air and without any wiring is called WPT (wireless power transmission). The first theoretical basis of WPT was proposed by Maxwell in the 18^{th} century followed by the first WPT experiment which was performed by Nikola Tesla in the 19^{th} century [24, 26, 48-51].

2.4.1.1 WPT Categories

WPT concept can be categorised into two groups: near field and far field [5, 23, 62, 64-66].

In near field WPT systems, resonant or inductive coupling methods are utilised to transmit power wirelessly. This technique is suitable for power transfer systems over short to medium distances. In this scenario, high power can be transmitted efficiently using an electric or electromagnetic field (resonant coupling) or only using a magnetic field (inductive coupling).

In far-field WPT systems, antennas are utilised to capture radiated electromagnetic waves and rectifiers are used to convert RF energy to DC [5, 23, 62, 67]. This technique is suitable for power transfer over short to longer distance (compared to the near field approach due to a different attenuation rate).

In the far-field WPT scenario a dedicated RF source is employed which radiates RF signals at a specific frequency and with a certain power level. Various features of the transmitted signal are controllable and can be programmed based on requirements, such as effectively isotropic radiated power, beam pointing, polarisation of the RF source, etc.

In order to enhance the WPT efficiency, signal design at the transmitting terminal has been proposed to excite the rectification device (e.g. diode) more efficiently [27, 47, 68-70]. To address this, modulated and chaotic waveforms have been offered as a potential solution to increase the rectifier efficiency [47, 71, 72]. It has been proved that a 20% improvement in the rectifier efficiency can be achieved using chaotic waveforms instead of using a single tone signal. This is due to the fact that chaotic waveform with a higher peak-to-average power ratio (PAPR) can overcome the SBD threshold voltage with lower average input RF power levels when comparing to the single-tone signal excitation.

Furthermore, as demonstrated theoretically and experimentally [69, 73], applying multi-sine signal (with constant total input power) to the rectifier circuit results in an increased DC

output over the single-tone signal excitation (with the same input power), due to a higher PAPR. However, power conversion efficiency (PCE) improvement is limited by the rectification device behaviour [47]. Moreover, various parameters should be taken in to consideration such as the signal bandwidth, tones spacing, phase arrangement and so on. It should be noted that these signal design techniques are not applicable to ambient RF energy harvesting where the input waveform is arbitrary.

2.4.1.2 WPT Applications

From an application point of view, various systems and devices can benefit from WPT, including space solar power [6, 74, 75], unmanned helicopters [25], small medical implants [33-35], home and office devices [76] and RFID systems [36].

WPT over several kilometres has been demonstrated, enabling the future feasibility of space solar power (SSP) and solar power satellite (SPS) [74]. For this reason, high wireless power transfer technique was proposed using efficient rectennas. The designed SPS system achieved a collection efficiency of 92%; however, due to the system losses the total power transfer efficiency of around 45% was reported for this system [74]. It should be noted that, due to human health hazards and safety regulations [27, 31, 77, 78], the number of applications at the high power levels are limited.

In 1969, William Brown performed a successful experiment using a microwave beam to supply power for a small helicopter [25]. In this experiment, a 5 kW magnetron operating at 2.45 GHz was used as a microwave power source in order to transfer sufficient power to the helicopter and enable it to fly continuously for ten hours at an altitude of 50 feet.

WPT can also provide energy and wireless data transmission simultaneously for intelligent medical implants which require small amount of power for continuous performance [33-35].

These medical implants play an important role in detecting and providing health status information permanently.

Home and office devices can also benefit from WPT. A proposed rectenna in [76] describes short-range wireless power transmission and reception (See Figure 2.4). A power transmission unit (PTU) generates electromagnetic radiation and transmits it to electronic loads over short ranges. A power receiving unit (PRU) which is connected to the surface of a device receives electromagnetic energy and converts it into electric current. Hence, each device needs to carry one or multiple PRUs, and is therefore not suitable from a design perspective. It is also possible to make the transmitted power available at further distances with the use of relay units at the cost of imposing additional expenses as well as adding complexity to the system. Furthermore, it is challenging to deliver sufficient power to portable devices while ensuring human safety.

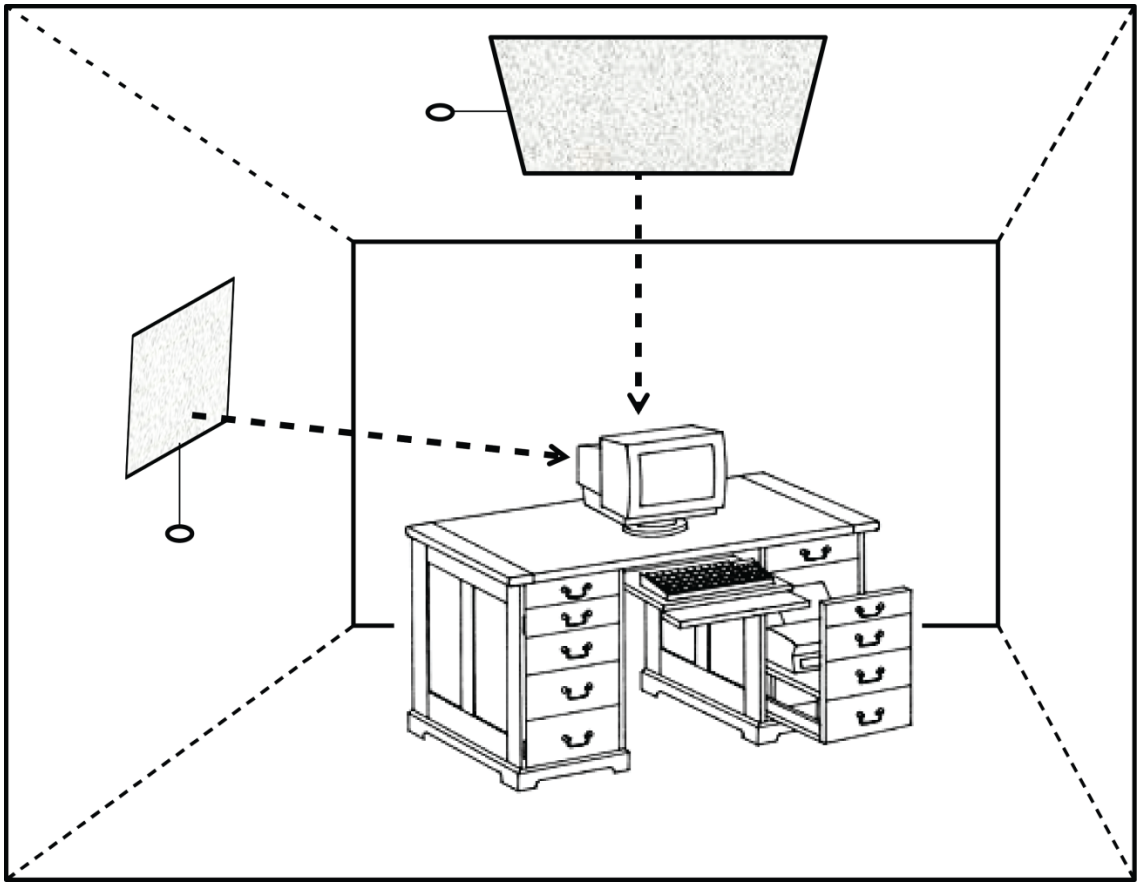

Figure 2.4 Far-field WPT system; short-range WPT and reception for home and office devices [76].

Finally, RFID systems are one of the most dominant applications of WPT technology [36]. These passive systems typically require small amount of power (microwatt level) which can be provided using a WPT design approach.

2.4.1.3 WPT Rectenna Design

From a design perspective, the majority of available literature on WPT have been dedicated to narrow band rectennas (essentially single-frequency, such as some of the previous section rectennas) [25, 33, 62, 74, 76, 79-81], while multi band and broad band structures have not often been used in WPT case [34, 82-84]. Since in WPT, sufficient input power level is available to turn on the rectification device, rectennas are mostly optimised to operate at a single frequency. This results in a higher RF-DC conversion efficiency compared to broadband rectennas [47]. Table 2.2 summarises some of the published rectennas for WPT. As will be presented, in all the below cited literature on WPT, high input powers were employed and hence, high efficiencies were reported.

Single Band WPT Rectennas

A 5.8 GHz rectenna has been designed using a dipole antenna and a silicon Schottky barrier mixer diode as a rectifying device [79]. The rectenna achieved high RF-DC conversion efficiency of 82% with high input power level of 50 mW (17 dBm) and a 327 Ω load resistance.

A circularly polarised rectenna array for WPT has been designed at 5.61 GHz [80]. An RF-DC conversion efficiency of 78% and output voltage of 11 V were reported for the proposed rectenna array with an input power density of 7.6 mW/cm^2 (30 dBm) and a 150 Ω load resistance.

In [81] a 2.4 GHz rectenna was proposed using a microstrip harmonic rejecting circular sector antenna and achieved a maximum conversion efficiency of 77.8% with 10 dBm input RF power and a 150 Ω load resistance.

Dual/Multi Band WPT Rectennas

A dual-frequency rectenna for WPT has been proposed using a uniplanar printed dipole antenna and GaAs Schottky barrier diode [82]. The proposed dual-frequency rectenna achieved a conversion efficiency of 84.4% and 82.7% at 2.45 and 5.8 GHz with a high input power level of 89.84 and 49.09 mW respectively. Furthermore, separate matching networks and filters were used to block the unwanted harmonics at each band which increased the total size and fabrication cost.

Another dual-band rectifier circuit for WPT has been designed operating at 2.45 GHz and 5.8 GHz concurrently [83]. Peak RF-DC conversion efficiencies of 66.8 % and 51.5 % were reported at 2.45 GHz and 5.8 GHz respectively with a high input RF power of 10 mW.

A dual-frequency rectenna for WPT at 2.45 and 5.8 GHz was proposed using two separate rectifier circuits. However, two individual rectifiers increased the circuit size and imposed additional costs to the system [84].

Finally, a rectenna for triple-band biotelemetry communications has been proposed using a triple-band antenna and a single frequency rectifier [34]. The proposed rectenna achieved an efficiency of 86% with 11dBm input power at 433 MHz.

It should be noted that, in a WPT scenario, there is a concern about the long term health effects of the transmitted microwave energy from base stations and wireless communication systems [27, 31, 77, 78]. The World Health Organization (WHO) has published an article which identifies potential health hazards and adverse effects of EM fields on human body

[78]. Furthermore, a relationship between early childhood cancers and mother's exposure to the radiated RF signals from mobile phone base station has been investigated in 2010 which revealed the harmfulness of the radiated microwave energy on our body [77]. Although safety regulations and restrictions are considered in wireless communication systems, it is recommended to keep a distance while charging portable devices wirelessly.

Furthermore, in a WPT case, rectenna systems for each device may be required [76], hence the rectenna attached to the device surface should be small and flat, which is often challenging from a design perspective especially at lower frequencies.

Table 2.2 Wireless Power Transmission Rectennas

Ref.	Publication Year	Measured Efficiency (%)	Input Power	Frequency	Rectification Technique	Rectification Technology	Load Ω
[25]	1969	80 (rectification) 55 (overall)	5KW (Magnetron)	2.45 GHz	Single band	Diode	dc load
[74]	2002	92 (collection) 45 (overall)	2.672 dc	5.8 GHz	Single band	Schottky diode (SPS)	–
[79]	1998	82	17 dBm (50 mW)	5.8 GHz	Single band	Schottky diode	327
[80]	2002	78	30 dBm	5.61 GHz	Single band	Schottky diode	150
[81]	2004	77.8	10 dBm	2.4 GHz	Single band	Schottky diode	150
[82]	2002	84.4 @ 2.45 GHz@ 89.84mW 82.7 @5.8GHz @ 49.09 mW	89.84 mW 49.09 mW	2.45 GHz 5.8 GHz	Dual band	Schottky diode	310
[83]	2013	66.8 @ 2.45 GHz 51.5 @ 5.8 GHz	10 mW	2.45 GHz 5.8 GHz	Dual band	Schottky diode	1050
[34]	2011	86@ 433 MHz	11dBm	433 MHz	Triple band antenna, Single band rectifier	Schottky diode	5000

1.10.2 Ambient RF Energy Scavenging

Instead of using a dedicated RF source, it is convenient, safe, and inexpensive to have a method for scavenging ambient RF signals which are freely available in the atmosphere. These abundant ambient signals are radiated by local electromagnetic (EM) sources such as FM radio stations, TV transmitters, cellular systems, wireless communication systems and many others. The environmental RF energy scavenging provides sufficient power for battery-assisted sensors to operate for a long time [5]. Moreover, a larger amount of total available energy can be scavenged by increasing the antenna gain and other techniques which will be discussed in this section.

In an ambient RF energy scavenging approach, as environmental power levels are lower than those that can be generated by a fixed RF source (WPT scenario), the efficiency, and sensitivity of the harvesting system are of paramount importance. Furthermore, the scavengeable power level is generally unknown (different to WPT scenario), incoherent and effected by environmental /free-space conditions such as the distance from the power source to a rectenna, propagation losses (free-path and attenuation), and the antenna orientation (polarisation). Hence, input power variation needs to be considered when designing a rectification network.

2.4.2.1 Ambient RF Energy Scavenging Applications and Rectenna Design

Various single band, multi band, and broad band rectenna configurations are deployed to enhance the PCE (power conversion efficiency) and sensitivity [40, 41, 56, 58, 85-107]. However, only a few attempts at using realistic ambient RF energy levels have been reported [41, 88, 94, 98, 100]. Table 2.3 summarises some of the published ambient RF energy harvesters.

Single Band Ambient Rectennas

Conventional ambient RF harvesting methods are focused on extracting power from a narrow spectral band. This is not an optimum solution in a real environmental case as typically RF sources are unknown, may shift, or are positioned in different locations. This would require constant re-tuning of the rectenna [56, 107].

A narrowband rectenna was presented to harvest ambient cellular signals at 1.96 GHz [85]. The proposed rectenna also included a smart power management system and maximum power point tracking (MPPT) unit to capture around seven times more energy in comparison to using a direct battery connection. An efficiency of 60% was achieved with input power levels over 30 μW (~ −15dBm) at a location 50 m away from the RF source. However, for lower power levels of 10 μW (−20 dBm), 10% efficiency was reported.

Another single band rectenna has been designed to harvest ambient digital TV signals at 540 MHz [86]. The sensing rate was improved by considering the storage capacitor leakage and using an adaptive duty cycle control scheme. Hence, an efficiency of 30% was reported for −10 dBm input power for a 50 KΩ load. Highest sensitivity of −20 dBm was also reported with very low efficiency of ~5%. However, more sensitive RF harvesters are required for more realistic ambient scavenging cases.

A compact single band RF energy harvester was designed and optimised to capture ambient medium wave signals at 909 kHz, taking the advantage of high transmit power and desirable signal propagation in contrast with higher frequencies [87]. It has been shown that a DC power of ~0.24 mW was delivered to a 1KΩ load at a distance of up to 20 km from a 150 kW transmitter, powering a wireless sensor. However, the sensitivity of the energy harvesting system was not identified.

A medium wave relatively sensitive single band rectenna was proposed operating at 1.27 MHz [88] and it was demonstrated that the scavenger can operate 10 km away from a

50 kW AM broadcasting station. However, the reflection properties of the antenna and rectifier were not provided to clarify their findings and the efficiency was almost zero at low input power (<2 μW [−27 dBm]).

Single band rectennas that operate in the UHF band are an efficient and cost-effective solution to power passive RFID systems. These passive systems typically require small amounts of power (microwatts) which can be efficiently and continuously captured from the reader. Extensive research has been conducted to enhance the RFID system performance [40, 89, 90]. Based on the published works, complementary metal-oxide-semiconductor (CMOS) technology has been widely utilised to harvest RF power for RFID applications, having the advantage of a compact design. However, it is very challenging to optimise CMOS-based rectifiers at different input powers and frequency bands [5].

In recent years, fully integrated CMOS technology rectifiers for passive RFID systems have been proposed, operating at 900 MHz [89]. An RF-DC conversion efficiency of 13% was achieved with −14.7 dBm received RF energy. Another fully integrated long-range RFID tag chip was fabricated in 0.35-μm CMOS using titanium–silicon Schottky diodes [90]. A sensitivity of −14.8 dBm and an efficiency of 36.2 % at 900 MHz were reported for this system. Furthermore, an RF harvesting system using compact planar antennas, coupled resonator impedance matching network, and MOS rectifier was presented for RFID applications [40]. This system achieved a power-up threshold of 6 μW (at 1 μW load) and 8.5 μW (at 2 μW load) at 950 MHz which results in extending the operating range of passive RFID systems.

Tunable impedance matching networks have been demonstrated in order to collect RF signals from various sources and convert them to DC power [91, 92]. In [91], the modified Greinacher's rectifier and static switches were utilised to provide a tuneable input response for channel selection in the Digital TV (DTV) band. This rectifier was designed to switch

between low band (470-505 MHz) and medium band (520-560 MHz). The proposed sensor power supply achieved an efficiency of 50% with an input power of −5 dBm. However from an application point of view, this is still single frequency rectification and it is not widely applicable to environmental RF energy scavenging where the available power is very low and variable.

Multi/Dual Band Ambient Rectennas

Efficient ambient RF energy harvesting is a very challenging issue, as it deals with the very low RF power levels available in the environment. From an ambient RF scavenging perspective, harvesting energy from various available frequencies could maximise power collection and hence increase the output DC power. To address this, dual-band or multi-band configurations have been proposed. This can maximise the PCE (power conversion efficiency) at the specific frequencies where the maximum ambient signal level is available. Various multi/dual band RF energy harvesting systems have been demonstrated, however in most cases a large signal analysis of the rectifier was not provided over a broad input power range.

A dual-band RF energy harvesting system using frequency limited dual-band impedance matching have been proposed and the PCE was shown over a high power range (up to 160 mW) [93]. However based on the reflection coefficient plot, it was only matched at a single input power level (10 dBm). Furthermore, a measured conversion efficiency of 73.76% (at 881 MHz) and 69.05% (at 2.4 GHz) with an individual input high power of 22 dBm was reported. When two tones with an overall power level of 22 dBm were applied to the RF harvester, a slightly better efficiency was achieved (77.13%) [93].

A CMOS dual-narrowband energy harvester circuit was modelled at typical environmental power levels [94]. However, the rectifier efficiency was demonstrated with only single input

power levels of −19 dBm and −19.3 dBm at 2 GHz and 900 MHz respectively, and a large signal analysis was not provided [94].

A compact dual-band rectenna operating at 915 MHz and 2.45 GHz with −9dBm and −15 dBm input power respectively, has been demonstrated [95]. The conversion efficiency of 37% and 20% was reported for 915 MHz (at −9dBm) and 2.45 GHz (at −15 dBm) band respectively. The efficiency is less than 1% for input power levels of below −33 dBm due to the diode behaviour [95]. However, the efficiency results with dual-tone excitation simultaneously and single-tone excitations (at 915 MHz) are very similar, hence the impact of applying a dual-band technique does not demonstrate a clear advantage over a single band. Furthermore, the reflection coefficient was evaluated at a single incident power level.

A conformal hybrid solar and electromagnetic (EM) energy harvesting rectenna has been presented which is capable of harvesting solar and RF power simultaneously [41]. Focusing on RF harvesting in this paper, two dual-band rectifiers were designed and optimised to harvest RF signals; one at 850 MHz and 900 MHz bands and the other one at 850 MHz and 2.45 GHz. RF-DC conversion efficiency of ~ 15% was reported for the first case, while the second rectifier achieved efficiencies between 10% to 12% with −20 dBm input power. The PCE was provided with −30 to 5 dBm input power range, achieving a maximum efficiency up to 40% at 1.85 GHz for higher input power levels (above −5 dBm) [41]. However, at lower power levels the PCE was quite low (less than 10%). Moreover, the dual band rectifier was not evaluated with two simultaneous signals to clarify the advantage of using dual band rectifier over a single band one and also the reflection coefficient was not provided over low input power range [41].

A multi-resonant rectenna that uses a multi-layer antenna and rectifier has been evaluated for a received RF power level ranging from −16 dBm to +8 dBm. However, the rectifier circuit layout and large signal analysis were not provided to clarify the findings [96].

A triple band rectenna presented RF-DC efficiency over the input power range of −14 to +20 dBm, using a triple-band antenna and a four-stage rectifier circuit [58]. However, the reflection coefficient results were only evaluated at a single input power level. The maximum efficiency of 80% was reported with high input RF power of 10 dBm at 940MHz. Moreover, with input powers of 8 dBm and 16 dBm, efficiencies of 47% (at 1.95 GHz) and 43% (at 2.44 GHz) were achieved respectively. This rectenna was shown to generate 7.06 μW of DC power from three sources simultaneously at a high input power level of +10 dBm. Hence, the proposed rectenna with a low-gain antenna and large number of rectifier stages is appropriate for high power energy harvesting [58].

A tetra-band rectenna is designed using genetic algorithm to harvest RF energy from available GSM 900, GSM 1800, UMTS, and WiFi sources in ambient [97]. However, the achieved sensitivity was not clarified and the overall system power conversion efficiency was evaluated for only two operating frequencies by applying a single RF source at a time. Hence, the impact of using a tetra-band technique does not demonstrate a clear advantage over a single band with respect to sensitivity and efficiency improvement.

Another multiband rectenna was demonstrated for urban and semi-urban environments, utilising four individual rectennas and a DC combining method to cover four frequency bands within the ultrahigh frequency range (0.3–3 GHz) [98]. However, a large signal analysis was not provided over a broad input power range. The low efficiency in the GSM (1.8 GHz) band was associated with the narrowband input impedance matching of the rectifier circuit. A minimum sensitivity of −25 dBm was reported for this rectenna [98], whilst in a real environment more sensitive systems are required as the available RF power levels are very low. Furthermore, utilising separate circuits to cover four bands increases the system size and also imposes additional fabrication cost.

Broad Band Ambient Rectennas

From an ambient RF harvesting viewpoint, harvesting energy over a wide frequency band could increase the output DC power by scavenging more RF signals. To address this, Ultra-wideband and broadband rectenna arrays have been proposed as a potential solution. However in some cases, simulation and experimental results were not provided to demonstrate the findings [99].

A broadband rectenna consisting of a dual-circularly polarised spiral rectenna array operating over a frequency range of 2-18 GHz was demonstrated in [100]. The rectified DC power was characterised as a function of DC load, RF frequency and polarisation for power densities between 10^{-5} and 10^{-1} mW/cm^2. However, the proposed rectenna was matched at a single input RF power level for a specified load resistance. Furthermore, due to the low Q value of the rectifier circuit, the conversion efficiency was a fraction of 1% at an input power level of −15.5 dBm.

A broadband arbitrarily-polarised rectenna array using self-similar right-hand and left-hand polarised spirals, operating over a broad range of 6-15 GHz was presented in [101]. A conversion efficiency ranging from 5 to 45% was reported with input power densities of 1-1.6 mW/cm^2 for two arrays consisting of different diodes. However, the sensitivity and large signal analysis were not provided.

Broadband rectenna arrays were proposed to collect randomly polarised RF signals from 4.5 to 8 GHz and 8.5 to 15 GHz [102]. It was shown by increasing the input power, higher efficiencies can be achieved. However, once again sensitivity was not clarified.

A compact broadband rectenna was reported operating within 2-2.7 GHz [103]. Measured RF-DC efficiency over the input power range of −3 to +13 dBm was provided with a maximum conversion efficiency of 72.5% at a high input power of 13 dBm [87].

A small size wideband rectenna for energy harvesting in the UHF band (0.7-1 GHz) was presented [104]. Output voltage versus frequency with 5 dBm input power at different distances was measured in an indoor environment. However, PCE was not provided over a broad low input power range to evaluate the system performance in realistic environmental cases.

Another wideband rectenna utilising a cross dipole antenna was designed operating from 1.7 to 3 GHz [105]. A maximum efficiency of 75% with high input power of 7.667 mW/cm^2 was reported, however, this rectenna is not efficient at ambient power levels which are much lower than the applied incident power.

A broadband microwave rectifier was proposed for ambient RF harvesting [106]. The rectifier was evaluated over a frequency range of 0.7-1.5 GHz with a constant high input power of 25 mW (14 dBm) from a signal generator which does not happen often in real environmental cases (probably very close to the base stations). A maximum measured efficiency of 81% at 1.04 GHz with 25 mW input power was reported and once again a large signal analysis was not presented.

A conformal hybrid solar and EM energy harvester was designed using a broadband printed monopole antenna to operate over 800 MHz-2.5 GHz [41]. However, due to the low quality factor of the matching network which is an adverse effect of a broadband structure, low conversion efficiencies between 4% to 8% was achieved with an input power of −20 dBm [47].

Although broadband rectennas can capture energy across a large section of the available spectrum, this typically results in very low efficiency at any particular source frequency as the quality factor of rectifier circuit is inversely proportional to its bandwidth (Bode-Fano limits [108]). Furthermore, from a design point of view, while it is relatively easy to achieve

a broadband antenna, it is very challenging to realise a broadband rectenna due to the non-linearity of the rectifier impedance with input power across a large frequency band.

Various patents have been also filed which focus on ambient RF harvesting, however the input power range far exceeds those found within a real environment. Recently, an apparatus for ambient microwave energy harvesting was invented in a US patent [109]. However, the microwave signals harvested were from close mobile base stations, broadcast repeaters and high-power wireless facilities and communication equipment. In all these circumstances a device has high amount of power as it is in close proximity to a high power transmitter. In a real ambient energy harvesting scenario, such a system is not feasible. Hence, the published method is not widely applicable for most realistic environmental cases where low RF power levels are present [1, 4, 5].

Despite all the achievements in rectenna designs, most of the published works are dedicated to maximising the system efficiency at a given and often quite high input power level (e.g. WPT scenarios). The effect of input power variation has not been widely considered which can cause unexpected variations in the matching network due to non-linearity characteristics of the diode. A sensitivity below −40 dBm has not been reported previously. This is however in the range of typical ambient free-space RF signals [1, 4, 5]. Furthermore, the achieved efficiencies of ambient rectennas at low input power levels (<−20 dBm) are seen to be quite low and hence are again not applicable in real environmental cases.

Hence, the aim of this thesis is to address some of the identified defects in the prior state-of-the-art solutions by designing highly sensitive and efficient RF energy scavenging circuits which operate over a broad input power range at a low level signal.

Table 2.3 Ambient RF Scavengers

Ref. Year	Sensitivity	Measured Efficiency (%)	RF Power Variation (in PCE evaluation)	Frequency	Rectification Technique	Rectification Technology	Load
[107] 2012	−30 dBm	83@ 1.95 μW/cm^2 50 @ 0.22 μW/cm^2	−30 to 15 dBm	2.45 GHz	Single band	Schottky diode	Resistor 1.4 KΩ
[56] 2013	−10 dBm	44@−10 dBm	—	830 MHz	Single band	Schottky diode	Resistor
[85] 2010	−20 dBm	60@ 30 μW 10@ 10μW	10 μW to 1 mW	1.96 GHz	Single band, 20-element rectenna array	Schottky diode	Battery
[86] 2013	−20 dBm	30 @−10 dBm 5 @ −20 dBm	−20 to −5 dBm	540 MHz	Single band	Schottky diode	Resistor 50 KΩ
[87] 2014	—	~ 50	—	909 KHz	Single band	—	Resistor 1 KΩ
[88] 2014	≈−27dBm*	0 @ <2 μW 28 @ 23 μW	2.5 to 23 μW	1.27 MHz	Single band Autotransforer	Diode	Capacitor
[91] 2011	−25 dBm	50@ −5 dBm	−25 to 0 dBm	470-505 MHz OR 520-560 MHz	Tunable	Diode	Resistor 8.2 KΩ
[93] 2013	—	77.13@22 dBm (158.49mW)	0 to 160 mW	881 MHz 2.4 GHz	Dual band	Schottky diode	Resistor 0.433 KΩ
[94] 2013	−19.3 dBm	9.1@−19.3dBm @900MHz 8.9@−19dBm @2GHz	−19.3dBm −19 dBm	870-940 MHz 1920-2030 MHz	Dual band	CMOS	Resistor 1.5 MΩ
[95] 2013	≈−33dBm*	37@−9dBm @915MHz 20@−15 dBm @2.45GHz <1@≈ −33 dBm	−40 to 0 dBm	915 MHz 2.45 GHz	Dual band	Schottky diode	Resistor 2.2 KΩ

Ref. Year	Sensitivity	Measured Efficiency (%)	RF power variation (in PCE evaluation)	Frequency	Rectification Technique	Rectification Technology	Load
[41] 2013	−30 dBm	15 @ −20 dBm ~2.5 @ −30 dBm	−30 to 5 dBm	850 MHz 900 MHz	Dual band	Schottky diode	Resistor 2.2 KΩ
[58] 2013	≈−14dBm	80@10 dBm @940MHz 47@8 dBm @1.95GHz 43@16 dBm @2.44GHz	−14 to 20 dBm	940MHz 1.95GHz 2.44GHz	Triple band	Schottky diode	Resistor 12 KΩ
[98] 2013	−25 dBm	40 (overall)	–	560 MHz 900 MHz 1.8 GHz 2.1 GHz	Tetra band	Schottky diode	Capacitor
[97] 2013	–	~ 45 @ 0.8 mW @900 MHz ~18 @0.15 mW @ 2.45 GHz	0 to 0.8 mW	900 MHz 1.75 GHz 2.15 GHz 2.45 GHz	Tetra band	Schottky diode	Resistor 50Ω
[100] 2004	10^{-5}mW/cm^2	0.1@5×10^{-5}mw/cm^2 20 @ 0.07 mW/cm^2	10^{-5} to 10^{-1} mW/cm^2	2-18 GHz	Broad band 64-element rectenna array	Schottky diode	Resistor
[101] 2001	–	5 to 45 @ 1to1.6 mW/cm^2	1 to1.6 mW/cm^2	6-15 GHz	Broad band 2 rectenna arrays	Schottky diode	Resistor 1Ω-10K Ω
[102] 2000	–	35@7.78mW/cm^2@ 5.7 GHz 45@1.56mW/cm2@ 10.7 GHz	–	4.5 - 8GHz 8.5- 1GHz	Broad band 2 rectenna arrays	Schottky diode	Resistor
[103] 2015	−3 dBm	72.5@ 13 dBm @2.45 GHz ~14 @ −3 dBm @2.45 GHz	−3 to +13 dBm	2-2.7 GHz	Broad band	Schottky diode	Resistor 900 Ω

Ref. Year	Sensitivity	Measured Efficiency (%)	RF power variation (in PCE evaluation)	Frequency	Rectification Technique	Rectification Technology	Load
[105] 2013	~0.7 mW/cm^2	75@ 7.667 mW/cm^2	~0.7 to 9.7 mW/cm^2	1.7- 3 GHz	Broad band	Schottky diode	Resistor
[106] 2014	14 dBm	81@25 mW @1.04 GHz	–	0.7-1.5 GHz	Broad band	Schottky diode	Resistor 510 Ω
[41] 2013	−20 dBm	4 to 8 @ −20 dBm	–	800MHz to 2.5 GHz	Broad band	Schottky diode	Resistor

Chapter 3 – RF Field Investigation and Maximum Available Power Analysis

2.1 Introduction

RF energy harvesting is attracting widespread interest to meet the goal of providing a sustainable energy source for the future growth and protection of the environment. As discussed in Chapter 2, while the power produced by electromagnetic (EM) energy harvesting has a low density [1,4, 5], there is a great range of ambient RF sources available to us whether in public, office or at home. Television, Radio, Mobile Phones and Wi-Fi are some of the most dominant sources. They all radiate RF energy and are widely available and hence are a potential scavenging source. However, there are various challenges in scavenging ambient RF energy, which will be discussed in this chapter.

In an ambient RF scavenging scenario as the EM source is unknown, field measurements should be conducted to investigate various suitable frequency bands with their associated signal strength. Hence, ambient rectennas can be efficiently designed based on realistic environmental RF signals.

A comprehensive literature review on previous RF field analyses for energy harvesting is conducted. In recent years, researchers have demonstrated that a single GSM telephone can

deliver enough energy for wirelessly powering small applications over a short distance of 20 cm [110]. In [111], broadcasting has been shown to be a reliable energy source for scavenging in comparison to wireless communication systems. More recently, in order to investigate the potential for ambient RF energy scavenging, an RF spectral survey from 0.3-3 GHz was conducted in urban and semi-urban areas of London. It was demonstrated that, digital DTV, GSM900, GSM1800, 3G and Wi-Fi are appropriate ambient RF energy scavenging sources [98].

In this chapter, in order to demonstrate the feasibility of RF energy harvesting, RF field investigations and analysis of maximum available power in the metropolitan areas of Melbourne, Australia are conducted, which have not been reported previously. Hence the great potential of vast power scavenging capabilities has not yet been fully discovered in order to generate a viable energy source for urban environments.

Therefore, measurements have been performed to determine the usable frequency ranges and to analyse maximum available power for different frequency bands based on antenna aperture and number of antennas in a given collecting area, estimating the potential of RF power harvesting. Furthermore, this chapter compares different rectenna configurations and recommends an alternative solution for ambient RF energy scavenging based on the RF measurement and analysis outcomes in Melbourne, Australia.

2.2 RF Field Measurement

In order to demonstrate the feasibility of RF energy harvesting, the suitable frequencies among several frequency bands are investigated. The map in Figure 3.1 depicts some of these investigations in different suburbs of the Melbourne metropolitan areas where precise measurements were performed (e.g. inner city, outer city, industrial areas, at RMIT University, etc.) at various times (e.g. peak and off-peak hours for telecommunication services) [112].

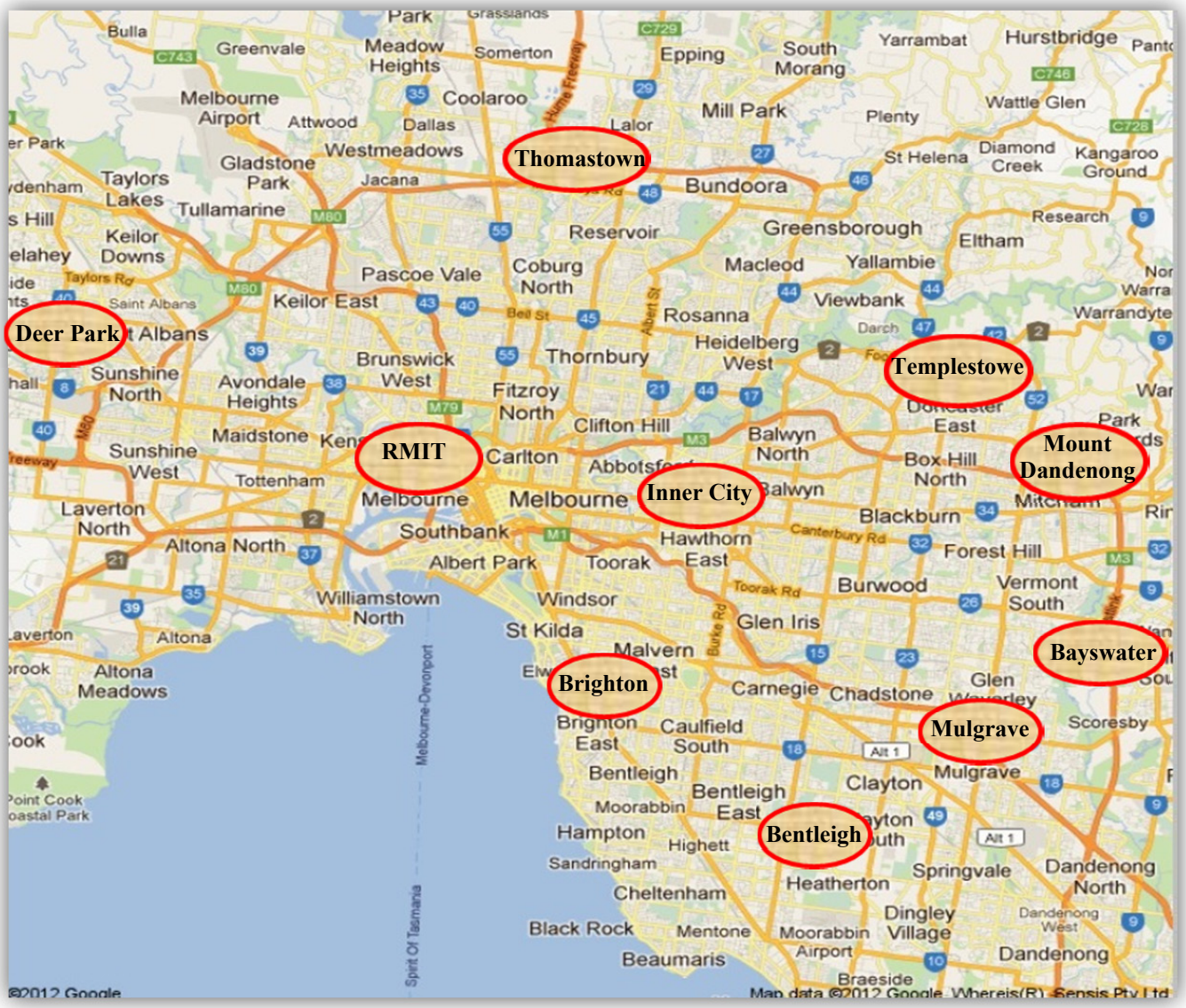

Figure 3.1 RF Field exploration locations, RMIT University, Inner city, Mount Dandenong, Templestowe, Bayswater, Mulgrave, Bentleigh, Thomastown, Deer Park, Brighton.

RF field measurements were conducted in two orthogonal polarisations (both horizontal and vertical polarisations), utilising omnidirectional monopole and discone antennas and a spectrum analyser.

The absolute value of the electric field intensity ($|E|$) in volts per meter is expressed in terms of power received using eqn. 3.1 [113].

$$P_r = \frac{E^2}{480\pi^2}\frac{C^2}{f^2}G \qquad (3.1)$$

Here, P_r represents the received power (watts), f denotes the frequency (Hz), C is speed of light (~3×10^8 m/s) and G refers to the realized gain of the antenna (dBi).

The gain of the antennas were measured in free-space over the frequency range of 50 MHz to 3 GHz and depicted in Fig 3.2 (a, b). An active diamond D707 monopole antenna was used to measure RF signals from 50 to 800 MHz, while 0.8 to 3 GHz signals were measured using a discone antenna. It should be noted that, both antennas were matched at 50 Ω for the selected frequency ranges.

Several RF field measurement results were collected and averaged to establish a comprehensive database. Figure 3.3 summarises the RF field measurement results for frequencies from 50 MHz to 3 GHz at various locations. Based on the Australian Radiofrequency Spectrum Plan [114], the investigated frequency bands are allocated to various applications such as broadcasting services and cellular systems (See Table 3.1).

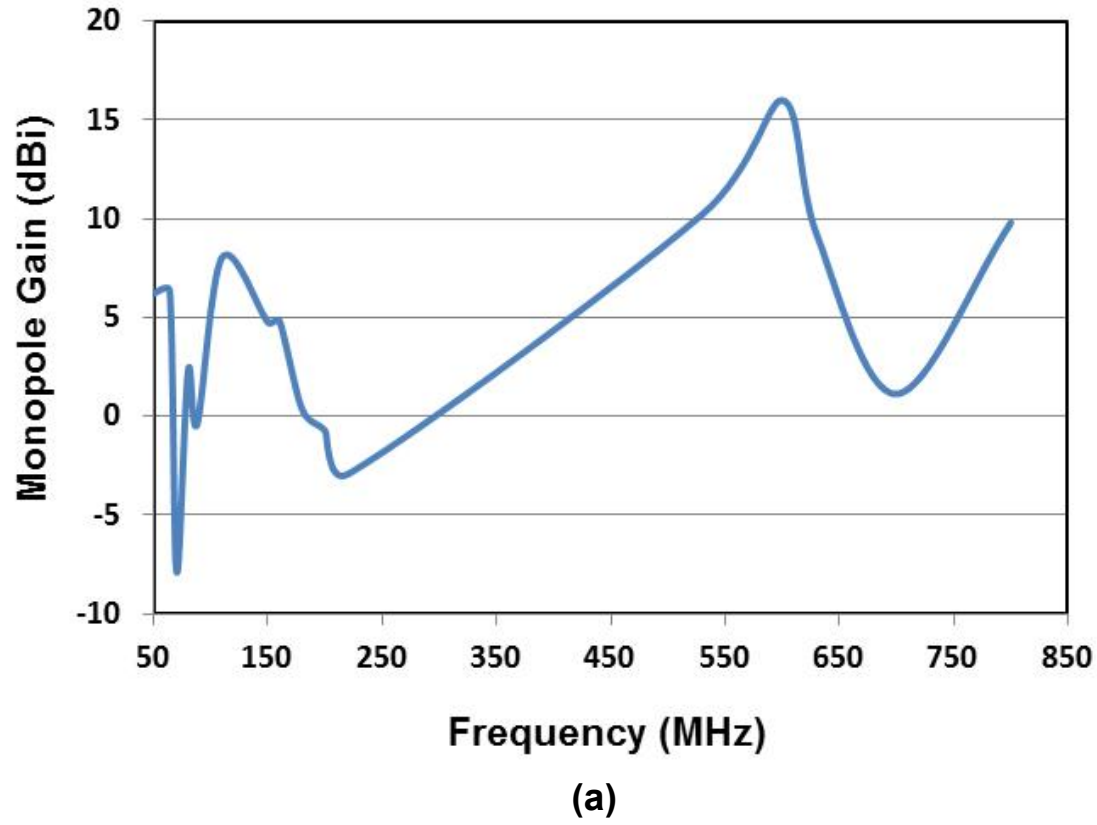

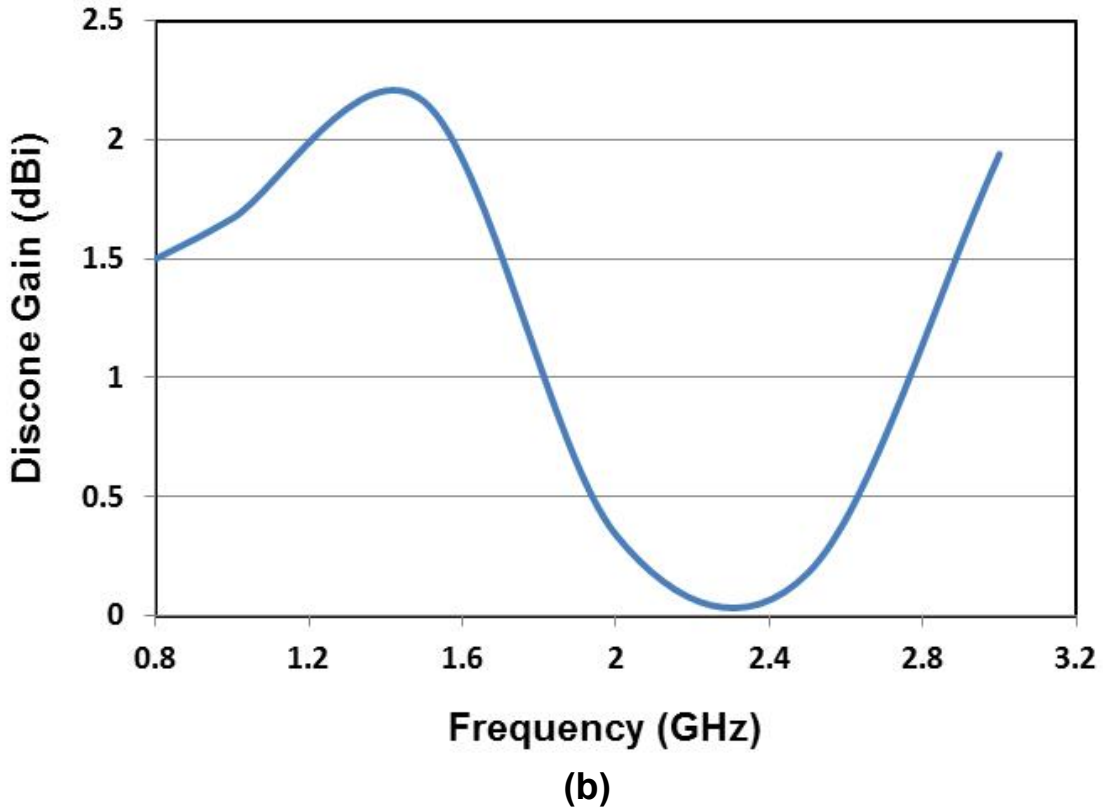

Figure 3.2 Antenna gain measurement from 50 MHz to 3 GHz. (a) Monopole antenna gain. (b) Discone antenna gain.

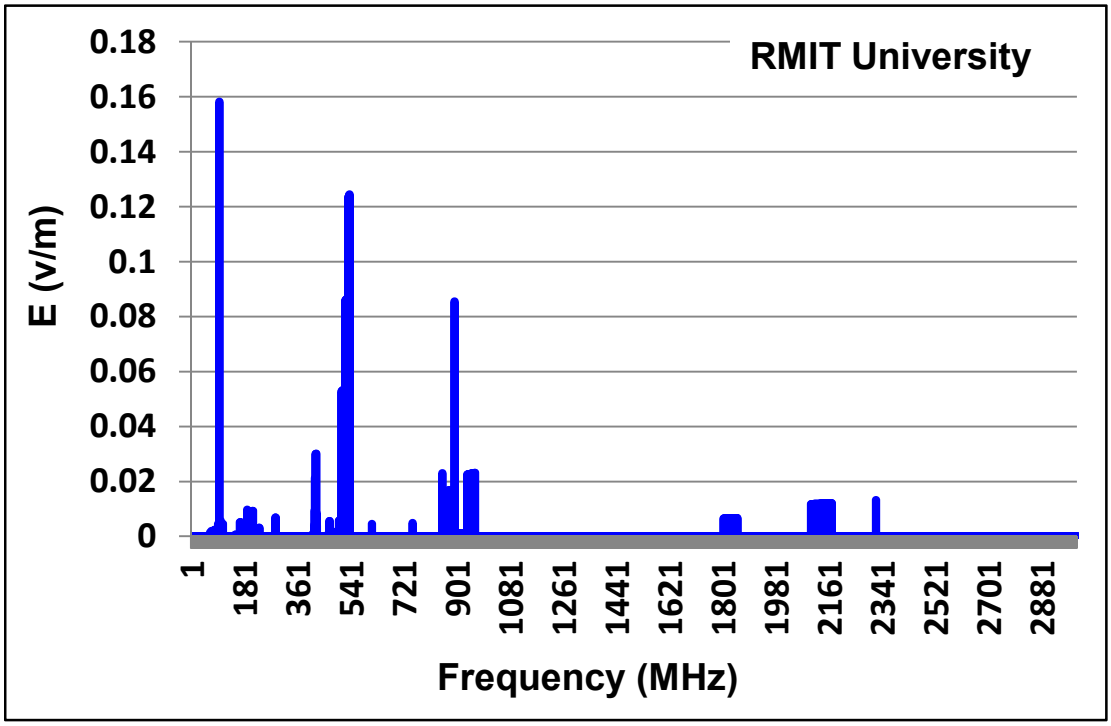
RMIT University
E (v/m)
0.18
0.16
0.14
0.12
0.1
0.08
0.06
0.04
0.02
0
1
181
361
541
721
901
1081
1261
1441
1621
1801
1981
2161
2341
2521
2701
2881
Frequency (MHz)

(a)

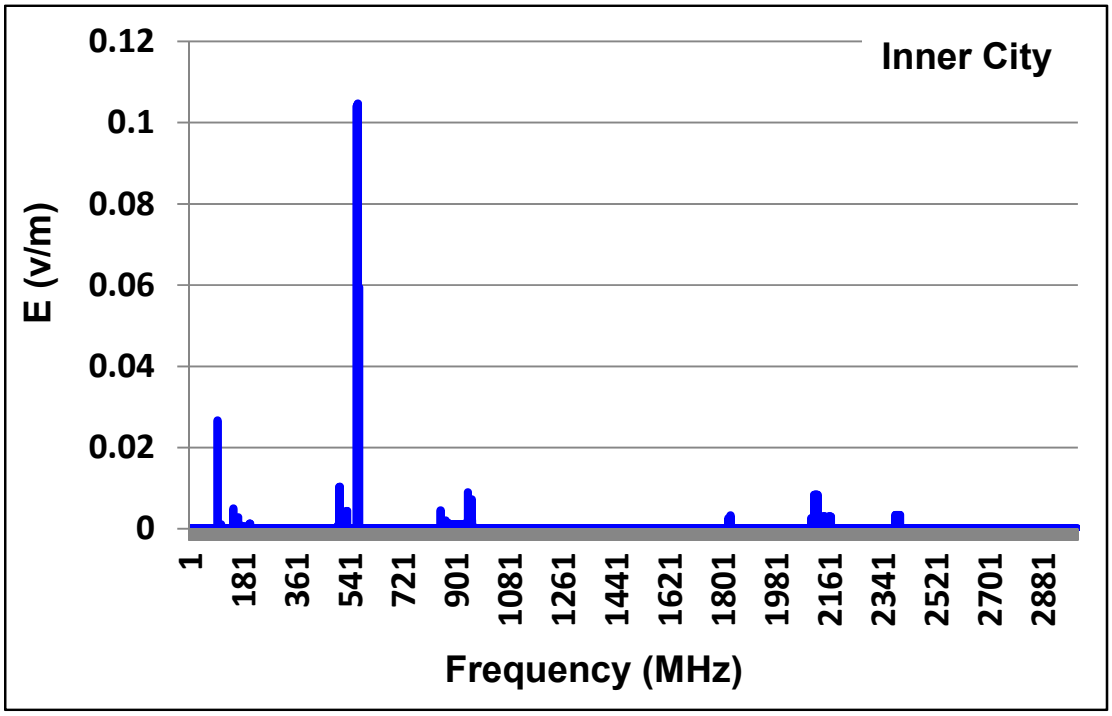
Inner City
E (v/m)
0.12
0.1
0.08
0.06
0.04
0.02
0
1
181
361
541
721
901
1081
1261
1441
1621
1801
1981
2161
2341
2521
2701
2881
Frequency (MHz)

(b)

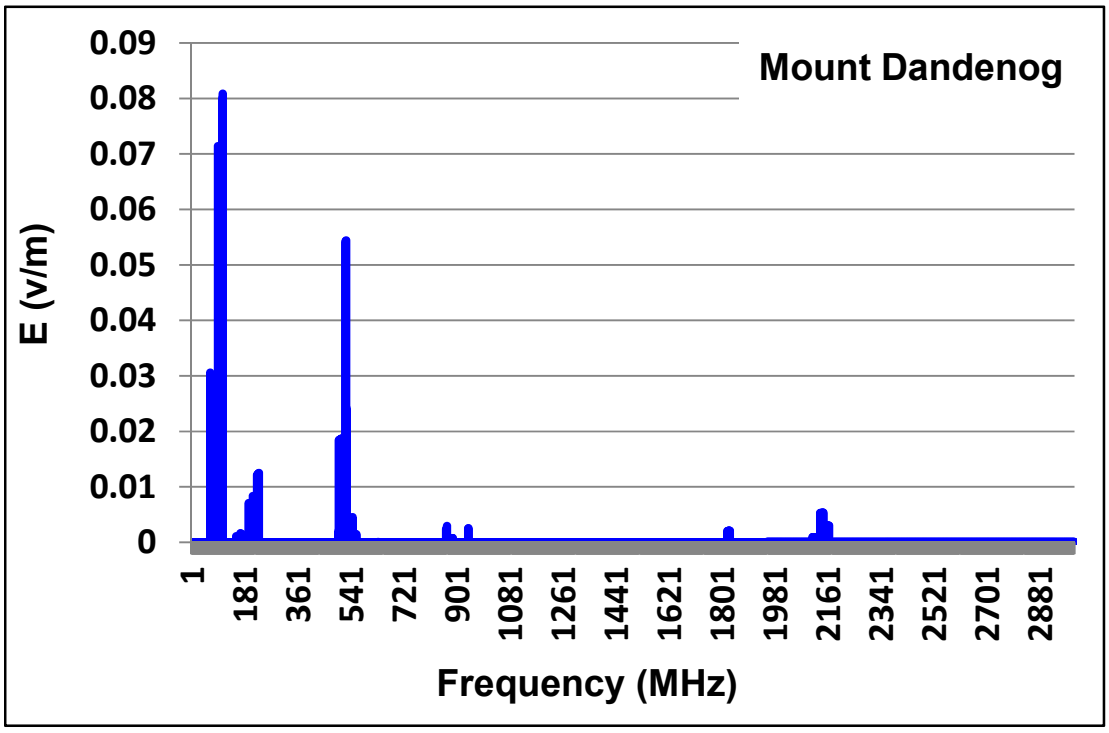
Mount Dandenog
E (v/m)
0.09
0.08
0.07
0.06
0.05
0.04
0.03
0.02
0.01
0
1
181
361
541
721
901
1081
1261
1441
1621
1801
1981
2161
2341
2521
2701
2881
Frequency (MHz)

(c)

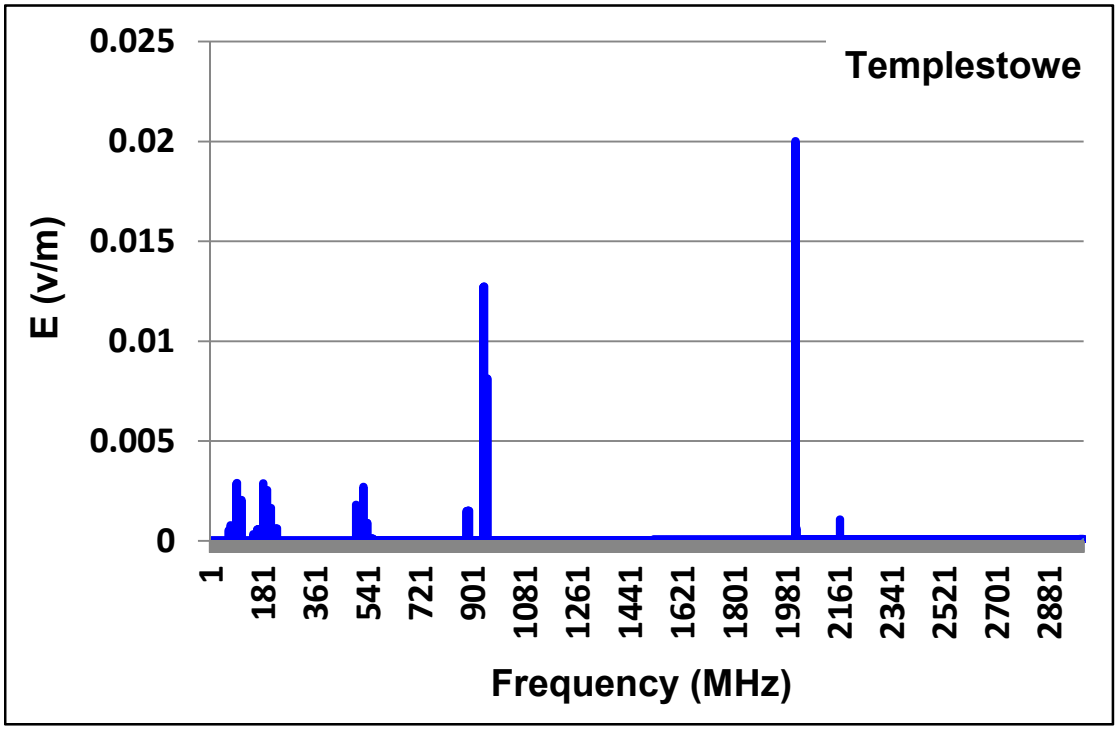
Templestowe
E (v/m)
0.025
0.02
0.015
0.01
0.005
0
1
181
361
541
721
901
1081
1261
1441
1621
1801
1981
2161
2341
2521
2701
2881
Frequency (MHz)

(d)

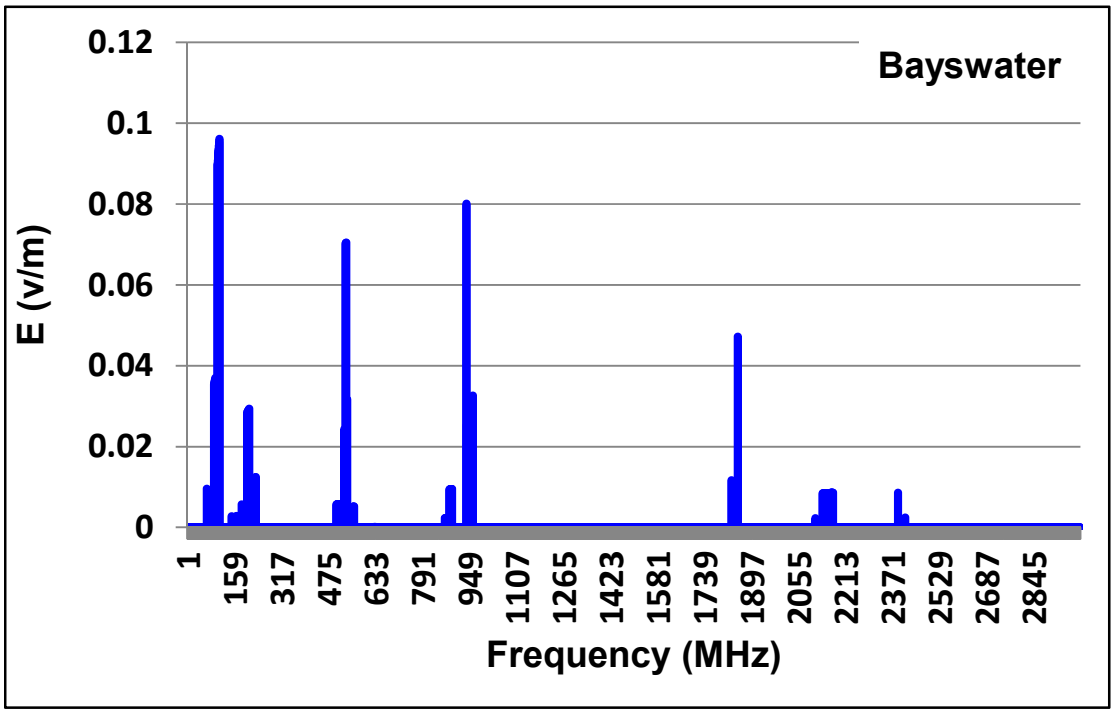
Bayswater
E (v/m)
0.12
0.1
0.08
0.06
0.04
0.02
0
1
159
317
475
633
791
949
1107
1265
1423
1581
1739
1897
2055
2213
2371
2529
2687
2845
Frequency (MHz)

(e)

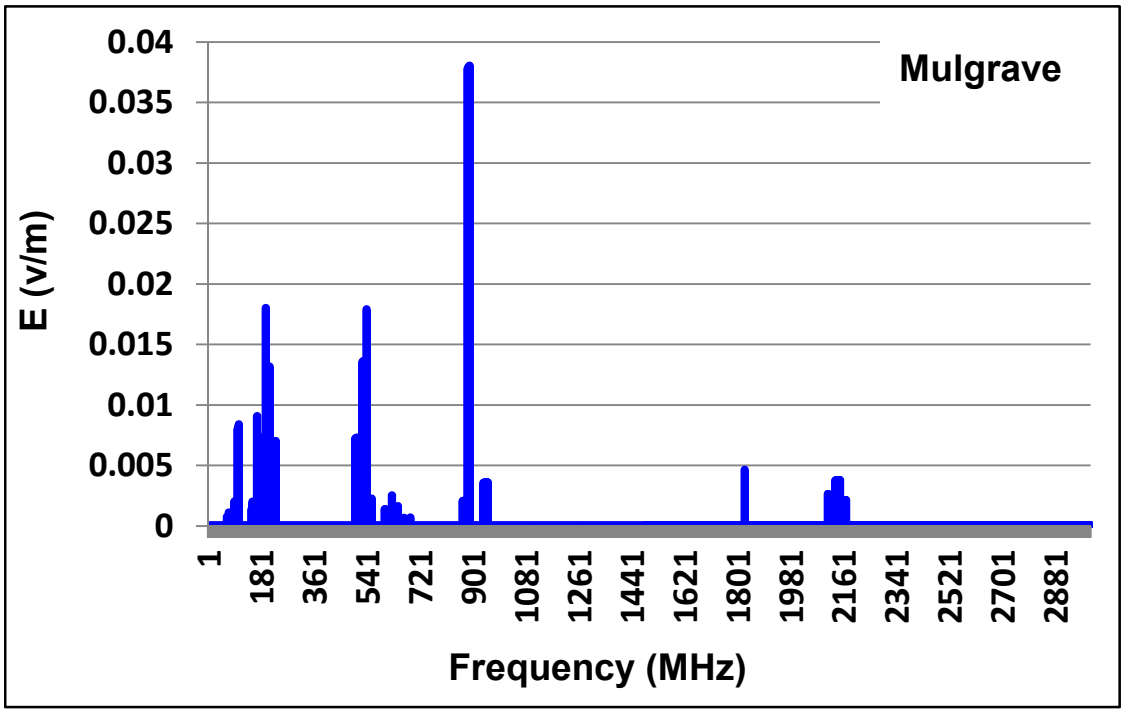
Mulgrave
E (v/m)
0.04
0.035
0.03
0.025
0.02
0.015
0.01
0.005
0
1
181
361
541
721
901
1081
1261
1441
1621
1801
1981
2161
2341
2521
2701
2881
Frequency (MHz)

(f)

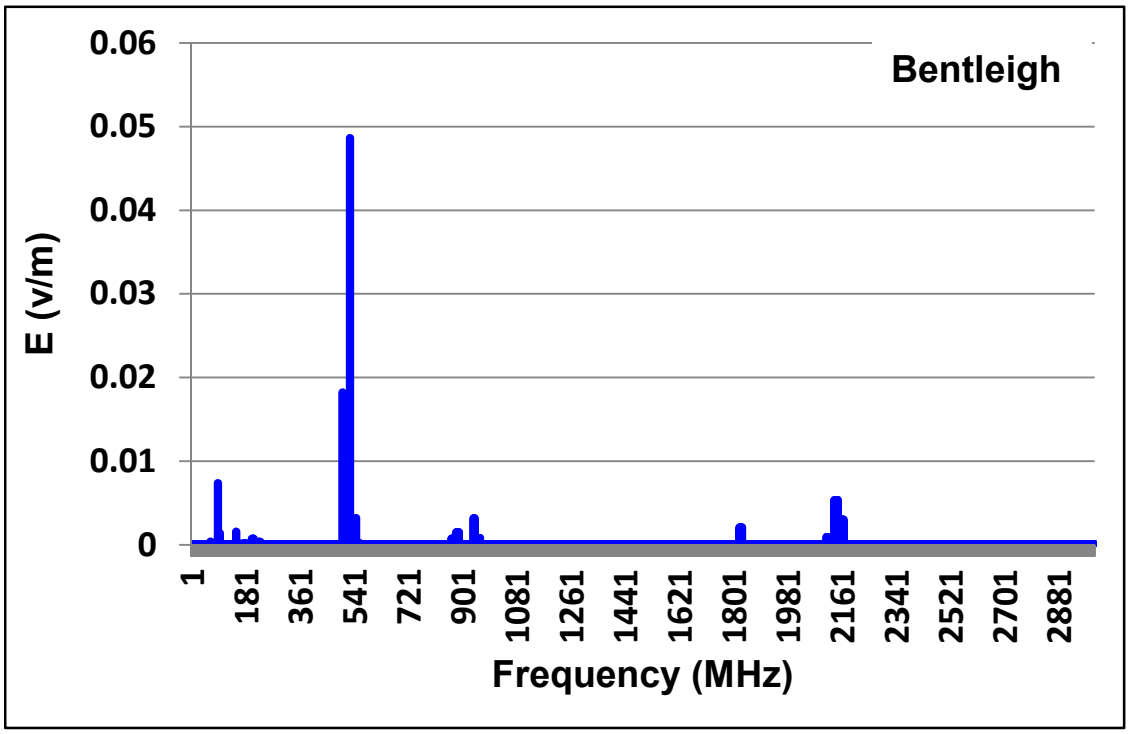
Bentleigh
E (v/m)
0.06
0.05
0.04
0.03
0.02
0.01
0
1
181
361
541
721
901
1081
1261
1441
1621
1801
1981
2161
2341
2521
2701
2881
Frequency (MHz)

(g)

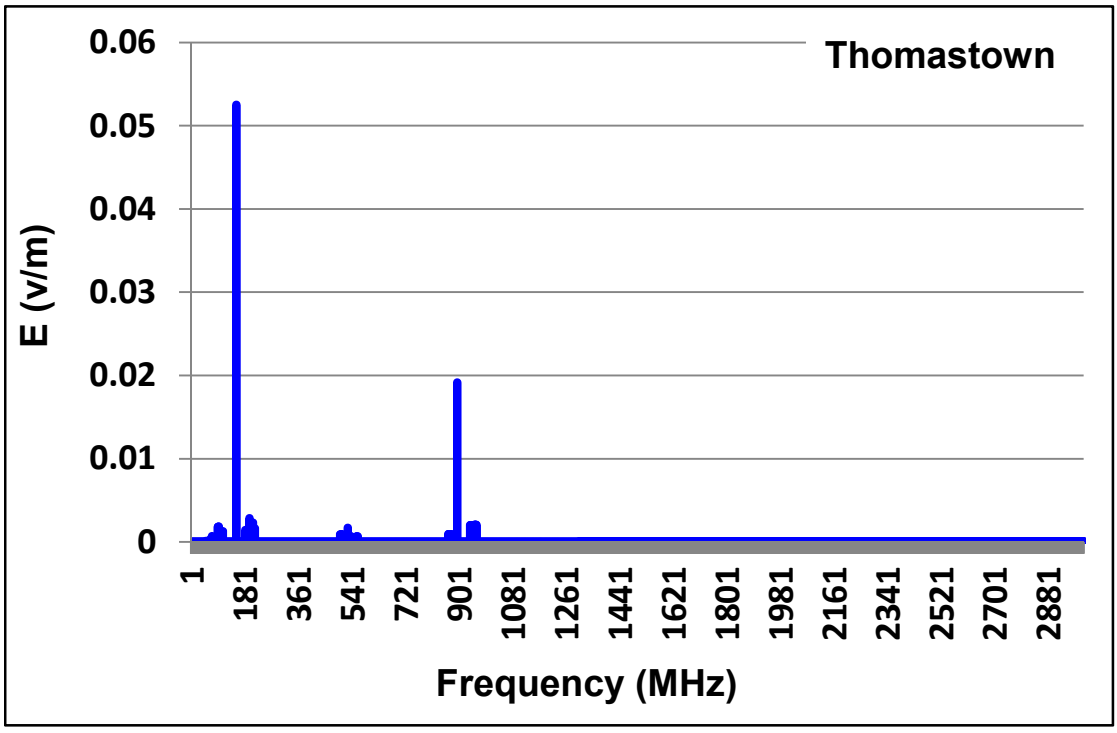
Thomastown
E (v/m)
0.06
0.05
0.04
0.03
0.02
0.01
0
1
181
361
541
721
901
1081
1261
1441
1621
1801
1981
2161
2341
2521
2701
2881
Frequency (MHz)

(h)

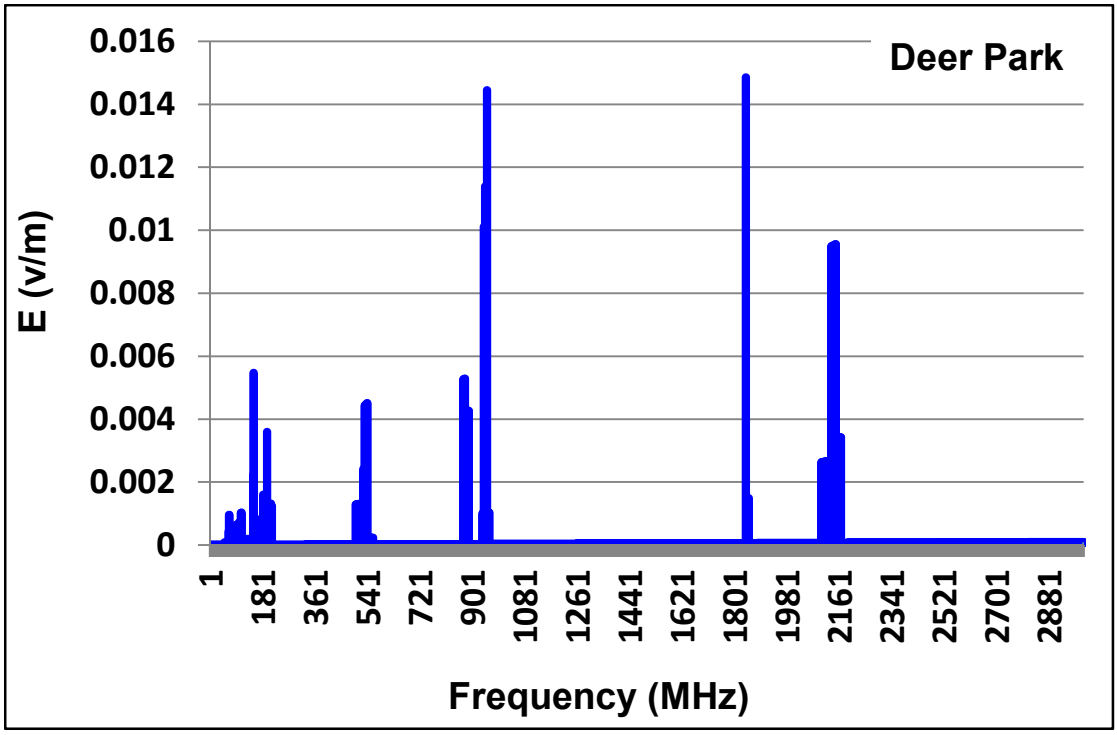

(i)

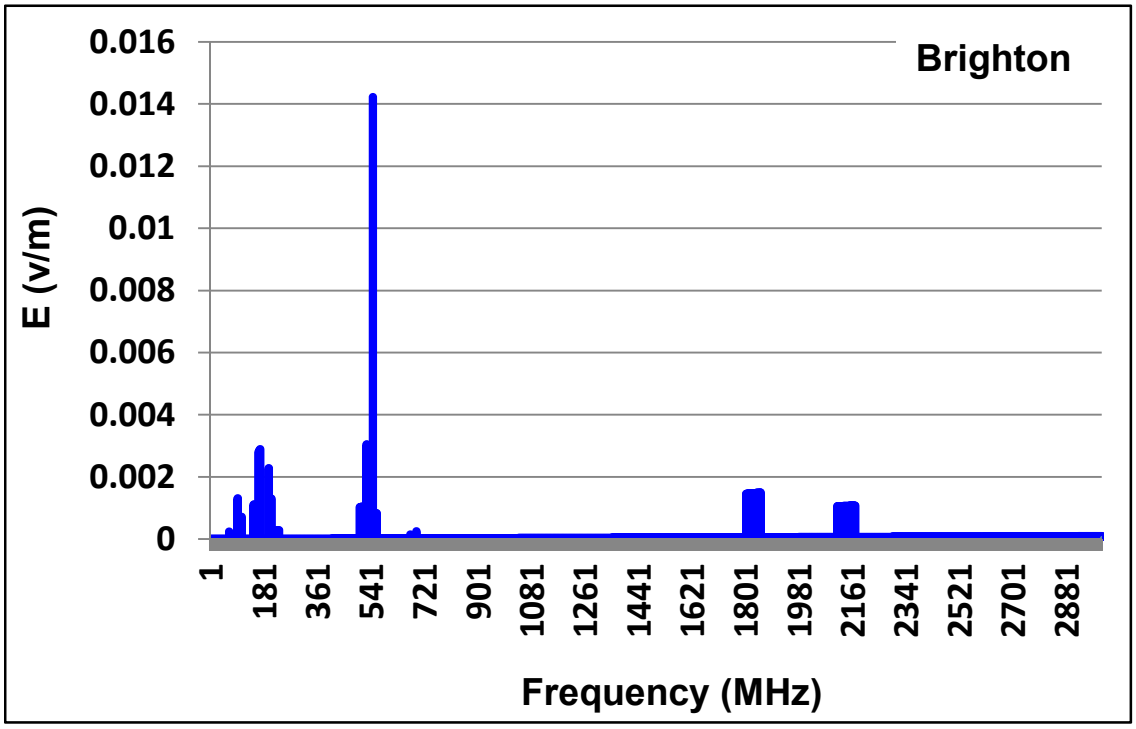

(j)

Figure 3.3 RF field measurement results in different Melbourne suburbs. (a) RMIT University, (b) Inner city, (c) Mount Dandenong, (d) Templestowe, (e) Bayswater, (f) Mulgrave, (g) Bentleigh, (h) Thomastown, (j) Deer Park, (j) Brighton.

Table 3.1 Australian Radio Frequency Spectrum Allocation

Frequency Band (MHz)	Australian Radio Frequency Allocation
88-108	FM Radio Broadcasting
137-144 and 174-230	Analogue and Digital TV Broadcasting
470-890	Analogue and Digital TV Broadcasting
800-1000	Cellular Mobile (GSM 850, 900 MHz)
1000-1800	Cellular Mobile (GSM 1800 MHz)
1800-2400	Cellular Mobile (GSM 1900, 2100 MHz) Wi-Fi, WiMAX
2500-3000	WiFi, Bluetooth

The RF field measurement results indicate that radio frequency signals from wireless communication services (e.g. mobile phone, Wi-Fi, etc.) are strong at various locations. However, the signal level is heavily dependent on the telecommunication traffic density and it varies during the day time. Hence, ambient RF energy harvesting from wireless communication services (e.g. at 900, 1800, 2100 MHz) is time dependant.

On the other hand, radio waves from broadcasting (e.g. FM radio, Digital and Analogue TV) are quite stable, although the strength varies with the distance from the broadcasting tower.

According to the RF field measurements results, it is evident that broadcasting systems (e.g. at 100 and 500 MHz) provide stable energy sources with high signal levels, as an efficient power scavenging source. Furthermore to clarify the findings, maximum available power for different frequency bands is analysed in the following section.

2.3 Maximum Available Power Analysis

In order to analyse the maximum available power for different frequency bands based on a set aperture area where the rectenna can be mounted, the frequency bands which had the highest signal levels (from Section 3.2) were selected. For the purpose of this exercise, it was assumed a limited area of 16 m² was available where patch antenna(s) with the gain of 6 dBi could be mounted (e.g. on the roof or wall of a building). The antenna size is assumed to be λ/2, and a spacing of λ/4 to ensure minimal coupling between the elements. The maximum number of elements in the given area was calculated and is presented in Table 3.2.

It should be highlighted that the purpose of assuming this large area (16 m²) is to investigate the practicality of embedding RF energy harvesting systems in building materials (roof tiles and wall/ceiling plaster boards), creating a structurally integrated energy scavenging system for home and office devices (this will be explained in Chapter 5).

Table 3.2 The Number of Elements in an Assumed Available Area Where the Rectennas Can be Mounted

Frequency (MHz)	Number of Patch Antennas in 16 m^2 Area
50	0
100	3
200	13
500	80
800	229
1000	400
2000	1600
3000	5926

As shown in Table 3.2, RF scavenging from broadcasting systems (at around 500 MHz) increases the antennas size and hence decreases the number of elements (*N*) in the available area in comparison to harvesting from wireless communication systems (at around 2000 MHz). However, according to the RF field measurement results, it is evident that broadcasting systems provide more stable energy sources with higher signal levels than wireless communication systems.

Therefore, for an accurate comparison of the different frequencies in Table 3.2, it is necessary to analyse the total signal level in terms of the number of antennas at the selected frequencies. By considering the factor of the number of elements, *N*, and the signal values that were measured in Section 3.2, the maximum available power can be calculated, which is shown in Figure 3.4.

For more clarity, as shown in Table 3.2, two cases are analysed as follows (assuming −10 dBm RF power is available in an ambient environmental scenario):

Case 1: Frequency=100 MHz

Number of elements =3

DC output of one element=X

Total DC output of elements=3×X

Total available RF power= −5.23 dBm

Case 1: Frequency=200 MHz

Number of elements =13

DC output of one element=X

Total DC output of elements =13×X

Total available RF power= 1.13 dBm

The total output DC value produced by rectenna elements can be determined by multiplying the DC value of each element and the number of elements *N* in a given area (assuming no loss in DC combining process). Hence, maximum available power would be calculated by

considering the operating frequency (which determines the *N*) and available input power (Section 3.2).

In order to present these results in terms of dBm, following conversion can be used:

$$\text{dBm} = \text{dB}\mu\text{V} - 107 \text{ dB} \qquad (3.2)$$

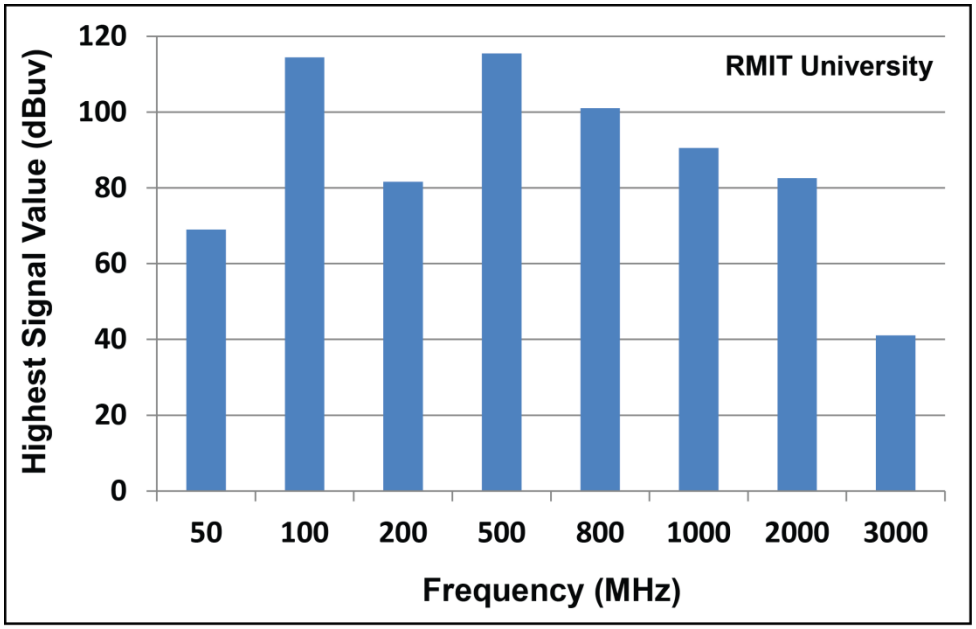

(a)

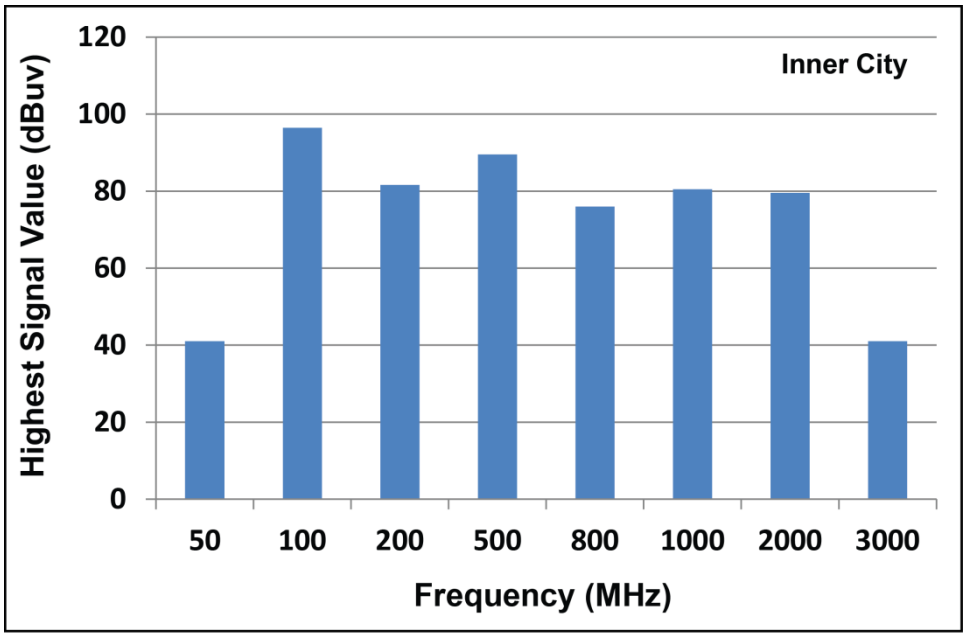

(b)

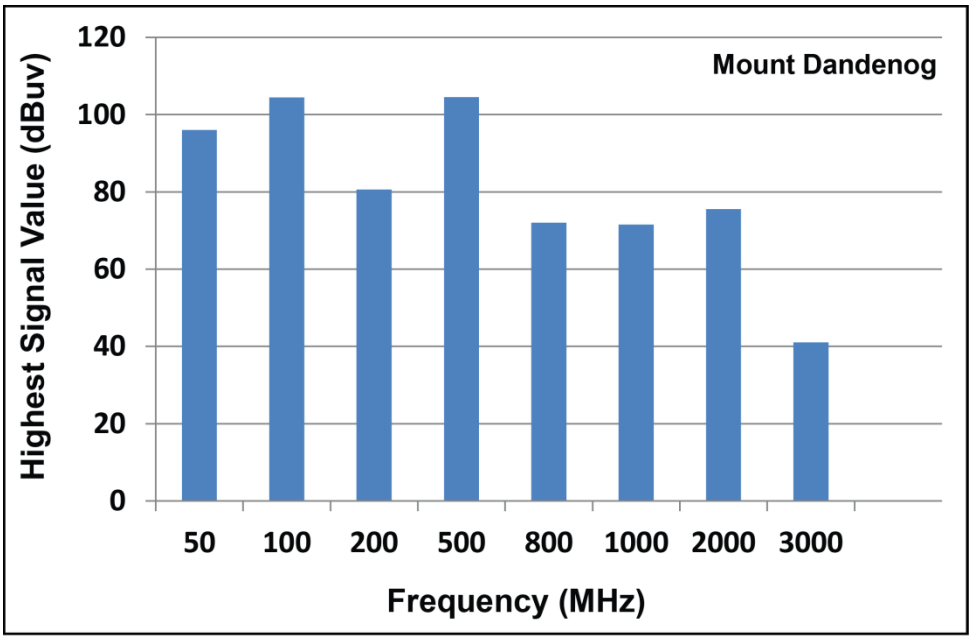
Mount Dandenog
Highest Signal Value (dBuv)
120
100
80
60
40
20
0
50
100
200
500
800
1000
2000
3000
Frequency (MHz)

(c)

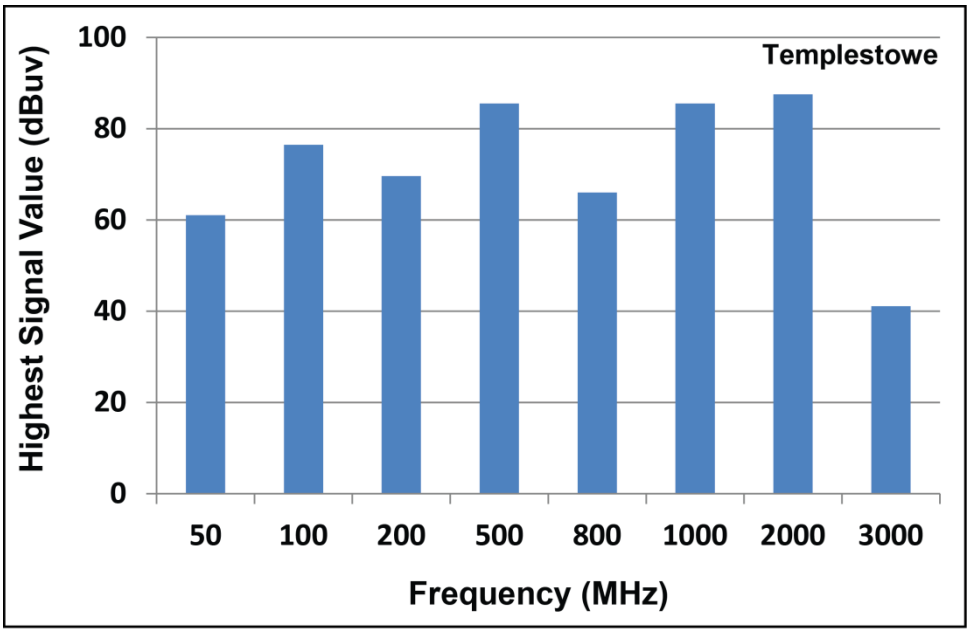
Templestowe
Highest Signal Value (dBuv)
100
80
60
40
20
0
50
100
200
500
800
1000
2000
3000
Frequency (MHz)

(d)

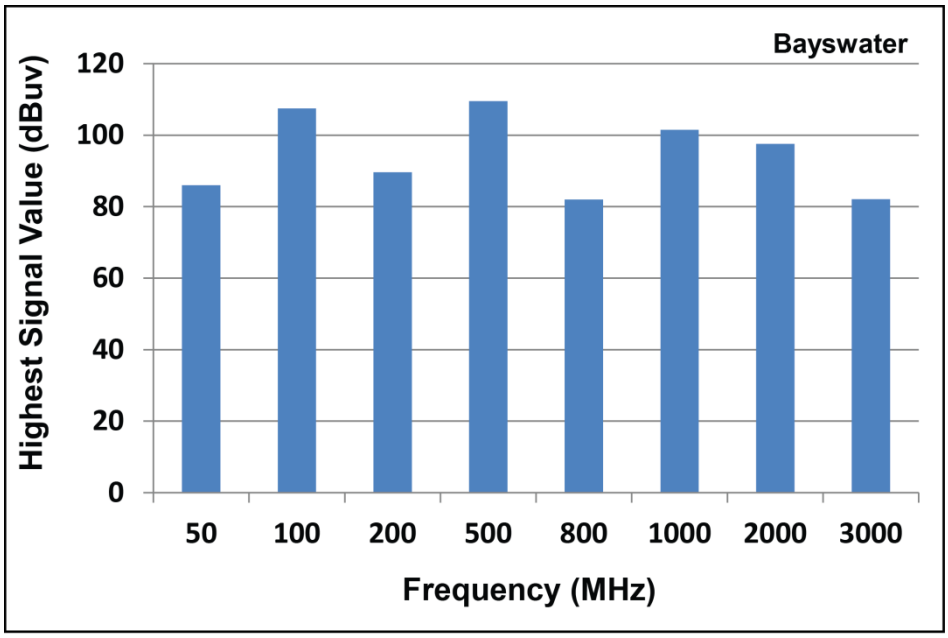
Bayswater
Highest Signal Value (dBuv)
120
100
80
60
40
20
0
50
100
200
500
800
1000
2000
3000
Frequency (MHz)

(e)

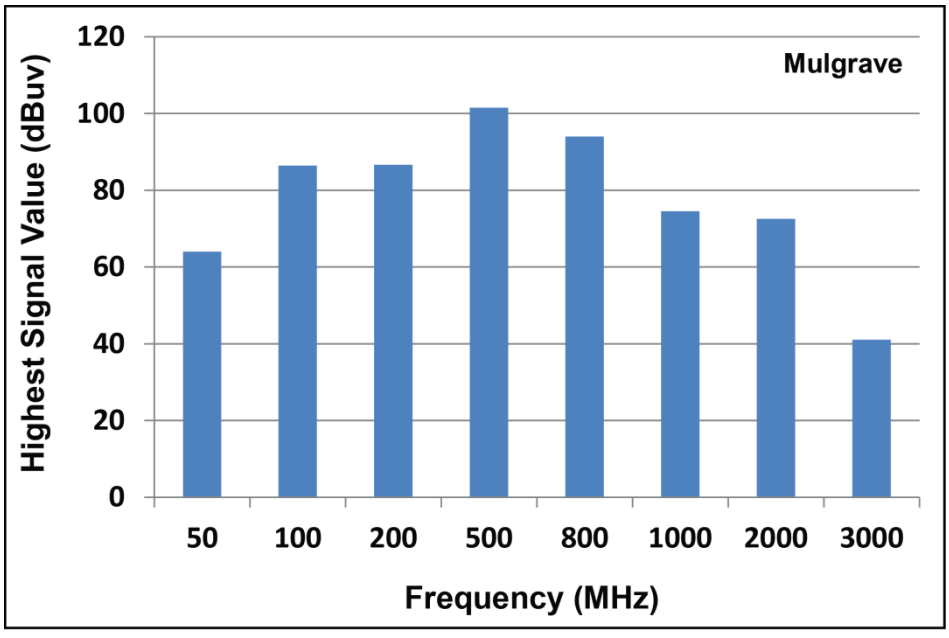
Mulgrave
Highest Signal Value (dBuv)
120
100
80
60
40
20
0
50
100
200
500
800
1000
2000
3000
Frequency (MHz)

(f)

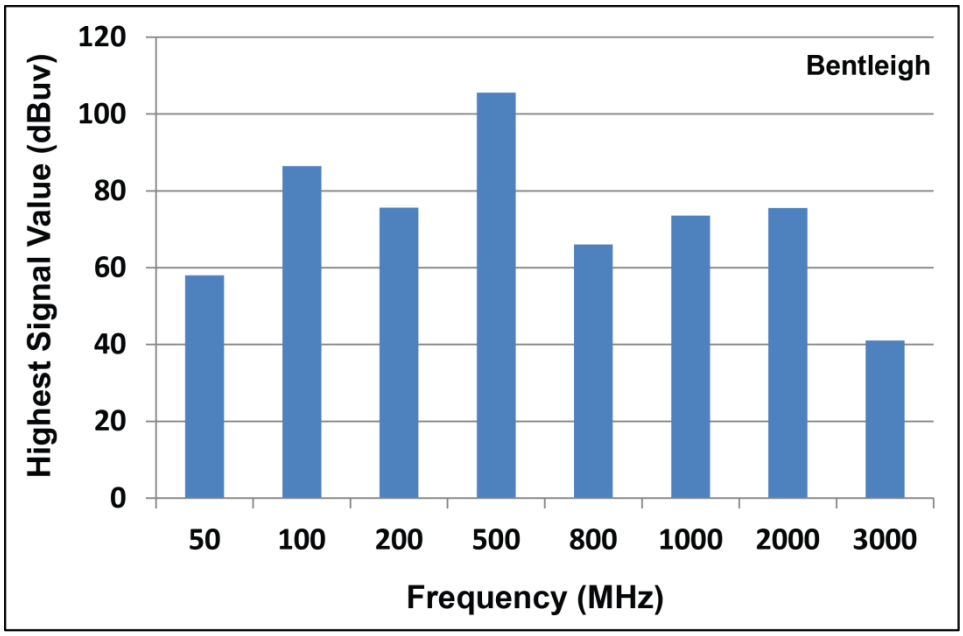
Bentleigh
Highest Signal Value (dBuv)
120
100
80
60
40
20
0
50
100
200
500
800
1000
2000
3000
Frequency (MHz)

(g)

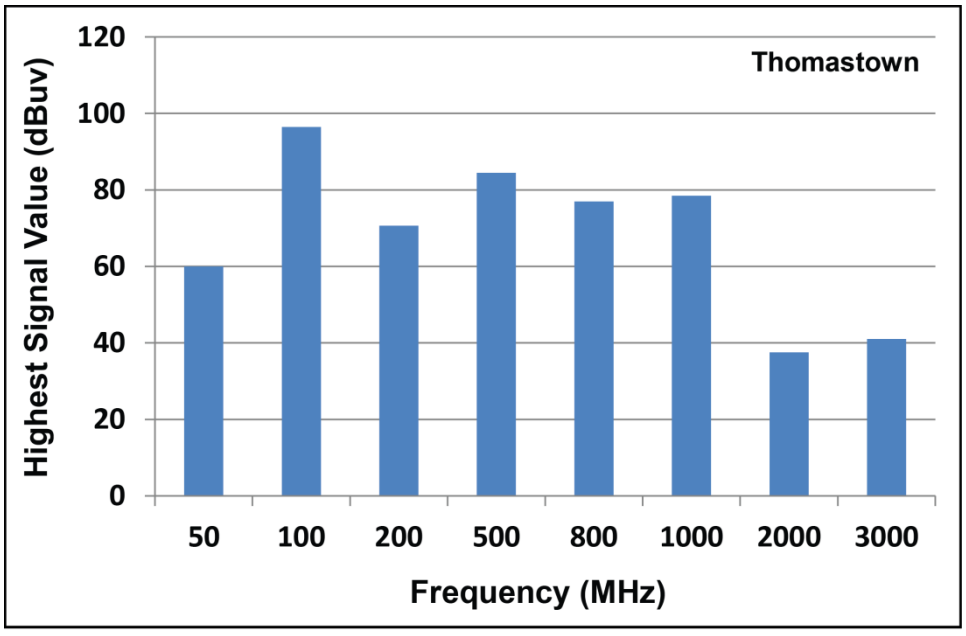
Thomastown
Highest Signal Value (dBuv)
120
100
80
60
40
20
0
50
100
200
500
800
1000
2000
3000
Frequency (MHz)

(h)

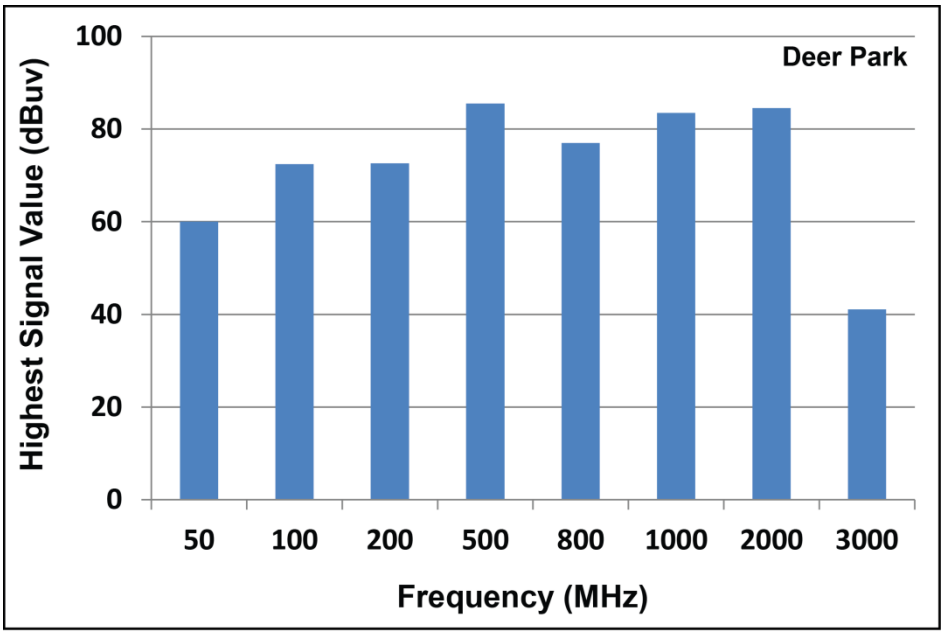

(i)

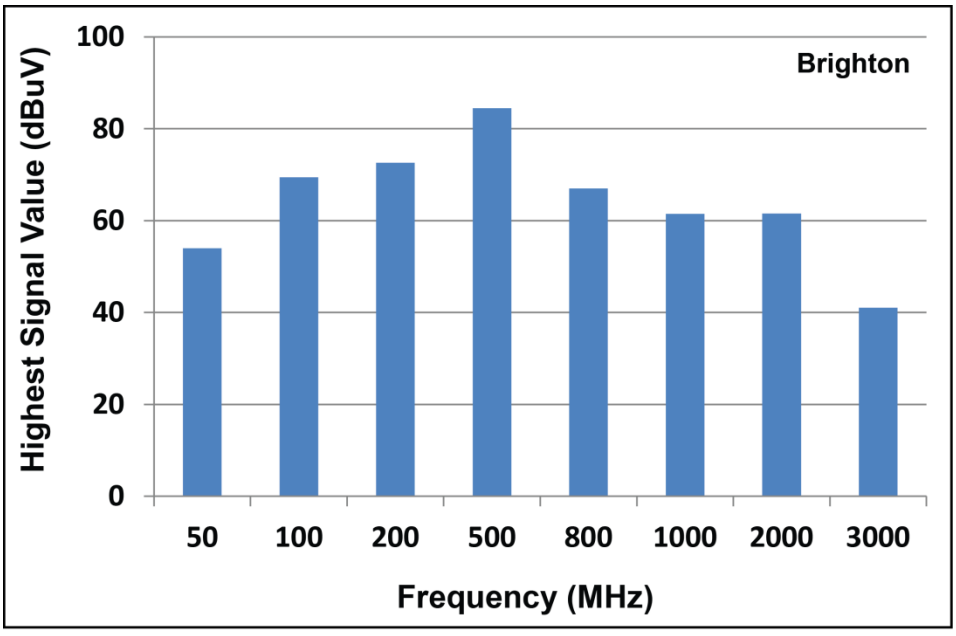

(j)

Figure 3.4 Maximum available signal level. (a) RMIT University, (b) Inner city, (c) Mount Dandenong, (d) Templestowe, (e) Bayswater, (f) Mulgrave, (g) Bentleigh, (h) Thomastown, (j) Deer Park, (j) Brighton.

Based on the RF field measurements and maximum available power analysis, it is evident that broadcasting bands (TV and FM radio) at 500 MHz (within 470-890MHz) and 100 MHz (88-108 MHz) are good scavenging sources (Figure 3.4). Even though both 500 MHz and 100 MHz ranges produce approximately similar results, in some cases the 500 MHz band possesses slightly higher amounts of average power.

From a design perspective, there is a significant reduction in the size of antennas operating at higher frequencies; therefore a greater number of rectennas can be mounted in an assumed available area. However, considering the cost scenario, utilising a large number of elements (i.e. antennas, diodes) creates additional expense.

Therefore depending on the specific application, where there is a limited available area, 500 MHz is a preferred band due to the small element size and high level of the incident power at this frequency. On the other hand, 100 MHz could provide more cost-effective implementation than higher frequencies. However, for applications with limited available area (less than 1 m^2), this frequency band is not feasible as a power scavenge source.

Furthermore, the amount of available signal at 0.8 and 1 GHz are comparable to 500 MHz and 100 MHz in some locations. Therefore, cellular and wireless communication systems could be alternative power scavenge sources for applications where miniaturisation is essential. However, more complicated design and fabrication technologies may result in a more expensive implementation. (It should be highlighted that, based on Table 3.2, 800 MHz band corresponds to both TV broadcasting and cellular systems in Australia.)

From the results of this study, the 500 MHz with around 20 MHz bandwidth range seems the most appropriate scavenging band, assuming a relatively large collection area. This frequency range provides stable RF signals and low atmospheric loss, promising to produce maximum available power in a variety of suburban locations. In addition, this broadcasting frequency

range is widely available at all times, and is simple to harvest with a cost-effective implementation.

2.4 Rectenna Configurations

The main goal in designing an efficient RF harvesting system is producing high level output power. Toward this goal, there are a few configuration options for the rectenna system.

One design approach is utilising an antenna array (multiple antennas) connected to a single rectifier circuit, using an RF combining method. This topology combines the RF signals from the antenna array to a single rectifier [115, 116] (See Figure 3.5(a)). This method increases the total directivity at the cost of potential misalignment with the incoming ambient signals. This is due to the fact that the array enhances the power delivered to the rectifier circuit by enlarging the antenna aperture and total gain, whilst the system becomes narrow in beam width [117, 118]. Consequently, such an implementation could lose scavengeable signals from different angles of incidence.

Another approach is to connect each individual antenna to a rectifier circuit (which essentially operate at a single frequency), using a DC combining method [100, 115] (See Figure 3.5(b)). This topology rectifies the received RF signal of each antenna element prior to combining it at the DC output. This enables the utilization of several broad-beam antennas to collect RF power from various sources and hence maximising power collection.

From an ambient RF scavenging perspective, this approach offers a more efficient power harvesting solution. This is due to the fact that the individual antenna elements provide a broader pattern which potentially increases the amount of energy collected by the antenna.

However, an important issue that should be taken into consideration is the non-linearity of the rectifier impedance with frequency and input power. To address this, a broadband impedance

matching network is essential for providing maximum power transfer from the antenna to the single rectifier circuit [118].

However, from a design point of view, whilst it is relatively easy to achieve a broadband antenna, it is very challenging to realise a broadband rectenna due to the non-linearity of the rectifier impedance with input power across the frequency band (as discussed in Chapter 2). Moreover, due to the low Q value (quality factor) of the broadband rectifier circuit, this method typically results in very low efficiency at any particular source frequency (based on the Bode-Fano limits [108]).

Hence, most of the published works on the second approach (Figure 3.5(b)) have used single band rectifiers [98, 119]. However, considering this method (individual antennas, individual rectifiers), it is very challenging to design a highly sensitive rectenna with individual single band rectifiers and DC combining method. As ambient RF energy levels are very low, the sensitivity of the harvesting system is of paramount importance and single band matching networks usually fail to deliver sufficient power to the rectification device (this has been discussed in Chapter 2).

Furthermore from a design and economic perspective, utilising a large number of components (i.e. antennas, diodes) to realise individual rectennas for each frequency band creates additional expense.

Therefore, an alternative approach is to use a multiband or broadband antenna and design a matching circuit at the specific frequencies (e.g. multiband matching network). It is important to select these frequencies where the maximum signal is available, which have been investigated in the previous sections.

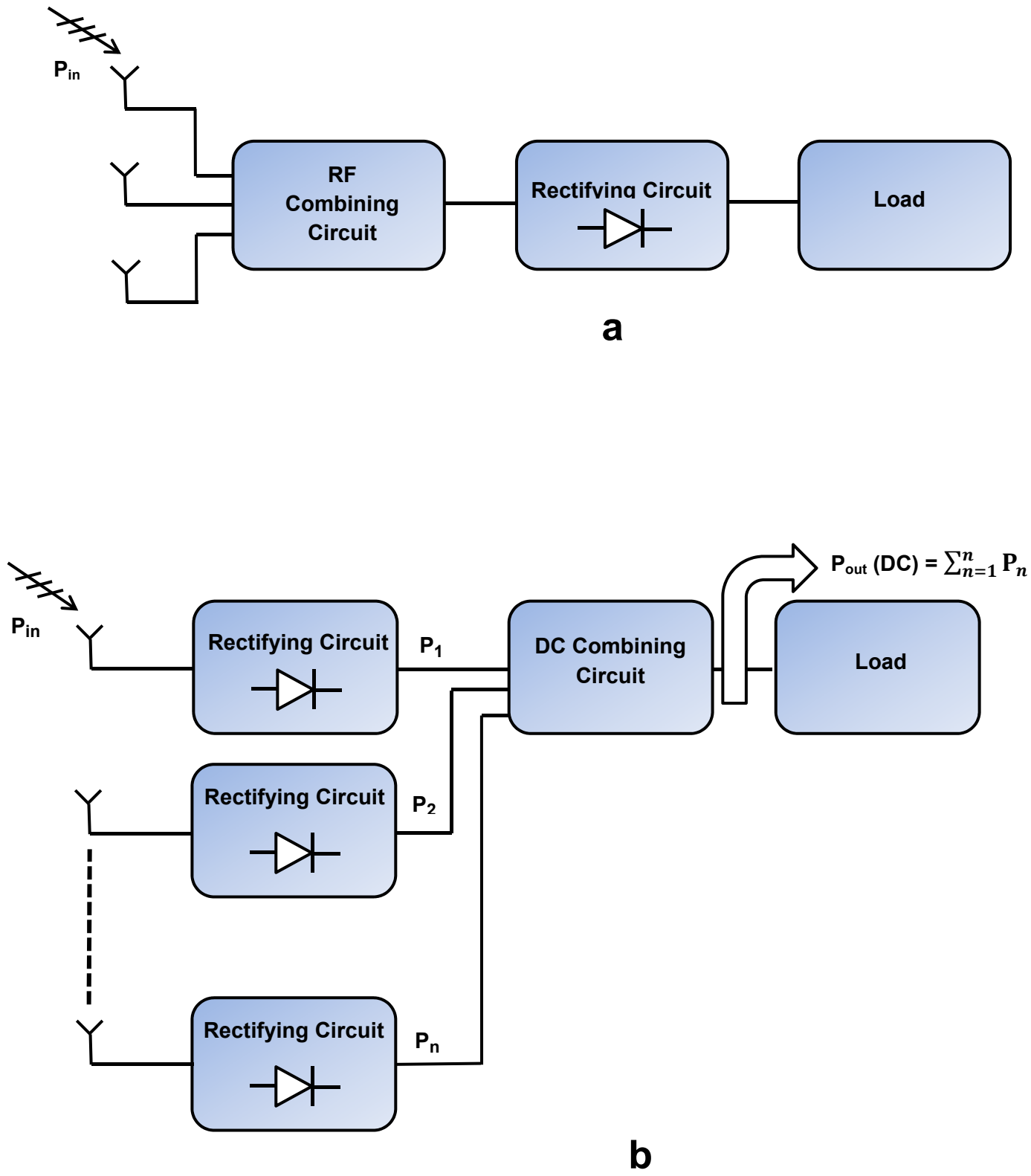

Figure 3.5 Schematics of the rectenna configurations (a) Single rectifier circuit using RF combining method. (b) Multiple rectifier circuits using DC combining method.

In order to elucidate this concept, a typical rectifier was simulated in Agilent ADS software and quantitative comparisons are provided in Table 3.3. As presented in Table 3.3, at high input RF power (e.g. −5 dBm), the DC output power of two rectifiers (using a DC combing method) is slightly higher than the output of a rectifier which combines two RF signals at the input (mainly due to the saturation of the rectifier in presence of high input power). However, at very low ambient power levels (e.g. −40 dBm), RF combing method provides higher DC power compared to adding the DC output of two rectifiers (due to delivering more power to rectification device).

Table 3.3 Rectenna Configurations Comparison

Rectifier Configuration	Output DC Power (µW) with input RF Power of −5 dBm	Outp0ut DC Power (µW) with input RF Power of −30 dBm	Output DC Power (µW) with input RF Power of −40 dBm
Single Rectifier	148	0.074	0.001
RF Combining of Two Signals at the Input of a Rectifier	277	0.217	0.004
DC Combining of Two Signals at the Output of Two Rectifiers	296	0.148	0.002

2.5 Conclusion

In this chapter, the feasibility of harvesting ambient EM energy in metropolitan areas of Melbourne, Australia has been investigated. Based on the RF field measurement results and maximum available power analysis, it is evident that broadcasting frequency ranges such as; FM and TV at 88-108 MHz and 470-890 MHz respectively are preferred power scavenge sources due to their suitable level of the ambient power at a variety of locations. In addition, these ranges offer a great deal of flexibility to deploy simple and cost-effective implementation, which is of paramount importance for optimal power harvesting systems. Furthermore, cellular and wireless communication systems (800-1000 MHz) have been recommended as alternative power scavenging sources.

Measurement results revealed that, available RF power from broadcasting services and cellular systems ranging from −40 to −10 dBm (there are also various signals below −40 dBm). This identifies two important considerations in the design of efficient rectenna for ambient RF energy harvesting: the scavengeable ambient RF power sources available, and the significant variance of this power.

Therefore, it has been demonstrated that the scavengeable levels of ambient RF power are orders of magnitude lower than previous published works. Furthermore, the scavengeable power level is generally unknown, incoherent and effected by environmental/free-space conditions such as the distance from the power source to a rectenna, propagation losses (free-path and attenuation), and the antenna orientation (polarisation).

This chapter also presented different rectenna configurations, and an optimum approach was proposed based on the RF field measurement outcomes. The solution is to identify and harvest multiple ambient frequency sources over their realistic available energy range in order to increase the amount of RF energy scavenged by a rectenna.

Therefore, with the creation of efficient rectenna arrays, there is potential to generate a viable energy source for urban environments, predominantly for low power applications.

The investigations and analysis of this chapter enable the design of an appropriate RF rectifier circuit based on the real environmental cases. The outcome of this chapter built up the baseline knowledge of low power RF harvesting which is the foundation for the proceeding chapters.

Chapter 4 – Multi-Service Highly Sensitive Rectifier

4.1 Introduction

Literature characterizes energy harvesting circuits by two important metrics; efficiency and sensitivity. Efficiency can be expressed as total energy-harvesting circuit efficiency or power conversion efficiency (PCE). While related to energy-harvester efficiency, sensitivity is defined as the minimum power necessary to turn on a rectification circuit.

Efficient RF energy harvesting is a very challenging issue, as it deals with very low RF power levels available in the environment. Furthermore, the scavengeable ambient power level can vary unpredictably, depending on several factors such as the distance from the power source, the transmission media, the telecommunication traffic density and the antenna orientation (as discussed in Chapter 3). Hence, accommodation of this input power variation should be considered when designing a rectification network. Importantly, the nonlinearity of a rectification device (Schottky Diode) in energy harvesting circuits makes impedance matching a challenging endeavour.

RF to DC rectifier solutions proposed in recent literature have mainly focused on maximising the system efficiency at a given, and often quite high, input power level (as discussed in

Chapter 2). This neglects the issues related to input power variation which can lead to unexpected variations in the matching network due to diode non-linearity. Also, the scavangeable levels of ambient RF power have been shown to be orders of magnitude lower than previous published works (based on the results from Chapter 3).

From a design point of view, the majority of available literature on RF rectification has been dedicated to narrowband rectennas, which essentially operate at a single frequency and hence provide low DC output power.

From an ambient RF scavenging perspective, harvesting energy from various available frequencies can maximise power collection and hence increase the output DC power (discussed in Chapter 2, Chapter 3). Ultra-wideband and broadband rectenna arrays have been proposed as a potential solution [99, 100]. However, due to the low Q value of the broadband rectifier circuit, this method typically results in very low efficiency at any particular source frequency (based on Bode-Fano limits).

From a design point of view, while it is relatively easy to achieve a broadband antenna, it is very challenging to realise a broadband rectenna due to the non-linearity of the rectifier impedance with input power across the frequency band. Hence, multi-band rectification approach has been proposed where individual antennas were connected to individual rectifier circuits (which essentially operate at a single frequency) and a DC combining method was used (discussed in Chapters 2 and 3). This topology rectifies the received RF signal of each antenna element prior to combining it at the DC output. This enables the utilization of several broad-beam antennas to collect RF power from various sources and hence maximises power collection. However, it is very challenging to design a highly sensitive rectenna with individual narrow-band rectifiers. Furthermore, utilising separate circuits to cover multiple bands increase the total system size and impose additional fabrication cost.

As ambient RF energy levels are very low (−40 to −10 dBm found in Chapter 3), the sensitivity of the harvesting system is of paramount importance and a narrow band matching network usually fails to deliver sufficient power to the rectification device to turn it on. Furthermore from a design and economic perspective, utilising a large number of components (e.g. diodes) and realizing individual rectifier circuits for each frequency band creates additional expense.

To address this, a promising approach is to use a multi-band configuration. Various environmental RF energy sources of different frequencies are collected by an efficiently designed antenna, and delivered to the rectification circuit via a multi-band matching network. This can maximise the PCE at the specific frequencies where the maximum ambient signal level is available. This is due to the fact that harvesting RF energy from various available frequencies simultaneously increases the delivered power to the rectifier, enhancing the diode conversion efficiency and consequently increasing the output DC power.

Therefore, in order to increase the amount of RF energy scavenged by a rectenna, it is crucial to identify and harvest multiple ambient frequency sources over their realistic available energy range.

The previous chapter has demonstrated the feasibility of RF energy harvesting through RF field investigations and maximum available power analysis in metropolitan areas of Melbourne, Australia. The maximum available power for different frequency bands based on antenna aperture and number of antennas in a given collection area was analysed.

Measured results and analysis indicated that cellular systems and broadcast sources are well suited to harvesting, with scavengeable RF power ranging from −40 to −10 dBm. This identifies two important considerations in the design of efficient rectenna for RF energy

harvesting: the scavengeable ambient RF power sources available, and the significant variance of this power.

Therefore, based on the previous research outcomes and recommendations (Chapter 3), an efficient power harvesting solution could encompass a multi-band matching circuit at the specific frequencies where maximum signal power is available, enabling greater power harvesting. This also results in a higher power being fed to a single rectifier, utilising the diode function more efficiently. Delivering multiple RF signals into a single rectification stage results in a high sensitivity rectifier, which can provide higher DC power than the post rectification combining of separate single frequency rectifier circuits operating at the same frequencies with very low input powers.

This chapter presents an RF energy harvesting method that can scavenge a wide range of ambient power levels which are orders of magnitude lower than previous reported techniques in the literature. An efficient dual resonant rectifier circuit is proposed, matched to a 50 Ω input port at 490 and 860 MHz over a broad low input RF power range from −40 to −10 dBm. Based on the Australian Radiofrequency Spectrum Plan, these bands are allocated to broadcasting services and cellular systems [114].

The proposed dual resonant matching network operates efficiently at two identified harvesting frequency bands over a wide input power range, maximising DC power by scavenging two sources simultaneously.

4.2 Dual Resonant Rectifier Design

The major goal in designing an efficient RF harvesting system is to produce high DC output power. Toward this goal, a high sensitivity rectifier is crucial for optimum RF scavenging. A significant factor governing the sensitivity of a rectifier is the threshold voltage of the diode used for rectification. The diode must be able to "switch on" for very low ambient energy levels. To address this sensitivity issue, a system that scavenges power from multiple frequency bands and delivers them to activate a rectification circuit is proposed.

The general block diagram of the proposed system is depicted in Figure 4.1. Various environmental RF energy sources of different frequencies are collected by an appropriately designed antenna, and delivered to the rectification circuit via a multi-band matching network. The rectification circuit converts multiple RF signals into DC power for low-powered applications.

This thesis realizes a dual resonant matching circuit as a transition between a 50 Ω nominal antenna output and the non-linear rectification device at 490 and 860 MHz. Since the rectifier is a critical part of the RF energy harvesting system and its efficiency and sensitivity determine the whole system functionality, this research focuses on the rectifier circuit design.

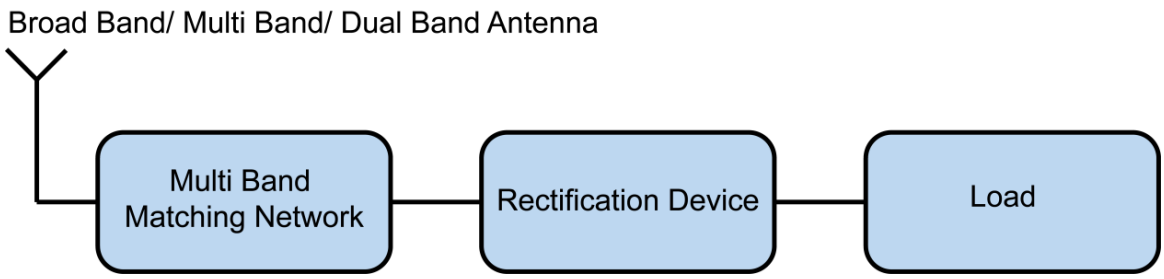

Figure 4.1 General block diagram of the RF energy harvesting system.

4.2.1 Device Selection

Due to the very low ambient power available in a real environment (Chapter 3 outcomes) a very low threshold voltage rectification device is required in order to increase the sensitivity. For this reason, Schottky diodes (GaAs or Si) are commonly employed for RF energy harvesting. In this work, a microwave Schottky detector HSMS2820 (C_{j0} = 0.7 pF, R_s = 6 Ω, $I_s = 2.2e^{-8}$ A) is chosen due to its excellent high frequency performance, low series resistance (R_s) and junction capacitance (C_j), and low threshold voltage with high-saturation current [52]. This low threshold voltage (~0.3 V) supports rectification at low input power levels.

Note that, high *Cj* degrades the diode efficiency and hence the rectifier performance. Also high value of *Rs* increases the ohmic loss on the diode; hence, careful selection of the rectification device is essential to achieve a desired performance.

4.2.2 Voltage Doubler

In order to design an efficient RF harvesting system, the non-linearity of the rectifier impedance with frequency and input power should be matched to the 50 Ω output of the antenna at the desired frequency bands. Therefore, the diode input impedance as a function of frequency for different power levels was calculated and analysed [120].

In order to match the input impedance of the rectifier to the 50 Ω output of the antenna, the total load impedance for different input power and frequencies should be determined.

A circuit consisting of a pair of Schottky Barrier Diodes (SBD) terminated with a load resistor (R_{Load} = 11 KΩ) and an output bypass capacitor (*C2* = 6.8 pF) was simulated using Agilent ADS software. Figure 4.2 shows the proposed geometry of the voltage-doubler

topology [52, 121].

In this work a single stage voltage multiplier is considered [31, 57, 62]. It is formed by combining two sets of half wave rectifiers in a cascading structure and the output DC voltage can be charge-pumped by the diode-capacitor pair. The capacitor nearest to R_{load} will hold the total charges accumulated by each diode-capacitor pair. However, the rise of output DC voltage will not be significant if there are too many diode-capacitor stages. This is due to the component loss and low amplitude of the input RF power. Hence, only single multiplying stage is considered for this ambient energy harvesting application.

Therefore, the voltage doubler rectifier structure is employed for the design of the RF-DC power conversion system as this topology is well suited to low power rectification. Furthermore, advantages of using a voltage doubler are summarised as follows:

1. The output voltages of two diodes are added in series increasing the overall magnitude of the output voltage.
2. The RF impedances of the two diodes are added in parallel, hence making the process reactive impedance matching easier.
3. The rectified current produced by the first diode constitutes the external bias current for the second diode. Therefore, at very low power levels the use of this technique allows to reduce the junction resistance of the diode and hence increase the detection sensitivity.

The resistor and capacitor at the output will filter higher frequencies. The high load resistor (11 KΩ) was chosen to observe a reasonable output voltage at very low currents. Using Large Signal S-Parameters analysis in Agilent ADS software, the load impedance and bypass

capacitor were determined and optimised.

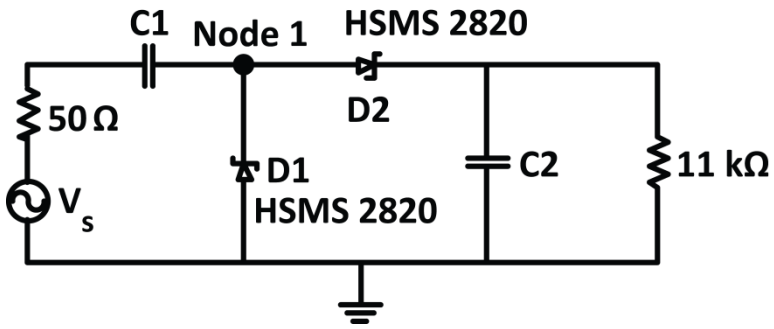

Figure 4.2 Schematic of a voltage-doubler rectifier without matching network.

The voltage doubler rectifier in Figure 4.2 consists of a peak rectifier formed by *D2* and bypass capacitor *C2* (6.8 pF) and a voltage clamp formed by *D1* and *C1* (total capacitance of the transmission lines and diode's parasitic capacitance (C_p)). In the negative phase of the input, current flows through *D1* while *D2* is cutoff. The voltage across *D1* stays constant around its threshold voltage and the voltage at node 1 is charged to $-V_{th1}$ (where $-V_{th1}$ is the threshold voltage of *D1*). At the negative peak, the voltage across *C1* is: $V_s - V_{th1}$.

In the positive phase of the input, current flows through *D2* while *D1* is cutoff. The voltage across *C1* remains the same as the previous phase because it has no way to discharge. At the positive peak, the voltage across *D1* is: $2V_s - V_{th1}$. Since *D2* is conducting current to charge *C2*, the voltage at the output is: $V_{out} = 2V_s - V_{th1} - V_{th2}$.

4.2.3 Dual Resonant Matching Network Design and Analysis

The DC equivalent circuit of the SBD is a voltage source in series with the junction resistor R_j which is obtained by differentiating the diode voltage–current characteristic and is given by eqn. (4.1) [52, 122]:

$$R_j = \frac{nKT}{q(I_s + I_b)} \qquad (4.1)$$

Where n is the diode ideality factor, K is Boltzmann's constant, T is the temperature in degrees Kelvin, q is the electric charge, I_s is the diode saturation current and I_b is the external bias current.

At low power levels, the saturation current is very small (I_s = 2.2e^{-8} A) and for a zero-biased diode, I_b = 0. Therefore, the resulting value of junction resistance at room temperature is approximately 1.7 MΩ [122]. Since, the saturation current is highly temperature dependent, R_j will be even higher at lower temperatures which tends to decrease the output voltage [122].

As the input power increases, some circulating rectified current will cause a drop in the value of R_j and this phenomenon will increase the value of the DC output voltage. Furthermore, it is worth to highlight that the rectified current produced by the first diode (*D1*) in Figure 4.2 constitutes the external bias current of the second diode (*D2*) which will help to reduce R_j and hence the detection sensitivity will be improved.

Therefore, depending on the amount of available bias current, R_j varies (equation (4.1)), hence the matching network changes which impacts the amount of delivered power to the diode and results in different values of PCE.

A Schottky barrier diode can be modeled by the linear equivalent circuit shown in Figure 4.3, where L_p and C_p are the diode's parasitic inductance and capacitance respectively due to packaging (L_p = 2 nH and C_p = 0.08 pF) which are generally unwanted [123]. This linear model is used for determining the diode impedance at a given input power.

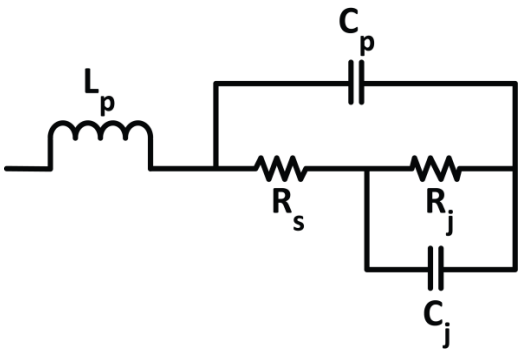

Figure 4.3 HSMS 2820 Schottky diode equivalent circuit.

The diode impedance was analysed using a Harmonic Balance (HB) simulator and a nonlinear model of the diodes over the frequency range of 400 to 900 MHz at various input power levels (Figure 4.4).

Due to the large junction resistor at low input RF power levels (e.g. −10 dBm); the rectification device is turned off in absence of an appropriate matching network. Large Signal S-parameter analysis was conducted and higher input power (associated with the signal source) was applied directly to the Schottky diodes configuration of Figure 4.2 which does not include a matching network in order to turn on the diodes (reduce the value of R_j) and extract approximate input impedance values as our starting point in design of a matching network.

As it can be seen in Figure 4.4, by increasing the source power (−5 to 5 dBm), the diode impedance is varies and it is beginning to switch on. Hence, the input impedance needs to be

determined when the diode is turned on to realise the matching network for a rectifier circuit. It is clear, in the presence of an appropriate matching network the rectification device can be turned on at lower power levels, whilst in the absence of a matching network a higher input power should be applied to switch on the diode.

Note: With an unmatched rectifier the total applied input power from the signal source cannot be delivered to the diode due to the high reflection in the circuit.

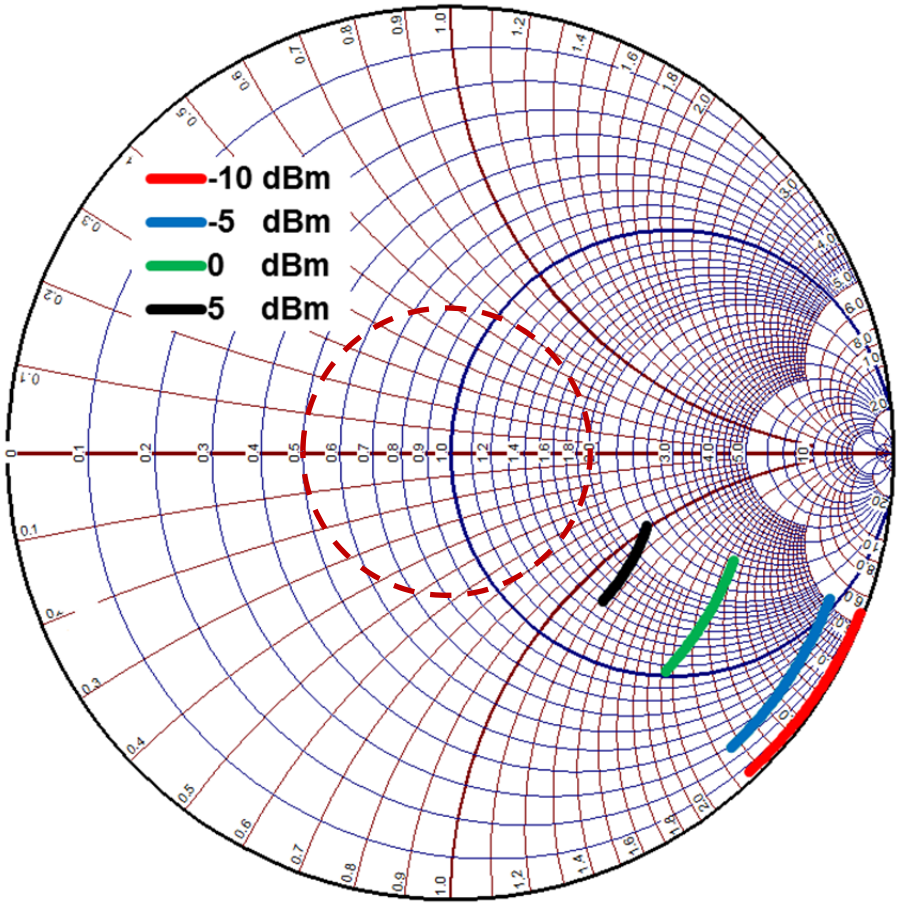

Figure 4.4 Diode input impedance calculated with Large Signal S-parameter analysis over the frequency range of 400 to 900 MHz with various unmatched input power levels.
(The 2:1 voltage standing wave ratio (VSWR) boundary is shown with a dashed circle on the Smith Chart).

In order to provide maximum power transfer from the antenna to the rectifier circuit, an impedance matching stage is essential. Designing the matching network is not straight-forward, since the rectifier is a nonlinear load with a complex impedance that varies with frequency and input power level. The impedance matching network is responsible for a low loss (minimum reflection) transmission between the receiving antenna and the rectifier. Without impedance matching, the RF energy will be reflected to the source and not delivered to the rectifier efficiently.

Hence, the aim is to match the input impedance of the device to 50 Ω at 478-496 MHz and 852-869 MHz bands over a broad range of input RF powers (−40 to −10 dBm). The procedure commences by matching the diode input impedance at high unmatched source power and shifting the diode input impedance at various power levels to within the voltage standing wave ratio (VSWR) < 2 circle on the Smith Chart. This procedure is based on that the diode input impedance does not change drastically in this low power range since the rectification device is turned off. The simulation results of Figure 4.4 prove that this was the case.

In this chapter, a dual resonant rectifier network is designed as a transition between a 50 Ω nominal antenna output and the non-linear rectification device over the power range of −40 to −10 dBm (See Figure 4.5). This can maximise the PCE at the specific frequencies where the maximum ambient signal level is available.

Hence, a coupled-resonator structure with both series and shunt resonators were designed to achieve a dual-band network [124]. The linear equivalent circuit model of the SBD chip has been taken into consideration to design a dual band matching circuit at the desired frequency bands [123].

In Figure 4.5 (a), $C_{equivalent}$ represents the total capacitance of the diodes and bypass capacitor and $L_{equivalent}$ is the overall parasitic inductance of the diodes. The series *L-C* resonator (*L4* + $L_{equivalent}$ and $C_{equivalent}$) and the parallel *L-C* resonator (*C3* and *L3*) define the dual resonant circuit. The series resonator corresponds closely to the higher band specification of 852-869 MHz, whilst the parallel resonator approximates the lower 478-496 MHz band. A minimum number of components were used in order to reduce the ohmic and parasitic losses.

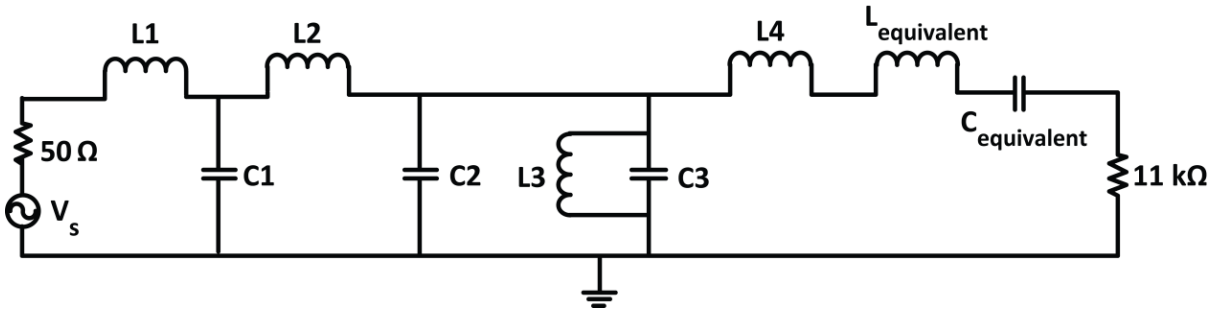

Figure 4.5 Schematic of the proposed dual resonant rectifier. Optimised parameters of the chip components are: *L1*= 3.9 nH, *C1*= 0.2 pF, *L2*= 12 nH, *C2*= 1.8 pF, *L3′*= 3.9 nH, *C3′* = 7.5 pF, *L4′* = 11.6 nH, $L_{equivalent} \cong$ 1 nH, $C_{equivalent} \cong$ 1.3pF.

The resonant frequency of each sub-circuit was determined in isolation using the following equation:

$$f = \frac{1}{2\pi\sqrt{LC}} \qquad (4.2)$$

The 852-869 MHz band resonator circuit components were calculated. Here, $C = C_{equivalent} \cong$ 1.3 pF consists of the combination of the bypass capacitor (6.8 pF) and the overall junction (C_{j0} = 0.7 pF) and parasitic capacitance (C_p = 0.08 pF) of *D1*and *D2*. Thus, *L* is calculated to be 26.5 nH in order to achieve an appropriate resonant frequency. Note that, *L* consists of L_4

and the overall parasitic inductance ($L_{equivalent} \cong 1$ nH) of *D1* and *D2*. The 478-496 MHz band resonator circuit components were calculated as $C3 \cong 15$ pF and $L3 \cong 7.2$ nH. Hence, the initial component values are determined for the two resonant circuits.

Initially these resonators were combined to achieve a dual-band structure. Then standard *LC* matching technique [124] are utilised to determine *C1*, *C2*, *L1*, and *L2* to achieve minimum reflection at the resonant frequencies. The substitution of realistic chip component values with their associated parasitics, and additions of 50 Ω microstrip lines and T-junctions introduce delays and shift the imaginary part of the input impedance. The via-holes also contribute to extra inductance in the circuit. Hence minor circuit adjustments are made in order to fine tune the resonant frequencies to the desired values. The final optimised values of the standard chip components are: $L3' = 3.9$ nH, $C3' = 7.5$ pF and $L4' = 11.6$ nH.

Large Signal S-parameter (LSSP) analysis is performed to demonstrate the matching network performance as the input power is varied. Simulation results for the input impedance of the circuit depicted in Figure 4.5 are illustrated in Figure 4.6. The proposed dual-resonant matching circuit achieves a VSWR < 2 at 478-496 MHz and 852-869 MHz for input power ranging from −40 to −10 dBm.

It should be noted that the matching circuit was designed based on the input impedance of two diodes and the output resistor and capacitor (Figure 4.2). Therefore, selecting a different value for the load resistor requires a new matching circuit.

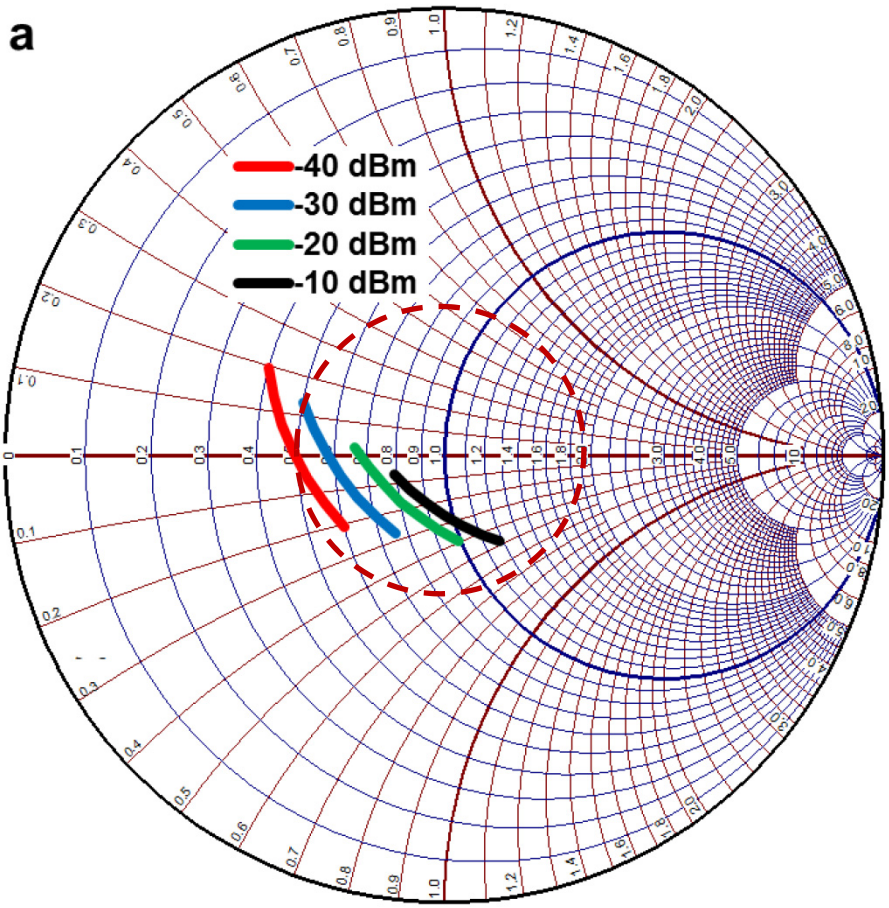
a
-40 dBm
-30 dBm
-20 dBm
-10 dBm

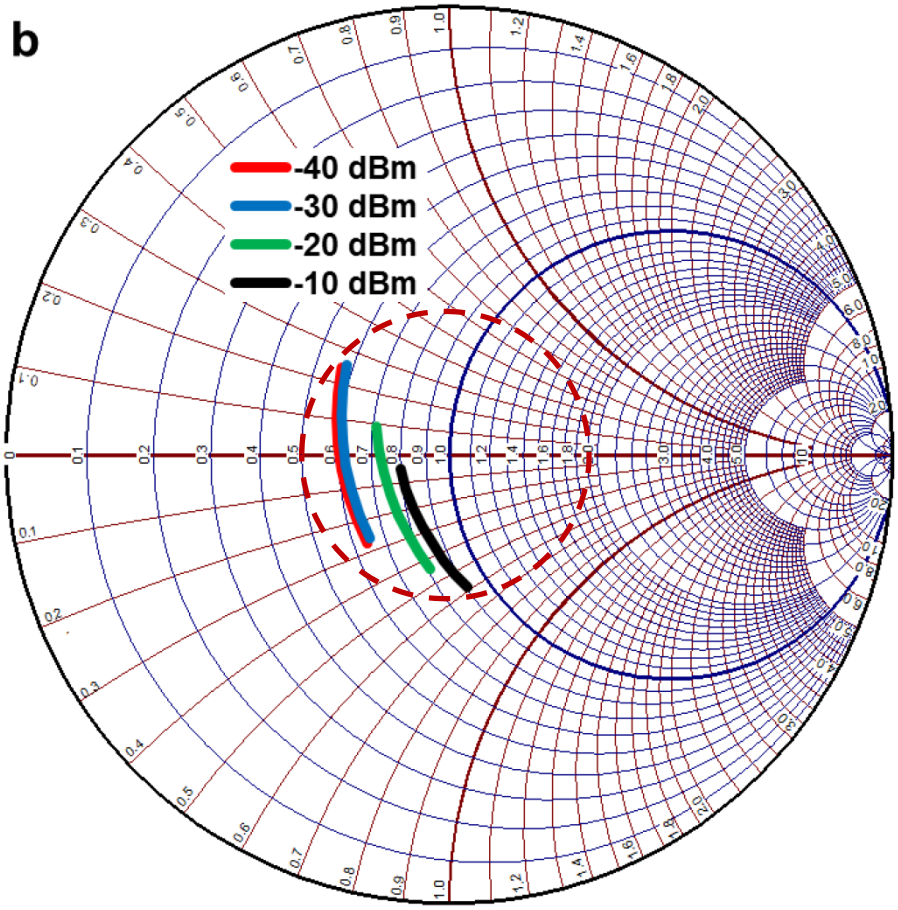

Figure 4.6 Dual resonant impedance matching with −40 to −10 dBm Input RF power. (a) 478-496 MHz. (b) 852-869 MHz. (The 2:1 voltage standing wave ratio (VSWR) boundary is shown with a dashed circle on the Smith Chart).

4.3 Results and Discussion

In order to confirm the rectification performance, the proposed dual resonant rectifier was fabricated on a 1.58 mm FR-4 substrate with a dielectric constant $\varepsilon_r \approx 4.5$ and a loss tangent $\delta \approx 0.025$. These substrate parameters were measured using the Nicolson-Ross method [125], so accurate values could be used in the rectifier design. A photograph of the fabricated dual resonant rectifier is shown in Figure 4.7 which depicts input RF port, dual-band matching network lumped components, Schottky diodes and the output terminal.

It should be noted that, in order to design a compact rectifier circuit with a reasonable size, using distributed transmission line (TL) elements are not applicable at the selected operating frequencies (478-496 MHz).

The performance of the rectifier was verified by measuring the input reflection properties, and the output power was calculated from the measured output DC voltage for the input powers ranging from −40 to −10 dBm (0.1 to 100 μW).

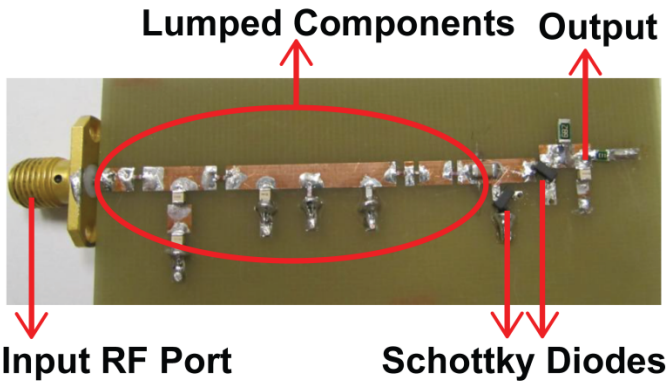

Figure 4.7 Fabricated dual resonant rectifier prototype.

4.3.1 Reflection Coefficient

The $|S_{11}|$ of the rectifier was evaluated using a vector network analyser (VNA). The VNA was re-calibrated for each input power level. Figure 4.8 compares the simulated and measured $|S_{11}|$ versus frequency for the dual resonant rectifier circuit at four different input power levels from −40 to −10 dBm. The measured results show very good agreement to the simulations. A slightly higher reflection was observed for the resonant frequencies at the lower part of the input power range (due to the diode characteristics). However, the proposed rectifier circuit is

well-matched ($|S_{11}| < -10$ dB) at the desired frequency bands of 478-496 MHz and 852-869 MHz over the broad range of input powers from −40 to −10 dBm. The small difference between simulation and measurement is due to the parasitic extraction accuracy.

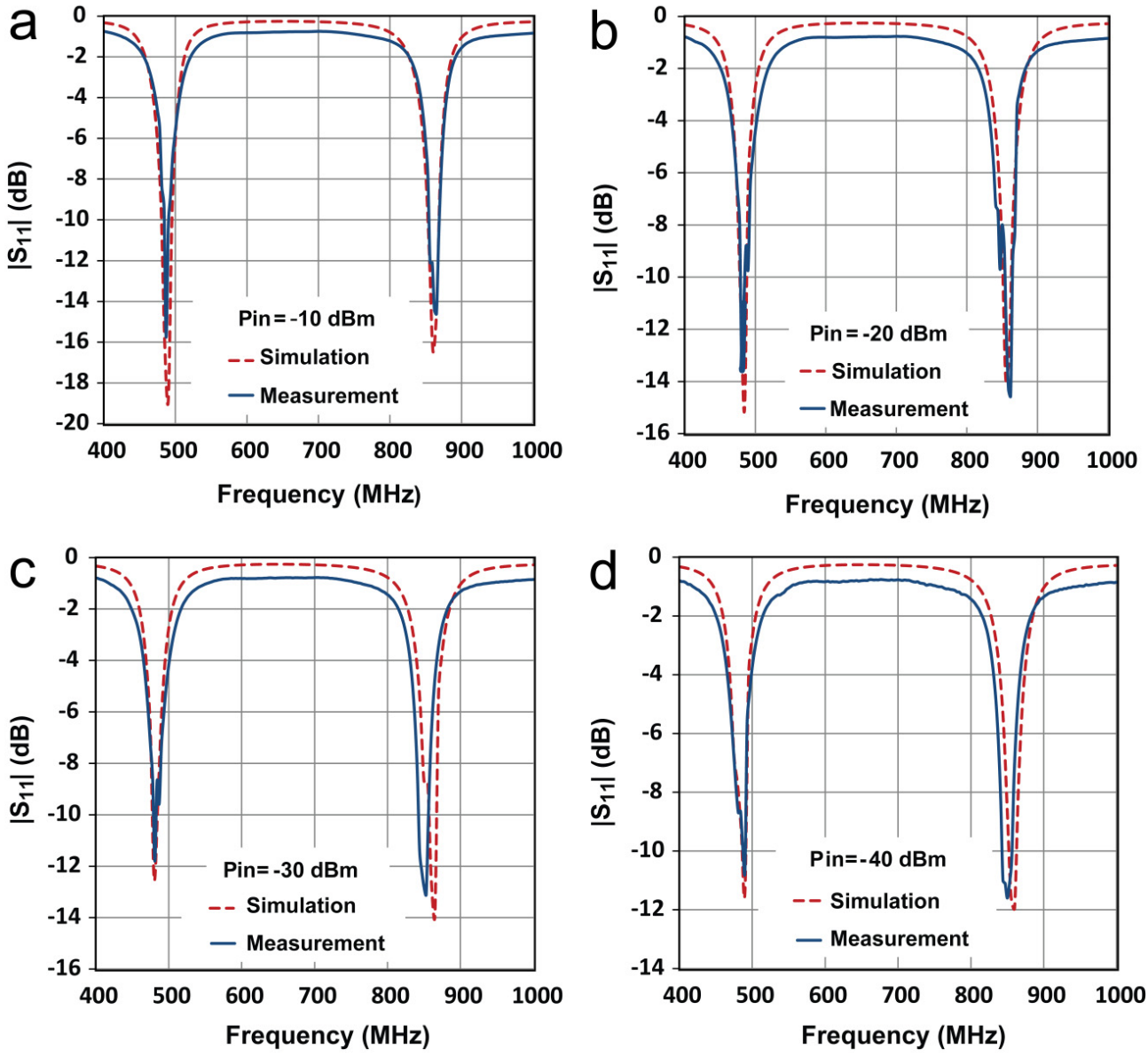

Figure 4.8 Simulated and measured $|S_{11}|$ as a function of frequency and input RF power for the proposed dual resonant rectifier circuit. (a) −10 dBm. (b) −20 dBm. (c) −30 dBm. (d) −40 dBm.

4.3.2 Output DC Power and Efficiency

In the frequency domain, the Harmonic Balance method of analysis provides a comprehensive treatment of a multispectral problem [100]. The method intrinsically takes into account the DC component and a specified number of harmonics, while allowing the ability to specify the source impedance and harmonic terminations.

A Harmonic Balance simulation was used to numerically evaluate the output DC voltage of the dual resonant rectifier for both single and dual input tones. The output DC voltage across the load resistor was also measured and used to calculate output DC power. Measurements were performed using a Wiltron 68247B synthesised signal generator as a RF power source for the rectifier circuit. Recording of the output DC voltage across the load resistance was achieved with a Fluke 79III digital voltage meter. The RF source power was initially set at −10 dBm, and decreased in 2 dB steps. In the dual-band measurement case, two RF signal generators were fed to the rectifier circuit simultaneously via a power combiner (to provide a real life scenario).

The simulation and measurement results for single and dual input tones are summarised in Figure 4.9 (a) and (b). A measured DC voltage of 772.8 mV is achieved with two simultaneous input tones at an input power of −10 dBm. For single tone measurements, DC voltages of 436 mV and 286 mV at 490 MHz and 860 MHz respectively are produced.

The comparison between the 490 and 860 MHz single rectifiers highlights the impact of the input frequency on the PCE. A higher amount of DC voltage can be generated at the lower frequency. This difference comes from decreasing diode performance at the higher frequency due to the higher junction capacitance of the diode [52].

Importantly, a slightly higher DC voltage can be generated with the dual resonant rectifier if compared to the sum of output voltage from the two single bands, particularly at the lower input power levels as can be seen in Figure 4.9 (b) which shows the lower power section of Figure 4.9 (a) in more detail.

By maximising power collection from various sources of different frequencies and delivering the combined power to the rectification circuit, the diode conversion efficiency is enhanced which results in a higher level of rectified voltage.

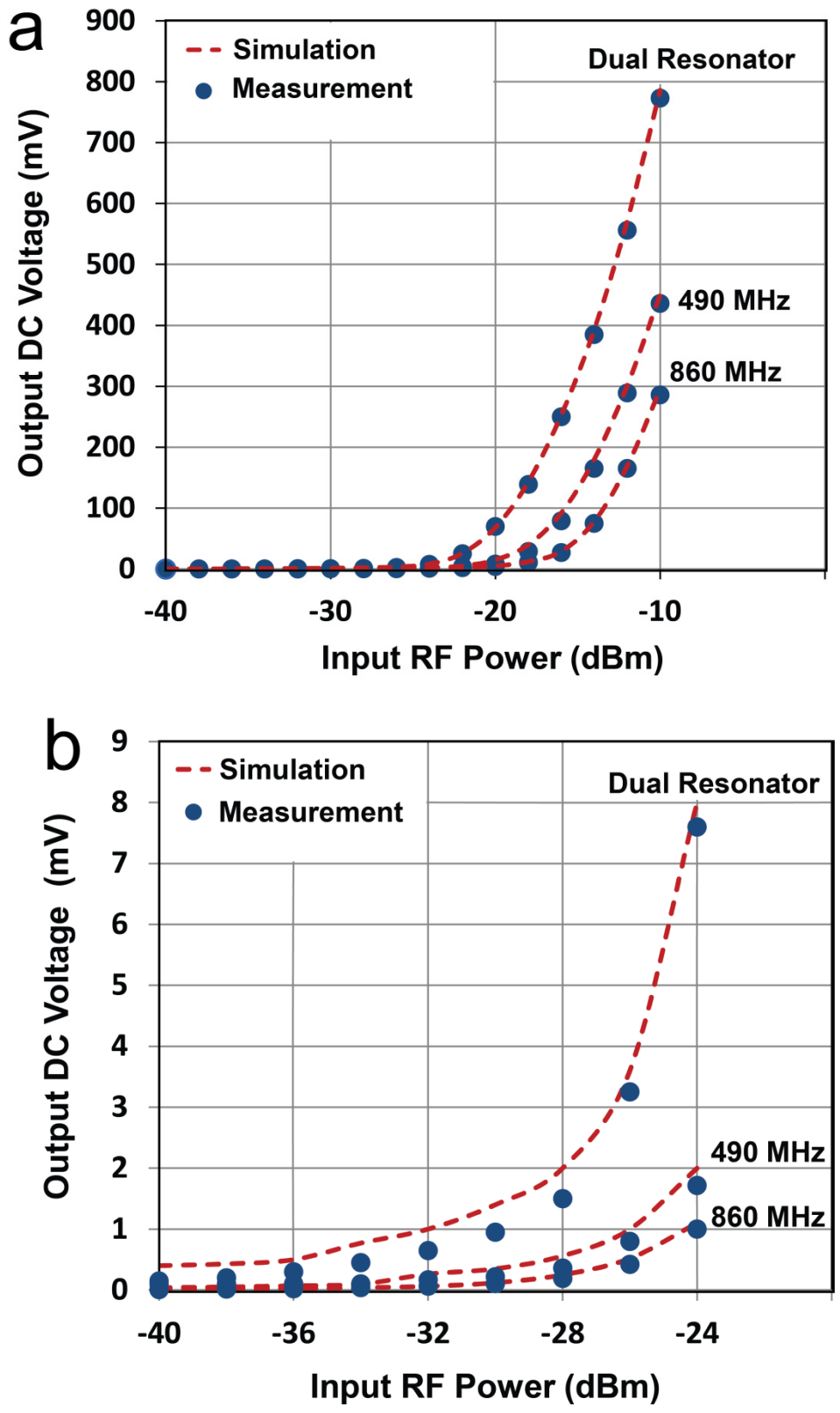

Figure 4.9 Output DC voltage as a function of input RF power for single input tone at both 490 MHz and 860 MHz and for dual input tones (a) with −40 to −10 dBm (0.1 to 100 µW) Input RF power (b) with −40 to −24 dBm (0.1 to 3.98 µW) Input RF power. (This power range is associated with the signal source).

Figure 4.10 (a) and (b) compares the simulated and measured output DC power for the dual resonant rectifier circuit with both single and dual input tones (Figure 4.10 (b) shows the lower power section of Figure 4.10 (a) in more detail). A measured DC power of 17.3 μW and 7.5 μW can be generated at 490 MHz and 860 MHz respectively with a single input tone of −10 dBm (100 μW). This represents true efficiencies of 17.3% and 7.5% for the individual single band rectification (See Figure 4.11). However, the measured DC output power with two concurrent input tones of −10 dBm is 54.3 μW which corresponds to an "effective efficiency" of 54.3% for the dual-band rectifier (See Figure 4.12 (a) and (b)). This represents a 3.14 and 7.24 times increase in output DC power over the single tone excitation at 490 MHz or 860 MHz respectively.

This trend is evident down to low input power levels (around 40 μW). Furthermore, there is a significant increase in the PCE of the dual resonant rectifier for lower input power levels (< 40 μW) compared to the single resonant rectifier.

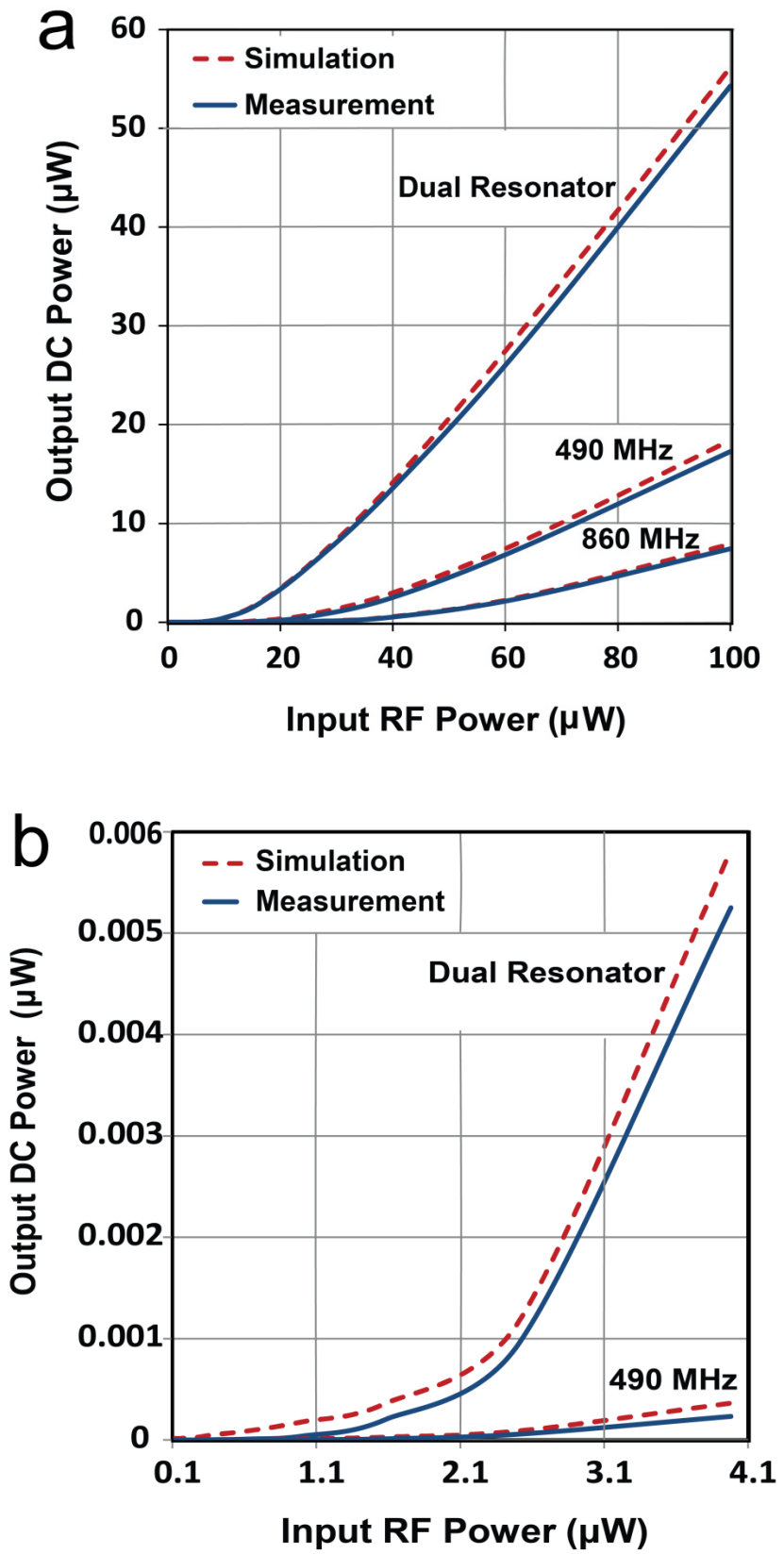

Figure 4.10 Output DC power as a function of Input RF power for single and dual input tones**.** (a) With 0.1 to 100 µW (−40 to −10 dBm) Input RF power. (b) With 0.1 to 3.98 µW (−40 to −24 dBm) Input RF power (at very low input power, the output power of single tone at 860 MHz is very low compared to the dual resonator output power.)

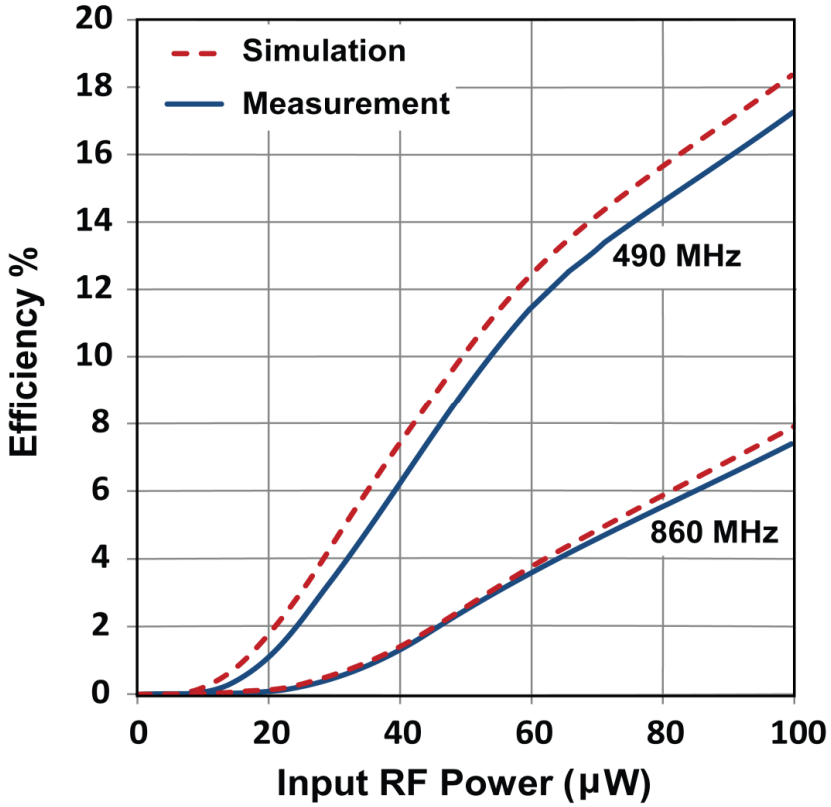

Figure 4.11 RF to DC conversion efficiency as a function of input RF power for single band rectification.

Here, the effective efficiency (Figure 4.12 (a) and (b)) is defined as the ratio of output DC power to the available input RF power rather than the power delivered to the diodes (equation (4.3)). The available power level is associated with the signal source. For the single resonator, the available input power is −10 dBm and the delivered power is also −10 dBm (assuming no loss). However, by creating a dual resonant matching network the power delivered to the diodes is close to −7 dBm (combined total input power from two signal generators) but the available power is still −10 dBm. Hence, in the "effective efficiency" calculation where two tones of −10 dBm are applied to the rectifier, the input power is considered as −10 dBm (which is the available input power).

$$\eta = \frac{P_o}{P_i} = \frac{\left(\frac{{V_o}^2}{R_L}\right)}{P_i} \qquad (4.3)$$

Therefore, delivering multiple input RF signals into a single rectification stage results in a high sensitivity rectifier, which is widely applicable to real environmental RF energy scavenging.

This multi-band technique can provide higher DC power than combining two separate single frequency rectifier circuits operating at the same frequencies. This is due to the fact that harvesting RF energy from various available sources simultaneously increases the delivered power to the rectifier, which improves the diode conversion efficiency and consequently enhances the output DC power. Table 4.1 summarises this work as compared to previous published works.

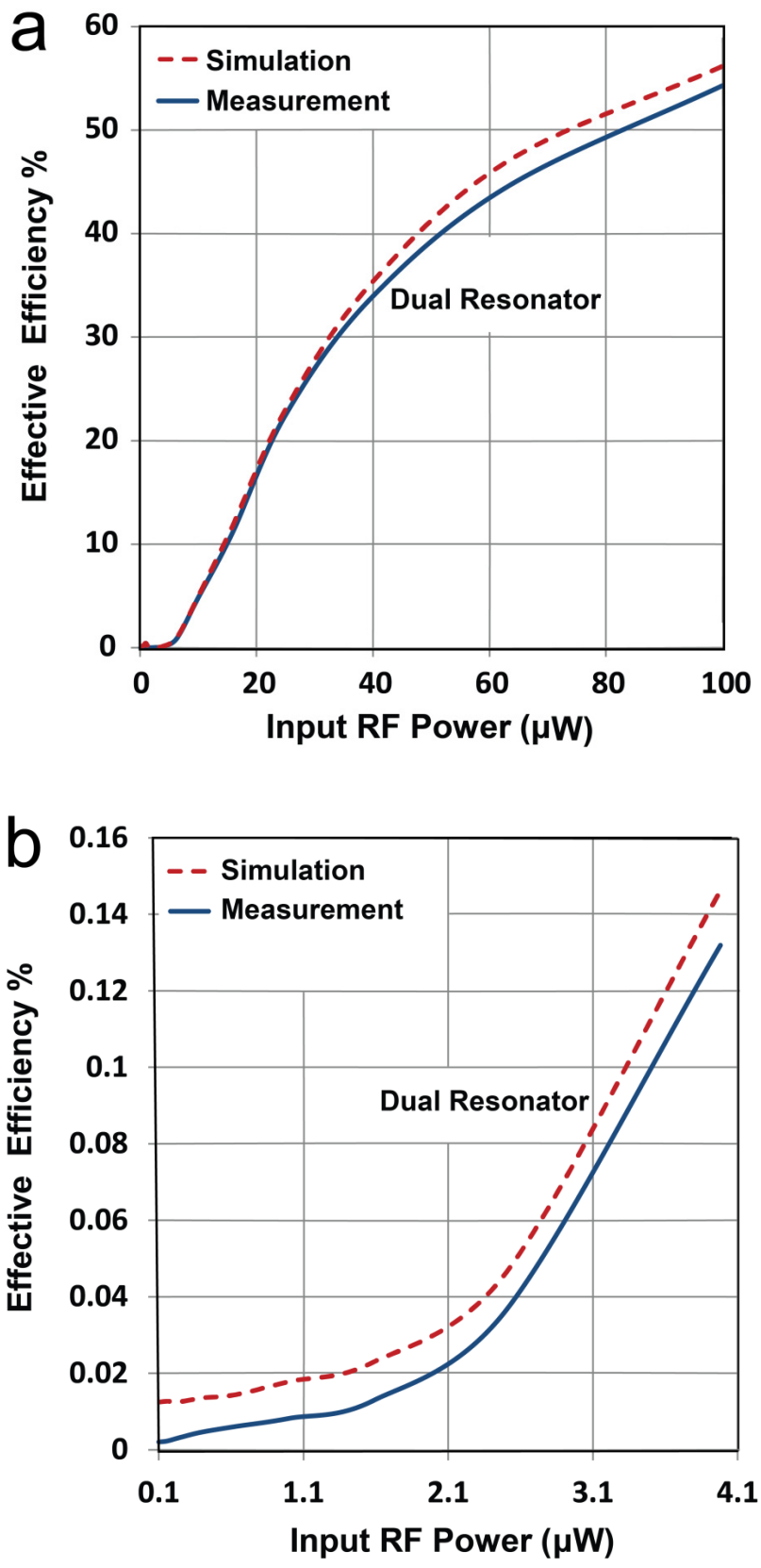

Figure 4.12 Effective RF to DC conversion efficiency as a function of Input RF power for dual resonant rectification. (a) With 0.1 to 100 μW (−40 to −10 dBm) input RF power.
(b) With 0.1 to 3.98 μW (−40 to −24 dBm) RF input power.

Table 4.1 RF Energy Scavengers Comparison

Ref.	Technology	Measured Efficiency (%)	RF Power Variation (in PCE Evaluation)	Rectification Technique
[79]	Schottky diode	82@50 mW	N/A	Single resonator
[56]	Schottky diode	44@−10 dBm	N/A	Single resonator
[100]	Schottky diode	20@0.07 mW/cm^2 0.1@10^{-5} mW/cm^2	10^{-5} to10^{-1} mW/cm^2	Broad band
[93]	Schottky diode	77.13@22 dBm (158.49mW)	0 to 160 mW	Dual resonator
[94]	CMOS	9.1@−19.3 dBm(900MHz) 8.9@−19 dBm(2GHz)	N/A	Dual resonator
[95]	Schottky diode	37(915MHz)@−9 dBm 30(2.45MHz)@−9 dBm	−40 to 0 dBm	Dual resonator
[82]	Schottky diode	84.4@89.84 mW (2.45GHz) 82.7@49.09 mW (5.8GHz)	0 to 100 mW	Dual resonator
[58]	Schottky diode	80@10 dBm (940MH) 47@8 dBm (1.95GHz) 43@16 dBm (2.44GH)	−14 to 20 dBm	Triple resonator
[91]	Schottky diode	50@−5 dBm	−25 to 0 dBm	Dual resonator with tunable input response
This work	Schottky diode	54.3@−10 dBm 11.25@−18 dBm (490 and 860 MHz)	−40 to −10 dBm (0.1 to 100 µW)	Dual resonator

It should be highlighted that, although using different loads for different input powers results in maximum power transfer, this is not applicable in a real life scenario. In reality, a fixed rectifier circuit is required to harvest a broad range of RF power with a determined load resistor. Hence, the optimised value of the load (11 KΩ) was used for all power levels (as discussed in Section 4.2.3). In order to evaluate the sensitivity of PCE to the load, different values of resistors are selected and efficiencies are simulated (See Figure 4.13). It is evident that, when the load value is altered by 20% (e.g. 9.1 KΩ and 13 KΩ), PCE only degrades by about 1%. This shows PCE is quite insensitive to the load resistor. However, by changing the load value substantially (e.g. 1 KΩ and 51 KΩ), PCE degrades significantly.

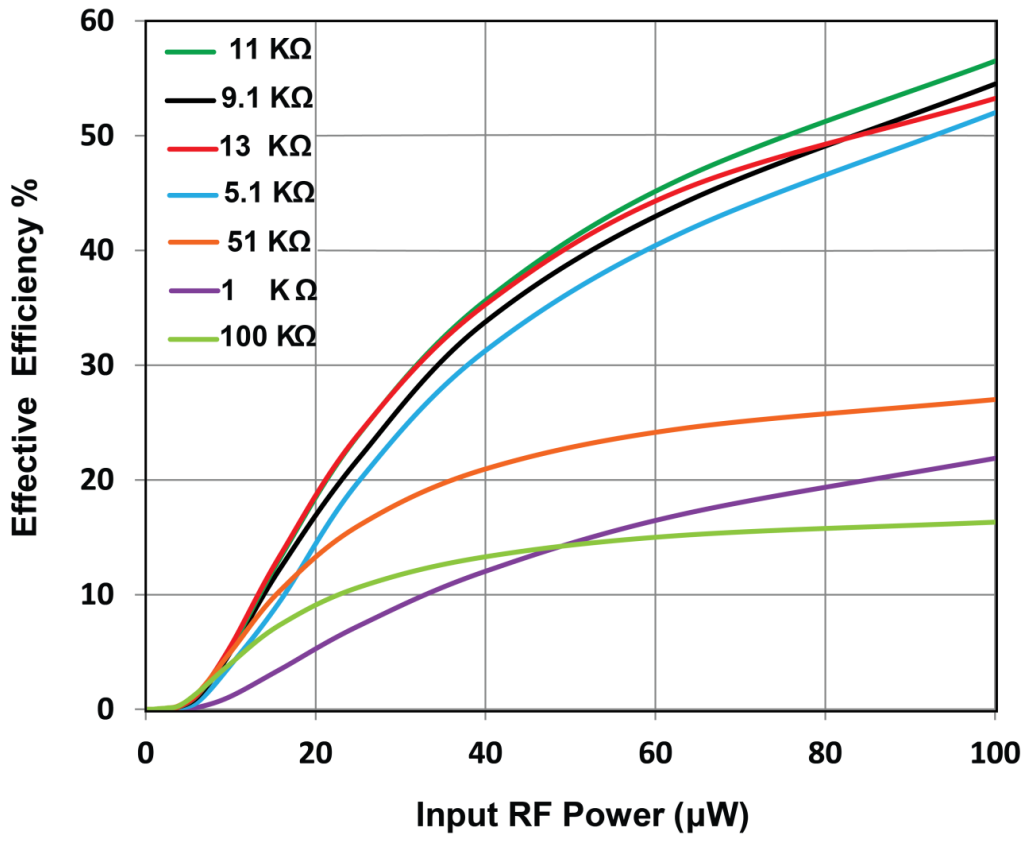

Figure 4.13 Effective RF to DC conversion efficiency as a function of input RF power for dual resonant rectification with different load resistors over 0.1 to 100 µW (−40 to −10 dBm) Input RF power.

4.3.3 Real Environmental Measurements of the Dual-Band Rectifier

In order to provide a realistic scenario for the proposed dual-band rectifier, measurement results were taken in three suburbs of Melbourne, Australia, congruent with Chapter 3 outcomes. Table 4.2 summarises these environmental measurement results.

It should be noted that the lower band (478-496 MHz) has a 3.67% fractional bandwidth and the higher band (852-869 MHz) has approximately 2% fractional bandwidth. Hence, various RF frequencies from different sources can be harvested within these two bands. The environmental measurement results demonstrate the feasibility of harvesting ambient EM energy from multiple sources simultaneously.

Table 4.2 Environmental Measurement Results of the Dual-Band Rectifier

Suburb	Available Frequencies (MHz)	Respective Available RF Power (dBm) [µW]	Measured DC Power (µW)	PCE (%)
Bayswater	486, 488, 489, 490 491, 867, 868, 869 870, 871, 872, 873 874	−19[12.5], −20[10], −17[19.95], −15[31.62] −22[6.3], −37[0.199], −37[0.199], −30[1] −24[3.98], −20[10], −30[1], −37[0.199] −40[0.1]	39.38	40.57
Bentleigh	491, 492, 494, 495 865, 866, 867, 868 869, 870, 871	−12[63.09], −46[0.02],−42[0.063],−57[0.001] −27[1.99], −27[1.99], −30[1], −37[0.199] −40[0.1], −40[0.1], −41[0.07]	30.9	45.02
RMIT University (Melbourne CBD)	487, 488, 489, 490 491, 851, 861, 862 866, 867, 868, 869	−30[1], −22[6.3], −29[1.25], −22[6.3] −20[10], −23[5.01], −21[7.94], −21[7.94] −30[1], −35[0.31], −40[0.1], −40[0.1]	14.5	30.68

4.4 Conclusion

The feasibility of harvesting ambient EM energy from multiple sources simultaneously is investigated in this chapter. The proposed dual resonant rectifier operates at two frequency bands (478-496 and 852-869 MHz), which are used for broadcasting and cellular systems. The dual resonant rectifier exhibits favourable impedance matching over a broad input power range (−40 to −10 dBm) at these two bands. The achieved sensitivity and dynamic range demonstrate the usefulness of this innovative low input power rectification technique.

Simulation and experimental results of input reflection coefficient and rectified output power are in excellent agreement. The measurement results demonstrate that a two-tone input to the proposed dual-band RF energy harvesting system can generate 3.14 and 7.24 times more power than a single tone at 490 or 860 MHz respectively, resulting in a measured effective efficiency of 54.3% for a dual-tone input power of −10 dBm.

It is evident that this dual resonant rectification technique increases the RF to DC effective conversion efficiency, and hence the recoverable DC power for low power applications. Furthermore from a design and economic perspective, utilising a large number of components (e.g. diodes) to realise individual rectifier circuits for each frequency band creates additional expense (e.g. multi-band rectifiers with DC combing method). The proposed dual-band rectifier circuit could harvest two bands concurrently, using a minimum number of components.

In order to provide more realistic measurement results, the proposed dual-band rectifier was tested in three suburbs of Melbourne, Australia. The proposed highly sensitive rectifier has 3.67% and 2% fractional bandwidth at the lower and the higher band respectively and hence, various RF source frequencies can be scavenged within these two bands. It was shown that

the rectifier could generate 39.38 μW by harvesting RF energy from two bands in the suburb of Bayswater.

Therefore, this dual-band technique offers a simple and cost-effective solution which is of paramount importance for environmental power harvesting systems. This innovative technique has the potential to generate a viable energy source for low power applications in urban environments.

Chapter 5 – Highly Sensitive Rectenna Embedded in Building Materials

5.1 Introduction

RF energy harvesting is a promising solution to provide a sustainable energy source for the long-term conservation of the environment and the global economy. RF energy scavenging has the advantage of diffracting from and penetrating inside building materials and hence can be harvested inside the buildings as well. Therefore, an innovative idea is proposed in this chapter to embed a highly sensitive and efficient rectenna system in building materials to harvest ambient RF energy and generate a viable energy source in urban environments, predominately for low power applications (e.g. home and office devices).

Since ambient RF energy levels are lower than those that can be generated by a dedicated RF source, the efficiency and sensitivity of the harvesting system are of paramount importance. Furthermore, the scavengeable power level is generally unknown; different to WPT (wireless power transmission); hence, input power variation should be considered when designing a rectification network.

In spite of all the achievements in rectenna design, a vast majority of the literature has focused on harvesting RF energy at a given and often high input power level (e.g. WPT

scenarios). As it has been discussed in Chapter 2 and demonstrated in Chapter 4, harvesting at a sensitivity of below −40 dBm (0.1 μW) has not been achieved.

Based on the outcomes from Chapter 3 and 4, in order to increase the amount of RF energy scavenged by a rectenna, it is crucial to identify and harvest various ambient frequency sources over their realistically available energy range. In Chapter 4, a new approach to harvest ambient RF energy from multi tones simultaneously was proposed. A sensitive dual-band rectifier has been developed using a minimum number of components and has achieved an effective efficiency of 54.3% for dual input tones of −10 dBm. The power conversion efficiency (PCE) and large signal analysis were shown over a broad low input power range (−40 to −10 dBm), and a fractional bandwidth of less than 4% was reported at each band. However, higher sensitivity (as discussed in Chapter 3) and efficiency are required for environmental RF energy scavenging. To address this, harvesting energy over a wider frequency band could increase the sensitivity and hence the output DC power. This can be achieved by scavenging more RF signals and deliver more power to the rectification device.

Although widening the matching network bandwidth would be a solution to capture energy across a large section of the available spectrum, there are some drawbacks. Ultra-widening the bandwidth may not result in higher sensitivity, and efficiency. This is due to the reduction in the quality factor of rectifier circuit which is inversely proportional to its bandwidth [108].

Furthermore, from a design point of view, it is very challenging to realise a broadband rectifier due to the non-linearity of the diode impedance with input power across the frequency band. Hence, ultra wideband rectifier is not an optimum solution for ambient energy harvesting as this typically results in very low efficiency at any specific frequency [100].

Therefore, in this chapter a broadband matching network with an optimum bandwidth is selected in order to capture RF energy from various frequencies concurrently and also to satisfy the Bode-Fano limits in matching network design [108]. The proposed rectifiers are able to operate over a broad range of very low input RF power for low-power rectification.

It should be noted that, throughout this work, broad band refers to up to 22% fractional bandwidth with the low insertion loss.

Hence, the embodiment in this chapter realizes rectifier circuits with 12.6 % and 22% fractional bandwidths (neither narrow band, nor ultra-wideband) in the 520-590 MHz and 89-111 MHz bands respectively. These bands are allocated to the television and FM broadcasting services respectively, as shown in the Australian Radiofrequency Spectrum Plan [114]. When considering the measurements carried out in Chapter 3, these broadcasting bands provide stable RF scavenge sources with a suitable level of ambient RF power. They are also widely available in most metropolitan areas as demonstrated within Chapter 3.

Furthermore, the practicality of embedding RF energy harvesting systems in building materials is investigated, creating a structurally integrated energy scavenging system. To address this, the proposed FM band rectifier is integrated with a simple dipole antenna to realise a rectenna. The rectenna is then embedded into building materials (plaster board), creating an innovative harvesting system, aiming to provide a sustainable, green, and inexpensive energy source for use in urban environments.

This research focuses on real life RF energy scavenging methods to provide electrical energy for home and office devices. This chapter is dedicated to harvest RF energy from multiple frequencies simultaneously to enhance the sensitivity and hence increasing the output DC power. The proposed FM band rectenna achieves a sensitivity of −50 dBm (0.01 μW), which to the best of knowledge is the highest sensitivity reported for an ambient energy harvester.

5.2 Concept of Embedding Rectennas in Building Materials

The key vision of this section is to investigate the practicality of embedding efficient and sensitive RF energy harvesting systems in building materials. This synergy between a rectenna and the surrounding building materials can create a structurally integrated energy scavenging system.

A conceptual illustration of a RF energy harvesting system embedded in plaster is depicted in Figure 5.1. Here, rectified DC power will be available in the building through DC sockets with different voltage setting; removing the need for AC adaptors in many applications. With the integration of the rectenna within structural materials, there is no need for external panels to be mounted on the building. These structural panels can be integrated in existing building structures such as roofs or walls. Hence, additional installation and fabrication costs can be reduced. The creation of efficient rectenna arrays in buildings provides potential for a sustainable and green energy source in urban environments, predominately for low power applications (e.g. home and office devices).

Figure 5.2 also depicts the proposed system for exploiting embedded rectennas in building materials for RF energy harvesting (an antenna is integrated with the rectifier to realise a rectenna). In outdoor scenarios, numerous rectennas can be embedded in roof tiles and a DC path can be provided by roof tile hooks. For indoor scenarios, rectennas can be integrated with wall or ceiling plaster boards. DC current produced by each rectenna element will be combined and made available through DC sockets with different voltage settings.

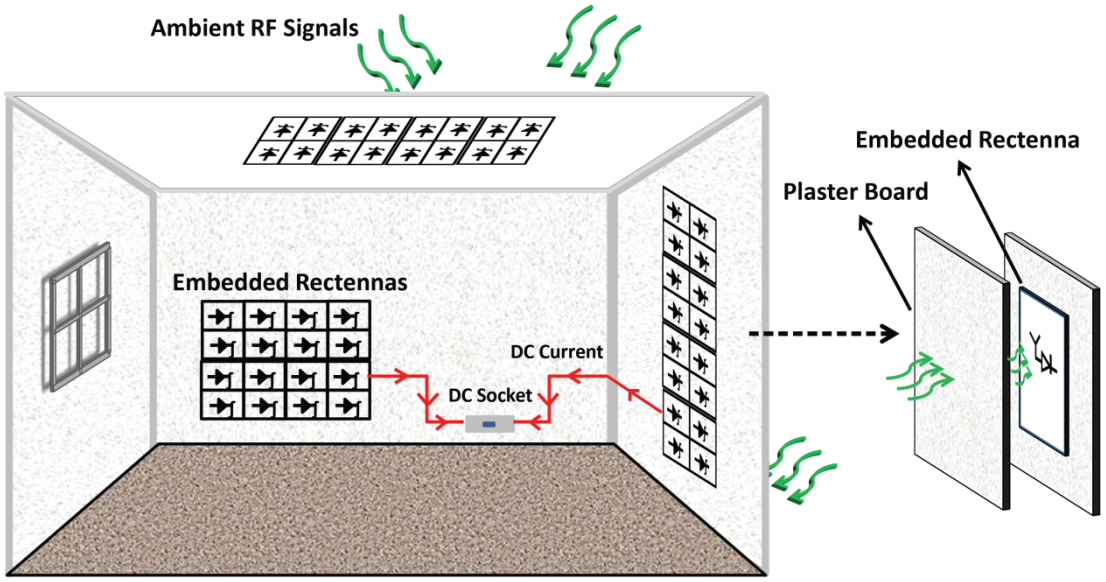

Figure 5.1 Embedded rectenna in plaster for RF energy harvesting.

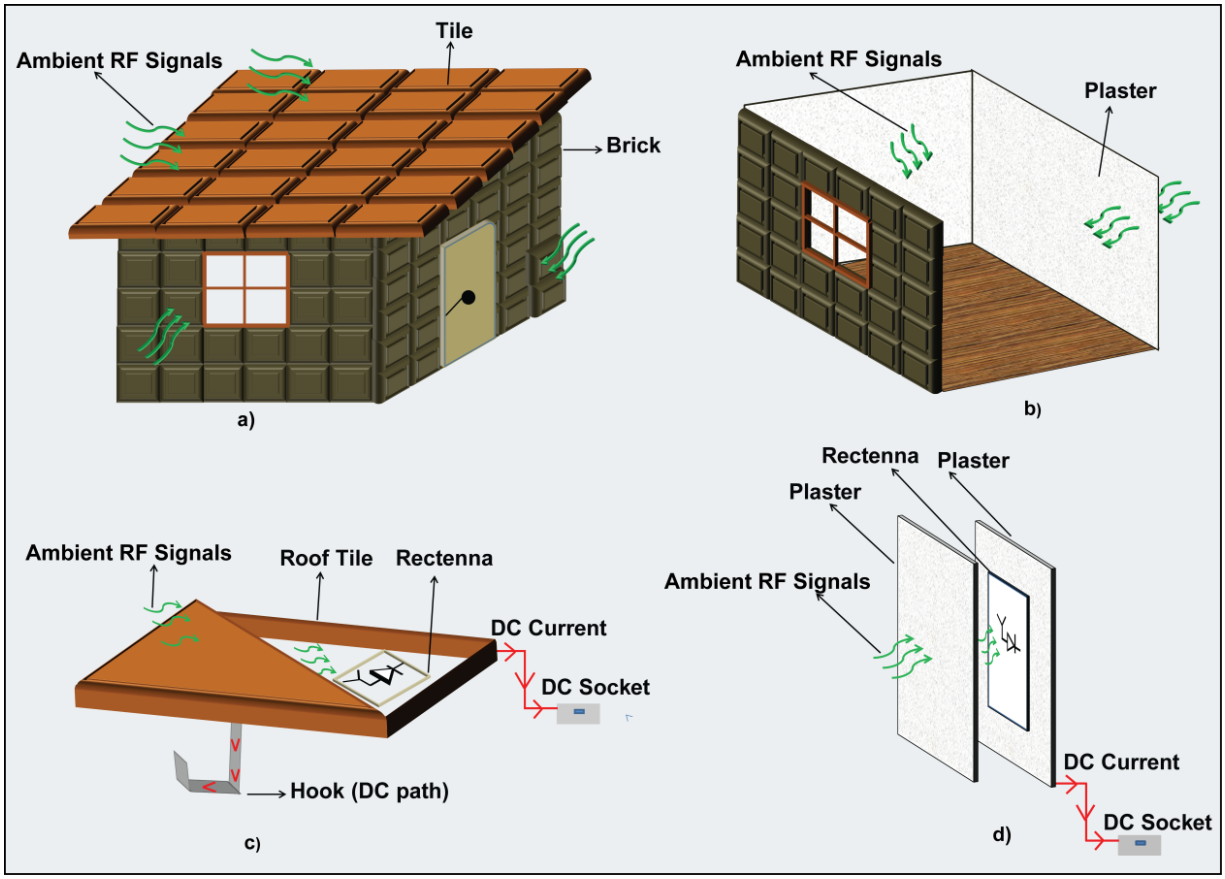

Figure 5.2 Embedded rectennas in building materials for RF energy harvesting. (a) Outdoor scenario. (b) Indoor scenario. (c) Embedded rectenna in a roof tile. (d) Embedded rectenna in a plaster board.

Various home and office devices will benefit from such an RF energy harvesting system. Devices can include laptops, mobile phones, chargers, portable devices (toothbrush, electric shaver, digital camera, hand held drilling machine, etc.), sensors in smart buildings, and generally any DC powered user devices (Figure 5.3). Hence, this innovative idea offers a simple and cost-effective alternative solution to generate DC power from dissipated RF signals.

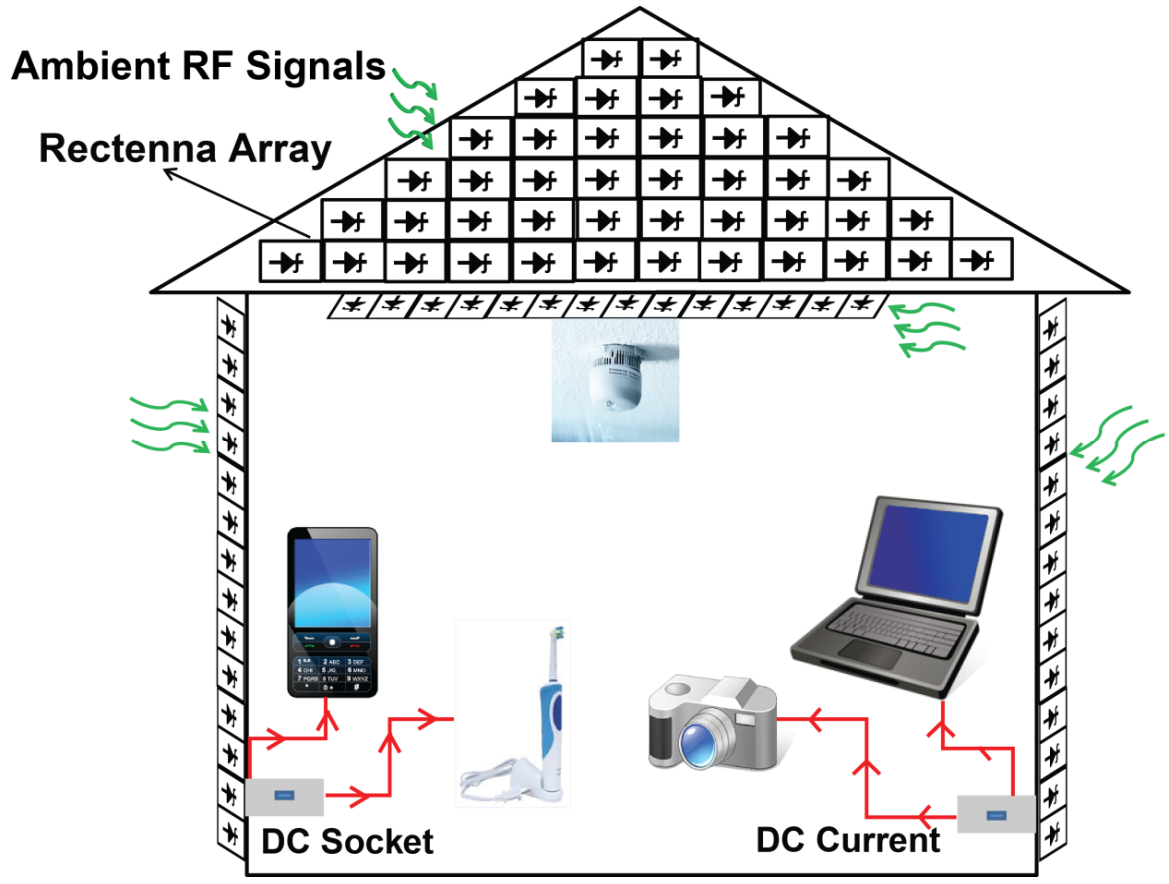

Figure 5.3 RF energy scavenging applications in urban environments.

5.3 Television Broadcasting Band (520- 590 MHz) Rectifier Design

Generating high DC output power is the main task when designing an efficient RF scavenger. Hence as discussed in previous chapters, a highly sensitive rectifier is essential for very low RF energy harvesting. Towards this goal, a sensitive rectification device with a very low turn on voltage is required. Therefore, in this work, a sensitive microwave Schottky detector HSMS2850 (C_j = 0.18 pF, R_s = 25 Ω, I_s = 3 × 10^{-6} A) [53, 126] is chosen with only 150 mV threshold voltage. This makes it suitable for rectification at low ambient energy levels. In order to enhance the sensitivity, the selected diode in this chapter is more sensitive than the diode used in Chapter 4 (HSMS2850 is more suitable for power levels below −20 dBm, however, it works reasonably up to 0 dBm).

The embodiment in this section realizes a rectifier circuit with 12.6% fractional bandwidth operating at 520-590 MHz over −40 to −10 dBm. This rectifier is able to produce a higher amount of DC power compared to the rectifier in Chapter 4, with a single tone excitation due to the high sensitivity rectification device and lower operating frequency (compared to the 860 MHz resonator in Chapter 4).

5.3.1 Voltage Doubler and Matching Network Design

As recommended in Chapter 4, in order to enhance the sensitivity, a voltage doubler rectifier structure (Figure 5.4), is considered as a core of the RF-DC power conversion system since this topology is appropriate for low power rectification. Large Signal S-Parameter analysis in Agilent ADS software was used to specify and optimise the load impedance and bypass capacitor (C_{bypass} = 2 pF, R_{load}= 7.5 KΩ).

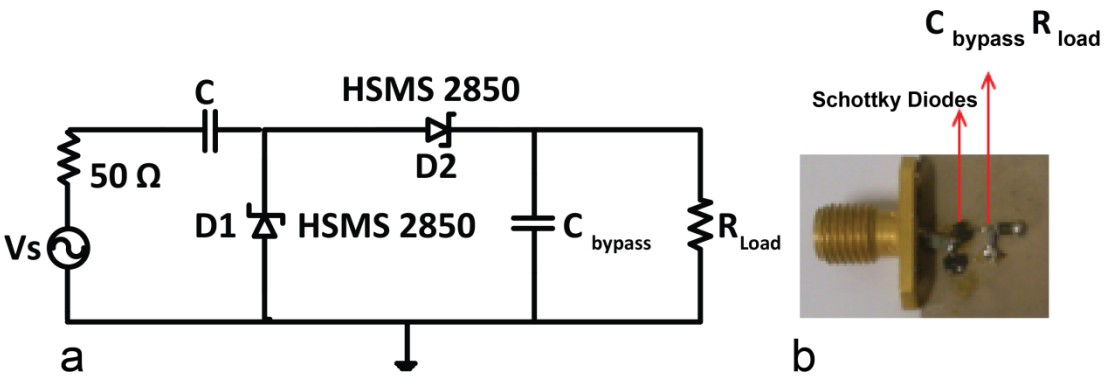

Figure 5.4 (a) Schematic of a voltage doubler rectifier without matching network. (b) Fabricated voltage doubler prototype.

The input impedance of the circuit depicted in Figure 5.4 (a) is analysed using a Harmonic Balance (HB) simulator and a nonlinear model of the diodes in ADS over the frequency range of 500 to 600 MHz at various low input power levels. Large Signal S-parameter (LSSP) analysis was performed and various input RF powers are fed directly to the Schottky diodes configuration of Figure 5.4 which does not have a matching network in order to find approximate input impedance value as the starting point (defining the load impedance). A vector network analyser (VNA) was also used to measure the input impedance of the device (Figure 5.4 (b)) and validate the simulation results as shown in Figure 5.5 and summarised in Table 5.1.

As it can be seen in Figure 5.5, with increasing the source power (−10 to 0 dBm), the diode impedance is changing and it is beginning to switch on. The simulation and measurement results of Figure 5.5 demonstrate that the diode input impedance does not drastically change with low power range (e.g. at −20 dBm) as the diode is turned off.

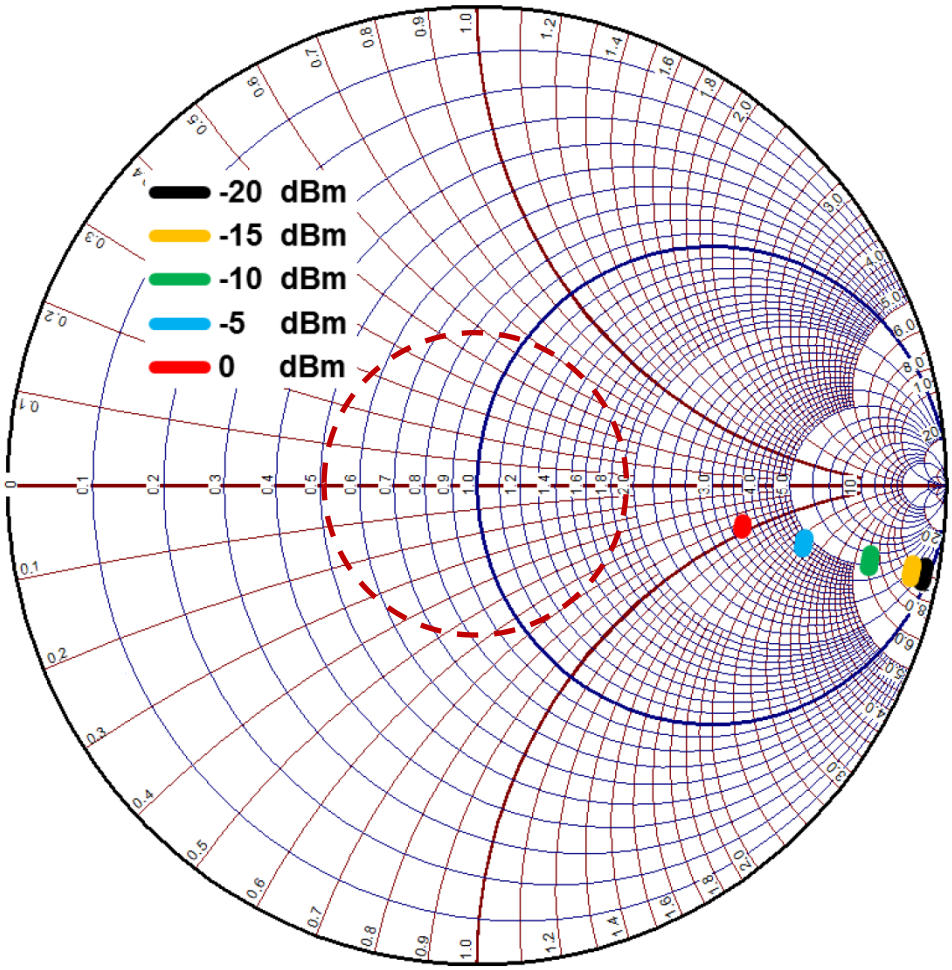

Figure 5.5 Voltage doubler input impedance calculated with Large Signal S-parameter (LSSP) analysis and measured with VNA over the frequency range of 500 to 600 MHz with various unmatched input power levels (−20 to 0 dBm). (The 2:1 voltage standing wave ratio (VSWR) boundary is shown with a dashed circle on the Smith Chart).

Table 5.1 Voltage Doubler Input Impedance Over 500-600 MHz

Input RF power (dBm) [µW]	500 MHz	600 MHz
−20 [10]	50*(1.98−j*11.25)	50*(1.42−j*9.44)
−15 [31.62]	50*(3.56− j*10.51)	50*(2.58−j*9.01)
−10 [100]	50*(6.1−j*6.27)	50*(4.97−j*6.1)
−5 [316.22]	50*(4.9−j*2.09)	50*(4.58−j*2.33)
0 [1000]	50*(3.49−j0.78)	50*(3.42−−j*0.91)

As discussed in Chapter 4, the objective is to match the input impedance of the device to 50 Ω at the television broadcasting band over a broad range of input RF powers (−40 to −10 dBm). Hence, a shunt-*C* coupled band pass filter consisting of series resonant *L*-*C* circuits coupled via shunt capacitors are used to design a matching network with desired bandwidth [124, 127].

The advantage of coupled-resonator filters is that they do not require a wide range of inductance values. Furthermore, by placing series capacitors on either side of the inductors, the inductors can be made to operate in differential mode around the pass band. Therefore, the high *Q* resonator decreases the pass band insertion losses [128]. Using filter synthesis [124, 127], a high *Q* band pass matching circuit with a fractional bandwidth of 12.6% is designed and is depicted in Figure 5.6.

Surface Mount Technology (SMT) components with their package parasitics were considered in the simulation to achieve accurate results. Further circuit optimizations are applied in order to fine tune the matching circuit components to achieve the desired bandwidth.

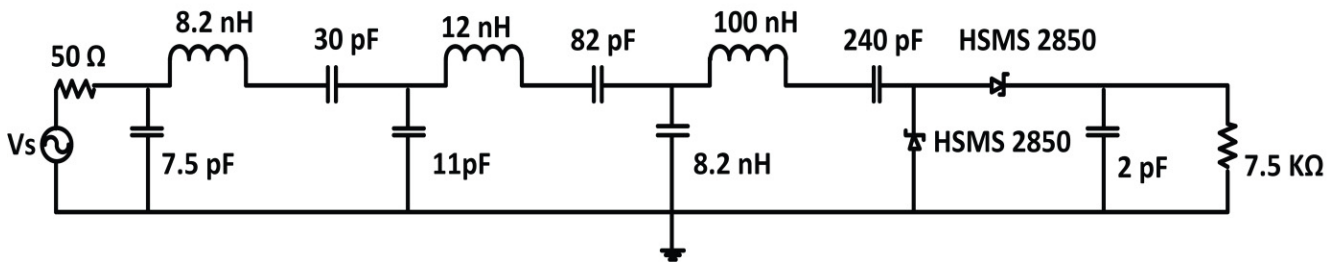

Figure 5.6 Schematic of the proposed TV band rectifier circuit.

5.3.2 Results and Discussions of the TV Band Rectifier

5.3.2.1 Reflection Coefficient

In order to evaluate the matching network performance with various input power levels, large Signal S-parameter (LSSP) analysis is conducted. Simulation results for the input impedance of the circuit depicted in Figure 5.6 are illustrated in Figure 5.7.

The proposed matching circuit achieves a VSWR < 2 over 520-590 MHz for input power ranging from −40 to −10 dBm (0.1 to 100 μW). Figure 5.8 shows the simulated |*S11*| versus frequency for the rectifier circuit at four different input power levels. The proposed rectifier circuit is well matched (|*S11*| < −10 dB) at the desired frequency band over the broad range of low input powers (−40 to −10 dBm).

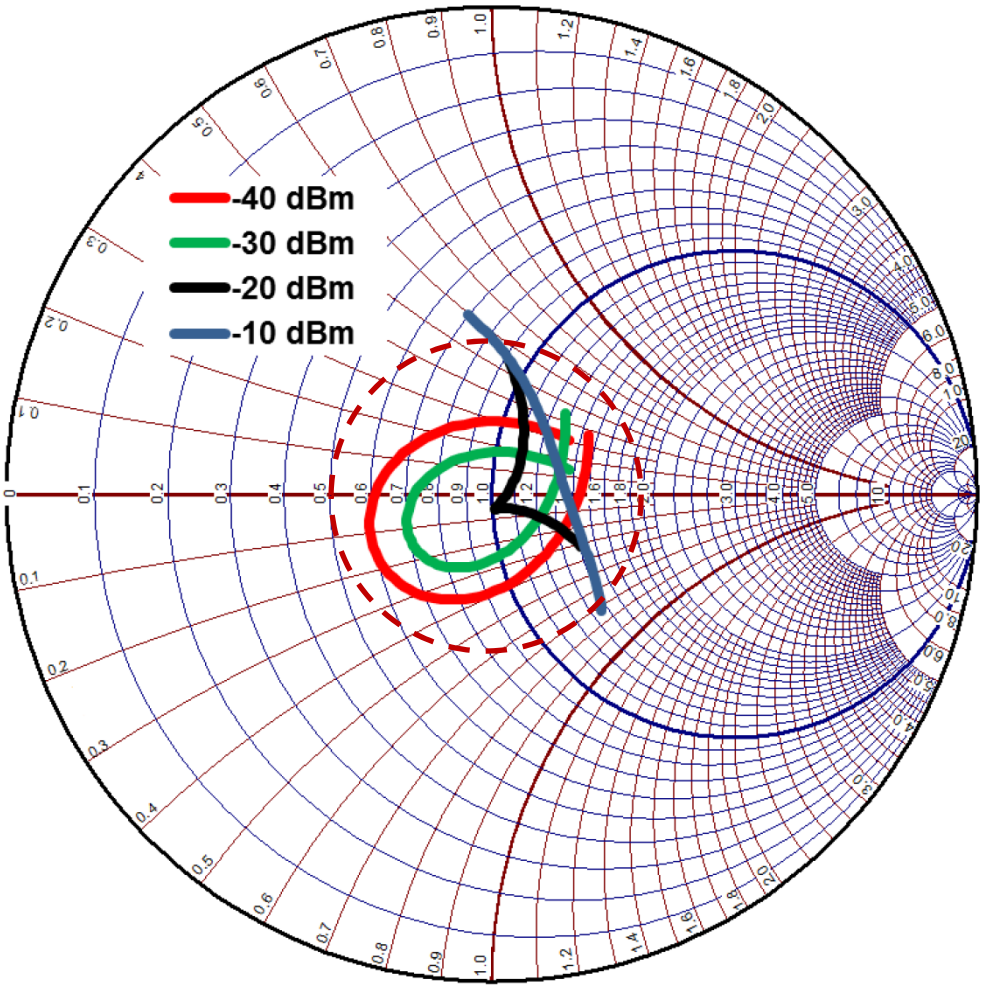

Figure 5.7 TV band rectifier impedance matching over 520-590 MHz, with −40 to −10 dBm (0.1 to 100 µW) Input RF power. (The 2:1 voltage standing wave ratio (VSWR) boundary is shown with a dashed circle on the Smith Chart).

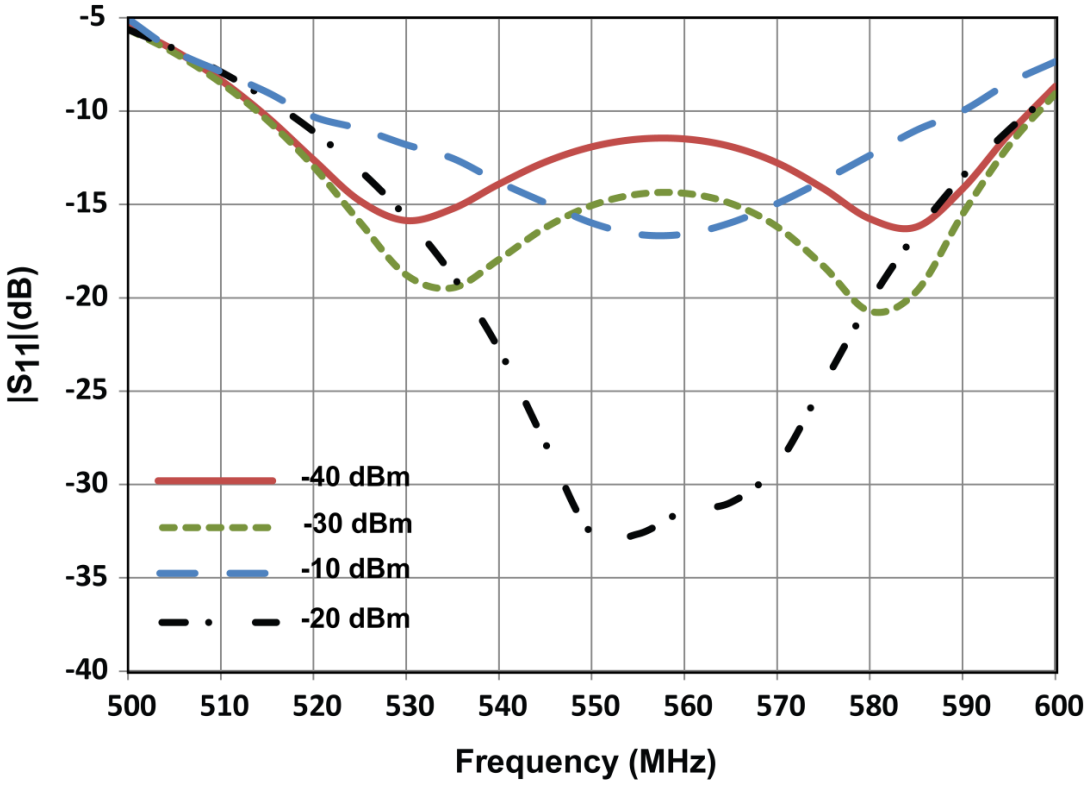

Figure 5.8 Reflection coefficient $|S_{11}|$ as a function of frequency and input RF power for the proposed sensitive TV band rectifier.

5.3.2.2 Output DC Power and Efficiency

Several properties of the diode (e.g. nonlinear capacitance and reflected harmonic energy from the diode) at microwave frequencies require a comprehensive frequency-domain approach (discussed in Chapter 4). Hence, in the frequency domain the output DC voltage of the rectifier was evaluated using a HB simulation. This method inherently considers the DC parts and a specified number of harmonics; also the source impedance and harmonic terminations can be determined. The output DC power was then calculated using the output DC voltage across the load resistor (Figure 5.9).

As demonstrated, the DC power of 53 µW and 0.0015 µW can be generated with a single tone input of −10 dBm (100 µW) and −40 dBm (0.1 µW) respectively, which demonstrates an improved performance over the rectifier of Chapter 4 with a single tone excitation (comparing simulation results only). This is mainly due to the high sensitivity rectification device utilised in this design. Furthermore, at higher frequencies (e.g. 860 MHz in Chapter 4), higher junction capacitance degrades the diode efficiency and hence the rectifier performance.

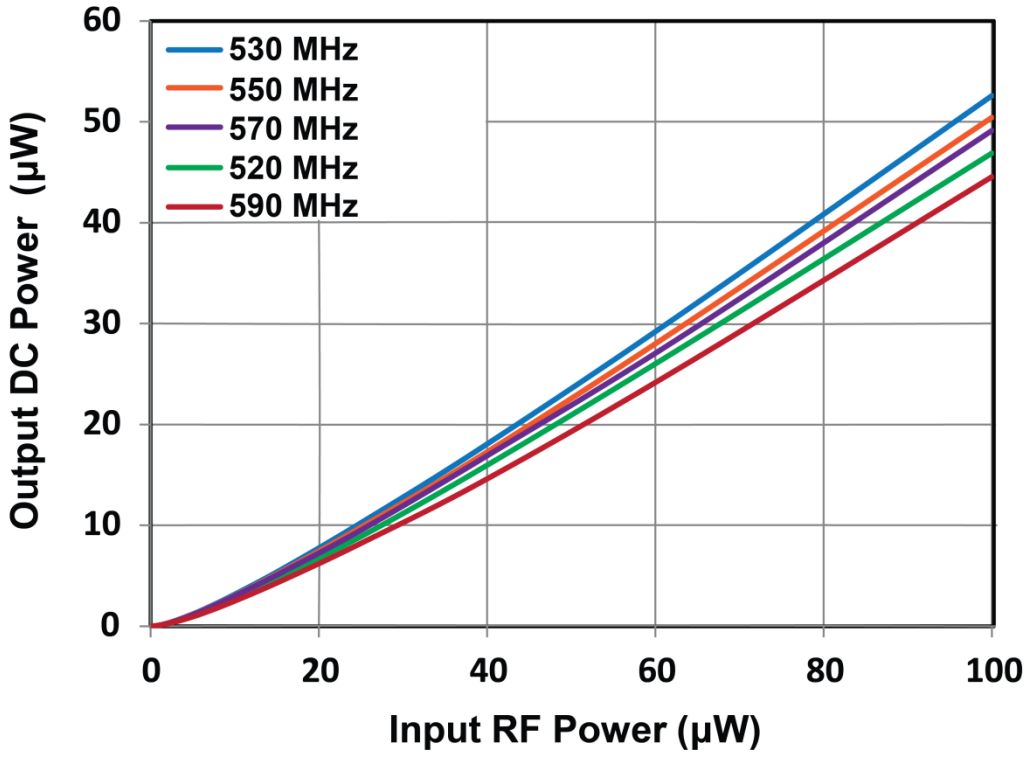

Figure 5.9 Output DC power as a function of input RF power for different frequencies within the matched TV frequency band (520-590 MHz). (The input power range corresponds to the signal level of each tone).

The RF to DC conversion efficiency is defined as the ratio of output power to the input power (eqn. 4.3). Figure 5.10 indicates power conversion efficiencies of 53% and 1.5% at a single tone input of −10 dBm (100 µW) and −40 dBm (0.1 µW) respectively. As depicted, there is a significant increase in the PCE for the lower input power levels (< 40 µW) compared to the rectifier of Chapter 4 with a single tone excitation. Furthermore, similar efficiency over the

frequency band is achieved for a wide range of input power, hence demonstrating the appropriate matching at the desired band (the small difference in the efficiency values at various frequencies is due to the diode characteristics.)

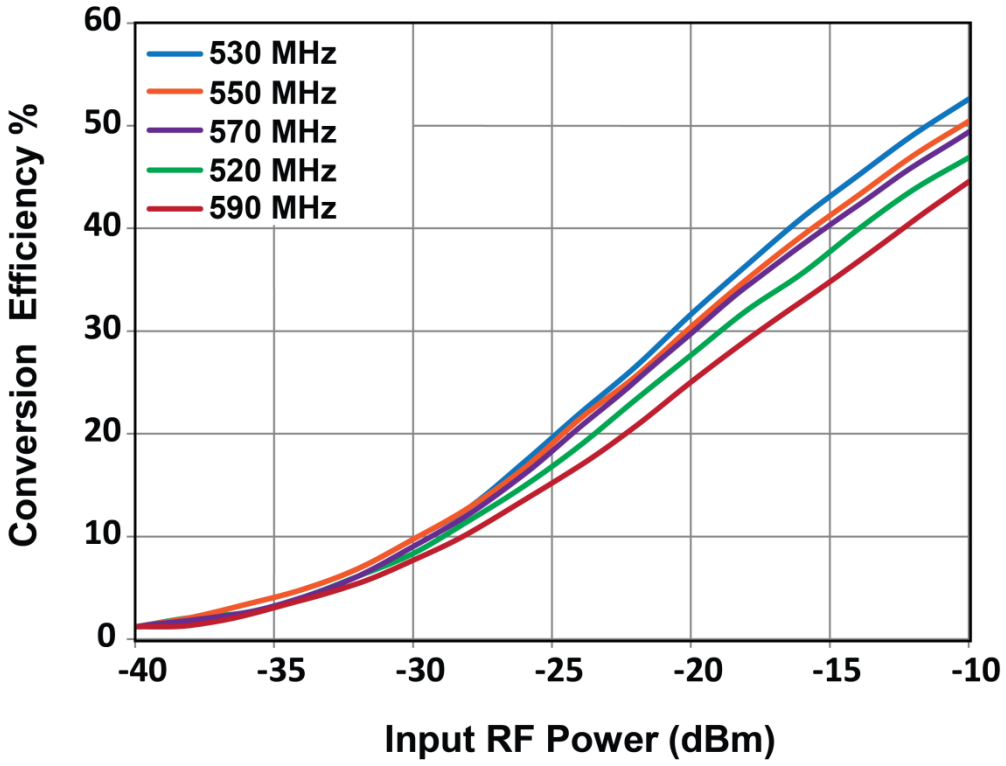

Figure 5.10 RF to DC power conversion efficiency as a function of input RF power for different frequencies.

5.4 FM Broadcasting Band (88- 108 MHz) Rectifier Design

In order to enhance the sensitivity and efficiency of the rectifier, not only a sensitive rectification device is required (previous section), but also harvesting energy over a wider frequency band to collect more RF signals and deliver more power to the rectification device is recommended (as discussed in Chapter 3 and Chapter 4). Hence, a system that harvests power from several ambient RF energy sources of different frequencies and combines them to activate a single rectification circuit via a matching network with 22% fractional bandwidth is proposed.

It is worth highlighting that the notion of combining RF signals refers to harvesting various signals with a broadband antenna and delivering more signals simultaneously to the diode via a broad band matching network - it is not referring to an actual combiner device.

Similar to Section 5.3, a voltage doubler rectifier structure (as seen in Figure 5.4) is considered as a core of the RF-DC power conversion system. Using Large Signal S-Parameter analysis in Agilent ADS software, the load impedance and bypass capacitor was determined and optimised (C_{bypass}= 43 pF, R_{load}= 18 KΩ).

Harmonic balance analysis and a nonlinear model of the diodes in ADS were used to calculate the impedance of the circuit depicted in Figure 5.4 (a) over the frequency range of 80 to 120 MHz at different low input power levels. A vector network analyser (VNA) was used to measure the input impedance of the device (Figure 5.4 (b)) and validate the simulation results as shown in Figure 5.11. These have been summarised in Table 5.2.

As demonstrated in Figure 5.11 and Table 5.2, increasing the source power (−10 to 0 dBm) has a direct influence on the impedance of the diode, which is varying and beginning to

switch on (e.g. at 0 dBm). Hence, the input impedance of the device was determined by applying a high unmatched power (e.g. 0 dBm) and then used in design of a matching network. Similar to the previous section, the simulation and measurement results of Figure 5.11 demonstrate that the diode's input impedance does not significantly change with low power range (e.g. –20 dBm).

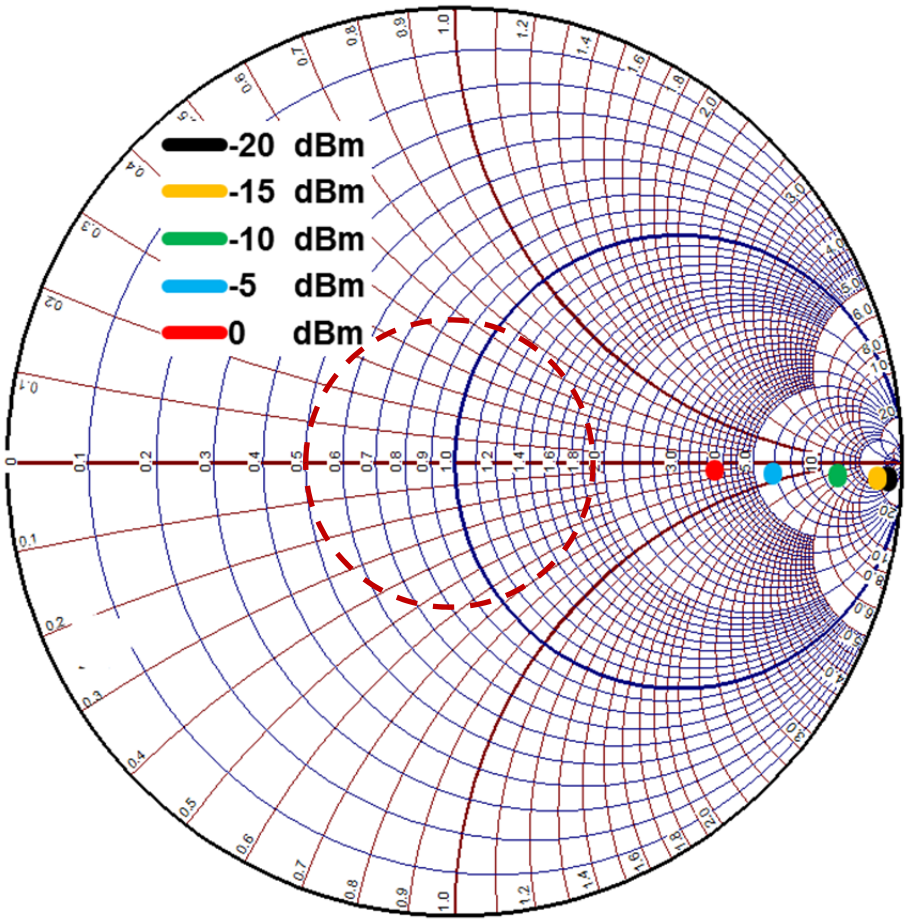

Figure 5.11 Voltage doubler input impedance calculated with Large Signal S- parameter (LSSP) analysis and measured with VNA over the frequency range of 80 to 120 MHz with various unmatched input power levels (−20 to 0 dBm). (The 2:1 voltage standing wave ratio (VSWR) boundary is shown with a dashed circle on the Smith Chart).

Table 5.2 Voltage Doubler Input Impedance Over 80-120 MHz

Input RF power (dBm) [µW]	80 MHz	120 MHz
−20 [10]	50*(34.72−j34.43)	50*(21.48−j31.85)
−15 [31.62]	50*(28.81−j14.96)	50*(27.77−j*17.7)
−10 [100]	50*(12.66−j2.24)	50*(12.19−j3.24)
−5 [316.22]	50*(5.93−j*0.43)	50*(5.89−j*0.64)
0 [1000]	50*(3.766−j0.14)	50*(3.75−j0.21)

In order to transfer maximum power, a matching network is required as a transition between a 50 Ω nominal antenna output and the rectification device at the FM band over a broad range of low input RF power (–50 to –10 dBm).

Similar to the previous rectifier design, using filter synthesis [124, 127], a high *Q* band pass matching circuit with a fractional bandwidth of 22% is designed and is depicted in Figure 5.12. The input impedance of the device at 0 dBm (high unmatched power) was used as the seed value in the design of the matching network.

Initially, ideal components from the ADS library were used to design a matching network. Then, similar to the previous design section, SMT components with their package parasitics were considered in the simulation to achieve accurate results. The substitution of realistic chip component values with their associated parasitics, and addition of 50 Ω microstrip lines and T-junctions introduce delay and shift the imaginary part of the input impedance. The via-holes also contribute to extra inductance in the circuit. Further, circuit optimizations are applied in order to fine tune the matching circuit components to achieve the desired bandwidth.

The final optimised values of the standard chip components are defined in Figure 5.12. A minimum number of components were used in order to reduce the ohmic and parasitic losses.

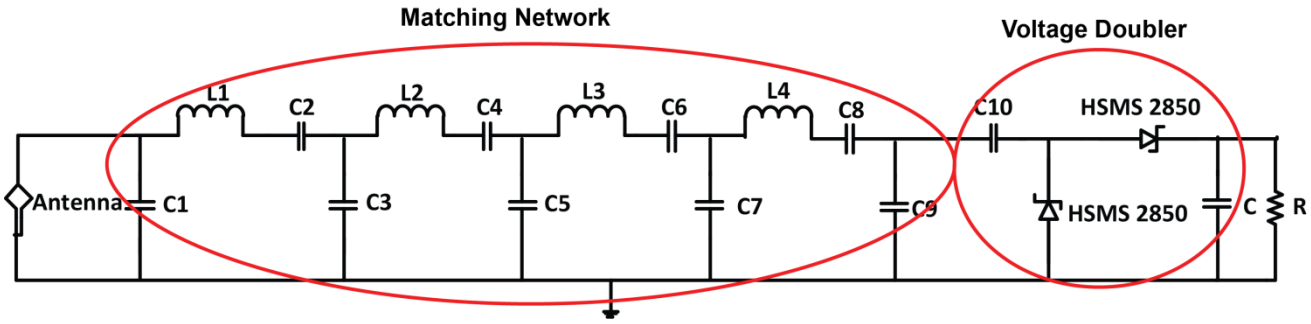

Figure 5.12 Schematic of the FM rectenna. The optimised values of the standard chip components are: C1=30 pF, L1=150 nH, C2=33 pF, C3=82 pF, L2=150 nH, C4=24 pF, C5=160pF, L3=82 nH, C6=62 pF, C7=82 pF, L4=560 nH, C8=150 pF, C9=3.6 pF, C10=1 nF, C=43 pF, R=18 KΩ.

In order to evaluate the matching network performance with various input power levels, large Signal S-parameter (LSSP) analysis is conducted. Figure 5.13 demonstrates the simulation results for the input impedance of the circuit presented in Figure 5.12.

The proposed matching circuit achieves a VSWR < 2 over 89-111 MHz for input power levels of –50 to –10 dBm (0.01 to 100 μW).

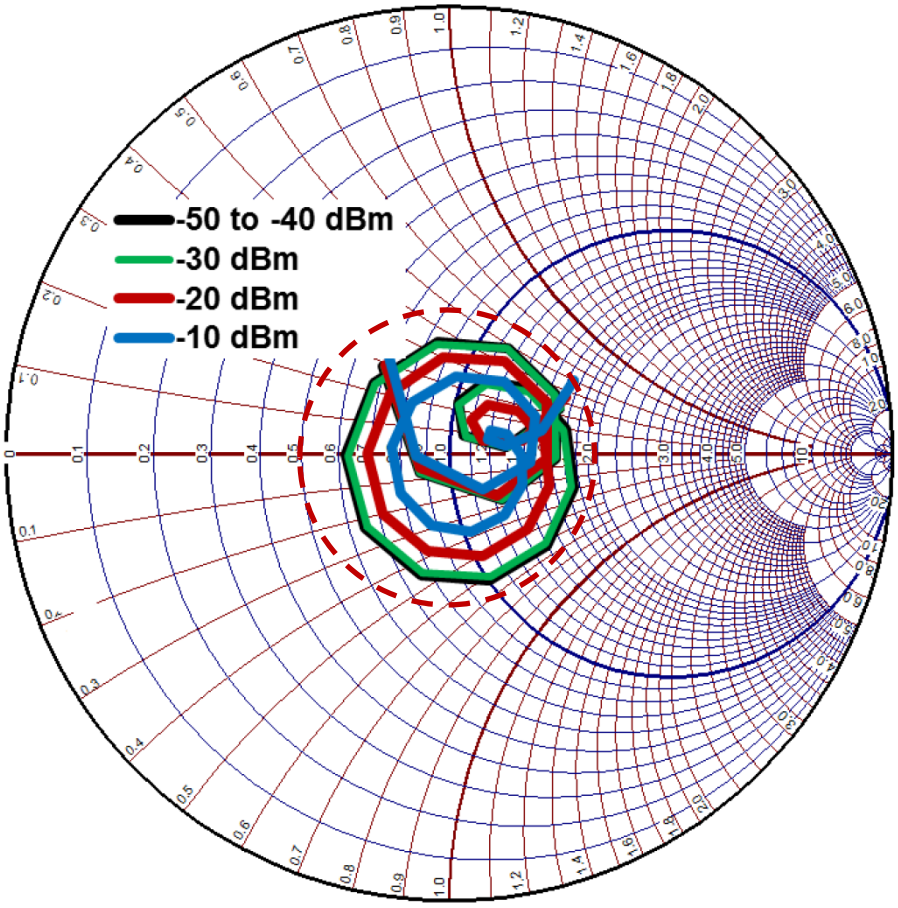

Figure 5.13 FM band rectifier impedance matching over 89-111 MHz, with −50 to −10 dBm (0.01 to 100 µW) Input RF power. (The 2:1 voltage standing wave ratio (VSWR) boundary is shown with a dashed circle on the Smith Chart).

5.4.1 Results and Discussion of the FM Band Rectifier

A rectifier circuit with 22% fractional bandwidth that harvests various ambient signals to enhance the sensitivity is designed with the aid of Agilent ADS software. In order to confirm the rectification performance, the proposed FM rectifier is fabricated on a 0.535 mm Rogers TMM4 substrate with a dielectric constant εr ≈ 4.7 and a loss tangent δ ≈ 0.002. A photograph of the fabricated rectifier is shown in Figure 5.14 (a) which depicts matching network lumped components, Schottky diodes and the output terminal.

The proposed rectifier has a small footprint hence, multiple circuits can be accommodated in building materials, which is important from a design perspective (this will be discussed in Section 5.6).

It should be noted that, due to parasitics and inaccuracy in the values of lumped components at the 89-111 MHz frequency band, precise component measurements were performed to find exact values and provide accurate results as generated from the simulation. In this work American Technical Ceramic (ATC) components were used. Measurement results of the scattering parameter ($|S_{11}|$) and the output DC voltage are used to validate the RF scavenger performance.

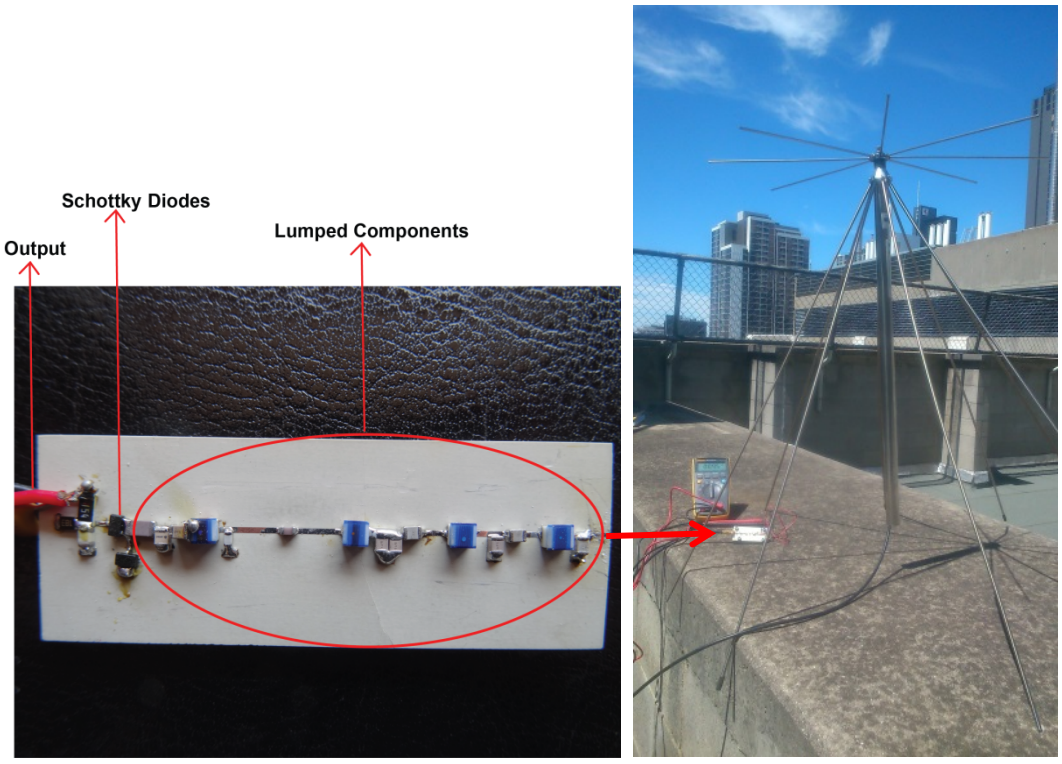

Figure 5.14 (a) Fabricated FM rectifier prototype. (b) Environmental measurement of the FM rectifier using a broadband discone antenna.

5.4.1.1 Reflection Coefficient

Figure 5.15 illustrates the $|S_{11}|$ of the rectifier which was measured using a vector network analyser (VNA) and simulated using Large Signal S-Parameter analysis in Agilent ADS software. The measured results are in good agreement with the simulations. The proposed rectifier circuit is well matched ($|S_{11}| < -10$ dB) at the favourable frequency band (89-111 MHz) over the wide range of very low input powers from –50 to –10 dBm (0.01-100 µW). The small difference between simulation and measurement is due to the diode parasitic extraction accuracy and tolerance of the circuit lumped components.

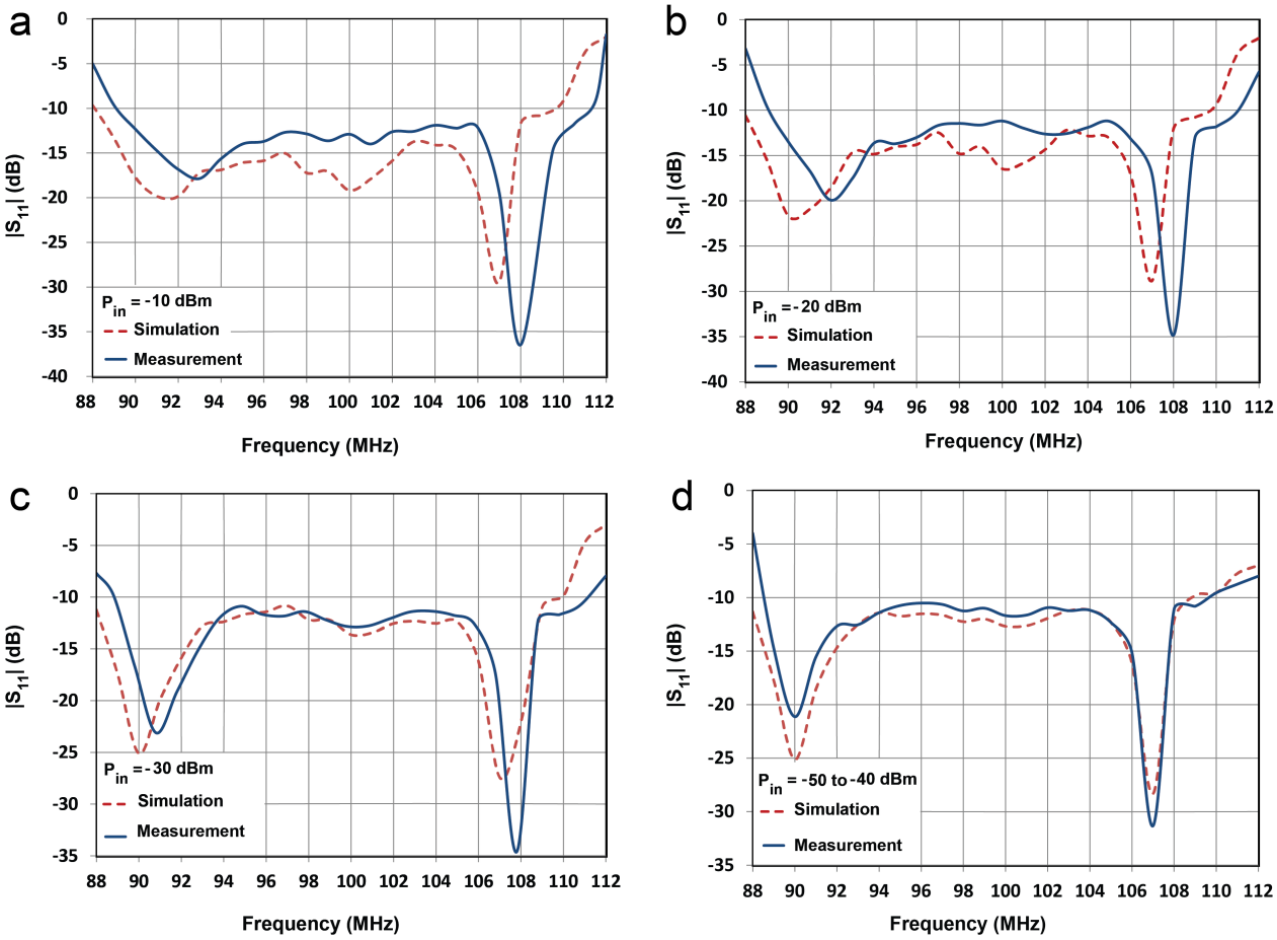

Figure 5.15 Simulated and measured $|S_{11}|$ as a function of frequency and input RF power for the proposed FM rectifier circuit. (a) −10 dBm (100 µW), (b) −20 dBm (10 µW), (c) −30 dBm (1 µW), (d) −50 dBm to −40 dBm (0.01 to 0.1 µW).

5.4.1.2 Output DC Power and Efficiency

Similar to the Section 5.3, HB simulation was used to numerically evaluate the output DC voltage of the rectifier. The output DC voltage across the load resistor was then used to calculate output DC power.

Two scenarios were analysed; laboratory and real environmental measurements. In the laboratory case, a Wiltron 68247B signal generator was connected to the rectifier circuit as an RF power source to carry out measurements. The output DC voltage across the load resistance was measured using a Fluke 79III voltage meter. The RF source power was set at −10 dBm at the beginning, and reduced in 1 dB steps.

Figure 5.16 (a) and (b) compares the simulated and measured output DC voltage of the proposed rectifier circuit. Figure 5.16 (b) shows the lower power section of Figure 5.16 (a) in more detail. The small difference between simulation and measurement is due to the component model accuracy in ADS and the ohmic loss. As illustrated, a measured DC voltage of 860 mV and 1.6 mV is achieved with a single tone input power of –10 dBm (100 μW) and –50 dBm (0.01 μW) respectively at 96 MHz, highlighting the impressive sensitivity.

The simulation and measurement results for the output DC power are depicted in Figure 5.17 (a) and (b). As illustrated a measured DC power of 41 μW and 0.14 nW can be achieved with a single tone input of –10 dBm (100μW) and –50 dBm (0.01 μW) respectively at 96 MHz.

The RF-DC conversion efficiency is also calculated as discussed in Section 5.3. The single tone excitation delivers a measured power conversion efficiency of 41% and 1.4 % at –10 dBm and –50 dBm respectively. Efficiency versus input power is provided in Figure 5.18.

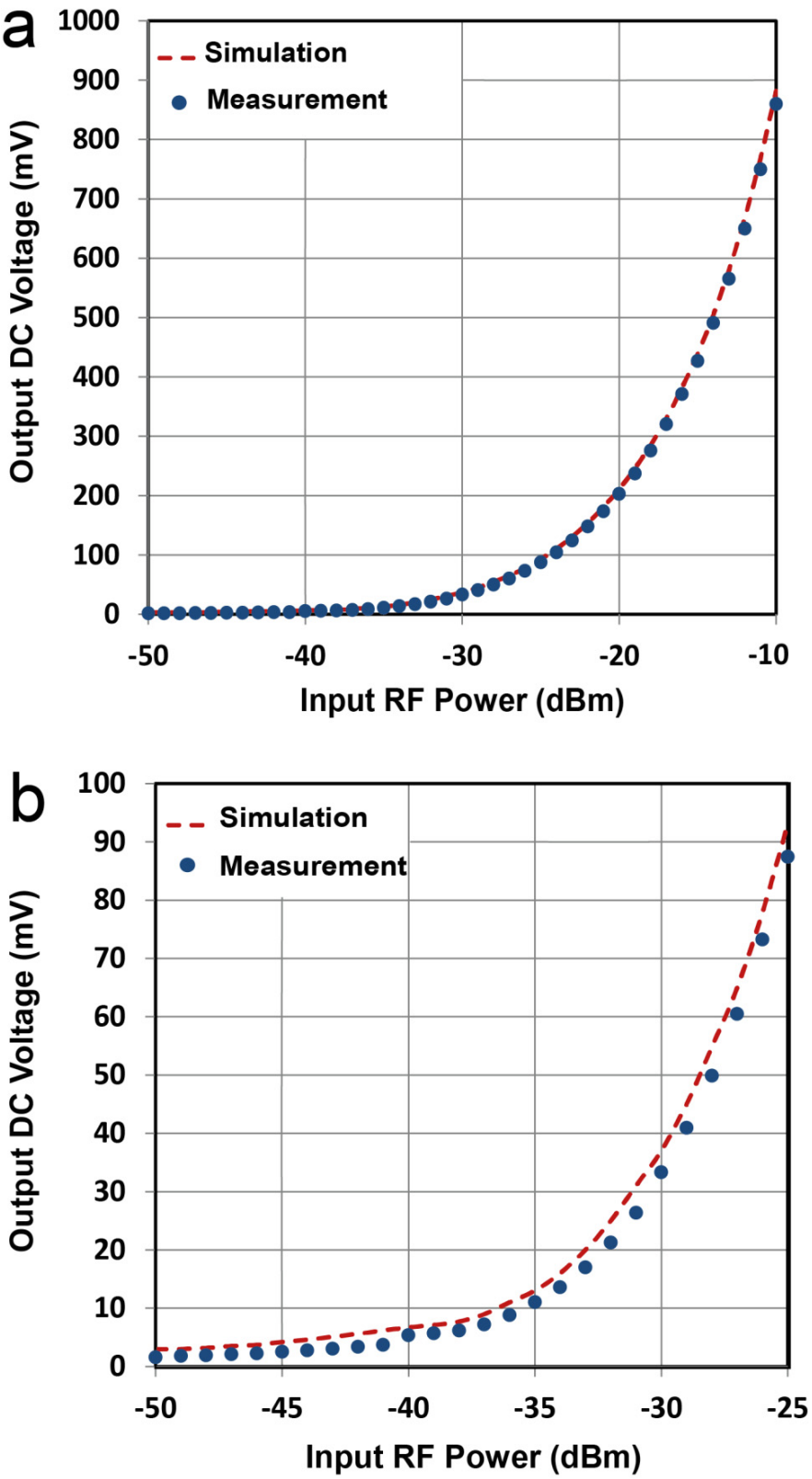

Figure 5.16 Output DC voltage as a function of input RF power with a single tone excitation at 96 MHz: (a) With –50 to –10 dBm (0.01 to 100 µW) Input RF power. (b) With –50 to –25 dBm (0.01 to 3.16 µW) Input RF power. (This power range is associated with the signal source.)

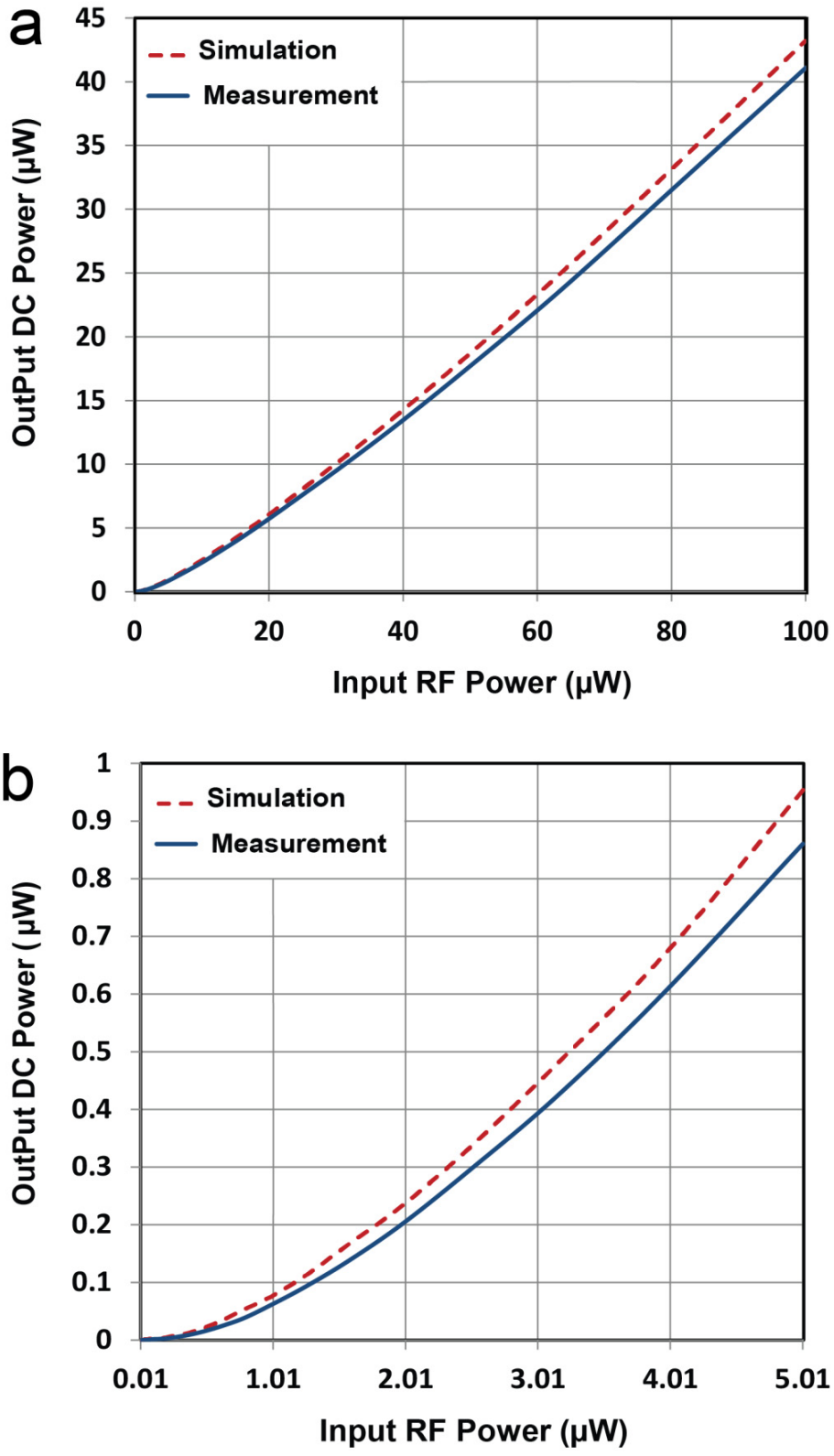

Figure 5.17 Output DC power as a function of input RF power with a single tone excitation at 96 MHz for the proposed rectifier circuit: (a) With 0.01 to 100 µW (–50 to –10 dBm) Input RF power (b) With 0.01 to 5.01 µW (–50 to –23 dBm) Input RF power.

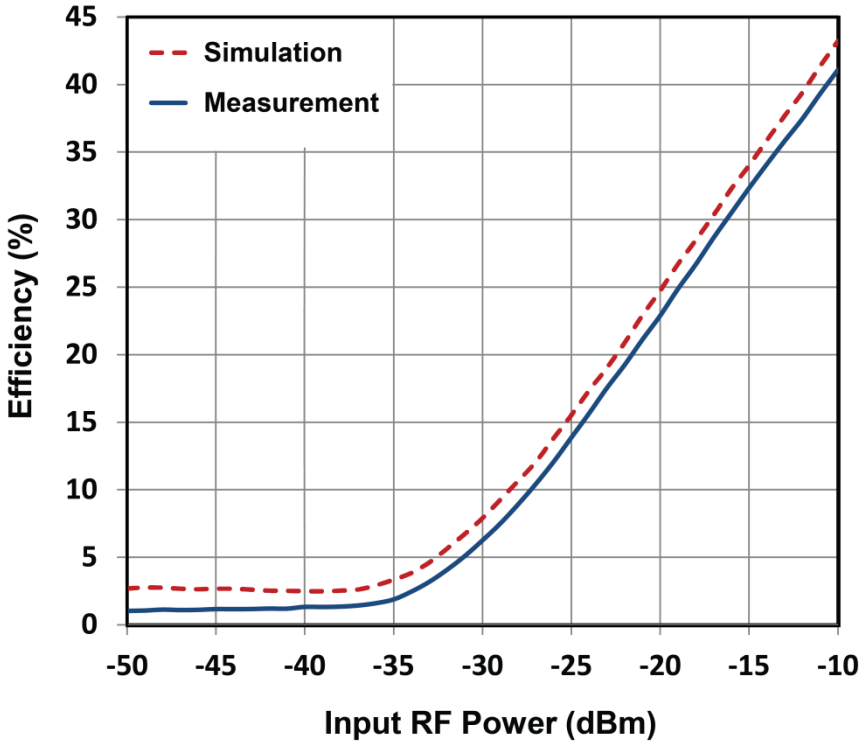

Figure 5.18 RF to DC efficiency as a function of Input RF power with a single tone excitation at 96 MHz over –50 to –10 dBm (0.01 to 100 µW) Input RF power.

5.4.1.3 Multi-tone Excitation Measurements

In order to demonstrate the effect of multi-signal excitation on the DC response and sensitivity of the rectifier [69], seven multiple tones of various frequencies (in the matched FM frequency band), are generated simultaneously with seven signal generators (from −50 to −10 dBm), summed using a power combiner and passed to the rectifier.

Note that a power combiner was used to provide a real life case.

The DC output voltage of the rectifier with various concurrent input tones is provided in Figure 5.19 (a), (b) and (c). Figure 5.19 (b) and (c) show the lower power levels of Figure 5.19 (a) in more detail, demonstrating the improved sensitivity.

As illustrated, a measured DC voltage of 1.8 V and 0.25 V can be achieved at –10 dBm (100 µW) and –25 dBm (3.16 µW) respectively with seven concurrent tones. In multi-tone case, total combined RF power from seven tones of –10 dBm and –25 dBm is around −1.54 dBm and −16.54 dBm respectively.

Focusing on the lower available powers in a real environment (Figure 5.19 (c)), the proposed highly sensitive rectifier can generate 25.87 mV and 15.5 mV of DC voltage with the combination of seven tones at –40 dBm (0.1 µW) and –50 dBm (0.01 µW) respectively. In this case, total available RF power from seven tones of –40 dBm and –50 dBm at the input is around −31.54 dBm and −41.54 dBm respectively.

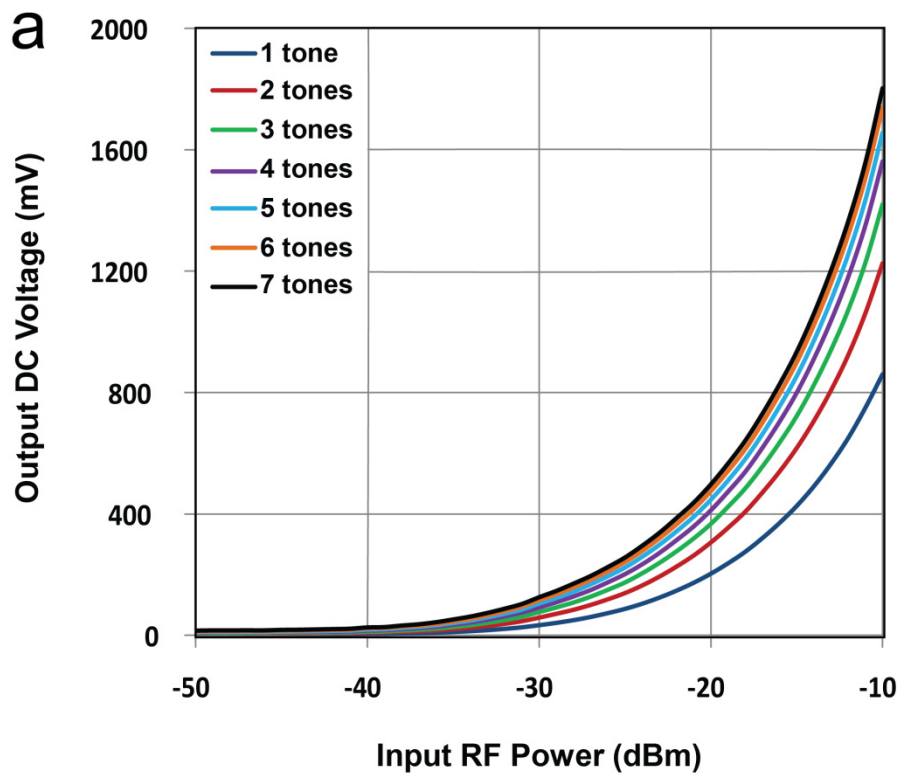

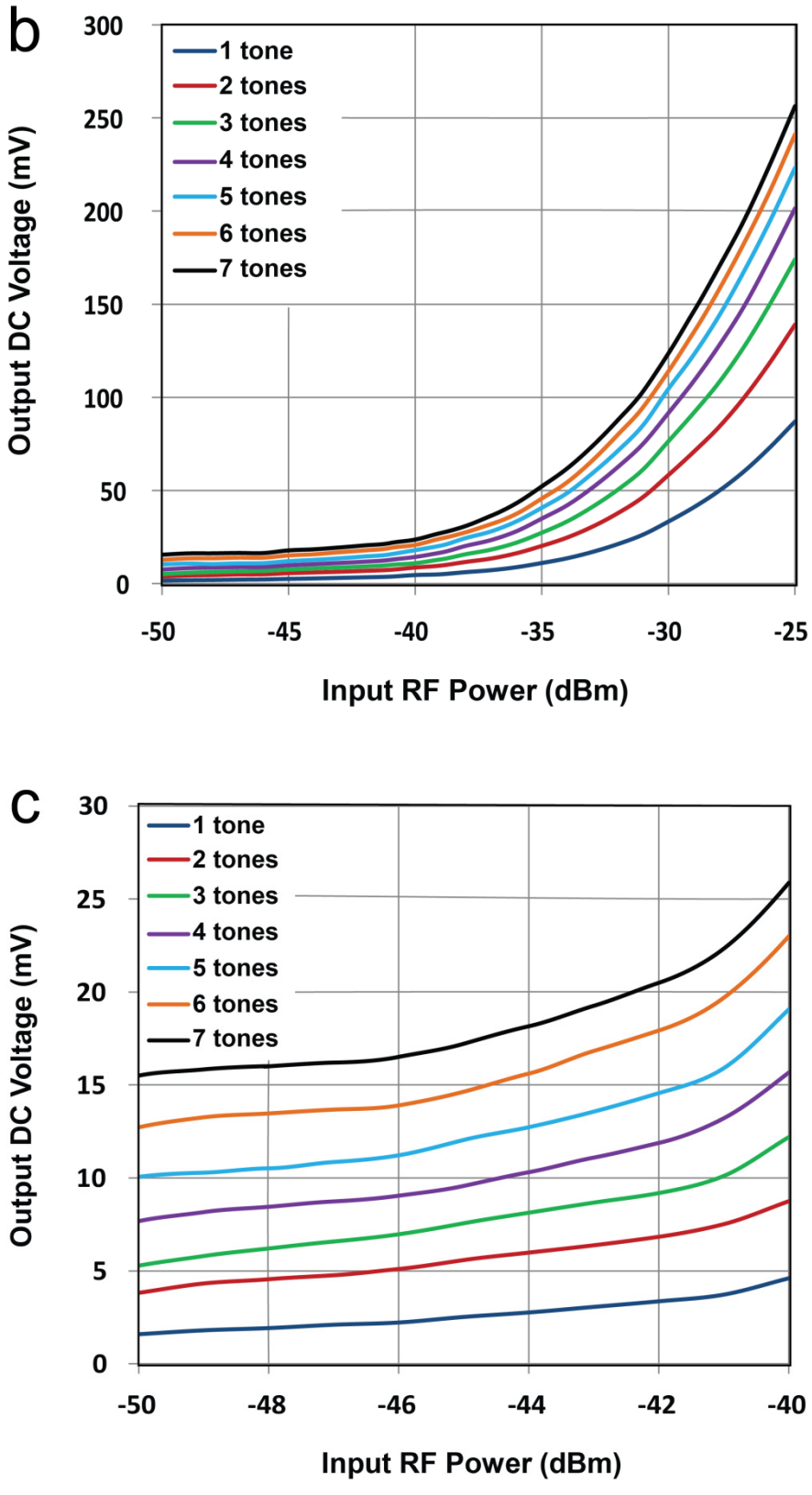

Figure 5.19 Measured output DC voltage as a function of input RF power for single tone and seven tones excitations: (a) With –50 to –10 dBm (0.01 to 100 µW) input RF power. (b) With 50 to –25 dBm (0.01 to 3.16 µW) input RF power. (b) With –50 to –40 dBm (0.01 to 0.1 µW) input RF power.
(The input power range corresponds to the signal level of each tone).

Figure 5.20 (a), (b) and (c) presents the measured output DC power of the proposed rectifier with seven-tone excitation and summarises the improved sensitivity and output DC power at very low input power levels (compared to the single tone excitation).

As shown, a measured DC power of 180.43 μW and 13.76 μW can be achieved at –10 dBm (100 μW) and –20 dBm (10 μW) respectively with seven concurrent tones. Focusing on the lower available powers in a real environment (Figure 5.20 (c)), the proposed highly sensitive rectifier can generate around 37 nW and 13.3 nW of DC power with the combination of seven tones at –40 dBm (0.1 μW) and –50 dBm (0.01 μW) respectively.

Hence, harvesting various RF signals and delivering more RF power to a single rectification step leads to a highly sensitive rectifier which can generate higher DC power, than the post rectification combining of individual single frequency rectifiers (using DC combing method) working at the same frequencies with very low input powers (<2 μW (−27 dBm)). The reason is harvesting RF energy from several available frequencies concurrently enhances the delivered power to the rectifier, improving the diode conversion efficiency which eventually results in a higher amount of output DC power. This is particularly obvious at the lower input power levels as can be seen in Figure 5.20 (b) and (c).

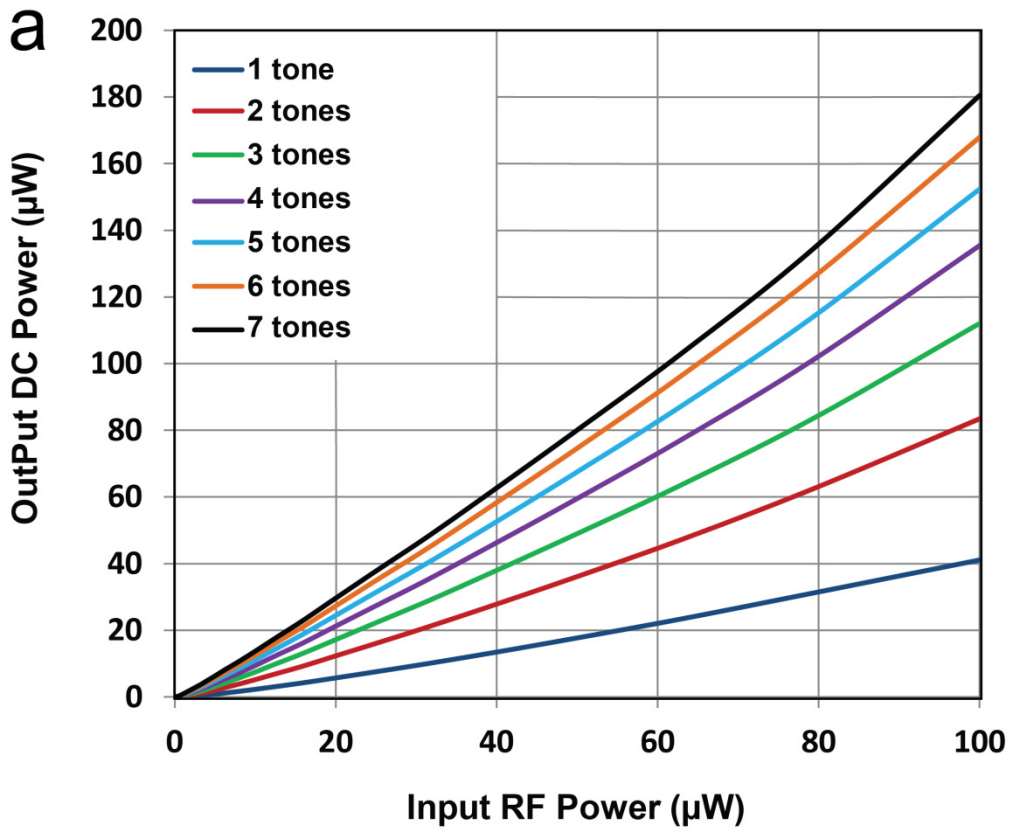
a
OutPut DC Power (μW)
200
180
160
140
120
100
80
60
40
20
0
1 tone
2 tones
3 tones
4 tones
5 tones
6 tones
7 tones
0
20
40
60
80
100
Input RF Power (μW)

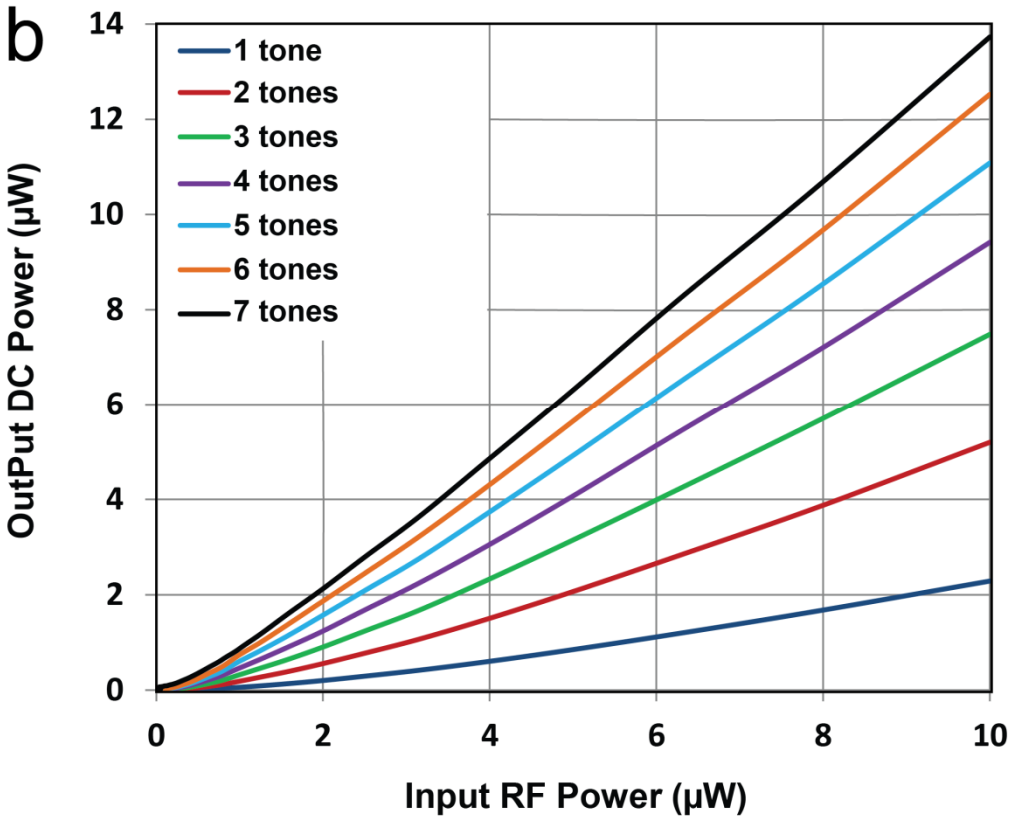
b
OutPut DC Power (μW)
14
12
10
8
6
4
2
0
1 tone
2 tones
3 tones
4 tones
5 tones
6 tones
7 tones
0
2
4
6
8
10
Input RF Power (μW)

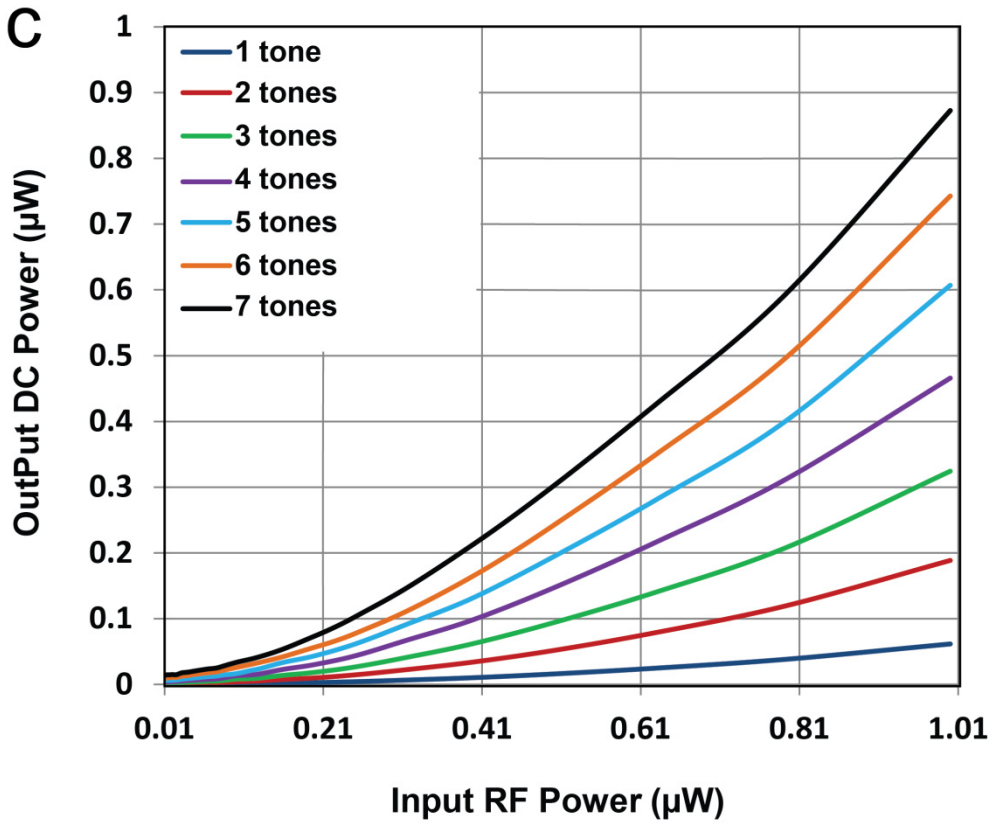

Figure 5.20 Measured output DC power as a function of input RF power with multi tones for the proposed FM rectifier circuit. Seven frequencies from 93-99 MHz are applied to the rectifier.
(a) With 0.01-100 µW (−50 to −10 dBm) input RF power, (b) with 0.01-10 µW (−50 to −20 dBm) input RF power. (c) With 0.01-1 µW (−50to −30 dBm) input RF power.
(The input power range corresponds to the signal level of each tone).

It should be noted that the rectifier has a quite similar output DC power (similar efficiency) at the selected frequencies between 93-99 MHz (Figure 5.21). Applying various tones at frequencies with widely variant efficiencies may result in different total DC outputs than those in Figure 5.20.

Evaluation of rectified output DC power over the matched frequency band for various input RF power levels can be seen in Figure 5.21 (a), (b), (c) and (d)

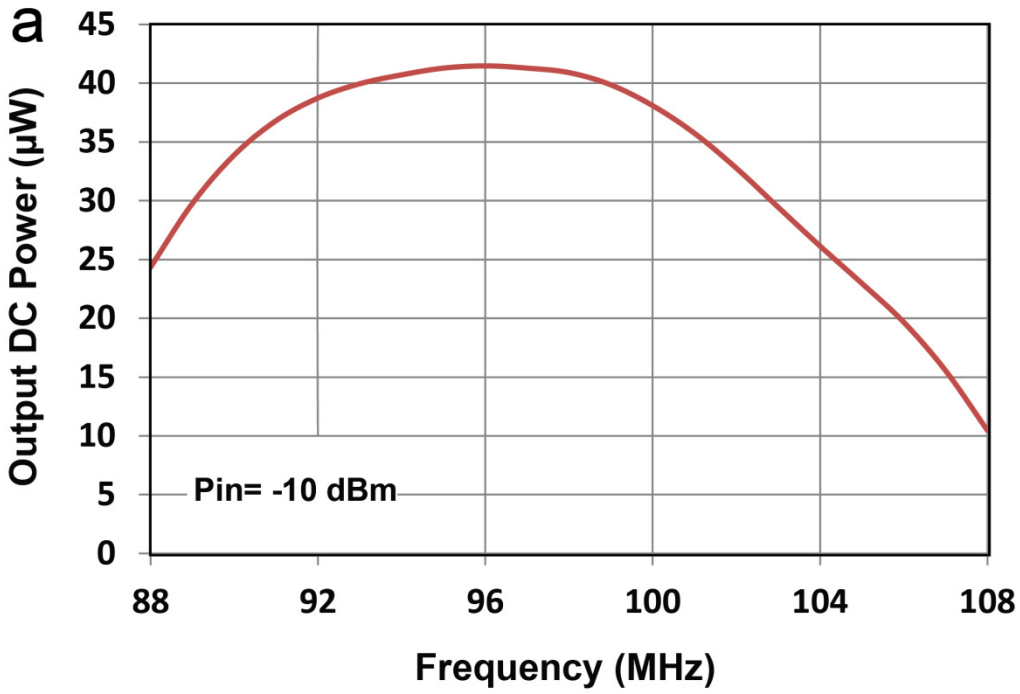
a
Output DC Power (μW)
45
40
35
30
25
20
15
10
5
0
Pin= -10 dBm
88
92
96
100
104
108
Frequency (MHz)

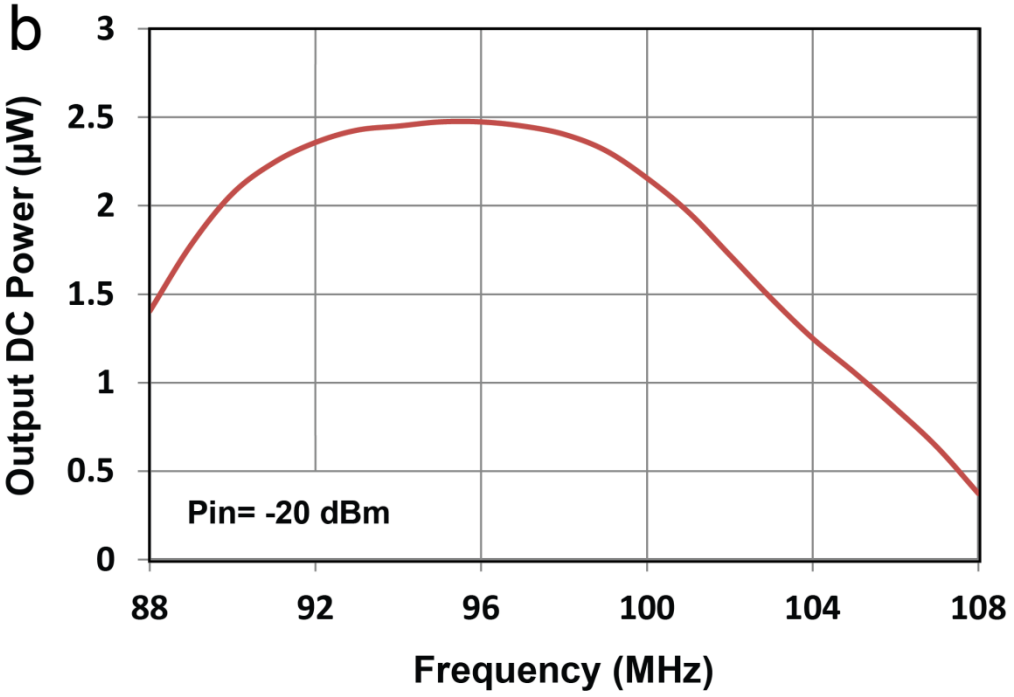
b
Output DC Power (μW)
3
2.5
2
1.5
1
0.5
0
Pin= -20 dBm
88
92
96
100
104
108
Frequency (MHz)

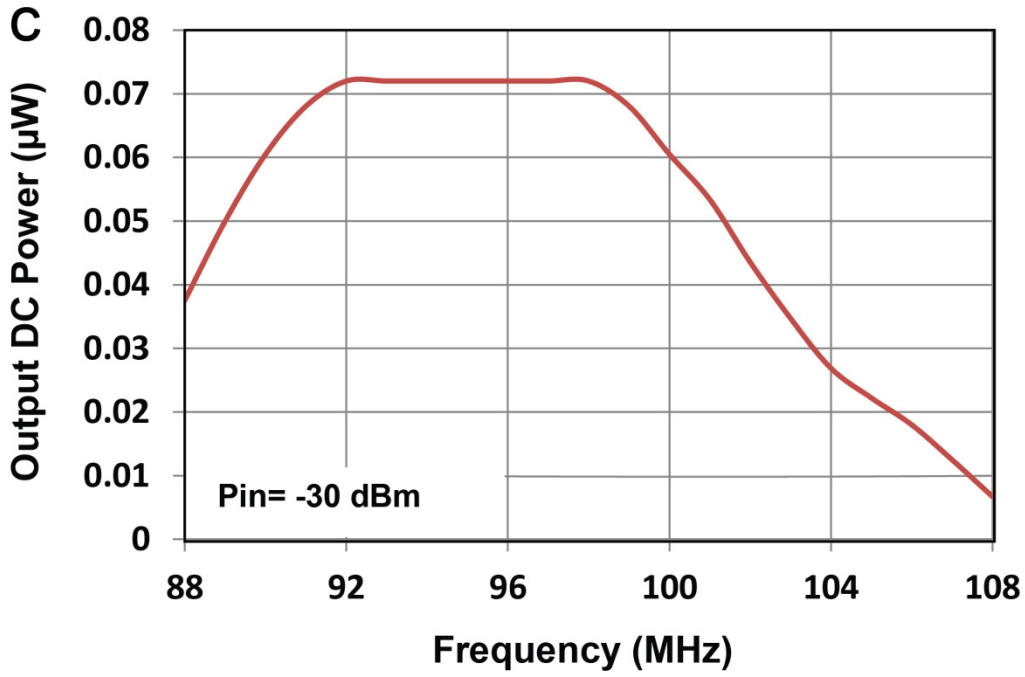
c
Output DC Power (μW)
0.08
0.07
0.06
0.05
0.04
0.03
0.02
0.01
0
Pin= -30 dBm
88
92
96
100
104
108
Frequency (MHz)

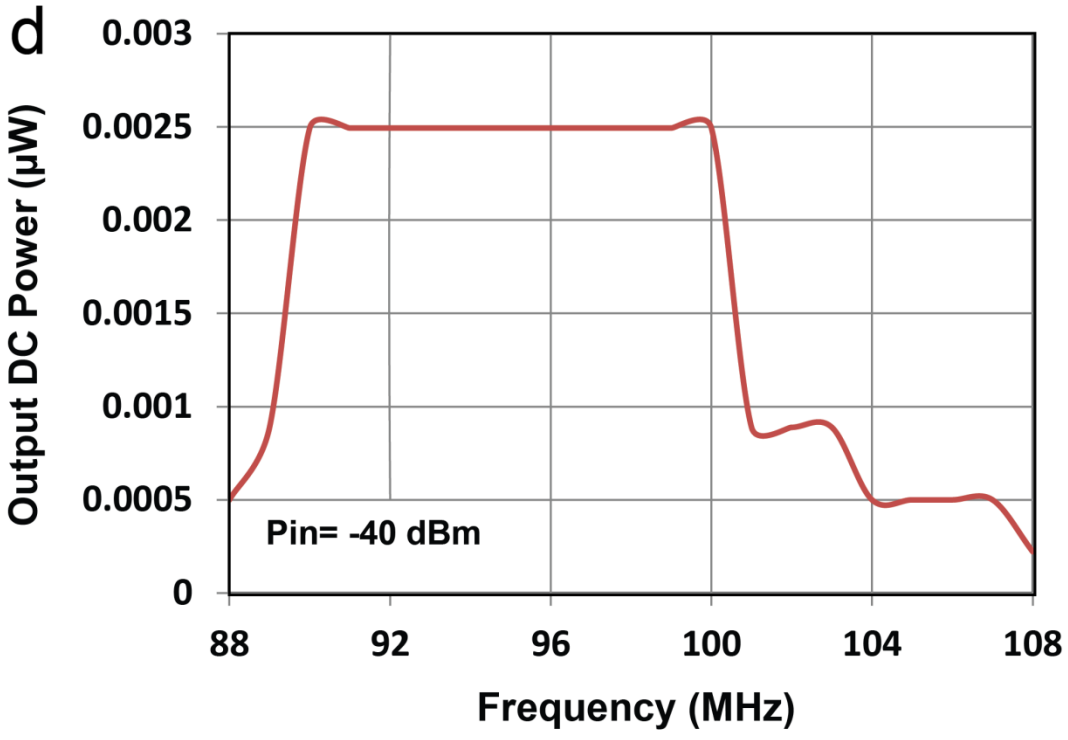
d
Output DC Power (μW)
0.003
0.0025
0.002
0.0015
0.001
0.0005
0
Pin= -40 dBm
88
92
96
100
104
108
Frequency (MHz)

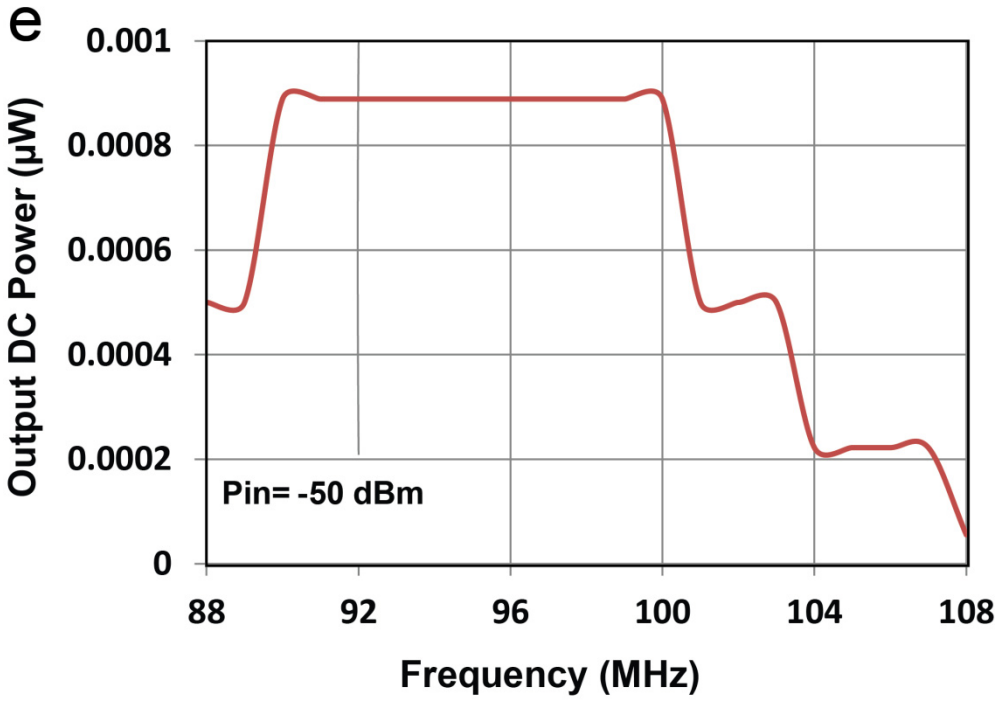

Figure 5.21 Output DC power versus frequency for the proposed rectifier circuit at different input power levels. (a) −10 dBm (100 μW), (b) −20 dBm (10 μW), (c) −30 dBm (1 μW), (d) −40 dBm (0.1 μW), (e) −50 dBm (0.01 μW).

5.4.1.4 Multi-tone Excitation Analysis

As seen in the previous section, applying multi-tone excitation to the rectifier (in the matched frequency band, results in a higher amount of output DC power when compared to a single tone excitation. It should be highlighted that, due to the non-linearity of the rectifier circuits, there is a non-linear relationship between the number of excited tones and output DC power, especially at very low power levels.

For more clarity, if we assume *N* is the number of applied tones, then at low power levels (when total applied power is <−20 dBm for this diode as shown in Figure 5.20 (c));

$$P_{DC\ N\text{-}TONE} > N^* P_{DC\ 1\text{-}TONE}$$

For example as depicted in Figure 5.20 (c), with a single tone of −30 dBm only around 0.07 μW DC power can be generated, however by applying seven tones of −30 dBm (total combined power at the input is −21.54 dBm, but still −30 dBm is available in ambient) around 1μW can be generated, which is 14.28 times higher than the single tone case.

This is due to the fact that, at very low input power levels (e.g. −50 to −30 dBm) the rectification device is almost off, while by applying multi-tones and increasing the total available power at the input, the non-linear diode can work more efficiently and shifts to its linear region. Hence, this proves the advantage of broadening the bandwidth so multiple signals are delivered to the diode hence harvesting very low energy density ambient signals. Therefore, one rectifier which is able to capture *N* signals of different frequencies simultaneously performs better than *N* single frequency individual rectifies operating at the same frequencies at very low input power levels.

It is evident that in real environmental cases where input RF levels are very low, this technique can capture these low level signals and improve the PCE (for example in a case where −21.54 dBm is not available, but there are seven signals at various frequencies with only −30 dBm power level).

Therefore, DC combing method ($N^* P_{DC\ 1\text{-}TONE}$) is not an optimum solution at very low ambient power levels, where high sensitivity rectifier is required [98]. Whereas RF combing method ($P_{DC\ N\text{-}TONE}$) can enhance the sensitivity of the rectifier by delivering various signals to the diode simultaneously (this was previously shown in Table 3.3).

It should be noted that the improvement in the output DC power by applying multi-tone excitation is limited by the non-linear diode performance. In presence of high power levels (~ > 0 dBm for HSMS2850) the diode starts working in a saturation mode and hence PCE and output DC power stop improving. (The selected diode for this rectifier (HSMS2850) is sensitive and although it could work reasonably up to 0 dBm, it is more suitable and efficient for power levels < −20 dBm.)

In order to better analyse the effect of multi-tone excitation, a power gain factor (G_p) has been introduced which is defined by eqn. 5.1 [69]. This factor demonstrates the power gain achieved with *N*-tone signal regarding to the one-tone case:

$$G_p = 10*LOG\left(\frac{P_{DC\ N-TONE}}{P_{DC\ 1-TONE}}\right) \qquad (5.1)$$

Figure 5.22 depicts the calculated power gain (based on Figure 5.20) and clarifies that at very low ambient power levels (−50 to −30 dBm) there is a significant improvement in G_p by applying multi tones. However, at higher power levels (e.g. −10 dBm), G_p improvement is insubstantial by applying multi tones due to the diode saturation effect.

As an example, for the seven-tone case, the gain is around 20 dB and 15 dB at 0.01 μW (−50 dBm) and 0.1 μW (−40 dBm) respectively compared to the one tone case.

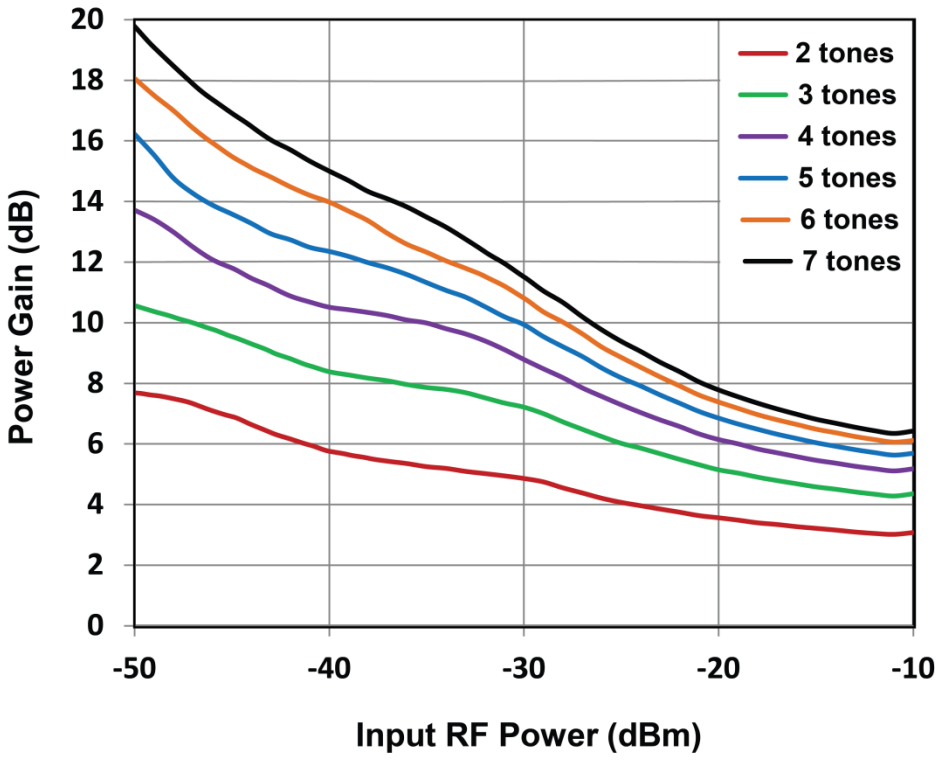

Figure 5.22 Power gain as a function of Input RF power over −50 to −10 dBm (0.01 to 100 µW). (The input power range corresponds to the signal level of each tone).

5.4.1.5 Real Environmental Measurements of the FM Rectifier

As proved in the previous sections, the rectifier could produce higher DC power in presence of various tones (which is the case in ambient RF energy scavenging) in comparison with a case when only one tone is available. Hence, in order to demonstrate a more realistic approach, environmental measurements were also performed in three suburbs of Melbourne, Australia. This is in accordance to the previous investigation results from Chapter 3.

Figure 5.14 (b) shows one of the field measurements on the roof of the RMIT University. A broadband discone antenna was connected to the rectifier to perform the measurement. Real environmental measurement results are provided in Table 5.3 and demonstrate the feasibility of ambient RF energy scavenging from the FM frequency band.

The proposed rectifier has a 22 % fractional bandwidth, and hence several RF source frequencies can be scavenged within FM band.

It is evident that the combination of very low RF power levels (e.g. similar to those listed for RMIT University in Table 5.3) can turn on the proposed sensitive rectifier and generate around 7.22 µW of DC power. Furthermore, DC power of 196 µW can be achieved in the suburb of Bayswater, which has stronger ambient RF signals.

Table 5.3 Real Environmental Measurement Results of the FM Rectifier

Suburb	Available Frequencies (MHz)	Respective Available RF Power (dBm) [µW]	Measured DC Power (µW)
Bayswater	88, 89, 91, 92 93, 94, 95 96, 97 100 101, 102, 103 104, 105 107, 108, 109, 110, 111	−20 [10], −20 [10] , −20 [10] , −20 [10] −11 [79.43], −11 [79.43], −11 [79.43] −11[79.43], −11[79.43] −14 [39.8] −15 [31.62], −15 [31.62], −15 [31.62] −15 [31.62],−15 [31.62] −33 [0.5], −33 [0.5], −33 [0.5], −33 [0.5], −33 [0.5]	196
Dandenong	89 90 93, 94, 96 100, 101, 102 103, 104, 105 106, 107, 108, 109	−25 [3.16] −12 [63.09] −14 [39.81], −14 [39.81], −14 [39.81] −22 [6.3], −22 [6.3], −22 [6.3] −22 [6.3], −22 [6.3], −22 [6.3] −15 [31.62], −15 [31.62], −15 [31.62]	97.3
RMIT University (Melbourne CBD)	89 90 91 92 93 94 95, 96, 97, 98 99, 100 101, 102, 103, 104 105,106, 107 108, 109, 110	−20 [10] −27 [1.99] −38 [0.15] −45 [0.03] −20 [10] −27 [1.99] −28 [1.58], −28 [1.58], −28 [1.58], −28 [1.58] −32 [0.63], −32 [0.63] −33 [0.5], −33 [0.5], −33 [0.5], −33 [0.5] −33 [0.5], −33 [0.5], −33 [0.5] −46 [0.025], −46 [0.025], −46 [0.025]	7.22

5.5 Embedded FM Rectenna in Plaster

In order to provide a sustainable and inexpensive energy source in urban environments, the practicality of embedding the RF energy harvesting system in building materials is investigated. Firstly the proposed rectifier is encased in plaster with a dielectric constant $\varepsilon r \approx 2$ and it was also sandwiched within a plasterboard panel as shown in Figure 5.23 (a) and (b). The plaster dielectric constant was measured using the Nicolson-Ross method [125]. In evaluating the performance of the rectifier encapsulated in the plaster, under identical input conditions as detailed in Section 5.4, it was found that its performance was maintained.

To further evaluate the performance of a plaster encapsulated rectenna, a simple dipole antenna was also embedded and its reflection properties were measured (See Figure 5.24). The dipoles reflection coefficient is detailed within Section 5.5.1 below. Finally, the proposed embedded rectifier and dipole antenna are integrated together to realise a rectenna system embedded in plaster board (Figure 5.23 (c)).

(a) **(b)**

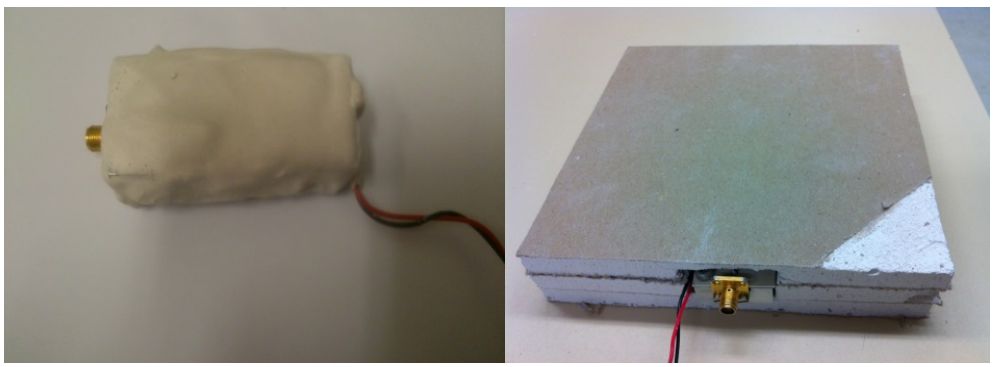

(c)

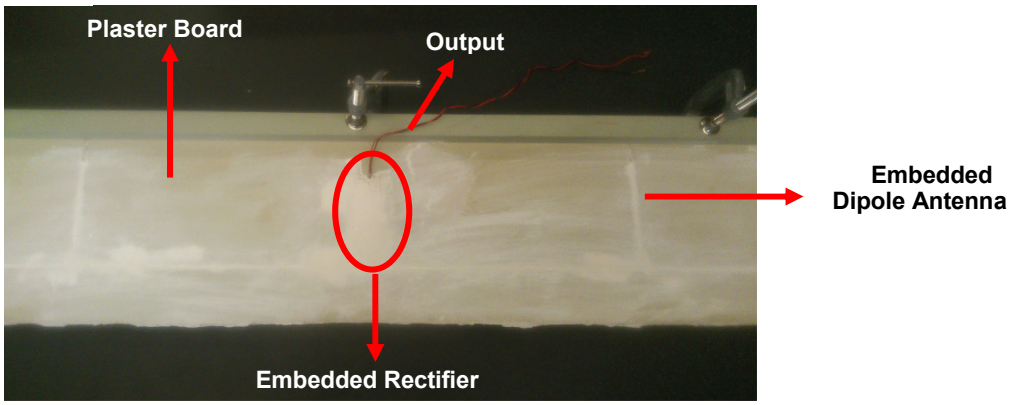

Figure 5.23 (a) Embedded rectifier in plaster and (b) sandwiched in plasterboard. (c) Embedded rectenna in plaster board.

5.5.1 Reflection Coefficient of the Antenna

A simple dipole antenna with a gain of ~1.2 dBi is fabricated to be integrated with the rectifier and to realise a proof of concept of a rectenna. The $|S_{11}|$ of the antenna was measured before and after embedding in a plaster board and the results are depicted in Figure 5.24. It is demonstrated that the antenna is matched within the desired frequency band. However, it should be noted that the antenna was not optimised for this frequency band and has a lower fractional bandwidth of around 16% (88-104 MHz) compared to the rectifier with 22% fractional bandwidth (89-111 MHz). Furthermore, after embedding the antenna in a plaster board the matched bandwidth decreased to around 13 % (90-103 MHz) which is due to the adverse effects of plaster on the antenna. The antenna could be designed with the plaster; however, this is not the scope of this thesis.

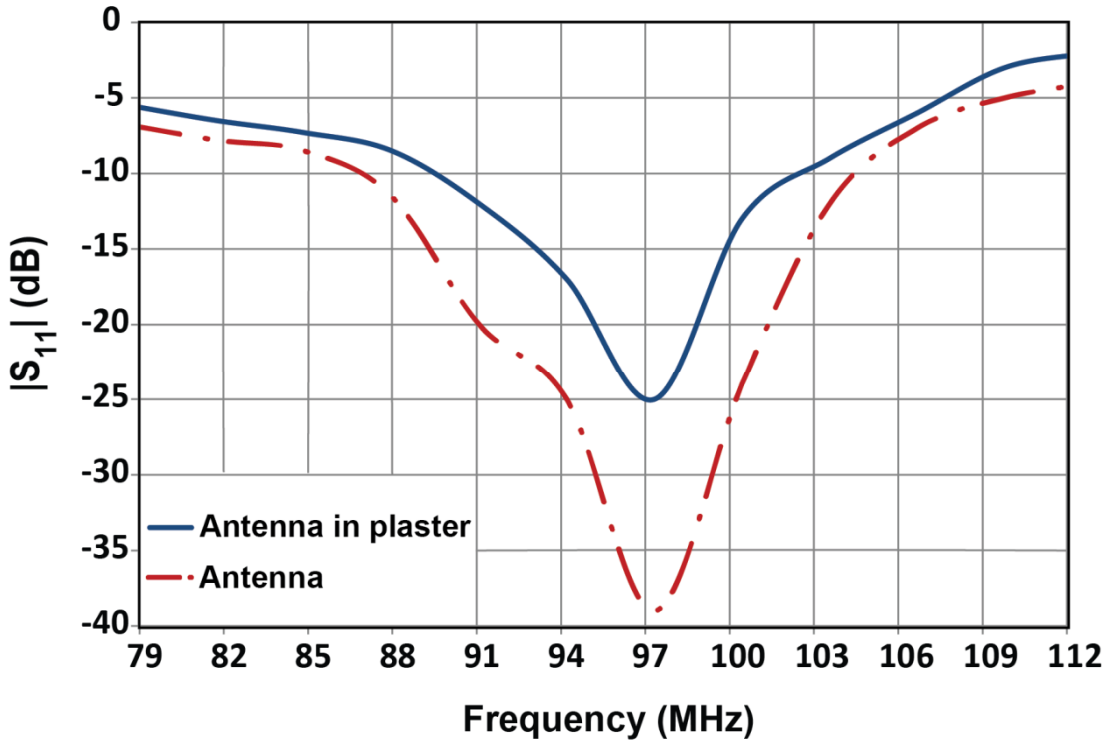

Figure 5.24 Measured $|S_{11}|$ as a function of frequency for the dipole antenna, before and after embedding in plaster.

5.5.2 Output DC Power of the Embedded Rectenna in Plaster

The proposed rectifier was then integrated with the dipole antenna, so various RF frequency sources can be harvested within the FM band. The rectenna was embedded in a plaster board (Figure 5.23 (c)) and its DC output in response to the entire range of input powers was measured. Measurements were again conducted using a broadband discone antenna as a transmitter. Taking into account the free space path loss (around −20 dB in this case), appropriate power levels were generated and applied to the transmitting antenna to deliver a received power range of approximately −50 to −10 dBm (0.01 to 100 μW) at the input of the rectenna.

Figure 5.25 shows the measured output DC power of the proposed embedded rectenna in plaster. A measured DC power of 40 µW and 0.11 nW can be generated with a single tone input of −10 dBm (100 µW) and −50 dBm (0.01 µW) respectively at 96 MHz.

The measurements of the complete embedded rectenna showed a similar output DC power and efficiency to that of the rectifier evaluated in Section 5.4 (as shown in the Figure 5.17 and Figure 5.18). Detailed efficiency values of the embedded rectenna in plaster are provided in Table 5.4. The measurement results indicate that the proposed highly sensitive rectenna is matched over a broad range of input power and can operate at power levels as low as −50 dBm (0.01 µW), exhibiting improved performance over previously published works for low power density levels. Table 5.4 compares this work to Chapter 4 results and previous published works.

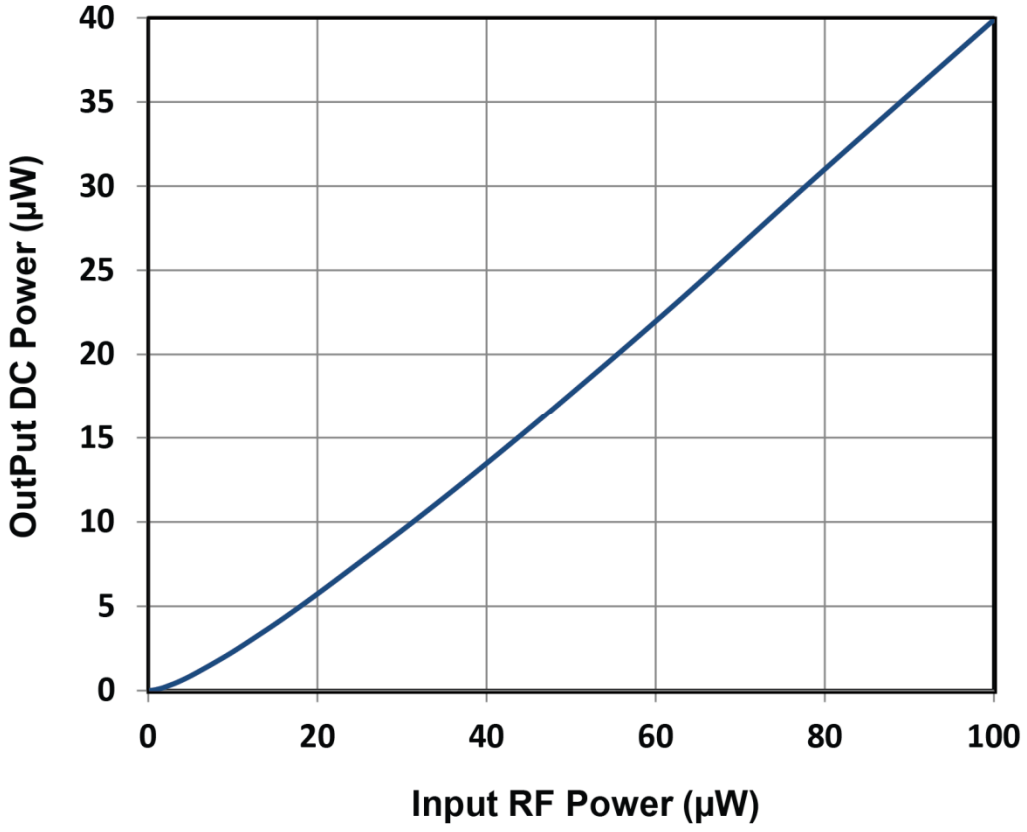

Figure 5.25 Measured output DC power as a function of input RF power with a single tone excitation at 96 MHz for the proposed embedded rectenna in plaster.

Table 5.4 RF Energy Scavengers Comparison

Ref.	Sensitivity	Measured Efficiency (%)	RF Power Variation (in PCE evaluation)	Frequency Range	Rectification Technique	Rectification Device
[94]	−19.3 dBm	9.1 @−19.3 dBm (900MHz) 8.9 @−19 dBm (2GHz)	−19.3 dBm (900MHz) −19 dBm (2GHz)	870-940 MHz 1920-2030 MHz	Dual resonator	CMOS
[88]	≈ −27 dBm*	0 @ <2 µW (1.27 MHz) 28 @ 23 µW (1.27 MHz)	2.5 to 23 µW	1.27 MHz	Auto-transformer	Diode
[100]	10^{-5} mW/cm^2	0.1 @ 5×10^{-5} mw/ cm^2 20 @ 0.07 mW/cm^2	10^{-5} to 10^{-1} mW/cm^2	2-18 GHz	Broad band	Schottky diode
Chapter 4	−40 dBm	54.3 @ −10 dBm (490 and 860 MHz) 11.25@ −18 dBm (490 and 860 MHz)	−40 to −10 dBm (0.1 to 100 µW)	(478-496 MHz and 852-869 MHz)	Dual resonator	Schottky diode
This Work**	−50 dBm	1.1 @ 0.01 µW (96 MHz) 1.4 @ 0.1 µW (96 MHz) 3 @ 0.5 µW (96 MHz) 6 @ 1 µW (96 MHz) 11 @ 2.5 µW (96 MHz) 16 @ 5 µW (96 MHz) 22 @ 10 µW (96 MHz) 28 @ 20 µW (96 MHz) 40 @ 100 µW (96 MHz)	−50 to −10 dBm (0.01 to 100 µW)	FM band (89-111 MHz)	Broad band (not ultra-wideband)	Schottky diode

* Based on the efficiency graph and main text, the efficiency is almost zero at low input power (<2 µW) which indicates a maximum sensitivity of −27 dBm.

* * Efficiency values are measured in laboratory and correspond to the embedded rectenna in the plaster.

5.5.3 Real Environmental Measurements of the Embedded Rectenna in Plaster

Similar to the previous section, environmental measurements were performed in three suburbs and the results are summarised in Table 5.5. It should be highlighted that, since the embedded rectenna in plaster has a lower fractional bandwidth (13%) compared to the rectifier circuit (22%), a lower amount of power could be harvested with rectenna. Therefore, improved results can be obtained with a specifically designed antenna. However, these field measurement results show that RF energy harvesting systems integrated in buildings provide a promising solution as a sustainable and stable energy source for low power applications within urban environments.

Table 5.5 Environmental Measurement Results of the Embedded Rectenna in Plaster.

Suburb	Available Frequencies in the Matched FM Frequency Band (MHz)	Respective Available RF Power (dBm) [µW]	Measured DC Power (µW)
Bayswater (outdoor)	91, 92 93, 94, 95 96, 97 100 101, 102, 103	−20 [10], −20 [10] −11 [79.43], −11 [79.43], −11 [79.43] −11 [79.43], −11 [79.43] −14 [39.8] −15 [31.62], −15 [31.62], −15 [31.62]	175
Bayswater (indoor)	91, 92 93, 94, 95 96, 97 100 101, 102, 103	−21 [7.94], −21 [7.94] −20 [10], −20 [10], −20 [10] −20 [10], −20 [10] −17[19.95] −20 [10], −20 [10], −20 [10]	68
Dandenong	90 93, 94, 96 100, 101, 102, 103	−12 [63.09] −14 [39.81], −14 [39.81], −14 [39.81] −22 [6.3], −22 [6.3], −22 [6.3], −22 [6.3]	78.2
RMIT University (Melbourne CBD)	90, 91, 92 93, 94 95, 96, 97, 98 99, 100 101, 102, 103	−27 [1.99], −38 [0.15], −45[0.03] −20 [10], −27 [1.99] −28 [1.58], −28 [1.58], −28 [1.58], −28 [1.58] −32 [0.63], −32 [0.63] −33 [0.5], −33 [0.5], −33 [0.5]	4.15

5.6 Realistic Case Analysis

In order to estimate the total harvested DC power by the proposed RF energy harvesting system in a typical building, a realistic case is analysed. Hence, total number of rectennas could be embedded in building materials (Figures 5.26 and 5.27) is estimated. In order to verify the findings, two RF energy harvesting scenarios have been taken into consideration; outdoor and indoor (Figure 5.1 and Figure 5.2).

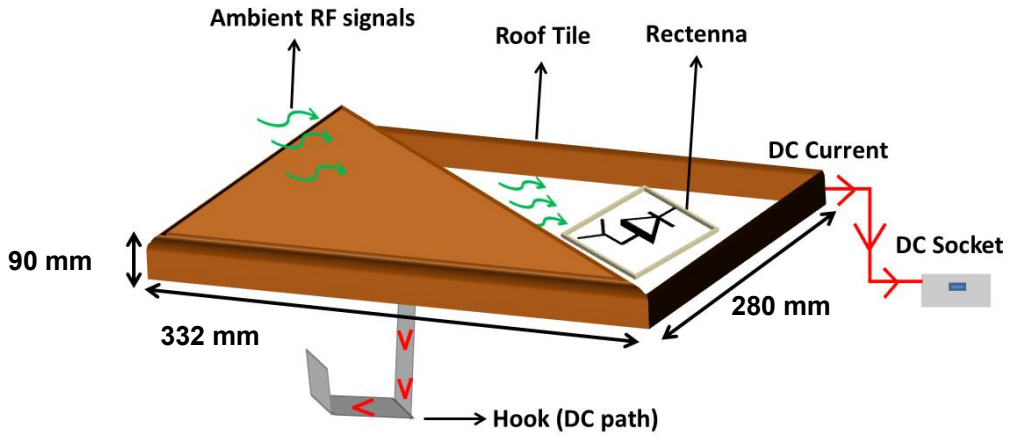

Figure 5.26 Embedded rectenna in roof tile.

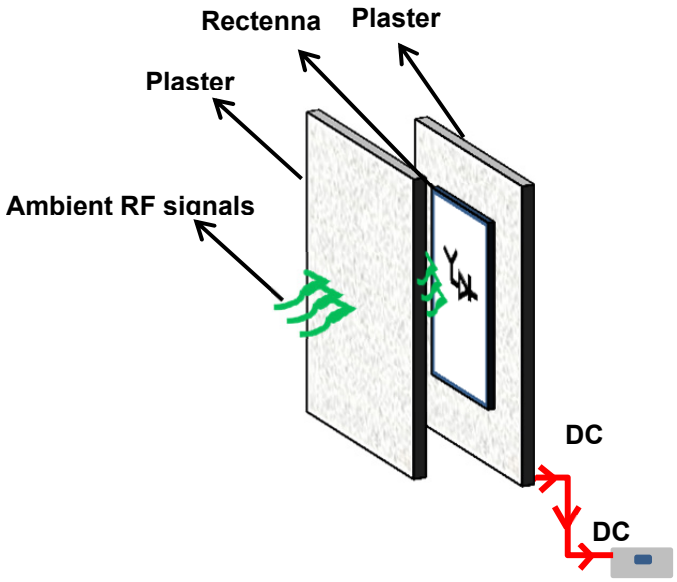

Figure 5.27 Embedded rectenna in plaster board.

.

5.6.1 Number of rectennas per Building (e.g. house)

An average house size in Melbourne, Australia is approximately 250 metre-squared and the average roof size was assumed to be around 250 metre-squared and the ceiling height is around 2.5 metres which also indicates each wall height (Figures 5.28 and 5.29). Obviously, apartments provide more wall areas than houses and hence more power could be harvested from the embedded rectennas in walls.

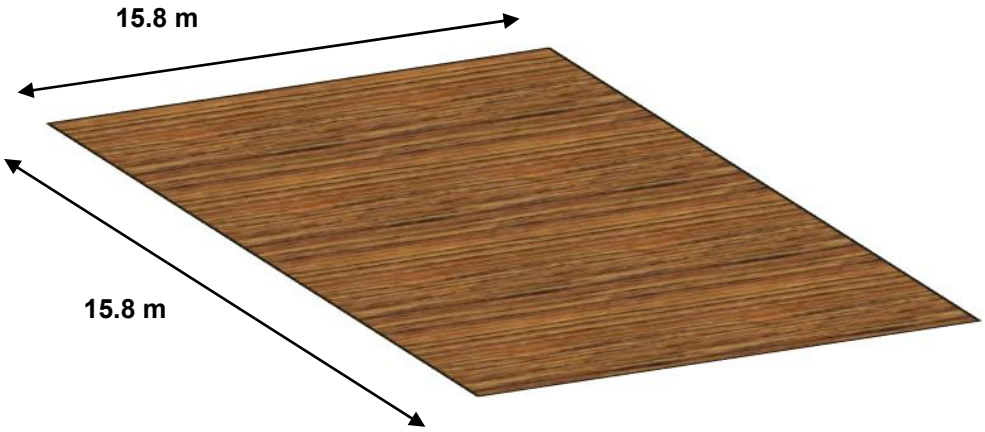

Figure 5.28 Typical land size (≈roof dimension).

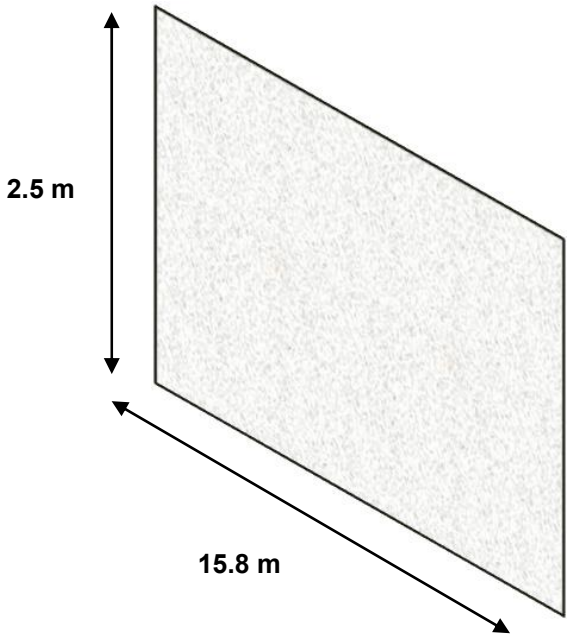

Figure 5.29 Typical wall dimensions.

It should be noted that, the work size of a standard roof tile is around: Length=332 mm, and Width=280 mm (Figure 5.26) [129] and the work size of a standard plaster board is: Length=2.4 m, Width=1.2 m (Figure 5.27). In order to verify the findings, two scenarios have been taken into consideration; outdoor and indoor.

5.6.1.1 Outdoor Scenario (Embedded Rectennas in Roof Tiles)

Considering the outdoor scenario (Figure 5.2), a flat roof tile is selected since it has a simple design and unique striated surface, and would make it a popular choice for all kinds of roofs. As previously mentioned, each roof tile surface area is around $0.332 \times 0.280 = 0.093$ m^2 (around 10.8 tiles can be mounted per metre-squared). Hence, around 2700 tiles can be mounted on the roof of a 250 metre-squared house, which means totally 2700 rectennas can be embedded in roof tiles. It should be noted that the rectenna's thickness is less than 2 mm and hence, it can be easily embedded in a roof tile.

Total number of embedded rectennas in the roof tiles= 2700

$$250\ m^2 / 0.093\ m^2 \approx 2700 \qquad (10.8 \times 250 = 2700)$$

5.6.1.2 Indoor Scenario (Embedded Rectennas in Wall and Ceiling Plaster Boards)

Considering indoor scenario (Figure 5.1 and Figure 5.2), rectennas can be embedded in wall and ceiling plaster boards. The surface area of each plaster board is around $2.4 \times 1.2 = 2.88$ m^2. Hence, around 86.8 plaster boards are required to cover the ceiling of a 250 metre-squared house.

$$250/2.88=86.8$$

Since each plaster board can accommodate at least 50 rectennas, total number of embedded rectennas in the ceiling plaster boards is 4340:

$$50 \times 86.8=4340$$

In order to calculate the total wall area of the 250 metre-squared house, it was assumed a quarter of two walls are occupied by windows and doors, hence,

Wall #1 surface area: $15.8 \times 2.5 = 39.5\ m^2$ (See Figure 5.29 for wall dimensions)

Wall #2 surface area: $15.8 \times 2.5 = 39.5\ m^2$

Wall #3 surface area: $(15.8 - (15.8/4)) \times (2.5 - 2.5/4) = 22.21\ m^2$

Wall #4 surface area: $(15.8 - (15.8/4)) \times (2.5 - 2.5/4) = 22.21\ m^2$

Hence, the number of plasterboards required to cover indoor walls are defined as follows:

(The surface area of each plaster board is around $2.4 \times 1.2 = 2.88\ m^2$)

Number of plaster boards of wall #1 39.5/ 2.88 = 13.7

Number of plaster boards of wall #2 39.5/ 2.88 =13.7

Number of plaster boards of wall #3 22.21/2.88=7.7

Number of plaster boards of wall #4 22.21/2.88=7.7

Total number of plaster boards of inner walls=43

Assuming each plaster board can accommodate at least 50 rectennas, total number of embedded rectennas in inner walls plaster boards: 43×50=2125

Hence, total number of indoor rectennas (ceiling and walls): 4340+2125=6465

5.6.2 Approximate Amount of Harvested Power for a Typical Building

As can be seen in Table 5.5, based on the real environmental field measurement**,** a single embedded rectenna in plaster is able to generate approximately 175 μW from outdoor RF signals and 68 μW from indoor RF signals (in the suburb of Bayswater). Hence, approximate amount of DC power could be harvested from all the embedded rectennas in building materials (outdoor and indoor) is calculated as follows.

5.6.2.1 Outdoor Scenario:

Total number of outdoor rectennas (embedded rectennas in the roof tiles) is equal to 2700. Hence, approximate amount of harvested DC power (e.g. in the suburb of Bayswater):

$$2700\times175=472500\ \mu W \approx 473\ mW$$

5.6.2.2 Indoor Scenario:

Total number of indoor rectennas (embedded rectennas in the ceiling and wall plaster) is equal to 6465. Hence, approximate amount of harvested DC power (e.g. in the suburb of Bayswater):

$$6465\times68=439620\ \mu W \approx 440\ mW$$

Therefore, total amount of harvested DC power for a 250 metre-squared house from outdoor and indoor RF signals can be estimated (e.g. in the suburb of Bayswater):

$$472.5+439.62 \approx 912 \text{ mW}$$

It is worth to highlight that, these calculations shows the amount of DC power which can be produced instantly. Hence during day and night the total harvested DC power will be increased significantly and could be stored in a super capacitor or a battery. Therefore, RF energy harvesting has the potential to generate a viable energy source in urban environment (predominately for low power applications), cleanly, safely and cheaply.

5.7 Conclusion

The feasibility of harvesting ambient EM energy from television and FM broadcasting frequency bands are investigated in this chapter. The proposed sensitive and efficient RF scavengers operate at 520-590 MHz and 89-111 MHz bands and present desirable impedance matching over broad low input power ranges of −40 to −10 dBm (0.1-100 μW) and −50 to −10 dBm (0.01-100 μW) respectively, enabling the harvesting of RF energy in urban environments. The achieved high sensitivity and dynamic range shows the usefulness of this new very low input power rectification method. The characteristics of the proposed rectifiers in this chapter are summarised in Table 5.6.

Furthermore, apart from the rectifiers' performance, the practicality of embedding RF energy harvesting systems in building materials is investigated, aiming to provide a sustainable, green and inexpensive energy source in urban environments. To address this, the proposed FM rectifier is integrated with a simple dipole antenna to realise a rectenna. The rectenna is then embedded into building materials (plaster), creating an innovative harvesting system. A realistic case is also presented to estimate the total amount of DC power that could be harvested from outdoor and indoor RF signals for a typical building.

Simulation results of the input reflection coefficient and output DC power agreed well with the measurements. The proposed sensitive FM rectenna takes the advantage of harvesting energy over a broad frequency band. It was shown that it could generate higher DC power than using different separate single frequency rectifiers operating at the same frequencies with very low input powers (<2 μW). Sensitive Schottky diodes and a highly efficient broadband matching network result in a sensitivity of −50 dBm (0.01 μW) for the proposed FM band rectenna, which has not been reported previously. This is achieved by scavenging

multiple RF signals and delivering more power to the rectification device, hence harvesting very low density ambient signals.

The output DC power from seven input frequency tones simultaneously fed to the FM scavenger, exhibits improved sensitivity and output DC power over the single tone excitation. It is proved that broadening the bandwidth (not ultra-widening) enhances the RF to DC conversion efficiency, and hence the rectified DC power for low power applications in urban environments (e.g. home and office devices).

Table 5.6 Specifications of the Proposed Rectifiers (without plaster)

RF Scavenger	Sensitivity (dBm)	RF power variation (in PCE evaluation)	Efficiency (%)	Frequency Range (MHz)	Rectification Technique	Rectification Device
TV band Rectifier	−40	−40 to −10 dBm (0.1 to 100 µW)	(Simulated) 53 @ 100 µW	520- 590	Broad bandwidth (12.6 % Fractional Bandwidth)	Schottky diode
FM band Rectifier	−50	−50 to−10 dBm (0.01 to 100 µW)	(Measured) 1.4 @ 0.01µW 1.6 @ 0.1 µW 3.2 @ 0.5 µW 6.2 @ 1 µW 12 @ 2.5 µW 17 @ 5 µW 23 @ 10 µW 29 @ 20 µW 41 @ 100 µW	89-111	Broad bandwidth (22% Fractional Bandwidth)	Schottky diode

Chapter 6 - Multi-tone Excitation Analysis in RF Energy Harvesting Systems

6.1 Introduction

As proved in Chapter 4 and 5, the rectifier can produce a higher amount of DC power when multiple tones of various frequencies (in the matched frequency bands) are applied at the input of the rectifier or exist in ambient signals.

In Chapter 4, a new approach to evaluate the RF to DC conversion efficiency in the case of multiple tones was proposed; "effective efficiency" was defined as the ratio of output DC power to the available input RF power rather than the power delivered to the diodes (available power level is associated with the signal source).

For example, for a single tone excitation, the available input power is −10 dBm and the delivered power is also −10 dBm (assuming no loss). However, by applying two tones the power delivered to the diodes is close to −7 dBm (combined total input power from two signal generators) but the available power in ambient is still −10 dBm. Hence, in "effective efficiency" calculation where two tones of −10 dBm are applied, the input power was considered as −10 dBm.

In order to determine the true efficiency of the rectifier for the case of multi-tone excitation, the input power should be constant regardless of the number of tones. This was not the case in Chapters 4 and 5 as they were dealing with ambient cases in which there is no control over the input power.

For more clarity, the DC output power of the rectifier when one tone of −10 dBm is available at the input can be compared with the output of the rectifier when two tones of −13 dBm or three tones of −14.77 dBm or four tones of −16.02 dBm are available at the input, since in all these cases the total combined input power is the same (−10 dBm).

It is worthwhile to mention that, in the WPT (wireless power transmission) scenario, it has been demonstrated theoretically and experimentally [69] that applying a multi-tone signal with a constant total input power level to the rectifier circuit, results in an increased output power over the single-tone excitation (with the same input power) due to a higher PAPR (peak-to-average power ratio) of the multi-tone signal. However, various parameters should be taken into consideration during the design phase, such as signal bandwidth, tone spacing, and phase arrangement, which are unknown and hence, out of the control in an ambient energy scavenging scenario. Furthermore, the achieved outcomes [69] are exclusively valid for the proposed rectifier circuit and cannot be generalised.

In this chapter in order to facilitate the comparison between single tone and multiple tones, regardless of the number of excited tones, the total input power is kept constant in all cases. Hence, the effect of applying multi tones with different phases and frequency spacing on the DC output of the rectifier will be investigated. To address this, frequency domain (harmonic balance) and time domain analyses are conducted. Furthermore, measurements are performed to verify the findings.

6.2 Circuit Topology for Multi-sine Excitation Analysis

Figure 6.1 depicts the FM rectifier which was used for multi-sine analysis in Chapter 5. The red circles indicate the points where simulation and measurements were carried out (for both voltage and current).

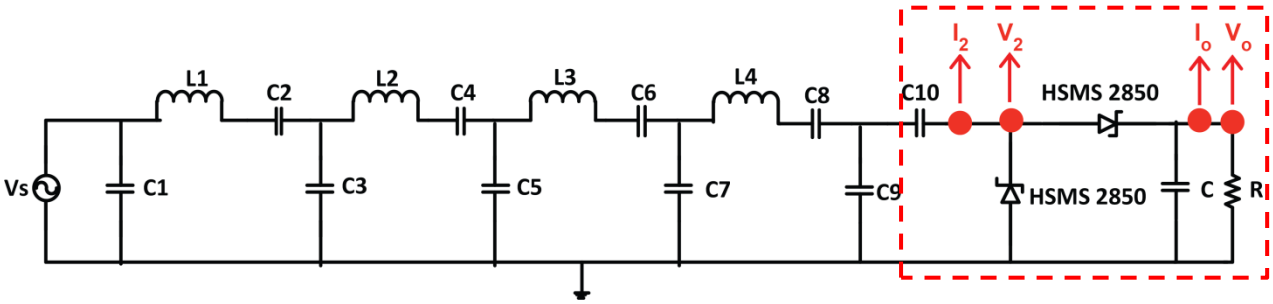

Figure 6.1 Schematic of the FM rectifier. The optimised values of the standard chip components are: C1=30 pF, L1=150 nH, C2=33 pF, C3=82 pF, L2=150 nH, C4=24 pF, C5=160pF, L3=82 nH, C6=62 pF, C7=82 pF, L4=560 nH, C8=150 pF, C9=3.6 pF, C10=1 nF, C=430 pF, R=18 KΩ.
(Here, I_2 refers to I_ probe2 which is the current over C10.)

6.3 Harmonic Balance (HB) Analysis

In order to demonstrate the effect of multi-signal excitation on the output DC power of the rectifier, various concurrent tones (in the matched FM frequency band) are applied to the circuit using Agilent ADS software. In the measurement case, multi-tones are generated simultaneously with different signal generators, summed using a power combiner, and passed to the rectifier.

As it was demonstrated in Chapter 5, the proposed rectifier circuit with 22% fractional bandwidth is well-matched within 89-111 MHz over a broad low input power range of −50 to −10 dBm (0.01-100 µW). Furthermore, Figure 6.2 illustrates the frequency response of the rectifier and indicates that it has a similar output DC power (i.e. efficiency) at the selected

frequencies between 94-99 MHz (due to the diode characteristics); hence, a fair comparison between various tones can be performed.

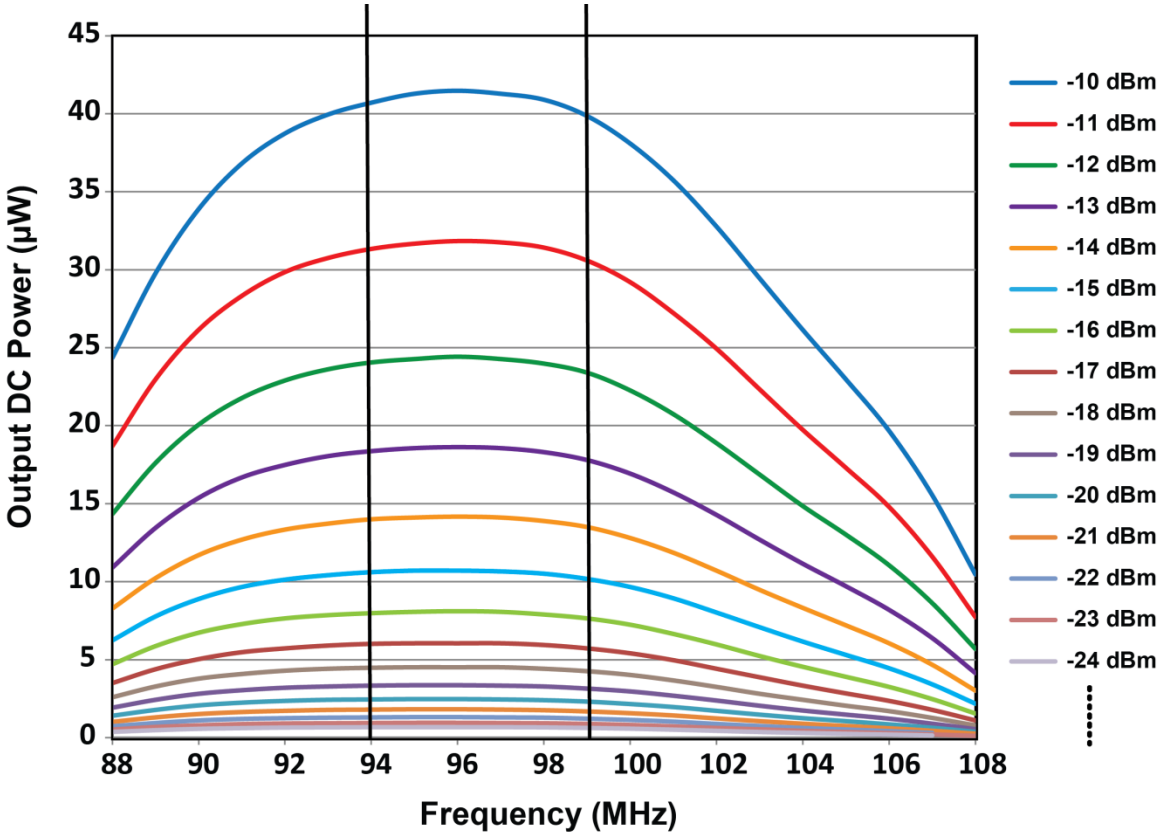

Figure 6.2 Output DC power versus frequency for the FM rectifier circuit at different input power levels. Various frequencies from 94 to 99 MHz with similar output were selected for multi-sine analysis.

The following sub-sections demonstrate the output DC power of the rectifier with various concurrent input tones over a broad range of input power −40 to −10 dBm (0.1 to 100 µW) with various frequency spacing between input signals. As discussed earlier for the purpose of this study, in all cases the input power (P_{in}) is kept constant (eqn. 6.1). Hence, the input power is the same for both the single-tone and multi-tone case (*N* refers to the number of tones).

$$P_{in} = P_1 + P_2 + P_3 + \ldots\ldots\ldots P_N \qquad (6.1)$$

6.3.1 Harmonic Balance Analysis and Measurement Results for Multi-tones with 1MHz Frequency Spacing over −40 dBm to −10 dBm (0.1 µW to 100µW)

Various tones within the matched frequency band with 1 MHz frequency spacing (94-99 MHz) were applied to the rectifier and the output DC power was analysed. Figure 6.3 depicts the output voltage that can be obtained from various simultaneous tones. The output voltage across the load is then used to calculate the output power (Figure 6.4).

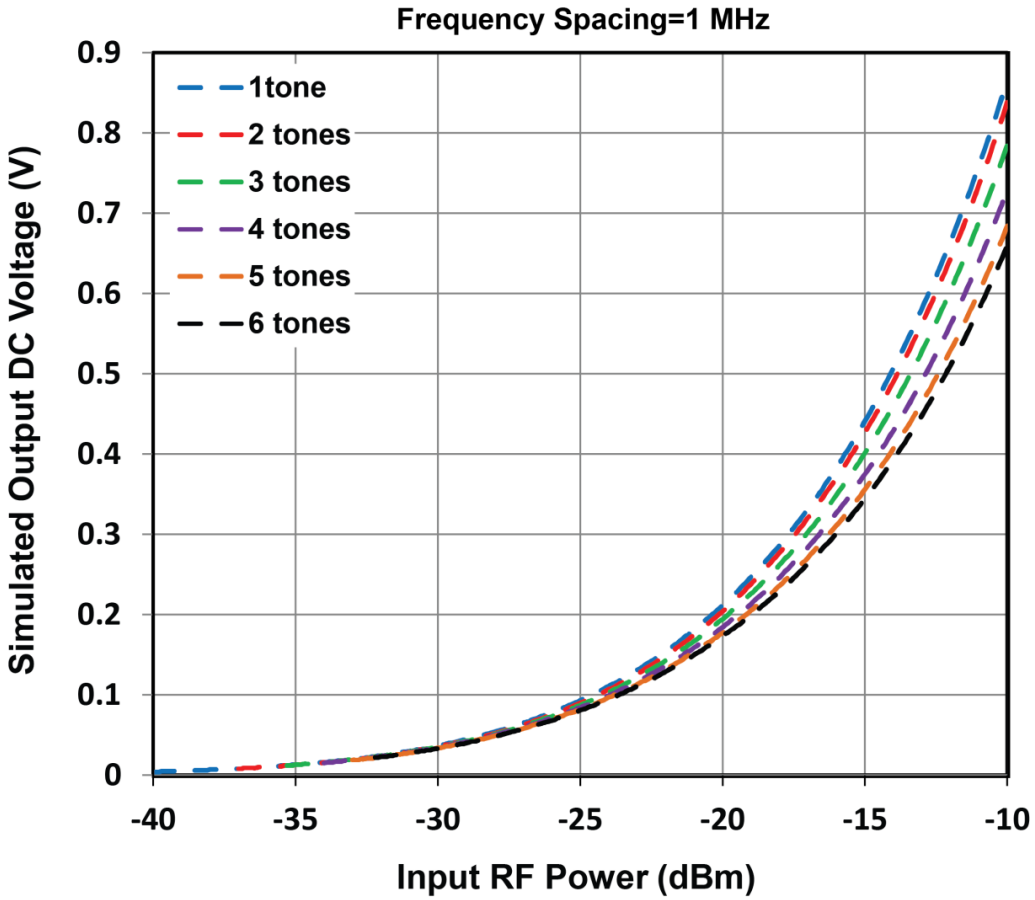

(a)

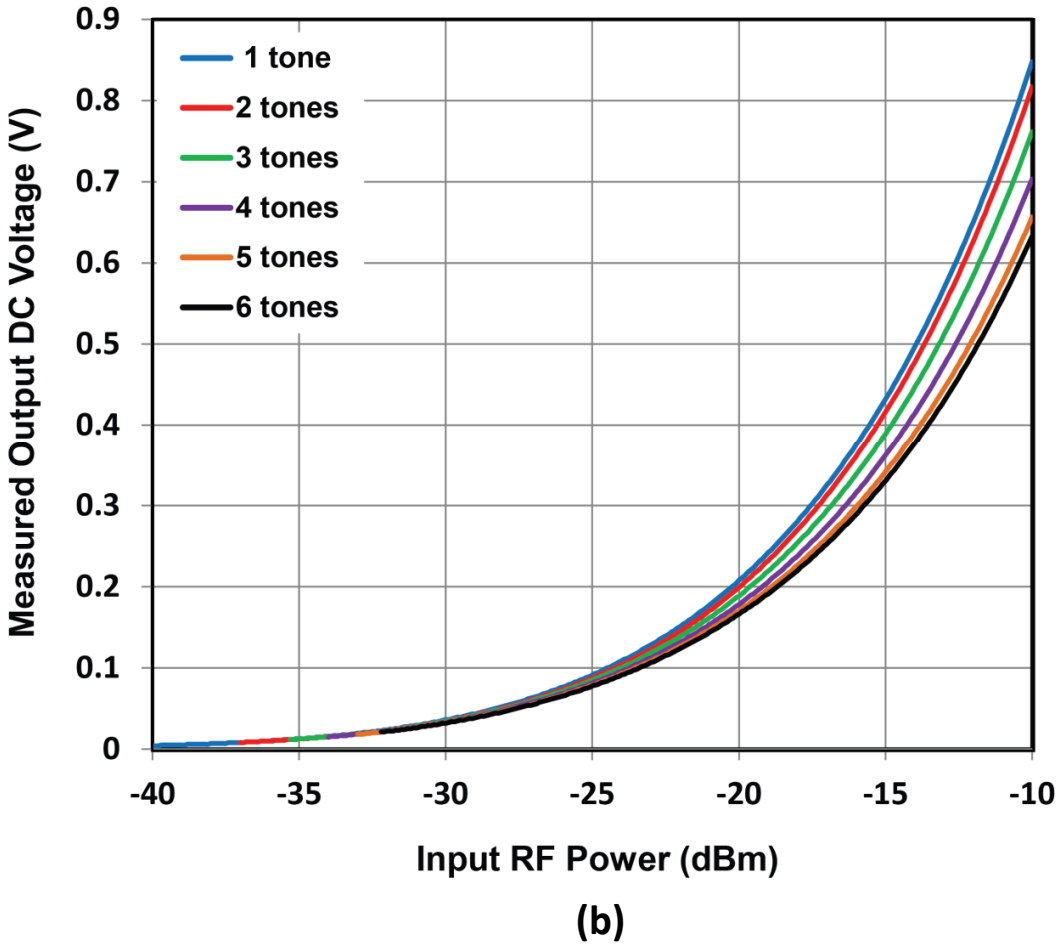

Figure 6.3 Output DC voltage as a function of input RF power for single-tone and multi-tone excitations with constant total input power over −40 to −10 dBm. Six frequencies from 94-99 MHz with 1 MHz spacing are applied to the FM rectifier. (a) Simulation. (b) Measurement.

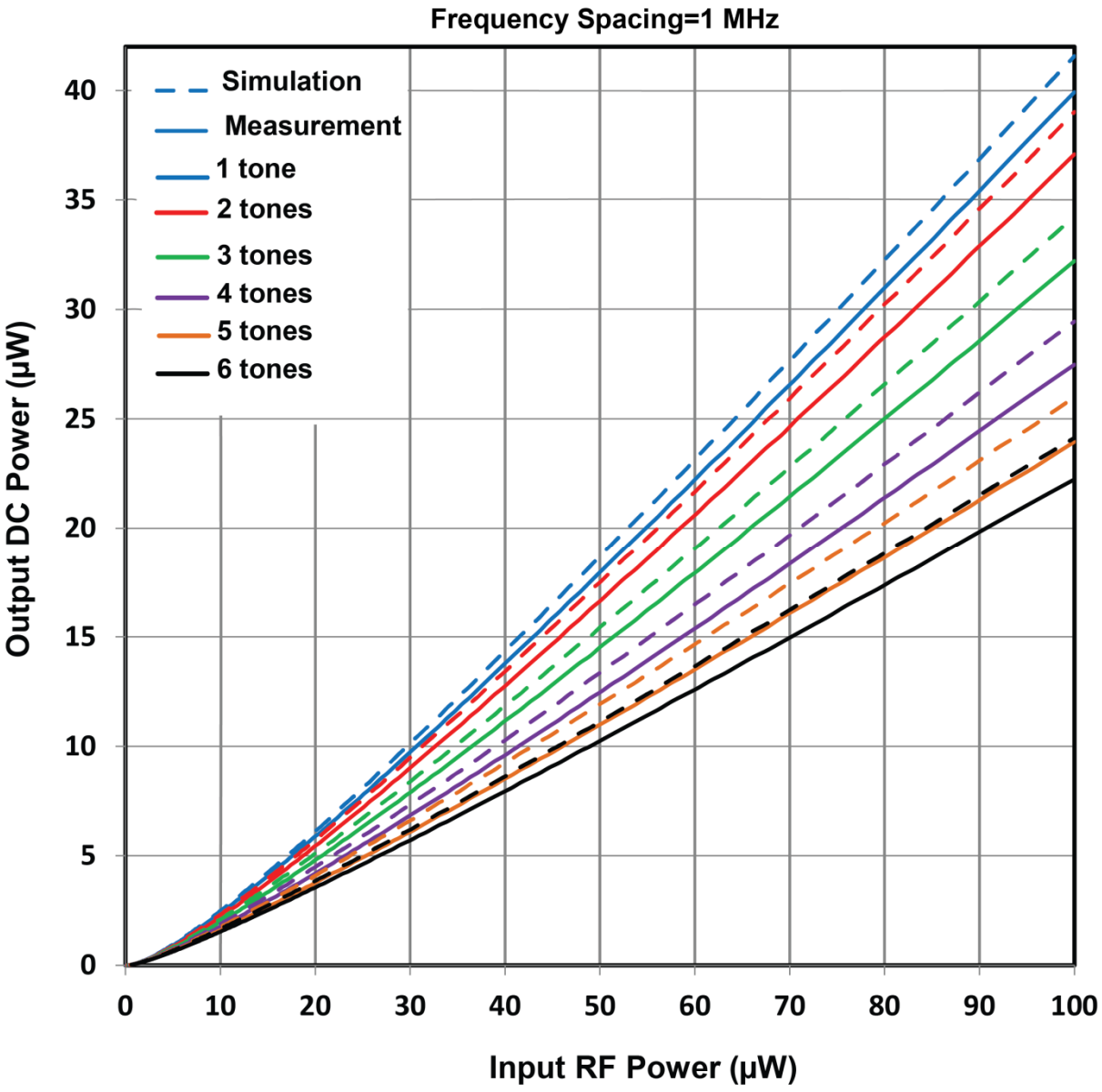

Figure 6.4 Simulated and measured output DC power as a function of input RF power for single-tone and multi-tone excitations with 1 MHz frequency spacing from 94-99 MHz over –40 to –10 dBm (0.01-100µW).

Measurement results and HB analyses show that applying multi-tones with a constant input RF power results in a lower output DC power when compared to the single-tone case with the same input power. In order to understand the phenomena, various cases are analysed in the following sub-sections.

6.3.2 Harmonic Balance Analysis for Multi-tones with 0.5 MHz Frequency Spacing

In this case, eight tones with 0.5 MHz frequency spacing (94-97.5 MHz) were applied to the rectifier and the output DC power is depicted in Fig 6.5.

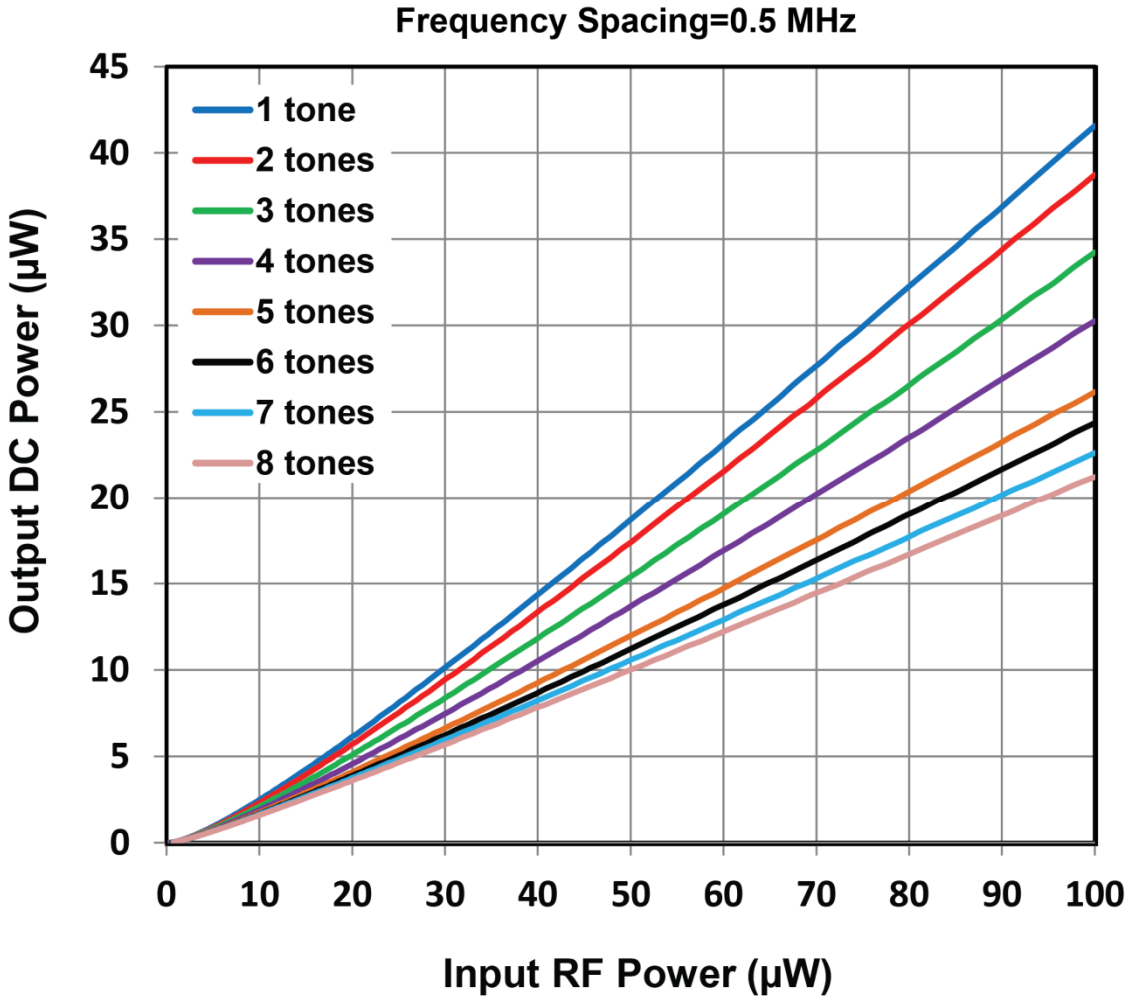

Figure 6.5 Simulated output DC power as a function of input RF power for single-tone and multi-tone excitations with 0.5 MHz frequency spacing.

As shown, when eight tones with a total input power of 100 μW (−10 dBm) (which means 12.5 μW (−19 dBm) each), with 0.5 MHz spacing are applied to the rectifier, approximately

half of the output DC power (21 µW) can be generated when compared to the single tone of 100 µW (−10 dBm).

6.3.3 Harmonic Balance Analysis for Multi-tones with 0.01 MHz Frequency Spacing

In this case, eight tones with 0.01 MHz frequency spacing (94-94.07 MHz) were applied to the rectifier and the output DC power is depicted in Figure 6.6.

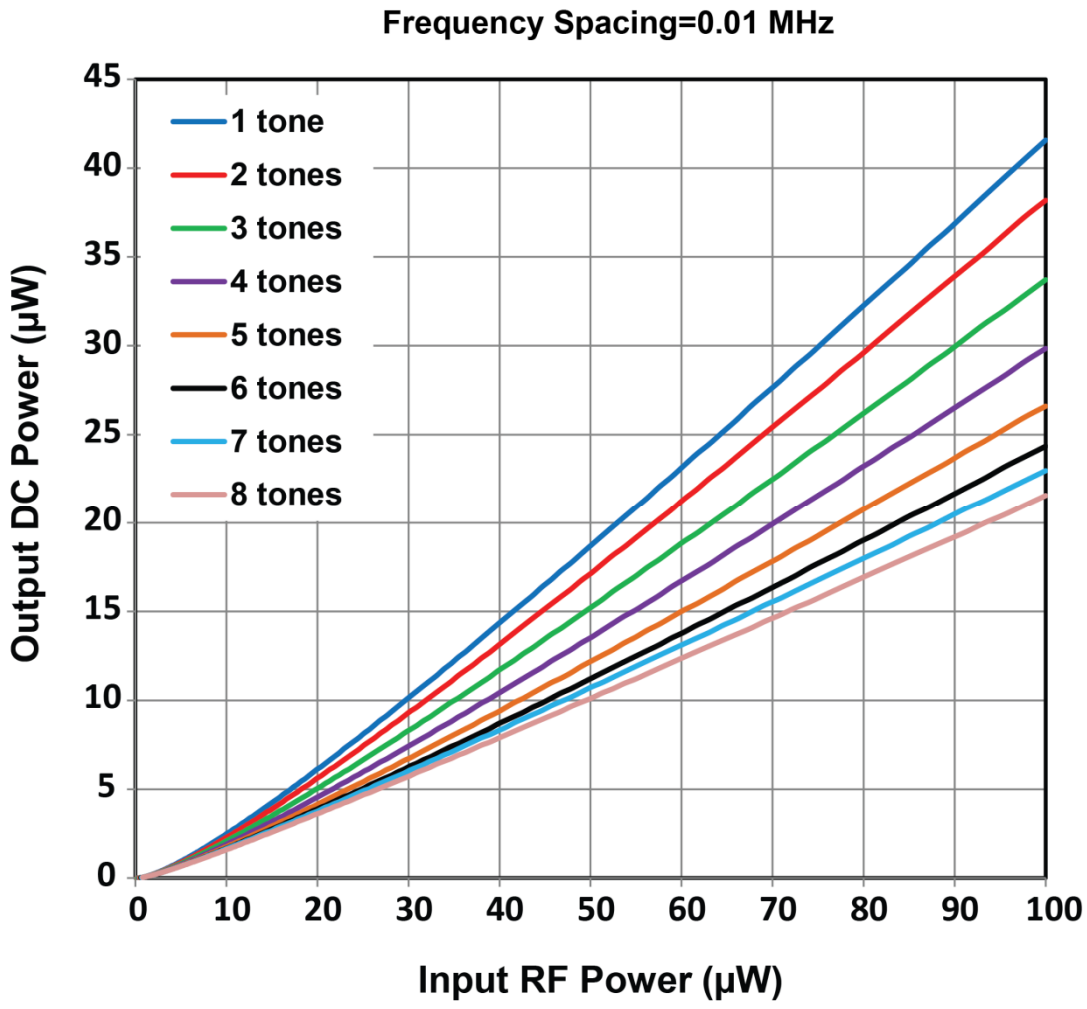

Figure 6.6 Simulated output DC power as a function of input RF power for single-tone and multi-tone excitations with 0.01 MHz frequency spacing.

As demonstrated in all the above cases, multi-tone excitation with constant input power levels and various frequency spacing, results in a lower output DC power when compared to the single-tone case with the same input power. Furthermore, the effect of changing the frequency spacing was insignificant. This is due to the diode characteristic and the matching performance which are similar at the selected frequencies. However, further analysis needs to be performed in the time domain.

6.4 Time Domain Analysis

Time domain (TD) analysis is performed to investigate the reason for obtaining a lower amount of output DC power when increasing the number of tones (as seen in the previous section). Therefore, delivered voltage/current to the rectification device and also output voltage/current of the rectifier are evaluated (these points are shown in Figure 6.1).

Time domain analysis for single-sine and multi-sine excitations with varying frequency spacing and input power levels (P_{in} is constant in each case) are conducted. Phase variation has also been evaluated, however, it did not have a significant change in analysis results, and hence the phase is assumed to be zero.

Figure 6.7 demonstrates time domain analysis of the rectifier with single-tone (a) and multi-tone (b-d) excitations. Comparing Figure 6.7 (a) and (b), show TD analysis of the rectifier with one tone and four-tone excitations respectively with total input power of −20 dBm. It is demonstrated that although, applying various tones simultaneously results in a higher peak value of the current (I_probe 2), the total average output DC voltage (V_o) reduces, as was shown in Section 6.3 (HB analysis).

For more clarity, by comparing one-tone (Figure 6.7 (a)) and ten-tone excitation (Figure 6.7 (d)), in the multi-tone, the total output voltage is dropped from 176 mV (with one tone) to 122 mV (with ten tones) with total input power of −20 dBm at the input in both cases.

It is worthwhile to highlight that in Figure 6.7, the spacing between the two peaks (in μsec) corresponds to the beat frequency which shows the difference between various tones (in this case frequency spacing is 0.5 MHz).

It should be noted that by selecting a higher value output capacitor, the ripple at the output will be smoother by removing the beat frequency; however, simulation time increases and also the matching network performance can be effected.

6.4.1 Time domain Analysis with 0.5 MHz Frequency Spacing and Total Input Power of −20 dBm

a) 1 tone of −20 dBm (10 µW)

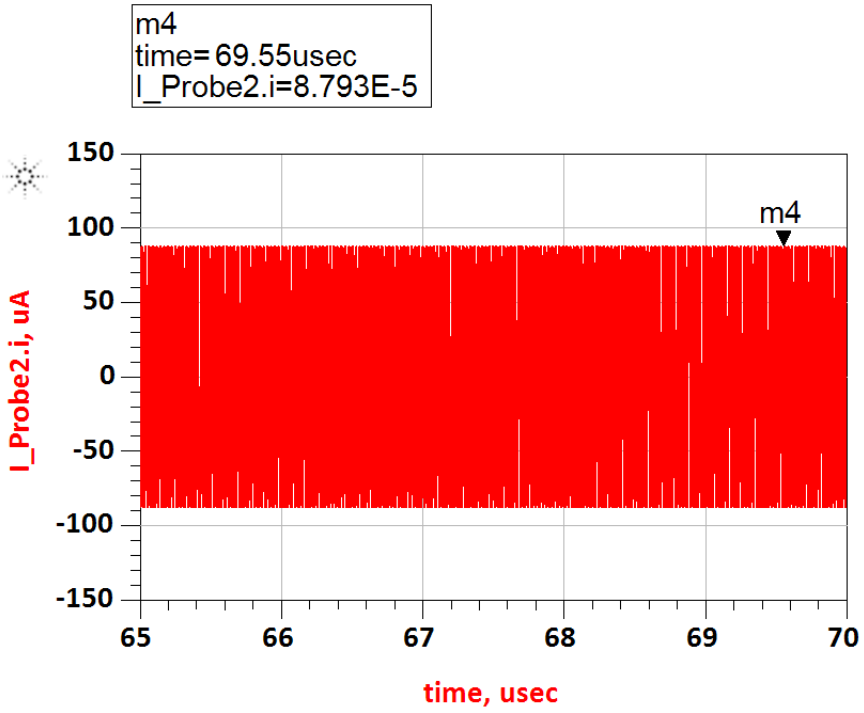

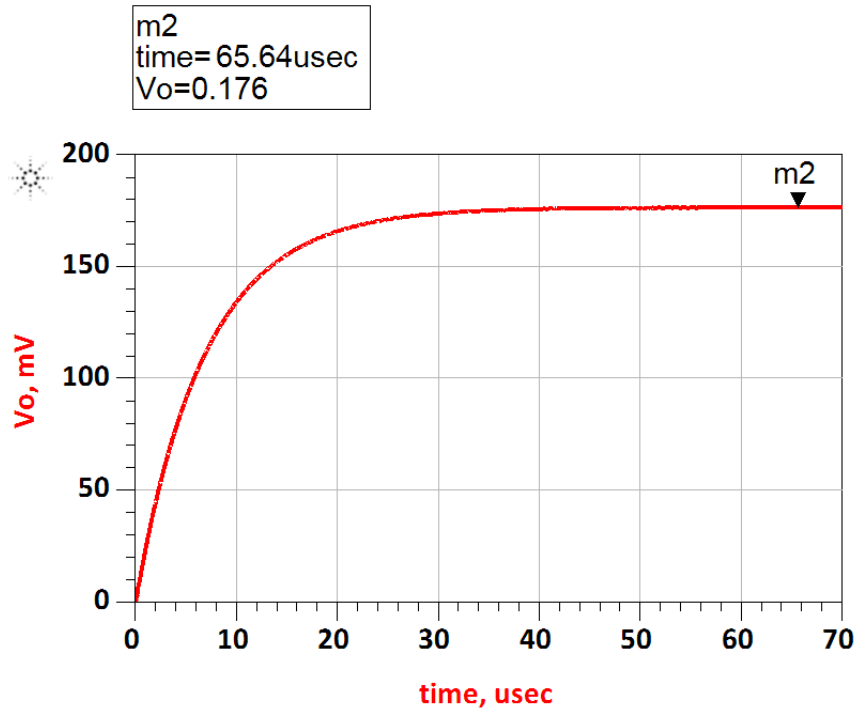

b) 4 tones of −26.02 dBm (total of −20 dBm)

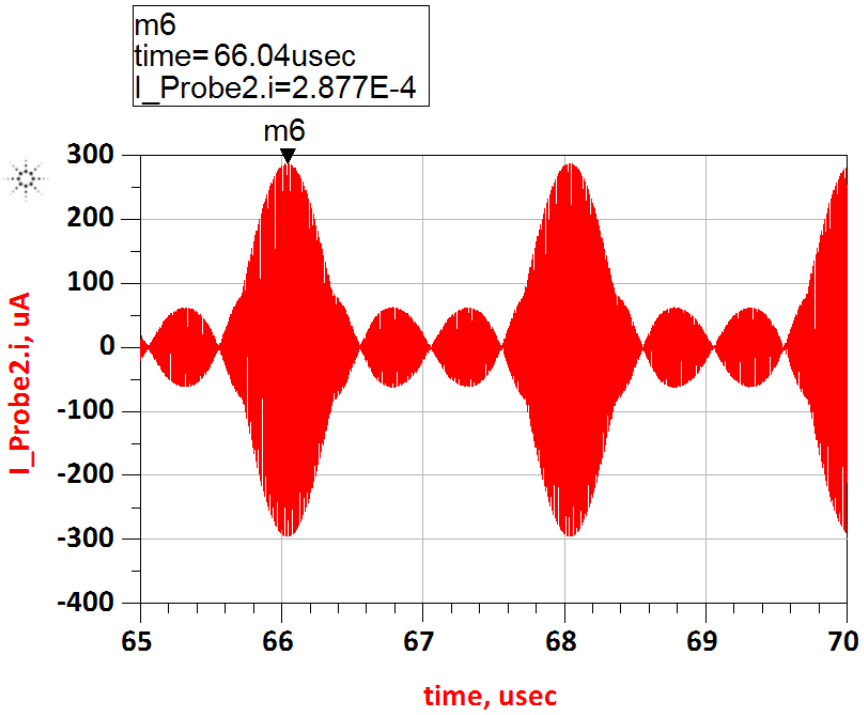

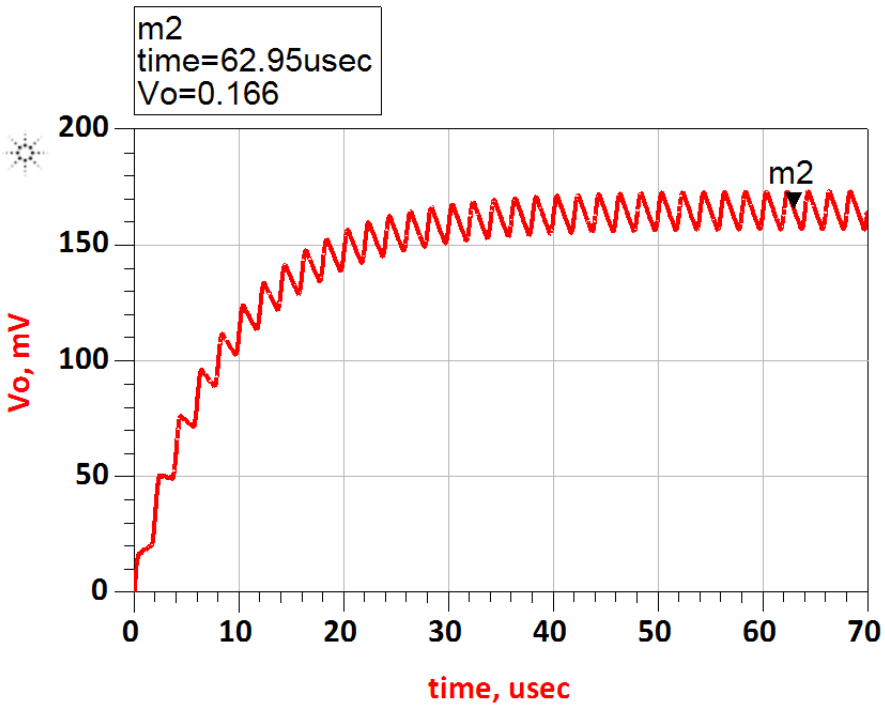

c) 8 tones of −29 dBm (total of −20 dBm)

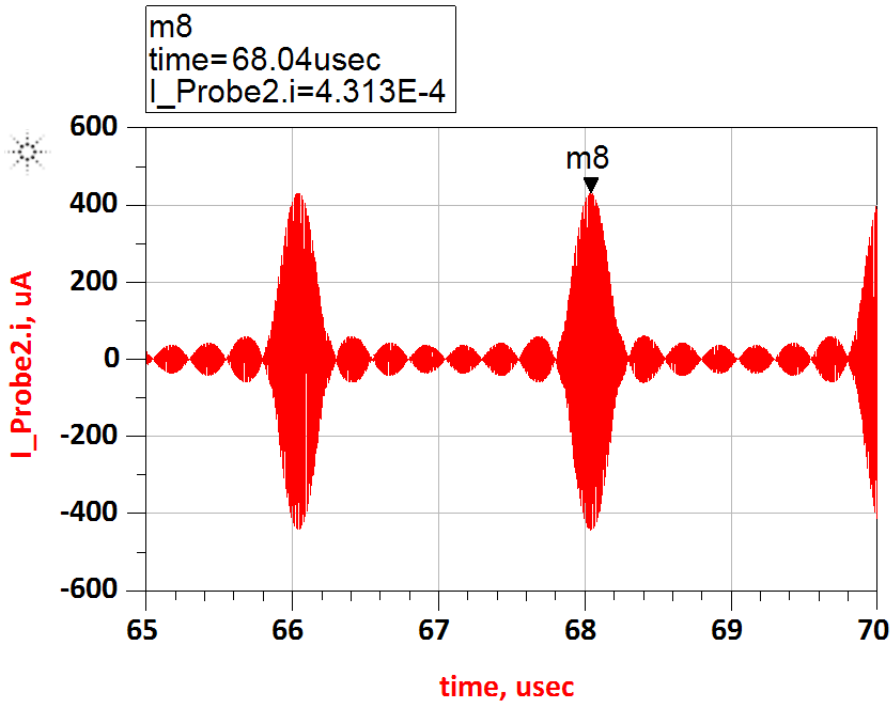

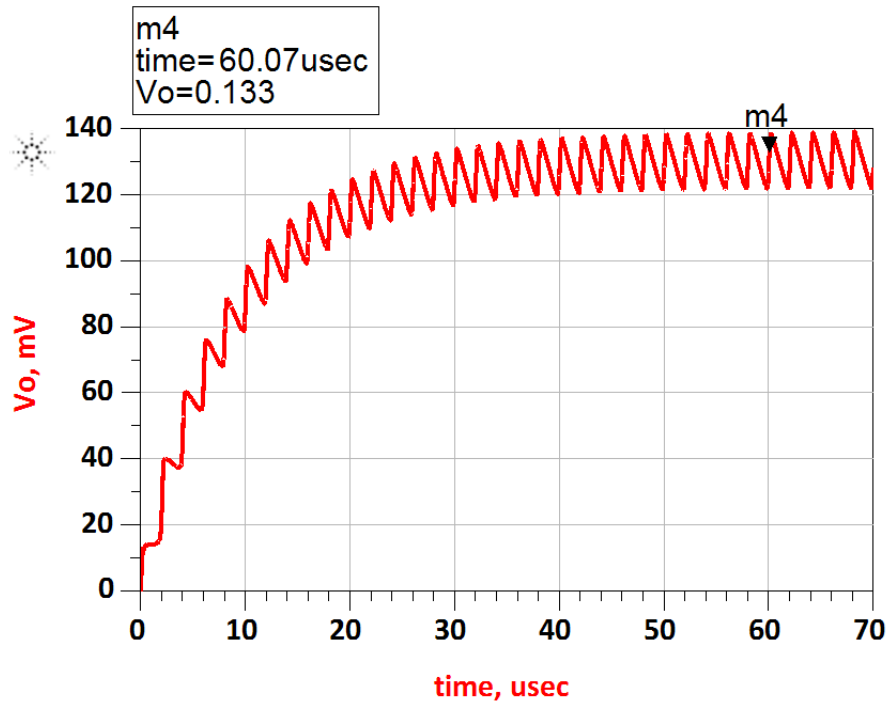

d) 10 tones of −30 dBm (total of −20 dBm)

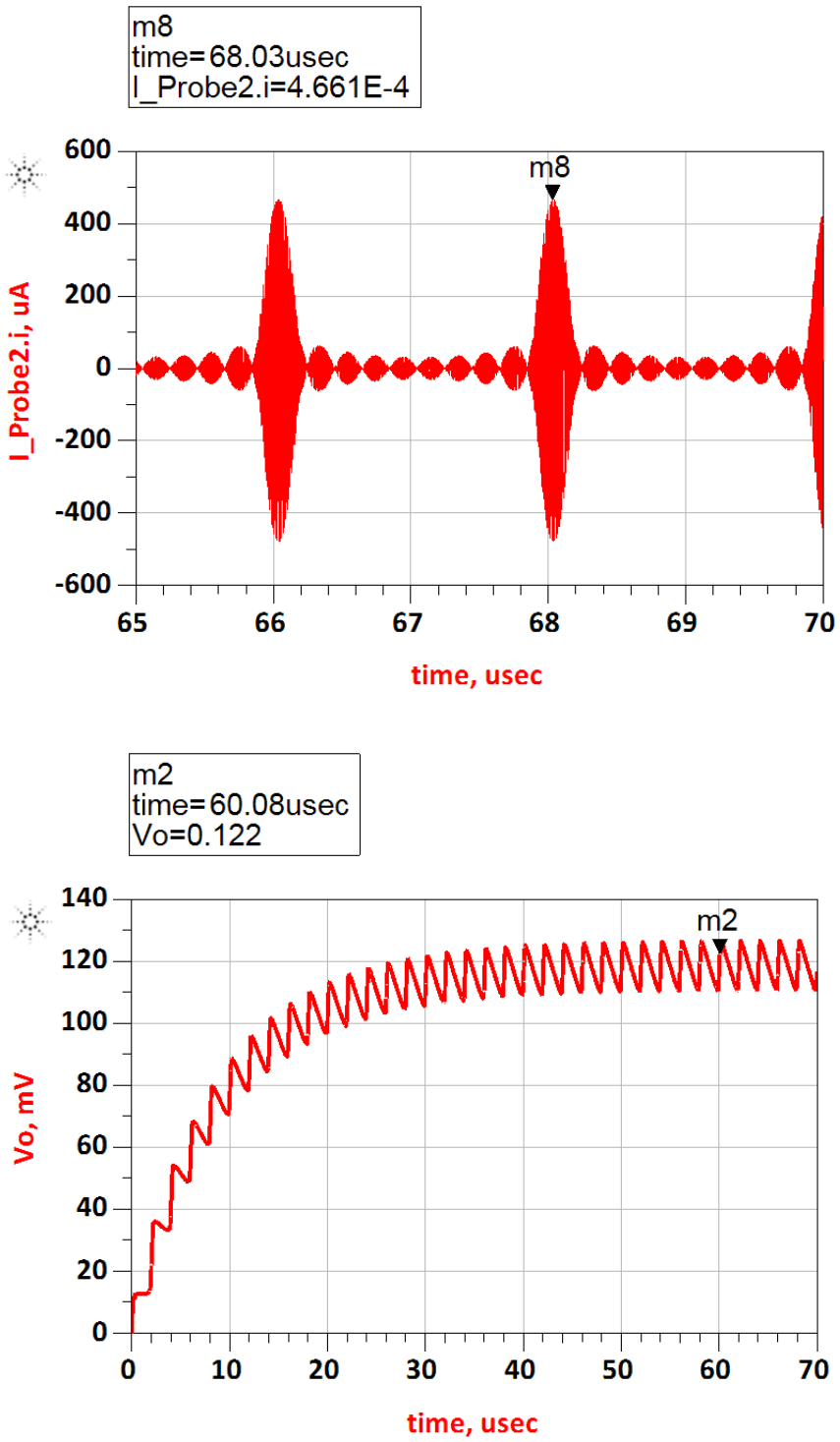

Figure 6.7 Time domain analysis for single-tone and multi-tone excitations with 0.5 MHz frequency spacing and total input power of −20 dBm. (a) 1 tone of −20 dBm. (b) 4 tones of −26.02 dBm. (c) 8 tones of −29 dBm. (d) 10 tones of −30 dBm.

As illustrated in Figure 6.7, with one tone of −20 dBm, 176 mV output DC voltage could be achieved, while by applying eight concurrent tones of −29 dBm (same total input power of −20 dBm), 123 mV was generated, which is in agreement with the HB and measurement results (Section 6.3).

Furthermore, in order to draw a conclusion, different cases were analysed such as:

- TD Analysis with 0.1 MHz Frequency Spacing and Total Input Power of −20 dBm.
- TD Analysis with 0.5 MHz Frequency Spacing and Total Input Power of −10 dBm.
- TD Analysis with 0.5 MHz Frequency Spacing and Total Input Power of −40 dBm.
- TD Analysis with 0.5 MHz Frequency Spacing and Total Input Power of −50 dBm.
- TD Analysis with 1 MHz Frequency Spacing and Total Input Power of −10 dBm.
- TD Analysis with 1 MHz Frequency Spacing and Total Input Power of −20 dBm.
- TD Analysis with 1 MHz Frequency Spacing and Total Input Power of −30 dBm.

In all the above cases, similar outcomes were achieved as depicted in Figure 6.7.

In order to investigate the reason for obtaining a lower amount of output DC power with the multi-tone excitation, the performance of the voltage doubler topology (the dashed circuit in Figure 6.1) should be analysed. As it was explained in Chapter 4, this topology was used to enhance the sensitivity and the efficiency of the rectifier circuit.

The performance of the voltage doubler depends on the input RF signal (delivered signal to the voltage doubler). However, as demonstrated in Figure 6.7 (b-d) for the multi-tone cases, the waveform changes (I_probe 2 plots) and is not a conventional sine wave; hence the operation of the voltage doubler is effected, which results in a lower output voltage.

6.5 Conclusion

This chapter discussed the effect of multi-tone excitation on the output DC response of the FM rectifier. In order to facilitate the comparison between single tone and multiple tones, regardless of the number of excited tones, the total input power was kept constant in all cases. Hence, the effect of applying multi-tones with various factors (e.g. frequency spacing, input power, and random phase) was analysed. Frequency and time domain analyses were conducted and measurements have been performed to clarify the findings.

It was demonstrated that, applying multi-tones simultaneously (with constant total input power and within the matched frequency band) results in a lower total average output voltage/power, when compared with single-tone case with the same input power. This trend was evident down with different frequency spacing, input power levels, and phase arrangements.

The reason for obtaining a lower amount of output DC power with the multi-tone excitation was the change in the signal waveform. In multi tone case, the input waveform (input of the voltage doubler) was not a conventional sine wave; hence the operation of the voltage doubler was effected, which results in a lower output voltage/power.

This analysis led us into future works which are explained in Chapter 7.

Chapter 7 – Conclusions and Future Work

7.1 Conclusions

The aim of this thesis was to investigate the feasibility of RF energy scavenging and to develop highly sensitive and efficient RF harvesting method and system. The ultimate goal was to generate a viable energy source in urban environments, predominately for low power applications (e.g. home and office devices).

This research study has demonstrated the possibility of scavenging very low-density ambient RF signals from various frequencies and has advanced the body of knowledge in the field of RF energy scavenging. It is believed that RF energy harvesting is a promising technique to provide a sustainable energy source for the long-term conservation of the environment and the global economy.

7.1.1 Chapter 3 – RF Field Investigation and Maximum Available Power Analysis

The aim of this chapter was to explore the feasibility of harvesting ambient EM energy in metropolitan areas of Melbourne, Australia, which has not been reported previously. Several RF field measurement results were collected and averaged to establish a comprehensive database. Hence, the usable frequency ranges with their associated scavengeable power levels were determined in this chapter. Furthermore, maximum available power analysis for different frequency bands based on antenna aperture and number of antennas in a given collecting area was provided to estimate the potential of RF energy harvesting.

This chapter identified three important conclusions;

1. The scavengeable levels of ambient RF power have been shown to be orders of magnitude lower than previous published works.
2. It was presented that the scavengeable power level is generally unknown, incoherent and effected by environmental/free-space conditions such as; the distance from the power source to a rectenna, propagation losses (free-path and attenuation), and the antenna orientation (polarisation).
3. Broadcasting frequency ranges such as; FM and TV at 88-108 MHz and 470-890 MHz respectively have been shown as preferred power-scavenge sources due to their suitable level of the ambient power at a variety of locations. Furthermore, cellular and wireless communication systems (800-1000 MHz) have recommended as alternative power scavenge sources.

This chapter also presented different rectenna configurations, and an optimum approach was proposed based on the field measurement outcomes. The solution was to identify and harvest multiple ambient frequency sources over their realistic available energy range in order to increase the amount of RF energy scavenged by a rectenna.

The investigations and analysis of this chapter enable the design of an appropriate RF rectifier circuit based on the real environmental cases. The outcome of this chapter built up the baseline knowledge of low power RF harvesting which was the foundation for the proceeding chapters.

7.1.2 Chapter 4 – Multi-Service Highly Sensitive Rectifier

Based on the recommendation of previous chapter, the feasibility of harvesting ambient EM energy from multiple sources simultaneously was investigated in this chapter. The proposed dual resonant rectifier was found to be most effective when operating a two frequency bands (478-496 and 852-869 MHz) simultaneously, which are allocated to Australia broadcasting and cellular systems.

The dual resonant rectifier achieved favourable impedance matching over a broad low input power range (−40 to −10 dBm) at these two bands. The measurement results demonstrated that a two-tone input into the proposed dual-band RF energy harvesting system can generate 3.14 and 7.24 times more power than a single tone at 490 and 860 MHz respectively, resulting in a measured effective efficiency of 54.3% for dual input tones of −10 dBm. Therefore, delivering multiple RF signals into a single rectification stage resulted in high sensitivity rectifier, which is widely applicable to real environmental RF energy scavenging. This multi-band technique could provide higher DC power than combining two separate single frequency rectifier circuits operating at the same frequencies. This was due to the fact

that harvesting RF energy from various sources simultaneously increased the delivered power to the rectifier, which improved the diode conversion efficiency and consequently enhanced the output DC power.

In order to provide more realistic measurement results, the dual-band rectifier was tested in three suburbs of Melbourne, Australia, congruent with the finding of Chapter 3. The proposed highly sensitive rectifier has 3.67% and 2% fractional bandwidth at the lower and the higher band respectively and hence, various RF source frequencies can be scavenged within these two bands. It was shown that the rectifier could generate 39.38 μW by harvesting RF energy from two bands simultaneously in the suburb of Bayswater.

7.1.3 Chapter 5 – Highly Sensitive Rectenna Embedded in Building Materials

As it was recommended in Chapter 4, harvesting energy over a wider frequency band (not ultra-wideband) could increase the sensitivity and hence the output DC power of the rectifier. This was achieved in this chapter by scavenging more RF signals and delivering more power to the rectification device through a broadband matching network (up to 22%), hence harvesting very low density ambient signal.

This chapter presented the feasibility of harvesting ambient EM energy from television and FM broadcasting frequency bands, congruent with the outcomes from Chapter 3. The proposed sensitive and efficient RF scavengers could operate at 520-590 MHz and 89-111 MHz bands and presented desirable impedance matching over broad low input power ranges of −40 to −10 dBm and −50 to −10 dBm respectively, enabling the harvesting of RF energy in urban environments.

The proposed sensitive FM rectenna with 22% fractional bandwidth, took the advantage of harvesting more energy over a broad frequency band and generated higher DC power than using different separate single frequency rectifiers operating at the same frequencies with very low input powers (<2 μW). Sensitive Schottky diodes and a highly efficient broadband matching network with low insertion loss resulted in a sensitivity of −50 dBm (0.01 μW) for the proposed rectenna, which has not been reported previously. It was also demonstrated that, a single tone excitation delivers a measured power conversion efficiency of 41% at −10 dBm.

The output DC power from seven input frequency tones simultaneously fed to the RF scavenger, demonstrated improved sensitivity, and output DC power over the single tone excitation. It was proved that, one rectifier which was able to capture *N* signals of different frequencies simultaneously performed better than *N* single frequency individual rectifies operating at the same frequencies (at very low input power levels <2 μW).

Furthermore, the practicality of embedding RF energy harvesting systems in building materials was investigated, aiming to provide a sustainable, green, and inexpensive energy source in urban environments. To address this, the proposed FM rectifier was integrated with a simple dipole antenna to realise a rectenna. The rectenna was then embedded into building materials (plaster), creating an innovative harvesting system. In order to verify the findings, both laboratory and real environmental measurements were conducted. Based on the environmental measurements of the embedded rectenna in plaster, 175 μW of DC power was achieved (in the suburb of Bayswater). Furthermore, the combination of very low RF power levels (e.g. at RMIT University), could turn on the proposed sensitive rectenna and generate 4.15 μW of DC power.

A realistic case was also presented to estimate the total amount of DC power that could be harvested from outdoor and indoor RF signals for a typical building. As it was estimated for a

typical building in the suburb of Bayswater, around 912 mW DC power could be harvested from outdoor and indoor RF signals.

7.1.4 Chapter 6 – Multi-tone Excitation Analysis in RF Energy Harvesting Systems

In order to determine the true efficiency of the rectifier for the cases of multiline excitations and also to facilitate the comparison between single tone and multiple tones, the input power should be constant regardless of number of tones. Hence, this chapter investigated the effect of multi-tone excitation (with constant total input power) on the output DC response of the FM rectifier. The effect of applying multi tones with various factors such as; different frequency spacing, low input power levels, and random phase arrangement were analysed. To address this, frequency and time domain analyses were conducted and measurements have been also performed to clarify the findings.

It was demonstrated that applying multi tones simultaneously within the matched frequency band and with a constant total input power resulted in a lower total average output voltage/power when compared with single-tone case for the same input power level. It was found that this was mainly due to the change in the signal waveform. In multi tone case, the input waveform was not a conventional sine wave; hence the operation of the voltage doubler was effected, which results in a lower output voltage. This trend was evident down with different frequency spacing and phase arrangements.

7.2 Future Work

Below provides a list of several opportunities for potential future work:

- As a result of Chapter 4, RF energy scavenging from multiple sources simultaneously enhances the rectifier sensitivity and PCE by delivering more input RF signals into a single rectification stage. Furthermore, Chapter 5 proved the advantage of broadening (not ultra-widening) the bandwidth so multiple signals could be delivered to the diode hence, harvesting very low density ambient signals. Therefore, developing a multi-broad-band rectifier circuit could be an optimum solution for ambient energy harvesting. One disadvantage of a broad-band rectifier is the large number of components (e.g. inductor and capacitor) that are required to achieve a multi-broad-band matching network. It is suggested that a more integrated technique is required to reduce the ohmic and parasitic losses present in all of the devices. Multi-broad-band rectenna arrays could be also developed for enhanced RF energy harvesting in buildings.
- Rectification device (e.g. Schottky diode) plays a significant role in the performance of the energy harvesting circuit. At very low input power (<−30 dBm), the use of Schottky diode can impact the PCE mainly due to its high zero-bias junction resistance and capacitance. Hence utilising more sensitive rectification devices could be investigated (e.g. spin diodes).

- The reason for obtaining a lower amount of output DC power with the multi-tone excitation (as demonstrated in Chapter 6) needs to be theoretically investigated.

  Furthermore, a mathematical method/model could be developed to predict the behaviour of the diode and output power when incoherent multi tones of various frequencies are available at the input. This model also enables to design RF energy scavenging circuits precisely according to the requirements and available RF signals in a real environment.

References

[1] R. Vullers, R. van Schaijk, I. Doms, C. Van Hoof, and R. Mertens, "Micropower energy harvesting," *Solid State Electron.,* vol. 53, pp. 684-693, 2009.

[2] R. Singh, N. Gupta, and K. F. Poole, "Global green energy conversion revolution in 21 st century through solid state devices," in *Microelectronics, 2008. MIEL 2008. 26th International Conference on*, 2008, pp. 45-54.

[3] S. Hemour and W. Ke, "Radio-Frequency Rectifier for Electromagnetic Energy Harvesting: Development Path and Future Outlook," *Proceedings of the IEEE,* vol. 102, pp. 1667-1691, 2014.

[4] J. A. Paradiso and T. Starner, "Energy scavenging for mobile and wireless electronics," *Pervasive Computing, IEEE,* vol. 4, pp. 18-27, 2005.

[5] K. Sangkil, R. Vyas, J. Bito, K. Niotaki, A. Collado, A. Georgiadis*, et al.*, "Ambient RF Energy-Harvesting Technologies for Self-Sustainable Standalone Wireless Sensor Platforms," *Proceedings of the IEEE,* vol. 102, pp. 1649-1666, 2014.

[6] P. Jaffe and J. McSpadden, "Energy Conversion and Transmission Modules for Space Solar Power," *Proceedings of the IEEE,* vol. 101, pp. 1424-1437, 2013.

[7] V. Raghunathan, A. Kansal, J. Hsu, J. Friedman, and M. B. Srivastava, "Design considerations for solar energy harvesting wireless embedded systems," in *Information Processing in Sensor Networks, 2005. IPSN 2005. Fourth International Symposium on*, 2005, pp. 457-462.

[8] M. A. Green, K. Emery, Y. Hishikawa, W. Warta, and E. D. Dunlop, "Solar cell efficiency tables (Version 38)," *Progress in Photovoltaics: Research and Applications,* vol. 19, pp. 565-572, 2011.

[9] S. H. Krishnan, D. Ezhilarasi, G. Uma, and M. Umapathy, "Pyroelectric-Based Solar and Wind Energy Harvesting System," *Sustainable Energy, IEEE Transactions on,* vol. 5, pp. 73-81, 2014.

[10] C. Tzuen-Lih, P. Ping-Lung, C. Yu-Lun, C. Wei-Ting, L. Whei-Min, C. Chih-Chiang*, et al.*, "Excitation Synchronous Wind Power Generators With Maximum Power Tracking Scheme," *Sustainable Energy, IEEE Transactions on,* vol. 5, pp. 1090-1098, 2014.

[11] K. Fanxin, D. Chuansheng, L. Xue, and Z. Haibo, "Quantity Versus Quality: Optimal Harvesting Wind Power for the Smart Grid," *Proceedings of the IEEE,* vol. 102, pp. 1762-1776, 2014.

[12] A. Varpula, S. J. Laakso, T. Havia, J. Kyynäräinen, and M. Prunnila, "Harvesting Vibrational Energy Using Material Work Functions," *Sci. Rep.,* vol. 4, p. doi:10.1038/srep06799, 2014.

[13] H. Kim, J.-H. Kim, and J. Kim, "A review of piezoelectric energy harvesting based on vibration," *International Journal of Precision Engineering and Manufacturing,* vol. 12, pp. 1129-1141, 2011/12/01 2011.

[14] A. Khaligh, Z. Peng, and Z. Cong, "Kinetic Energy Harvesting Using Piezoelectric and Electromagnetic Technologies—State of the Art," *Industrial Electronics, IEEE Transactions on,* vol. 57, pp. 850-860, 2010.

[15] Z. Qian and K. Eun Sok, "Vibration Energy Harvesting Based on Magnet and Coil Arrays for Watt-Level Handheld Power Source," *Proceedings of the IEEE,* vol. 102, pp. 1747-1761, 2014.

[16] G. Mahan, B. Sales, and J. Sharp, "Thermoelectric materials: New approaches to an old problem," *Physics Today,* vol. 50, pp. 42-47, Mar 1997.

[17] L. Long and H. Ye, "How to be smart and energy efficient: A general discussion on thermochromic windows," *Sci. Rep.,* vol. 4, p. doi:10.1038/srep06427, 2014.

[18] H. Lhermet, C. Condemine, M. Plissonnier, R. Salot, P. Audebert, and M. Rosset, "Efficient Power Management Circuit: From Thermal Energy Harvesting to Above-IC Microbattery Energy Storage," *Solid-State Circuits, IEEE Journal of,* vol. 43, pp. 246-255, 2008.

[19] Y. Du, K. Cai, S. Chen, H. Wang, S. Z. Shen, R. Donelson*, et al.*, "Thermoelectric Fabrics: Toward Power Generating Clothing," *Sci. Rep.,* vol. 5, p. DOI: 10.1038/srep06411, 2015.

[20] S. B. Inayat, K. R. Rader, and M. M. Hussain, "Nano-materials Enabled Thermoelectricity from Window Glasses," *Scientific Reports,* vol. 2, Nov 13 2012.

[21] A. H. Slocum, G. E. Fennell, G. Dundar, B. G. Hodder, J. D. C. Meredith, and M. A. Sager, "Ocean Renewable Energy Storage (ORES) System: Analysis of an Undersea Energy Storage Concept," *Proceedings of the IEEE,* vol. 101, pp. 906-924, 2013.

[22] Y.-K. Wang, G.-P. Sheng, B.-J. Shi, W.-W. Li, and H.-Q. Yu, "A Novel Electrochemical Membrane Bioreactor as a Potential Net Energy Producer for Sustainable Wastewater Treatment," *Sci. Rep.,* vol. 3, 05/21/online 2013.

[23] A. Costanzo, M. Dionigi, D. Masotti, M. Mongiardo, G. Monti, L. Tarricone*, et al.*, "Electromagnetic Energy Harvesting and Wireless Power Transmission: A Unified Approach," *Proceedings of the IEEE,* vol. 102, pp. 1692-1711, 2014.

[24] W. C. Brown, "The history of power transmission by radio waves," *IEEE Trans. Microw. Theory Tech.,* vol. 32, pp. 1230-1242, 1984.

[25] W. C. Brown, "Experiments involving a microwave beam to power and position a helicopter," *IEEE Trans. Aerosp. Electron. Syst.,* pp. 692-702, 1969.

[26] N. Shinohara, "Power without wires," *IEEE Microwave Magazine,* vol. 12, pp. S64-S73, 2011.

[27] N. B. Carvalho, A. Georgiadis, A. Costanzo, H. Rogier, A. Collado, J. A. García*, et al.*, "Wireless power transmission: R&D activities within Europe," *IEEE Trans. Microw. Theory Tech.,* vol. 62, pp. 1031-1045, 2014.

[28] N. M. Din, C. K. Chakrabarty, A. Bin Ismail, K. K. A. Devi, and W. Y. Chen, "Design of RF Energy Harvsting System For Energizing Low Powe Devices," *Progress in Electromagnetics Research-Pier,* vol. 132, pp. 49-69, 2012 2012.

[29] T. Le, K. Mayaram, and T. Fiez, "Efficient far-field radio frequency energy harvesting for passively powered sensor networks," *IEEE Journal of Solid-State Circuits,* vol. 43, pp. 1287-1302, May 2008.

[30] T. Paing, J. Morroni, A. Dolgov, J. Shin, J. Brannan, R. Zane*, et al.*, *Wirelessly-powered wireless sensor platform*, 2007.

[31] H. J. Visser and R. J. M. Vullers, "RF Energy Harvesting and Transport for Wireless Sensor Network Applications: Principles and Requirements," *Proceedings of the IEEE,* vol. 101, pp. 1410-1423, 2013.

[32] J. Paulo and P. D. Gaspar, "Review and Future Trend of Energy Harvesting Methods for Portable Medical Devices," *Lecture Notes in Engineering and Computer Science,* 2010.

[33] J. Walk, J. Weber, C. Soell, R. Weigel, G. Fischer, and T. Ussmueller, "Remote Powered Medical Implants for Telemonitoring," *Proceedings of the IEEE,* vol. 102, pp. 1811-1832, 2014.

[34] H. Fu-Jhuan, L. Chien-Ming, C. Chia-Lin, C. Liang-Kai, Y. Tzong-Chee, and L. Ching-Hsing, "Rectenna Application of Miniaturized Implantable Antenna Design for Triple-Band Biotelemetry Communication," *Antennas and Propagation, IEEE Transactions on,* vol. 59, pp. 2646-2653, 2011.

[35] L. T. G. Monti, and C. Trane, "Experimental characterization of a 434 MHz wireless energy link for medical applications," Progress In Electromagnetics Research C, Vol. 30, 53-64, 2012. .

[36] K. Finkenzeller, *RFID Handbook*: 2nd Edition ed. Wiley.

[37] D.-S. Liu, F.-B. Li, X.-C. Zou, Y. Liu, X.-M. Hui, and X.-F. Tao, "New Analysis and Design of a RF Rectifier for RFID and Implantable Devices," *Sensors,* vol. 11, pp. 6494-6508, Jul 2011.

[38] S. Scorcioni, A. Bertacchini, L. Larcher, A. Ricciardi, D. Dondi, and P. Pavan, "RF to DC CMOS rectifier with high efficiency over a wide input power range for RFID applications," in *Microwave Symposium Digest (MTT), 2012 IEEE MTT-S International*, 2012, pp. 1-3.

[39] A. Shameli, A. Safarian, A. Rofougaran, M. Rofougaran, and F. De Flaviis, "Power Harvester Design for Passive UHF RFID Tag Using a Voltage Boosting Technique," *Microwave Theory and Techniques, IEEE Transactions on,* vol. 55, pp. 1089-1097, 2007.

[40] S. Mandal and R. Sarpeshkar, "Low-Power CMOS Rectifier Design for RFID Applications," *Circuits and Systems I: Regular Papers, IEEE Transactions on,* vol. 54, pp. 1177-1188, 2007.

[41] A. Collado and A. Georgiadis, "Conformal Hybrid Solar and Electromagnetic (EM) Energy Harvesting Rectenna," *Circuits and Systems I: Regular Papers, IEEE Transactions on,* vol. 60, pp. 2225-2234, 2013.

[42] M. Danesh and J. R. Long, "Photovoltaic Antennas for Autonomous Wireless Systems," *Circuits and Systems II: Express Briefs, IEEE Transactions on,* vol. 58, pp. 807-811, 2011.

[43] B. G. Karthik, S. Shivaraman, and V. Aditya, "Wi-Pie: Energy Harvesting in Mobile Electronic Devices," in *Global Humanitarian Technology Conference (GHTC), 2011 IEEE*, 2011, pp. 398-401.

[44] W. C. Brown, G. R. H, H. Neil, and W. R. C, "Microwave to dc converter," ed: Google Patents, 1969.

[45] W.C.Brown, "The history of the development of the rectenna," presented at the SPS Microwave Syatem Workshop at JSC-NASA, 1980.

[46] W. C. Brown, "Adapting Microwave Techniques to Help Solve Future Energy Problems," *Microwave Theory and Techniques, IEEE Transactions on,* vol. 21, pp. 753-763, 1973.

[47] A. Boaventura, A. Collado, N. B. Carvalho, and A. Georgiadis, "Optimum behavior: Wireless power transmission system design through behavioral models and efficient synthesis techniques," *Microwave Magazine, IEEE,* vol. 14, pp. 26-35, 2013.

[48] N. Tesla, *Experiments with Alternate Currents of High Potential and High Frequency*: New York: McGraw-Hill, 1904.

[49] N. Tesla, *The Transmission of Electric Energy Withou Wires (The thirteenth Anniversary Number of the Electrical World and Engineer)*: new York: McGraw-Hill, 1904.

[50] W. Lumpkins, "Nikola Tesla's Dream Realized: Wireless power energy harvesting," *Consumer Electronics Magazine, IEEE,* vol. 3, pp. 39-42, 2014.

[51] J. L. W. Li, "Wireless power transmission: State-of-the-arts in technologies and potential applications (invited paper)," in *Microwave Conference Proceedings (APMC), 2011 Asia-Pacific*, 2011, pp. 86-89.

[52] Agilent Technologies. (22/11/2014). *Surface Mount RF Schottky Barrier Diodes HSMS-282X Series*. Available at: http://www.avagotech.com/docs/AV02-1320EN

[53] Agilent Technologies. *Surface Mount Zero Bias Schottky Detector Diodes HSMS-285X Series.* Available at:http://www.avagotech.com/docs/AV02-1377EN

[54] (19/08/2015). *Radio-Electronics*. Available: Radio-Electronics.Com.htm

[55] R. E. Barnett, L. Jin, and S. Lazar, "A RF to DC Voltage Conversion Model for Multi-Stage Rectifiers in UHF RFID Transponders," *Solid-State Circuits, IEEE Journal of,* vol. 44, pp. 354-370, 2009.

[56] H. Kanaya, S. Tsukamaoto, T. Hirabaru, D. Kanemoto, R. K. Pokharel, and K. Yoshida, "Energy Harvesting Circuit on a One-Sided Directional Flexible Antenna," *Microwave and Wireless Components Letters, IEEE,* vol. 23, pp. 164-166, 2013.

[57] T. Salter, G. Metze, and N. Goldsman, "Application of a parasitic aware model to optimize an RF energy scavenging circuit fabricated in 130 nm CMOS," in *Recent Advances in Microwave Theory and Applications, 2008. MICROWAVE 2008. International Conference on*, 2008, pp. 303-305.

[58] B. L. Pham and A. V. Pham, "Triple bands antenna and high efficiency rectifier design for RF energy harvesting at 900, 1900 and 2400 MHz," in *Microwave Symposium Digest (IMS), 2013 IEEE MTT-S International*, 2013, pp. 1-3.

[59] S. dela Cruz, M. G. de los Reyes, A. Alvarez, M. T. de Leon, and C. R. Roque, "Design and implementation of passive RF-DC converters for RF power harvesting systems," in *TENCON 2010 - 2010 IEEE Region 10 Conference*, 2010, pp. 1503-1508.

[60] S. Radiom, C. De Roover, G. Vandenbosch, M. Steyaert, and G. Gielen, "A Fully Integrated Pinless Long-Range Power Supply with On-Chip Antenna for Scavenging-Based RFID Tag Powering," in *Silicon Monolithic Integrated Circuits in RF Systems, 2009. SiRF '09. IEEE Topical Meeting on*, 2009, pp. 1-4.

[61] M. Arrawatia, M. S. Baghini, and G. Kumar, "RF energy harvesting system from cell towers in 900MHz band," in *Communications (NCC), 2011 National Conference on*, 2011, pp. 1-5.

[62] C. R. Valenta and G. D. Durgin, "Harvesting Wireless Power: Survey of Energy-Harvester Conversion Efficiency in Far-Field, Wireless Power Transfer Systems," *Microwave Magazine, IEEE,* vol. 15, pp. 108-120, 2014.

[63] N. Shinohara, "Rectennas for microwave power transmission," *Ieice Electronics Express,* vol. 10, 2013 2013.

[64] C. Qiang, K. Ozawa, Y. Qiaowei, and K. Sawaya, "Antenna Characterization for Wireless Power-Transmission System Using Near-Field Coupling," *Antennas and Propagation Magazine, IEEE,* vol. 54, pp. 108-116, 2012.

[65] A. Kurs, A. Karalis, R. Moffatt, J. D. Joannopoulos, P. Fisher, and M. Soljačić, "Wireless Power Transfer via Strongly Coupled Magnetic Resonances," *Science,* vol. 317, pp. 83-86, July 6, 2007 2007.

[66] J. A. Russer, M. Dionigi, M. Mongiardo, and P. Russer, "A moving field inductive power transfer system for electric vehicles," in *Microwave Conference (EuMC), 2013 European*, 2013, pp. 519-522.

[67] Z. Popovic, E. A. Falkenstein, D. Costinett, and R. Zane, "Low-Power Far-Field Wireless Powering for Wireless Sensors," *Proceedings of the IEEE,* vol. 101, pp. 1397-1409, 2013.

[68] M. S. Trotter and G. D. Durgin, "Survey of range improvement of commercial RFID tags with Power Optimised Waveforms," in *RFID, 2010 IEEE International Conference on*, 2010, pp. 195-202.

[69] A. S. Boaventura and N. B. Carvalho, "Maximising DC power in energy harvesting circuits using multisine excitation," in *Microwave Symposium Digest (MTT), 2011 IEEE MTT-S International*, 2011, pp. 1-4.

[70] C. R. Valenta and G. D. Durgin, "Rectenna performance under power-optimised waveform excitation," in *RFID (RFID), 2013 IEEE International Conference on*, 2013, pp. 237-244.

[71] A. Collado and A. Georgiadis, "Improving wireless power transmission efficiency using chaotic waveforms," in *Microwave Symposium Digest (MTT), 2012 IEEE MTT-S International*, 2012, pp. 1-3.

[72] N. B. Carvalho, J. C. Pedro, J. Wonhoon, and M. B. Steer, "Nonlinear RF circuits and systems simulation when driven by several modulated signals," *Microwave Theory and Techniques, IEEE Transactions on,* vol. 54, pp. 572-579, 2006.

[73] A. J. S. Boaventura, A. Collado, A. Georgiadis, and N. Borges Carvalho, "Spatial Power Combining of Multi-Sine Signals for Wireless Power Transmission Applications," *Microwave Theory and Techniques, IEEE Transactions on,* vol. 62, pp. 1022-1030, 2014.

[74] J. O. McSpadden and J. C. Mankins, "Space solar power programs and microwave wireless power transmission technology," *Microwave Magazine, IEEE,* vol. 3, pp. 46-57, 2002.

[75] P. E. Glaser, "The potential of satellite solar power," *Proceedings of the IEEE,* vol. 65, pp. 1162-1176, 1977.

[76] E. Vecchione and C. Keegan, "Short-range wireless power transmission and reception," 2005.

[77] P. Elliott, M. B. Toledano, J. Bennett, L. Beale, K. De Hoogh, N. Best*, et al.*, "Mobile phone base stations and early childhood cancers: case-control study," *BMJ,* vol. 340, 2010.

[78] "IARC classifies radiofrequency electromagnetic fields as possibly carcinogenic to humans," ed. Press Release: World Health Organization (WHO), 208, 2011.

[79] J. O. McSpadden, F. Lu, and C. Kai, "Design and experiments of a high-conversion-efficiency 5.8-GHz rectenna," *Microwave Theory and Techniques, IEEE Transactions on,* vol. 46, pp. 2053-2060, 1998.

[80] B. Strassner and C. Kai, "A circularly polarised rectifying antenna array for wireless microwave power transmission with over 78% efficiency," in *Microwave Symposium Digest, 2002 IEEE MTT-S International*, 2002, pp. 1535-1538 vol.3.

[81] P. Ji-Yong, H. Sang-Min, and T. Itoh, "A rectenna design with harmonic-rejecting circular-sector antenna," *Antennas and Wireless Propagation Letters, IEEE,* vol. 3, pp. 52-54, 2004.

[82] S. Young-Ho and C. Kai, "A high-efficiency dual-frequency rectenna for 2.45- and 5.8-GHz wireless power transmission," *Microwave Theory and Techniques, IEEE Transactions on,* vol. 50, pp. 1784-1789, 2002.

[83] W. Defu and R. Negra, "Design of a dual-band rectifier for wireless power transmission," in *Wireless Power Transfer (WPT), 2013 IEEE*, 2013, pp. 127-130.

[84] J. Heikkinen and M. Kivikoski, "A novel dual-frequency circularly polarised rectenna," *Antennas and Wireless Propagation Letters, IEEE,* vol. 2, pp. 330-333, 2003.

[85] A. Dolgov, R. Zane, and Z. Popovic, "Power Management System for Online Low Power RF Energy Harvesting Optimization," *Circuits and Systems I: Regular Papers, IEEE Transactions on,* vol. 57, pp. 1802-1811, 2010.

[86] R. Shigeta, T. Sasaki, Q. Duong Minh, Y. Kawahara, R. J. Vyas, M. M. Tentzeris*, et al.*, "Ambient RF Energy Harvesting Sensor Device With Capacitor-Leakage-Aware Duty Cycle Control," *Sensors Journal, IEEE,* vol. 13, pp. 2973-2983, 2013.

[87] T. Ajmal, V. Dyo, B. Allen, D. Jazani, and I. Ivanov, "Design and optimisation of compact RF energy harvesting device for smart applications," *Electronics Letters,* vol. 50, pp. 111-113, 2014.

[88] X. Wang and A. Mortazawi, "Medium Wave Energy Scavenging for Wireless Structural Health Monitoring Sensors," *IEEE Trans. Microw. Theory Tech.,* vol. 62, pp. 1067-1074, 2014.

[89] Y. Yao, W. Jie, S. Yin, and F. F. Dai, "A Fully Integrated 900-MHz Passive RFID Transponder Front End With Novel Zero-Threshold RF-DC Rectifier," *Industrial Electronics, IEEE Transactions on,* vol. 56, pp. 2317-2325, 2009.

[90] L. Jong-Wook and B. Lee, "A Long-Range UHF-Band Passive RFID Tag IC Based on High-Q Design Approach," *Industrial Electronics, IEEE Transactions on,* vol. 56, pp. 2308-2316, 2009.

[91] C. Mikeka and H. Arai, "Microwave tooth for sensor power supply in battery-free applications," in *Microwave Conference Proceedings (APMC), 2011 Asia-Pacific*, 2011, pp. 1802-1805.

[92] G. Seigneuret, E. Bergeret, and P. Pannier, "Auto-tuning in passive UHF RFID tags," in *NEWCAS Conference (NEWCAS), 2010 8th IEEE International*, 2010, pp. 181-184.

[93] P. Kim, G. Chaudhary, and Y. Jeong, "A Dual-Band RF Energy Harvesting Using Frequency Limited Dual-Band Impedance Matching," *Progress in Electromagnetics Research-Pier,* vol. 141, pp. 443-461, 2013 2013.

[94] L. Bo, S. Xi, N. Shahshahan, N. Goldsman, T. Salter, and G. M. Metze, "An Antenna Co-Design Dual Band RF Energy Harvester," *Circuits and Systems I: Regular Papers, IEEE Transactions on,* vol. 60, pp. 3256-3266, 2013.

[95] K. Niotaki, K. Sangkil, J. Seongheon, A. Collado, A. Georgiadis, and M. M. Tentzeris, "A Compact Dual-Band Rectenna Using Slot-Loaded Dual Band Folded Dipole Antenna," *Antennas and Wireless Propagation Letters, IEEE,* vol. 12, pp. 1634-1637, 2013.

[96] V. Rizzoli, G. Bichicchi, A. Costanzo, F. Donzelli, and D. Masotti, "CAD of multi-resonator rectenna for micro-power generation," in *Microwave Conference, 2009. EuMC 2009. European*, 2009, pp. 1684-1687.

[97] D. Masotti, A. Costanzo, M. Del Prete, and V. Rizzoli, "Genetic-based design of a tetra-band high-efficiency radio-frequency energy harvesting system," *Microwaves, Antennas & Propagation, IET,* vol. 7, pp. 1254-1263, 2013.

[98] M. Piñuela, P. D. Mitcheson, and S. Lucyszyn, "Ambient RF energy harvesting in urban and semi-urban environments," *IEEE Trans. Microw. Theory Tech.,* vol. 61, pp. 2715-2726, 2013.

[99] A. Buonanno, M. D'Urso, and D. Pavone, "An ultra wide-band system for RF Energy harvesting," in *Antennas and Propagation (EUCAP), Proceedings of the 5th European Conference on*, 2011, pp. 388-389.

[100] J. A. Hagerty, F. B. Helmbrecht, W. H. McCalpin, R. Zane, and Z. B. Popovic, "Recycling ambient microwave energy with broad-band rectenna arrays," *IEEE Trans. Microw. Theory Tech.,* vol. 52, pp. 1014-1024, 2004.

[101] J. A. Hagerty and Z. Popovic, "An experimental and theoretical characterization of a broadband arbitrarily-polarised rectenna array," in *Microwave Symposium Digest, 2001 IEEE MTT-S International*, 2001, pp. 1855-1858 vol.3.

[102] J. A. Hagerty, N. D. Lopez, B. Popovic, and Z. Popovic, "Broadband Rectenna Arrays for Randomly Polarised Incident Waves," in *Microwave Conference, 2000. 30th European*, 2000, pp. 1-4.

[103] N. Mei-Juan, Y. Xue-Xia, T. Guan-Nan, and H. Bing, "A Compact 2.45-GHz Broadband Rectenna Using Grounded Coplanar Waveguide," *Antennas and Wireless Propagation Letters, IEEE,* vol. 14, pp. 986-989, 2015.

[104] P. Binh, J. C. S. Chieh, and P. Anh-Vu, "A wideband composite right/left hand rectenna for UHF energy harvesting applications," in *Antennas and Propagation Society International Symposium (APSURSI), 2012 IEEE*, 2012, pp. 1-2.

[105] Z. Jingwei, H. Yi, and C. Ping, "A wideband cross dipole rectenna for rf wireless harvesting," in *Antennas and Propagation (EuCAP), 2013 7th European Conference on*, 2013, pp. 3063-3067.

[106] Z. Hongxian and Z. Xinen, "A broadband high efficiency rectifier for ambient RF energy harvesting," in *Microwave Symposium (IMS), 2014 IEEE MTT-S International*, 2014, pp. 1-3.

[107] S. Hucheng, G. Yong-Xin, H. Miao, and Z. Zheng, "Design of a High-Efficiency 2.45-GHz Rectenna for Low-Input-Power Energy Harvesting," *IEEE Antennas and Wireless Propagation Letters, ,* vol. 11, pp. 929-932, 2012.

[108] R. M. Fano, "Theoretical limitations on the broadband matching of arbitrary impedances," *Journal of the Franklin Institute,* vol. 249, pp. 57-83, 1950.

[109] I.-K. Cho, J.-I. Moon, J.-H. Yun, and J.-H. Kwon, "Apparatus for harvesting energy from microwave," 2010.

[110] H. J. Visser, A. C. F. Reniers, and J. A. C. Theeuwes, "Ambient RF Energy Scavenging: GSM and WLAN Power Density Measurements," in *Microwave Conference, 2008. EuMC 2008. 38th European*, 2008, pp. 721-724.

[111] Y. Kawahara, K. Tsukada, and T. Asami, "Feasibility and potential application of power scavenging from environmental RF signals," in *Antennas and Propagation Society International Symposium, 2009. APSURSI '09. IEEE*, 2009, pp. 1-4.

[112] (2015). Available: http://maps.google.com.au

[113] S. Y. Liao, "Measurements and Computations of Electric Field Intensity and Power Density," *Instrumentation and Measurement, IEEE Transactions on,* vol. 26, pp. 53-57, 1977.

[114] A. Government. (2013). *Australia Radio Frequency Spectrum Plan (ACMA)*. Available: http://acma.gov.au/~/media/Spectrum%20Transformation%20and%20Government/Information/pdf/Australian%20Radiofrequency%20Spectrum%20Plan%202013.pdf.

[115] U. Olgun, C. Chi-Chih, and J. L. Volakis, "Investigation of Rectenna Array Configurations for Enhanced RF Power Harvesting," *Antennas and Wireless Propagation Letters, IEEE,* vol. 10, pp. 262-265, 2011.

[116] J. Zbitou, M. Latrach, and S. Toutain, "Hybrid rectenna and monolithic integrated zero-bias microwave rectifier," *Microwave Theory and Techniques, IEEE Transactions on,* vol. 54, pp. 147-152, 2006.

[117] J. L. Volakis, *Antenna Engineering Handbook*, 4th ed.: McGraw-Hill, 2007.

[118] C. A. Balanis, *Antenna Theory: Analysis and Design*, 3th ed.: Wiley Interscience, 2005.

[119] A. N. Parks and J. R. Smith, "Sifting through the airwaves: Efficient and scalable multiband RF harvesting," in *RFID (IEEE RFID), 2014 IEEE International Conference on*, 2014, pp. 74-81.

[120] S. Keyrouz, H. J. Visser, and A. G. Tijhuis, "Rectifier analysis for Radio Frequency energy harvesting and Power Transport," in *Microwave Conference (EuMC), 2012 42nd European*, 2012, pp. 428-431.

[121] Agilent Technologies. (2005, 22/11/2014)). *Schottky Diode Voltage Doubler. Application Note 956-4*. Available: http://c1233384.r84.cf3.rackcdn.com/UK_HPA_HSCH-5331_7AN.pdf.

[122] H. Eriksson, Waugh, R.W. (2000, 22/11/2014). *A temperature compensated linear diode detector,Design Tip.*

[123] Agilent Technologies. (2005, 22/11/2014). *The Zero Bias Schottky Diode Detector at Temperature Extremes-Problems and Solutions, Application Note AN 1090*. Available at: http://www.efo.ru/download/Zero_bias_shottky_over_temperature.pdf.

[124] G. L. Matthaei, L. Young, and E. M. Jones, "Microwave filters, impedance-matching networks, and coupling structures," DTIC Document1963.

[125] T. Baum, L. Thompson, and K. Ghorbani, "Complex Dielectric Measurements of Forest Fire Ash at X-Band Frequencies," *Geoscience and Remote Sensing Letters, IEEE,* vol. 8, pp. 859-863, 2011.

[126] S. S. Keyrouz, H. Visser, and A. Tijhuis, "Rectifier analysis for radio frequency energy harvesting and power transport," 2012.

[127] A. I. Zverev, *Handbook of filter synthesis*: Wiley, 1967.

[128] R. C. Frye, K. Liu, G. Badakere, and Y. Lin, "A hybrid coupled-resonator bandpass filter topology implemented on lossy semiconductor substrates," *Resistor,* vol. 3, p. M3, 2007.

[129] Available: http://www.boral.com.au/home.asp

Appendix A
ADS Schematic - Dual-Band Rectifier (Chapter 4)

(a)

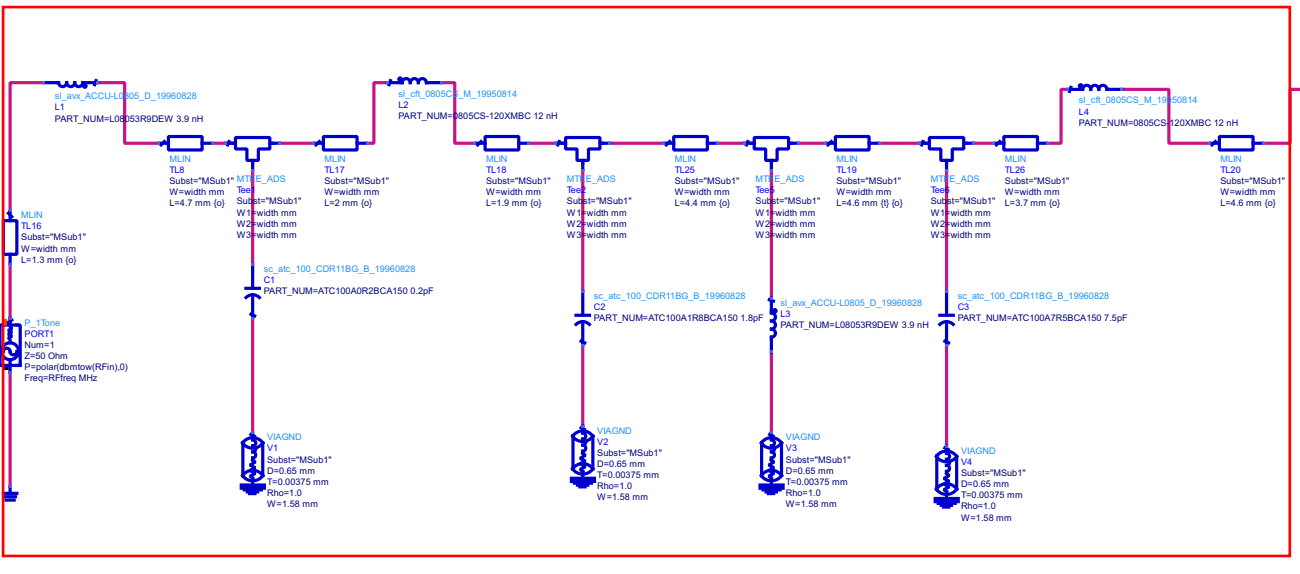

(b)

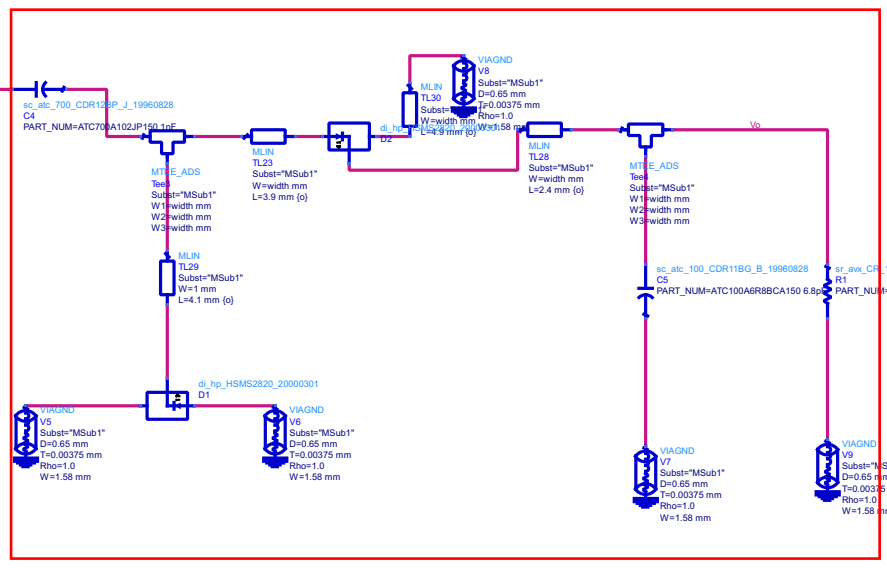

(a)

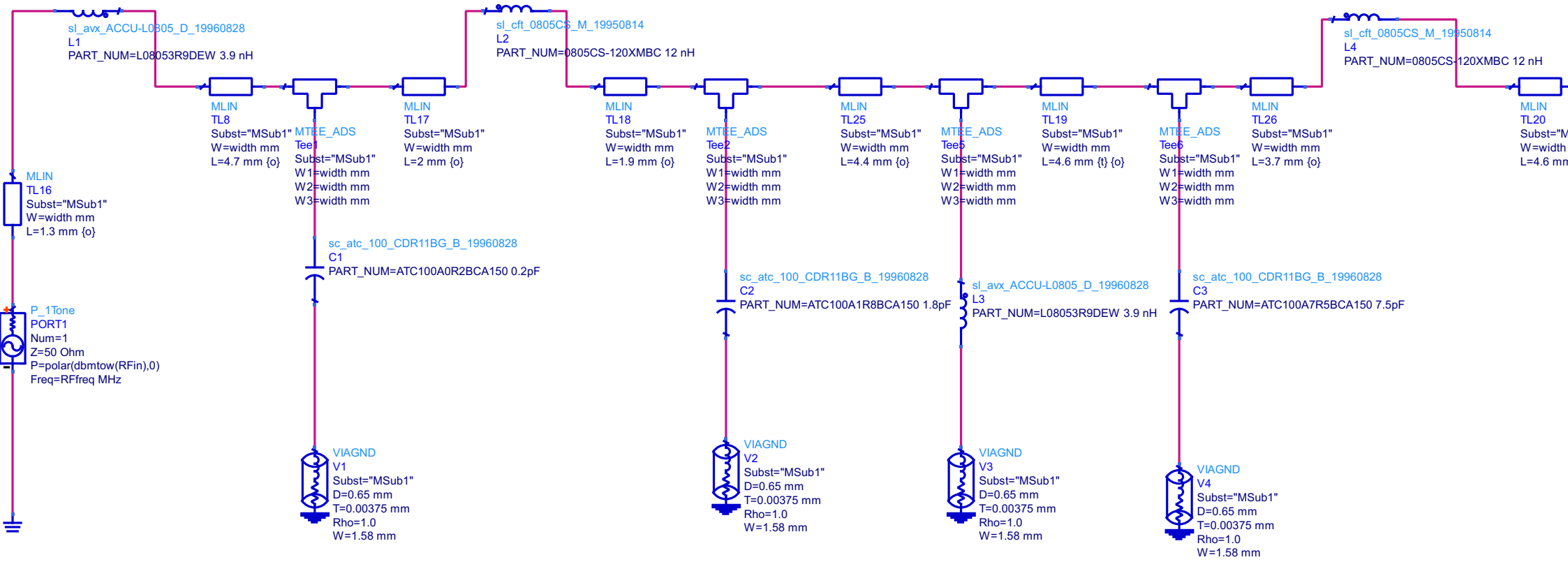
sl_avx_ACCU-L0805_D_19960828
L1
PART_NUM=L08053R9DEW 3.9 nH
MLIN
TL8
Subst="MSub1"
W=width mm
L=4.7 mm {o}
MTEE_ADS
Tee1
Subst="MSub1"
W1=width mm
W2=width mm
W3=width mm
MLIN
TL17
Subst="MSub1"
W=width mm
L=2 mm {o}
sl_cft_0805CS_M_19950814
L2
PART_NUM=0805CS-120XMBC 12 nH
MLIN
TL18
Subst="MSub1"
W=width mm
L=1.9 mm {o}
MTEE_ADS
Tee2
Subst="MSub1"
W1=width mm
W2=width mm
W3=width mm
MLIN
TL25
Subst="MSub1"
W=width mm
L=4.4 mm {o}
MTEE_ADS
Tee5
Subst="MSub1"
W1=width mm
W2=width mm
W3=width mm
MLIN
TL19
Subst="MSub1"
W=width mm
L=4.6 mm {t} {o}
MTEE_ADS
Tee6
Subst="MSub1"
W1=width mm
W2=width mm
W3=width mm
MLIN
TL26
Subst="MSub1"
W=width mm
L=3.7 mm {o}
sl_cft_0805CS_M_19950814
L4
PART_NUM=0805CS-120XMBC 12 nH
MLIN
TL20
Subst="M
W=width
L=4.6 mm
MLIN
TL16
Subst="MSub1"
W=width mm
L=1.3 mm {o}
P_1Tone
PORT1
Num=1
Z=50 Ohm
P=polar(dbmtow(RFin),0)
Freq=RFfreq MHz
sc_atc_100_CDR11BG_B_19960828
C1
PART_NUM=ATC100A0R2BCA150 0.2pF
sc_atc_100_CDR11BG_B_19960828
C2
PART_NUM=ATC100A1R8BCA150 1.8pF
sl_avx_ACCU-L0805_D_19960828
L3
PART_NUM=L08053R9DEW 3.9 nH
sc_atc_100_CDR11BG_B_19960828
C3
PART_NUM=ATC100A7R5BCA150 7.5pF
VIAGND
V1
Subst="MSub1"
D=0.65 mm
T=0.00375 mm
Rho=1.0
W=1.58 mm
VIAGND
V2
Subst="MSub1"
D=0.65 mm
T=0.00375 mm
Rho=1.0
W=1.58 mm
VIAGND
V3
Subst="MSub1"
D=0.65 mm
T=0.00375 mm
Rho=1.0
W=1.58 mm
VIAGND
V4
Subst="MSub1"
D=0.65 mm
T=0.00375 mm
Rho=1.0
W=1.58 mm

(b)

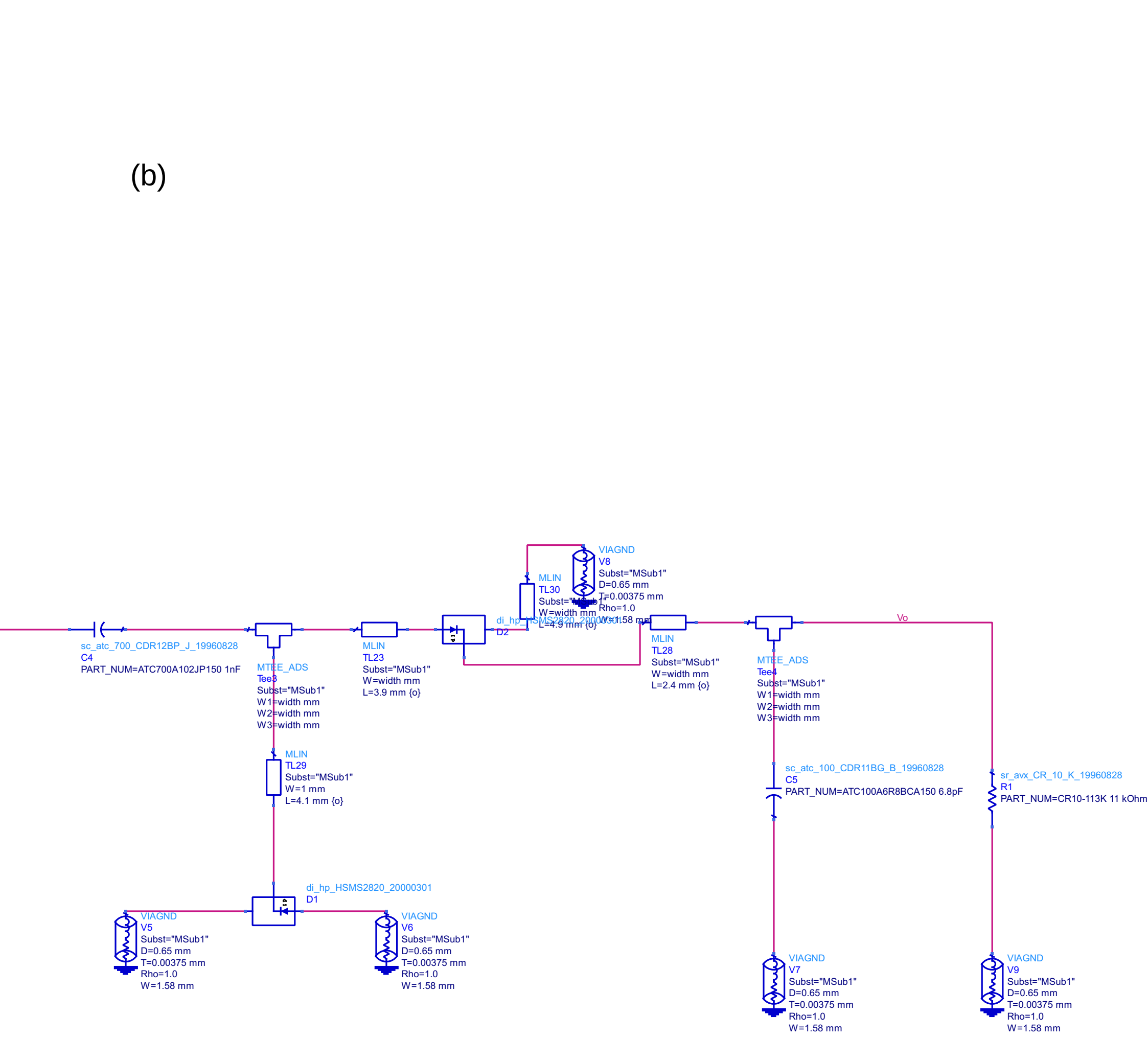
sc_atc_700_CDR12BP_J_19960828
C4
PART_NUM=ATC700A102JP150 1nF
MTEE_ADS
Tee3
Subst="MSub1"
W1=width mm
W2=width mm
W3=width mm
MLIN
TL23
Subst="MSub1"
W=width mm
L=3.9 mm {o}
di_hp_HSMS2820_20000301
D2
MLIN
TL30
Subst="MSub1"
W=width mm
L=4.9 mm {o}
VIAGND
V8
Subst="MSub1"
D=0.65 mm
T=0.00375 mm
Rho=1.0
W=1.58 mm
MLIN
TL28
Subst="MSub1"
W=width mm
L=2.4 mm {o}
MTEE_ADS
Tee4
Subst="MSub1"
W1=width mm
W2=width mm
W3=width mm
Vo
MLIN
TL29
Subst="MSub1"
W=1 mm
L=4.1 mm {o}
sc_atc_100_CDR11BG_B_19960828
C5
PART_NUM=ATC100A6R8BCA150 6.8pF
sr_avx_CR_10_K_19960828
R1
PART_NUM=CR10-113K 11 kOhm
di_hp_HSMS2820_20000301
D1
VIAGND
V5
Subst="MSub1"
D=0.65 mm
T=0.00375 mm
Rho=1.0
W=1.58 mm
VIAGND
V6
Subst="MSub1"
D=0.65 mm
T=0.00375 mm
Rho=1.0
W=1.58 mm
VIAGND
V7
Subst="MSub1"
D=0.65 mm
T=0.00375 mm
Rho=1.0
W=1.58 mm
VIAGND
V9
Subst="MSub1"
D=0.65 mm
T=0.00375 mm
Rho=1.0
W=1.58 mm

Appendix B

ADS Schematic - FM Band Rectifier (Chapter 5)

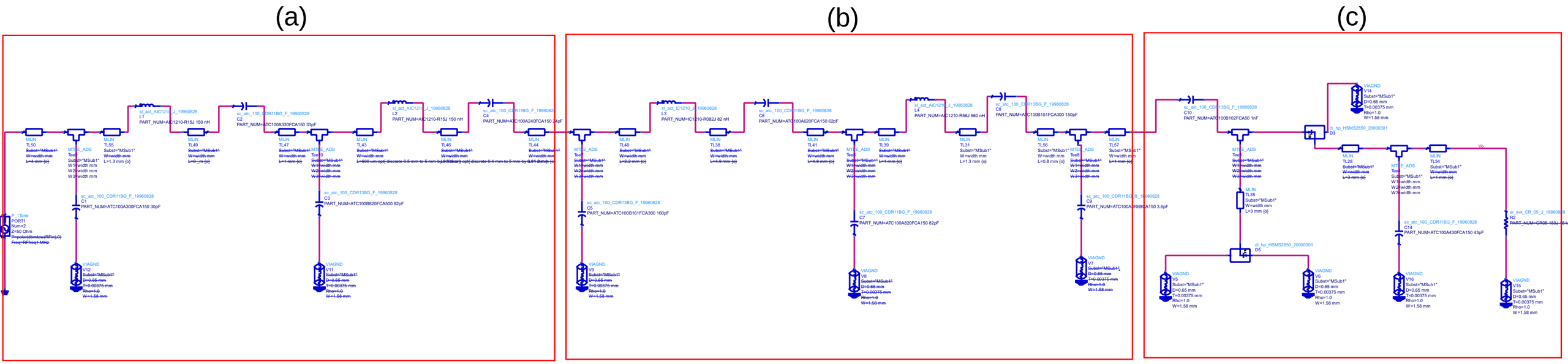

(a)

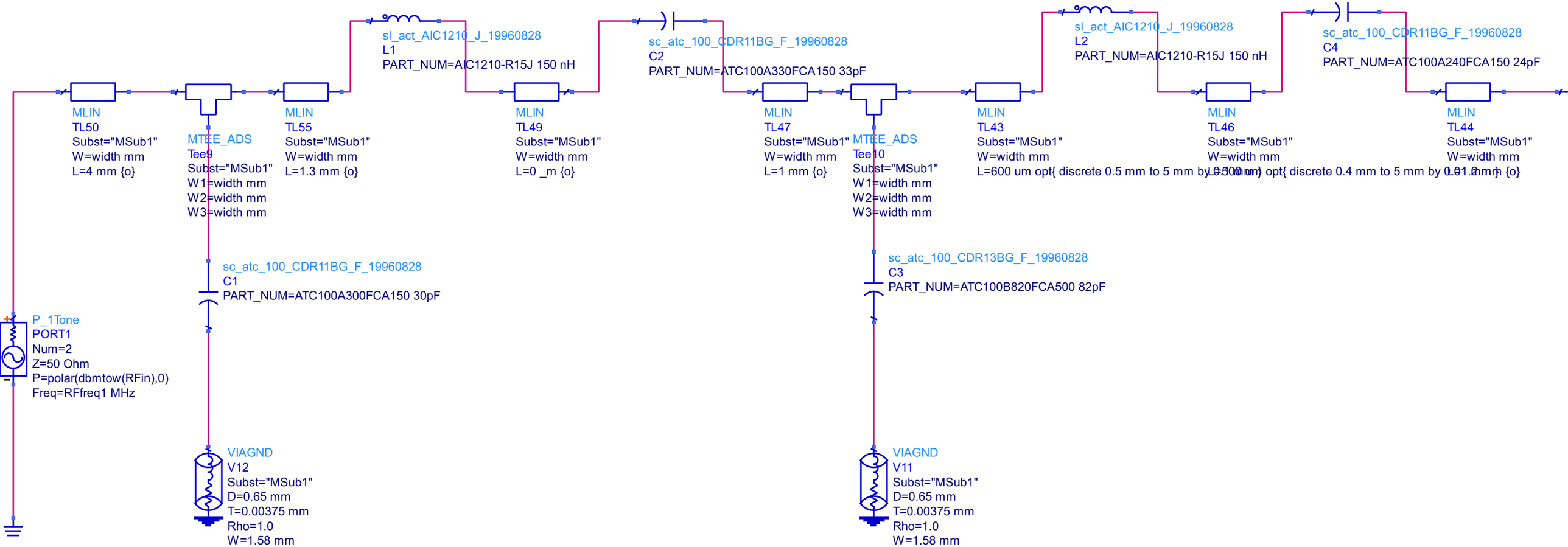
MLIN
TL50
Subst="MSub1"
W=width mm
L=4 mm {o}
MTEE_ADS
Tee9
Subst="MSub1"
W1=width mm
W2=width mm
W3=width mm
MLIN
TL55
Subst="MSub1"
W=width mm
L=1.3 mm {o}
sl_act_AIC1210_J_19960828
L1
PART_NUM=AIC1210-R15J 150 nH
MLIN
TL49
Subst="MSub1"
W=width mm
L=0 _m {o}
sc_atc_100_CDR11BG_F_19960828
C2
PART_NUM=ATC100A330FCA150 33pF
MLIN
TL47
Subst="MSub1"
W=width mm
L=1 mm {o}
MTEE_ADS
Tee10
Subst="MSub1"
W1=width mm
W2=width mm
W3=width mm
MLIN
TL43
Subst="MSub1"
W=width mm
L=600 um opt{ discrete 0.5 mm to 5 mm by 0.5 mm}
sl_act_AIC1210_J_19960828
L2
PART_NUM=AIC1210-R15J 150 nH
MLIN
TL46
Subst="MSub1"
W=width mm
L=300 um opt{ discrete 0.4 mm to 5 mm by 0.1 mm}
sc_atc_100_CDR11BG_F_19960828
C4
PART_NUM=ATC100A240FCA150 24pF
MLIN
TL44
Subst="MSub1"
W=width mm
L=1.2 mm {o}
sc_atc_100_CDR11BG_F_19960828
C1
PART_NUM=ATC100A300FCA150 30pF
P_1Tone
PORT1
Num=2
Z=50 Ohm
P=polar(dbmtow(RFin),0)
Freq=RFfreq1 MHz
VIAGND
V12
Subst="MSub1"
D=0.65 mm
T=0.00375 mm
Rho=1.0
W=1.58 mm
sc_atc_100_CDR13BG_F_19960828
C3
PART_NUM=ATC100B820FCA500 82pF
VIAGND
V11
Subst="MSub1"
D=0.65 mm
T=0.00375 mm
Rho=1.0
W=1.58 mm

(b)

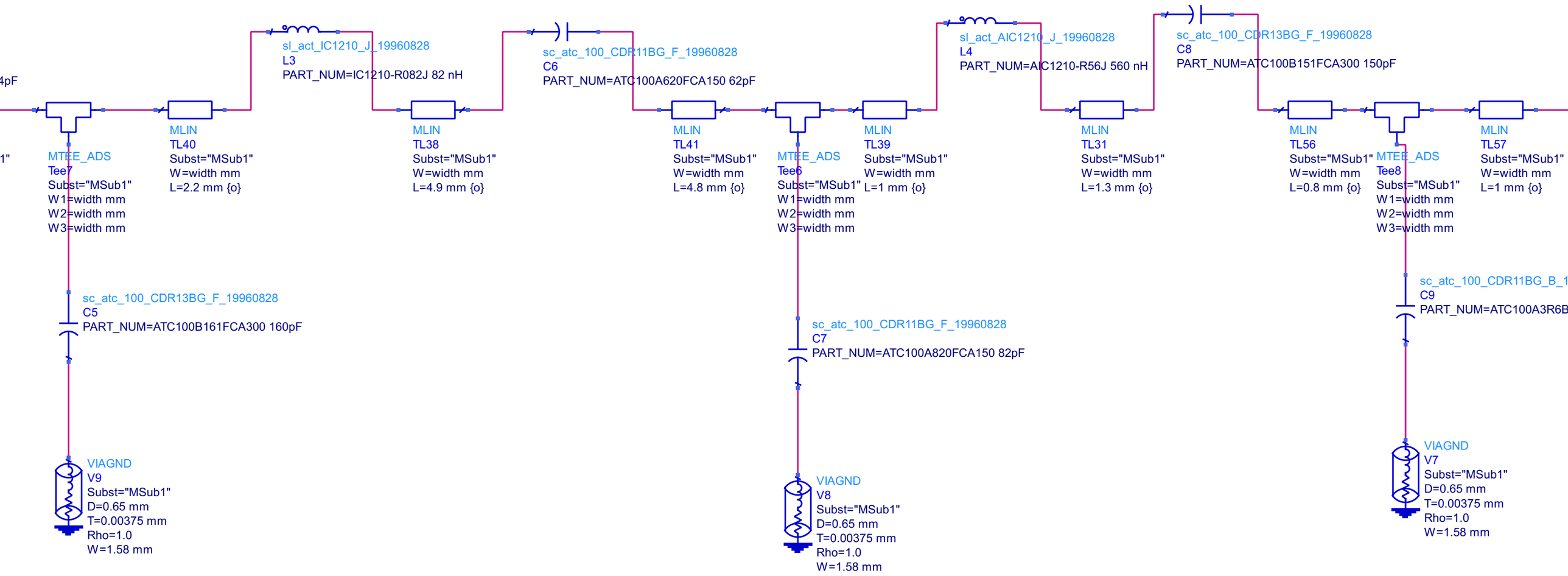
4pF
1"
MTEE_ADS
Tee7
Subst="MSub1"
W1=width mm
W2=width mm
W3=width mm
MLIN
TL40
Subst="MSub1"
W=width mm
L=2.2 mm {o}
sl_act_IC1210_J_19960828
L3
PART_NUM=IC1210-R082J 82 nH
MLIN
TL38
Subst="MSub1"
W=width mm
L=4.9 mm {o}
sc_atc_100_CDR11BG_F_19960828
C6
PART_NUM=ATC100A620FCA150 62pF
MLIN
TL41
Subst="MSub1"
W=width mm
L=4.8 mm {o}
MTEE_ADS
Tee6
Subst="MSub1"
W1=width mm
W2=width mm
W3=width mm
MLIN
TL39
Subst="MSub1"
W=width mm
L=1 mm {o}
sl_act_AIC1210_J_19960828
L4
PART_NUM=AIC1210-R56J 560 nH
MLIN
TL31
Subst="MSub1"
W=width mm
L=1.3 mm {o}
sc_atc_100_CDR13BG_F_19960828
C8
PART_NUM=ATC100B151FCA300 150pF
MLIN
TL56
Subst="MSub1"
W=width mm
L=0.8 mm {o}
MTEE_ADS
Tee8
Subst="MSub1"
W1=width mm
W2=width mm
W3=width mm
MLIN
TL57
Subst="MSub1"
W=width mm
L=1 mm {o}
sc_atc_100_CDR13BG_F_19960828
C5
PART_NUM=ATC100B161FCA300 160pF
VIAGND
V9
Subst="MSub1"
D=0.65 mm
T=0.00375 mm
Rho=1.0
W=1.58 mm
sc_atc_100_CDR11BG_F_19960828
C7
PART_NUM=ATC100A820FCA150 82pF
VIAGND
V8
Subst="MSub1"
D=0.65 mm
T=0.00375 mm
Rho=1.0
W=1.58 mm
sc_atc_100_CDR11BG_B_1
C9
PART_NUM=ATC100A3R6B
VIAGND
V7
Subst="MSub1"
D=0.65 mm
T=0.00375 mm
Rho=1.0
W=1.58 mm

(c)

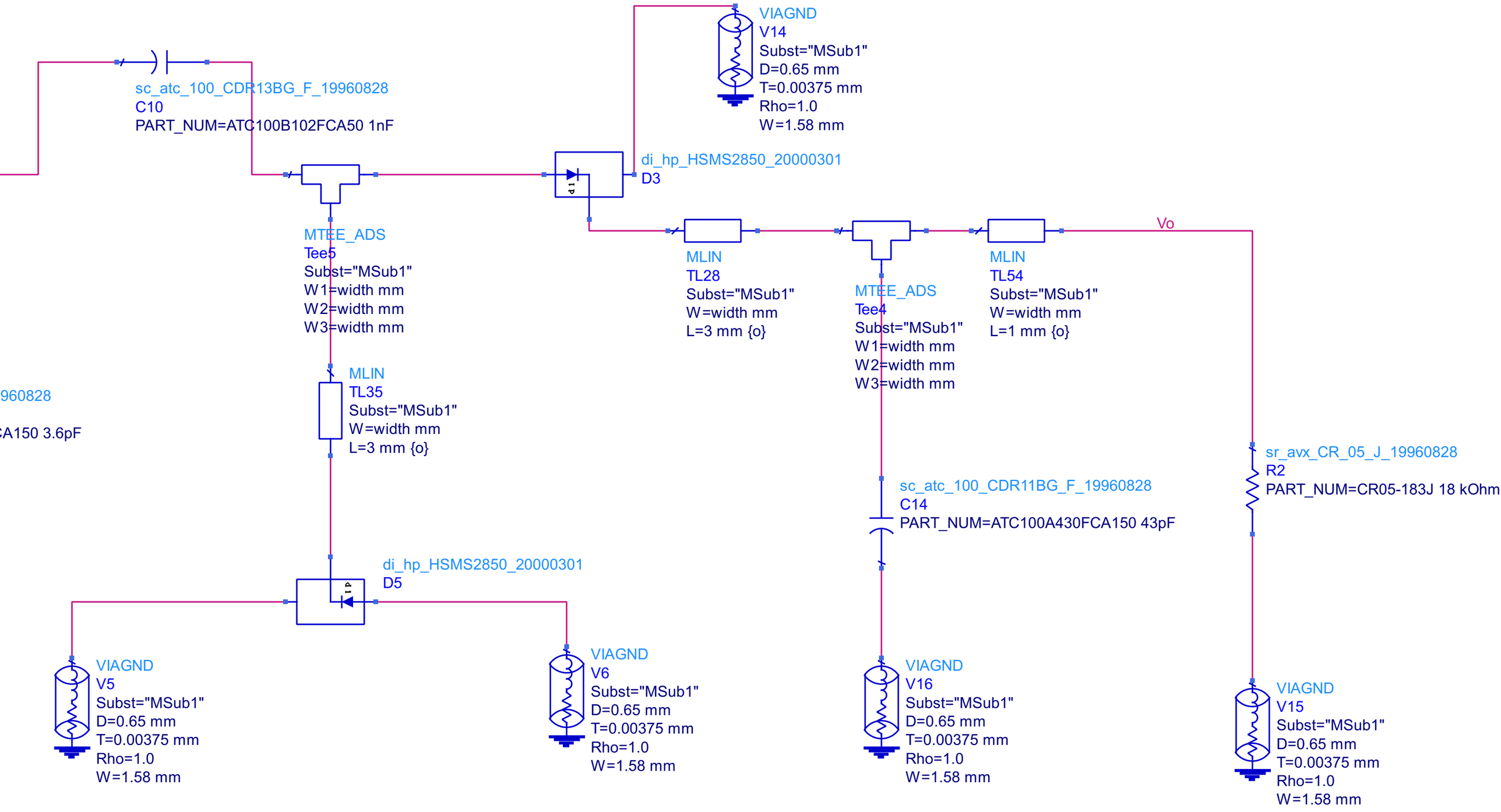
960828
CA150 3.6pF
sc_atc_100_CDR13BG_F_19960828
C10
PART_NUM=ATC100B102FCA50 1nF
MTEE_ADS
Tee5
Subst="MSub1"
W1=width mm
W2=width mm
W3=width mm
MLIN
TL35
Subst="MSub1"
W=width mm
L=3 mm {o}
di_hp_HSMS2850_20000301
D5
VIAGND
V5
Subst="MSub1"
D=0.65 mm
T=0.00375 mm
Rho=1.0
W=1.58 mm
VIAGND
V6
Subst="MSub1"
D=0.65 mm
T=0.00375 mm
Rho=1.0
W=1.58 mm
VIAGND
V14
Subst="MSub1"
D=0.65 mm
T=0.00375 mm
Rho=1.0
W=1.58 mm
di_hp_HSMS2850_20000301
D3
MLIN
TL28
Subst="MSub1"
W=width mm
L=3 mm {o}
MTEE_ADS
Tee4
Subst="MSub1"
W1=width mm
W2=width mm
W3=width mm
MLIN
TL54
Subst="MSub1"
W=width mm
L=1 mm {o}
Vo
sc_atc_100_CDR11BG_F_19960828
C14
PART_NUM=ATC100A430FCA150 43pF
VIAGND
V16
Subst="MSub1"
D=0.65 mm
T=0.00375 mm
Rho=1.0
W=1.58 mm
sr_avx_CR_05_J_19960828
R2
PART_NUM=CR05-183J 18 kOhm
VIAGND
V15
Subst="MSub1"
D=0.65 mm
T=0.00375 mm
Rho=1.0
W=1.58 mm